



國立中山大學海洋地質及化學研究所

博士論文

南海時間序列測站海水之碳化學參數與碳-13

之垂直分佈及其在混合層中的季節變化

Seasonal Variability of CO₂ Species and $\delta^{13}\text{C}_{\text{TCO}_2}$ in the Mixed-layer
and Their Vertical Distributions at the SEATS Site

研究生：周文臣撰

指導教授：許德惇博士、陳鎮東博士

中華民國 九十三年 七月

國立中山大學研究生學位論文審定書

本校海洋地質及化學研究所博士班

研究生周文臣 (學號：8953801) 所提論文

南海時間序列測站海水之碳化學參數與碳-13

之垂直分佈及其在混合層中的季節變化

經本委員會審查並舉行口試，符合博士學位論文標準。

學位考試委員簽章：

(召集人) 劉禎克

唐存真

陳偉東
黃國亨

許坤亨

白書祥

夏張國

指導教授 許坤亨 陳偉東

系主任/所長 _____

博碩士論文授權書

(國科會科學技術資料中心版本 93.2.6)

本授權書所授權之論文為本人在 國立中山大學(學院)海洋地質及化學系 所
組 92 學年度第 2 學期取得 博 士學位之論文。

論文名稱：南海時間序列測站海水之碳酸鹽類礦-13之垂直分佈及其在
及其在混合層中的季節變化
同意 不同意

本人具有著作財產權之論文全文資料，授予行政院國家科學委員會科學技術資料中心(或其改制後之機構)、國家圖書館及本人畢業學校圖書館，得不限地域、時間與次數以微縮、光碟或數位化等各種方式重製後散布發行或上載網路。

本論文為本人向經濟部智慧財產局申請專利(未申請者本條款請不予理會)的附件之一，申請文號為：_____，註明文號者請將全文資料延後半年再公開。

同意 不同意

本人具有著作財產權之論文全文資料，授予教育部指定送繳之圖書館及本人畢業學校圖書館，為學術研究之目的以各種方法重製，或為上述目的再授權他人以各種方法重製，不限地域與時間，惟每人以一份為限。

上述授權內容均無須訂立讓與及授權契約書。依本授權之發行權為非專屬性發行權利。依本授權所為之收錄、重製、發行及學術研發利用均為無償。上述同意與不同意之欄位若未鈎選，本人同意視同授權。

指導教授姓名：許德惇、陳鎮東

研究生簽名：周文臣

學號：8953801

(親筆正楷)

(務必填寫)

日期：民國 93 年 7 月 29 日

1. 本授權書(得自<http://sticnet.stic.gov.tw/sticweb/html/theses/authorize.html> 下載或至<http://www.stic.gov.tw> 首頁右下方下載)請以黑筆撰寫並影印裝訂於書名頁之次頁。
2. 授權第一項者，請確認學校是否代收，若無者，請個別再寄論文一本至台北市(106-36)和平東路二段106號1702室 國科會科學技術資料中心 黃善平小姐。(本授權書諮詢電話：02-27377606 傳真：02-27377689)

誌 謝

“天地間最大的人情失衡，第一產生於父母與子女之間，第二產生於老師與學生之間。”
霜冷長河……………余秋雨

這句話的前半段，在有了黎恩和沛恩後體會更深；而後半段，經歷過這四年來的淬煉也有了刻骨銘心的感受。四年來許德惇、陳鎮東兩位老師毫無保留的傾囊相授，不厭其煩的諄諄教誨，不僅使我在學業上受益良多，更讓我認識了科學的迷人之處，以及一個科學工作者對追求真理該有的執著。我知道這分在人情天平上嚴重的失衡，並無法以有形的方式來加以回報。除了真誠的感謝外，我將會以這分執著面對未來，並且將這分失衡繼續向下一代延續。

台灣大學白書禎教授、唐存勇教授、夏復國教授、中央大學劉康克教授和海洋大學龔國慶教授對論文初稿提出寶貴的指正與建議，口試時一針見血的提問，使學生受益匪淺，亦使本論文增色不少。在此謹致上十二萬分的謝意。

衷心感謝所上林慧玲老師、洪佳章老師、袁彼得老師、劉祖乾老師和鍾玉嘉老師在課業上的指導，諸位老師不同領域豐富的學養，使學生的視野與胸襟變的更為開闊。特別是林慧玲老師在生活上的關心，還得不時忍受黎恩和沛恩的騷擾，這分情誼學生永誌不忘。高雄海洋大學王樹倫老師在碳化學參數分析上的協助，海軍官校梁文德老師提供南海風速資料，以及楊穎堅老師有關於南海流場的文獻諮詢，海資系李玉玲老師，在固氮及新生產力上觀念的指導，海科中心溫良碩博士、曾鈞懋博士、楊益博士在相關資料的提供與討論，在此深表感謝。

實驗室的學弟妹，謹緒、子賢、志成、清芬、峰慧、信吉、福祥、詠嚴在實驗上的切磋與相互幫忙，歷任助理愛琳、蓮珠、震南在實驗及庶務上的協助，以及陳老師實驗室的修儀姊諸多的幫忙與鼓勵，在此特申謝忱。與你們的相處彷彿置身於一個大家庭中，希望大家可以做一生一世的朋友。感謝所辦康兄、莊姐在行政事務上的幫忙，圖書室桂蜜在文獻查尋上的協助，讓我的工作更有效率。學長洪國璋博士、冰潔學姐、小郭、美姐謝謝你們長期的關心與鼓勵。海上工作承蒙海研一號的船長及船員們的協助，還有許許多多一塊出海的伙伴們的照顧，謝謝你們陪伴著我度過那些吃風喝浪的日子。

謹以此論文獻給早逝的父親與一位堅苦卓絕的偉大女性—我的母親。我曾在碩士論文的誌謝中寫道：「我不清楚她是如何獨自一人，將三個孩子教養成人，卻從不曾讓他們有一絲的不安與牽掛」。如今我生為人父了，這個疑惑更深了。我真的她不了解她是如何做到的？我只知道我這一生中都會以她為傲，我只知道她是我這一生中最好的榜樣。黎恩和沛恩，爸爸必須跟你們說抱歉，因為你們不像別的小朋友有那麼多與爸爸相處的時間；爸爸也必須跟你們說謝謝，因為你們是爸爸最大的精神支柱。最後願將這分喜悅與榮耀和雅雲分享，感謝妳多年來付出的一切...

摘要

東南亞時間序列研究 (SEATS) 測站是全球海洋時間序列觀測網中, 唯一位於低緯度邊緣海域的測站。本研究利用 2002 年 3 月至 2003 年 8 月間八個 SEATS 探測航次所測得之 TA、TCO₂ 及 $\delta^{13}\text{C}_{\text{TCO}_2}$ 的數據, 探討了 SEATS 測站碳化學參數在混合層中季節變化的特性, 以及現今控制 NTA、NTCO₂ 和 $\delta^{13}\text{C}_{\text{TCO}_2}$ 垂直變化的作用機制。其目的乃在於增進吾等對此類型海域碳循環之瞭解, 並可作為日後探討在人為活動影響下, 南海碳化學系統所可能發生之變化時的對比依據。

研究結果顯示, 春、夏兩季, NTCO₂ 之遞減趨勢主要由生物生產作用所造成; 混合層的深化, 則是秋、冬兩季 NTCO₂ 濃度漸增的主因。根據冬、夏兩季 NTCO₂ 之濃度差所推算出全年之平均基礎生產力介於 177 ± 34 到 363 ± 69 mgC m⁻² day⁻¹ 之間。fCO₂ 呈現夏高冬低的季節性變化趨勢, 且幾與溫度成完美的同步變化。此種季節變化之形成機制為: 在溫度漸升的時期, 溫度上升對 fCO₂ 之增加效果較生物生產對 fCO₂ 之減少效果為大, 故 fCO₂ 隨溫度的增高而增大; 在溫度遞減的時期, 雖然次表層水加入混合層大幅提高了 fCO₂, 但其增加效果不若溫度降低與生物生產加總對 fCO₂ 的減少效果, 故 fCO₂ 呈現隨溫度而遞減的現象。SEATS 測站在夏季及秋初明顯是大氣二氧化碳的“source”, 冬季時為“sink”, 春季及秋末則大致呈現海氣平衡的狀態。最高之二氧化碳海氣交換通量出現在冬季, 此乃因東北季風之風速遠較其它季節為強所致。全年累計之二氧化碳海氣交換淨通量約介於 -1.28 ± 0.94 至 -2.73 ± 2.20 gC m⁻² yr⁻¹ 之間。

PO₄³⁻、NO₃⁻、AOU、NTA 和 NTCO₂ 之垂直分佈呈現典型的“nutrient type”型態, 意即隨深度增加而遞增。 $\delta^{13}\text{C}_{\text{TCO}_2}$ 之垂直變化, 則呈現與 PO₄³⁻、NO₃⁻ 及 AOU 相反的趨勢。PO₄³⁻ 與 AOU、NO₃⁻ 與 AOU 和 NO₃⁻ 與 PO₄³⁻ 在水深 100m 以下都呈現良好之線性相關, 但三者線性關係之斜率卻明顯偏離了 Redfield-ratio。PO₄³⁻ 和 AOU 線性關係斜率與 Redfield-ratio 的偏離, 可由不同深度水樣 PO₄³⁻ 起始值的差異所解釋; NO₃⁻ 和 AOU 以及 NO₃⁻ 和 PO₄³⁻ 之線性關係與 Redfield-ratio

的偏移，則可能與脫硝作用有關。

NTA 由表層至水深 150m 處濃度大致不變，此乃因起始值之增加與有機質分解所造成 TA 之變化量相互抵銷的結果。其後 NTA 隨深度的遞增，是由起始值之增加及碳酸鈣的溶解所共同造成，在 500m 以上起始值的增加較碳酸鈣溶解作用重要；500m 以下碳酸鈣溶解則是造成 NTA 隨深度遞增最重要的因素。NTCO₂ 在 400m 以上隨深度之增加，主要是由起始值的增加和有機質的分解所造成，兩者之相對貢獻大略相等。400m 以下，碳酸鈣溶解亦開始對 NTCO₂ 隨深度的增加有所貢獻，惟其仍較起始值和有機質分解作用之貢獻程度為小。IC/OC 比之計算結果顯示，此比值隨深度遞增，最大值約為 0.4，代表對任何深度而言，有機質的分解作用才是造成海水中 TCO₂ 增加的主因。此外根據 TA 所計算之碳酸鈣溶解量的結果顯示，在霰石及方解石化學飽和深度(分別為 600m 及 2500m) 之上，碳酸鈣即出現了溶解訊號。但由於碳酸鈣溶解並非 TA 唯一的來源，故此現象之真實性仍有待證實。由於有機質之 $\delta^{13}\text{C}$ 與海水 $\delta^{13}\text{C}_{\text{TCO}_2}$ 之差異極大，且有機質分解是海水中 TCO₂ 增加最重要的貢獻者。故 $\delta^{13}\text{C}_{\text{TCO}_2}$ 隨深度遞減趨勢是由有機質分解作用所主導形成。以碳化學及 $\delta^{13}\text{C}_{\text{TCO}_2}$ 資料所估算的結果都顯示，人為二氧化碳在 SEATS 測站的穿透深度約為 1200m。整個垂直剖面所累積人為二氧化碳之總儲量約為 18mol m^{-2} 。若將此結果套用於整個南海，則南海之人為二氧化碳總儲量約為 0.5 至 0.6Gt C，此量約佔全球海洋人為二氧化碳總儲量的 0.5%。在人为二氧化碳影響下，SEATS 測站海水中 TCO₂ 增加量 (ΔTCO_2) 與 $\delta^{13}\text{C}_{\text{TCO}_2}$ 減輕量 ($\Delta\delta^{13}\text{C}_{\text{TCO}_2}$) 的相對比值 ($\Delta\delta^{13}\text{C}_{\text{TCO}_2}/\Delta\text{TCO}_2$) 約為 $-0.024\text{‰} (\mu\text{mol kg}^{-1})^{-1}$ 。

ABSTRACT

With regard to the concerns on the role of oceanic uptake of the increasing atmospheric CO₂ concentration, a total of eight ocean time-series programs, have been established worldwide since the JGOFS era (i.e. late 1980s). Among these, the Southeast Asia Time-series Study (SEATS) site is the only one located in a “subtropical marginal sea”, namely the South China Sea (SCS). TA, TCO₂, δ¹³C_{TCO₂} and other pertinent chemical parameters were measured for seawater samples collected at the SEATS site from eight separate cruises between March 2002 and August 2003. Based on these measurements, the characteristics of the seasonal variability of CO₂ species in the mixed-layer, the processes controlling the vertical distributions of NTA, NTCO₂ and δ¹³C_{TCO₂}, and the magnitude of anthropogenic CO₂ influence throughout the water column are thoroughly investigated to better understand the carbon cycles in such a subtropical marginal sea.

Results show that the decline of NTCO₂ in spring-summer mainly results from *in situ* biological utilization in the mixed-layer, while the resurgence of NTCO₂ in fall-winter is due to entrainment of the CO₂-rich subsurface waters from below. Based on the drawdown of NTCO₂ from winter to summer, the primary production is estimated to be 177±34 ~ 363±69 mgC m⁻² day⁻¹ in the mixed-layer. fCO₂ increases progressively from spring to summer, then decreases from fall to winter. The seasonal variability of fCO₂ is in phase with temperature changes, suggesting that the fCO₂ seasonality is primarily controlled by temperature effect, though other factors have compensated partially to yield the observed low amplitude of its variability. The SEATS site is an atmospheric CO₂ “source” in summer and early fall, but a “sink” in winter. The largest CO₂ flux occurs in winter due to the high wind speed during winter monsoon. The annual sea-to-air CO₂ flux at the SEATS site is

estimated to be around -1.28 ± 0.94 to -2.73 ± 2.20 $\text{gC m}^{-2} \text{ year}^{-1}$.

A close examination on processes controlling the vertical variations of NTA, NTCO_2 and $\delta^{13}\text{C}_{\text{TCO}_2}$ reveals that the increasing trend of NTA is resulted mainly from higher preformed-NTA and carbonate dissolution at deep, while organic oxidation and greater preformed- NTCO_2 are responsible for the observed increasing trend in NTCO_2 . The decrease in $\delta^{13}\text{C}_{\text{TCO}_2}$ with depths, however, is principally owing to the decomposition of organic matter. Furthermore, carbonate dissolution accounts for approximately 30% of TCO_2 production in the SCS deep waters, and it may have taken place at depths well above aragonite and calcite saturation depths at 600 m and 2500 m, respectively, in the SCS. Moreover, the penetration depth of anthropogenic CO_2 at the SEATS site is estimated to be about 1200 m, based on both carbonate and $\delta^{13}\text{C}_{\text{TCO}_2}$ data. The ratio of the decrease of $\delta^{13}\text{C}_{\text{TCO}_2}$ to TCO_2 increase, i.e. $\Delta\delta^{13}\text{C}_{\text{TCO}_2}/\Delta\text{TCO}_2$, due to the uptake of anthropogenic CO_2 is about $-0.024\text{‰} (\mu\text{mol kg}^{-1})^{-1}$.

目錄

誌謝.....	I
摘要.....	III
ABSTRACT.....	V
目錄.....	VII
圖目錄.....	IX
表目錄.....	XI
一、緒論.....	1
1.1 海洋碳循環研究之重要性及其研究策略.....	1
1.2 海洋碳循環之作用機制及其在全球海洋之運作概況.....	6
1.3 東南亞時間序列研究之緣起與目的.....	13
1.4 研究區域之背景介紹.....	15
1.4.1 南海的地理型態.....	15
1.4.2 南海的氣候概況.....	17
1.4.3 南海的環流概況.....	19
1.4.4 南海的水文特性.....	21
1.5 論文目標.....	22
二、研究方法.....	25
2.1 研究材料.....	25
2.2 實驗方法.....	27
2.2.1 海水滴定總鹼度(TA)之測定.....	27
2.2.2 海水總二氧化碳(TCO ₂)之測定.....	27
2.2.3 海水總二氧化碳碳同位素組成($\delta^{13}\text{C}_{\text{TCO}_2}$)之測定.....	28
2.2.4 TA, TCO ₂ 和 $\delta^{13}\text{C}_{\text{TCO}_2}$ 分析精確度及準確度的評估.....	29
三、結果與討論.....	32
3.1 SEATS 測站混合層中滴定總鹼度/標準化鹼度(TA/NTA)、總二 氧化碳/標準化總二氧化碳(TCO ₂ /NTCO ₂)及二氧化碳	

分壓($f\text{CO}_2$)季節變化之初探.....	32
3.1.1 混合層中溫度、鹽度、TA/NTA、 $\text{TCO}_2/\text{NTCO}_2$ 及 $f\text{CO}_2$ 之季節變化型態.....	33
3.1.2 混合層中 $f\text{CO}_2$ 季節變化之控制機制.....	37
3.1.3 二氧化碳海氣交換通量之季節變化.....	47
3.1.4 基礎生產力之估算.....	50
3.1.5 碳氮消耗不平衡的現象.....	52
3.2 SEATS 測站標準化鹼度(NTA)、標準化總二氧化碳(NTCO_2)及 總二氧化碳碳同位素組成($\delta^{13}\text{C}_{\text{TCO}_2}$)之垂直分佈特徵: 控制機制及人為二氧化碳影響之探討.....	54
3.2.1 磷酸鹽(PO_4^{3-})、硝酸鹽(NO_3^-)、表觀溶氧消耗量(AOU)、 NTA、 NTCO_2 和 $\delta^{13}\text{C}_{\text{TCO}_2}$ 之垂直分佈.....	54
3.2.2 NTA、 NTCO_2 和 $\delta^{13}\text{C}_{\text{TCO}_2}$ 垂直變化之控制機制.....	61
3.2.3 人為二氧化碳之影響.....	72
四 結論.....	81
參考文獻.....	86
附錄一 各航次鹽度、位溫、磷酸鹽、硝酸鹽、溶氧、總滴定鹼度、總 二氧化碳及 $\delta^{13}\text{C}_{\text{TCO}_2}$ 之數據.....	99
附錄二 Chou, W.C., Sheu, D.D., Chen, C.T.A., Wang, S.L., Tseng, C.M., 2004. Preliminary investigation on seasonal variability of mixed-layer CO_2 , alkalinity, and $f\text{CO}_2$ at the SEATStime-series site, northern South China Sea, submitted to Deep-Sea Research I.....	106
附錄三 Chou, W.C., Sheu, D.D., Chen, C.T.A., Tseng, C.M., 2004. Vertical distributions of alkalinity, TCO_2 , $\delta^{13}\text{C}_{\text{TCO}_2}$ at South East Asia Time-series Study (SEATS) site: controlling processes and anthropogenic CO_2 influence (first draft).....	147
作者簡介.....	210

圖目錄

圖 1.1	過去四十萬年來，南極地區大氣溫度與二氧化碳濃度隨時間之變化圖.....	1
圖 1.2	西元 900 年至 2000 年，大氣二氧化碳濃度隨時間之變化圖.....	2
圖 1.3	西元 1850 年至 2000 年，全球地表平均溫度異常隨時間之變化圖.....	3
圖 1.4	西元 1960 年至 2000 年，大氣二氧化碳儲量月及年變化圖.....	5
圖 1.5	海洋碳循環運作機制：生物幫浦及物理幫浦之示意圖.....	7
圖 1.6	全球海域表水之二氧化碳分壓在二月及八月時之分佈圖.....	9
圖 1.7	二氧化碳海氣交換年淨通量在全球海域之分佈圖.....	10
圖 1.8	人為二氧化碳在大西洋 印度洋和太平洋之分佈圖.....	12
圖 1.9	JGOFS 海洋時間序列測站分佈圖.....	13
圖 1.10	南海海底地貌圖.....	16
圖 1.11	南海季風風速和風向月平均變化圖.....	17
圖 1.12	南海表層海水水溫月平均變化圖.....	18
圖 1.13	南海之表面環流系統(a)冬季，(b)夏季.....	20
圖 1.14	南海及西菲律賓海之溫鹽圖.....	21
圖 2.1	南海之水深等深線及 SEATS 測站之位置圖.....	25
圖 2.2	TA 和 TCO ₂ 標準品測量值與標定值之差異分佈圖.....	30
圖 3.1	2002 年 3 月至 2003 年 4 月 SEATS 測站，混合層之(a)平均溫度，(b)平均鹽度及(c)深度 之時間序列變化圖.....	35
圖 3.1	(續) 2002 年 3 月至 2003 年 4 月 SEATS 測站，混合層之平均(d)TA/NTA，(e)TCO ₂ /NTCO ₂ 及(f)fCO ₂ 之時間序列變化圖.....	36
圖 3.2	北大西洋高緯地區（冰島附近海域）表水溫度及 pCO ₂ 之季節變化圖.....	38
圖 3.3	BATS 和 ESTOC 時間序列測站，混合層中溫度及 pCO ₂ 之時間序列變化圖.....	39

圖 3.4	KNOT 時間序列測站 1998 年至 2000 年表水 $p\text{CO}_2$ 之時序變化圖.....	40
圖 3.5	OSP 時間序列測站混合層內 $p\text{CO}_2$ 及溫度之年時序變化圖.....	41
圖 3.6	HOT 時間序列測站 1988 年底至 1992 年上層海水溫度與 $p\text{CO}_2$ 之時序變化圖.....	42
圖 3.7	SEATS 測站“ $f\text{CO}_{2\text{mean}}$ corrected for ΔT ”、“ $f\text{CO}_2$ at 27 °C”以及 $f\text{CO}_2$ 觀測值之時序變化圖.....	43
圖 3.8	SEATS 和 HOT 時間序列測站位溫、磷酸鹽與總二氧化碳濃度之垂直分佈比較圖.....	48
圖 3.9	SEATS 測站 $\Delta f\text{CO}_2$ 之時序變化圖.....	49
圖 3.10	SEATS 測站 PO_4^{3-} 、 NO_3^- 、AOU、NTA、 NTCO_2 和 $\delta^{13}\text{C}_{\text{TCO}_2}$ 之垂直分佈圖.....	56
圖 3.11	SATS 測站(a) PO_4^{3-} 對 AOU, (b) NO_3^- 對 AOU 和 (c) NO_3^- 對 PO_4^{3-} 之關係圖.....	58
圖 3.12	SEATS 測站硝酸鹽異常值(N^*)之垂直分佈圖.....	60
圖 3.13	SEATS 測站 NTA 實測值、NTA 起始值和 (NTA 起始值 + 有機質分解所造成 TA 之變化量) 之垂直分佈圖.....	63
圖 3.14	SEATS 測站 NTCO_2 實測值、 NTCO_2 起始值和 (NTCO_2 起始值 + 有機質分解所造成 TCO_2 之變化量) 之垂直分佈圖.....	65
圖 3.15	SEATS 測站 IC/OC 比之垂直分佈圖.....	67
圖 3.16	SEATS 測站霰石與方解石飽和度和碳酸鈣溶解所造成 TCO_2 增加量之垂直分佈圖.....	68
圖 3.17	SEATS 測站 $\delta^{13}\text{C}_{\text{TCO}_2}$ 實測值、 $\delta^{13}\text{C}_{\text{TCO}_2}$ 起始值和 ($\delta^{13}\text{C}_{\text{TCO}_2}$ 起始值 + 有機質分解所造成 $\delta^{13}\text{C}_{\text{TCO}_2}$ 變化量) 之垂直分佈圖.....	71
圖 3.18	以“反算法”計算海水中人為二氧化碳含量之觀念流程圖.....	73
圖 3.19	SEATS 測站“人為二氧化碳”濃度之垂直分佈圖.....	75
圖 3.20	SATS 測站 $\delta^{13}\text{C}_{\text{TCO}_2}$ 對 PO_4^{3-} 之關係圖.....	78
圖 3.21	SEATS 測站 $\Delta\delta^{13}\text{C}_{\text{a-p}}$ 之垂直分佈圖.....	79

表目錄

表 2.1	各航次之編號、探測日期及採樣深度表.....	26
表 2.2	TCO ₂ 標準品重覆分析 8 次 $\delta^{13}\text{C}_{\text{TCO}_2}$ 之結果表.....	31
表 2.3	本實驗室與Dr. Spero實驗室針對南海2m, 400m, 1500m水樣 $^{13}\text{C}_{\text{TCO}_2}$ 之分析結果比較表.....	31
表 3.1	SEATS 與 HOT、BATS、KNOT 和 OSP 等時間序列測站， 溫度及生物效應對 fCO ₂ 影響之相對重要性比較表.....	46
表 3.2	SEATS 測站春、夏、秋、冬四季以及年平均二氧化碳海氣交 換通量之估算結果表.....	51

一、緒論

本論文所要探討的主題為東南亞時間序列研究測站其海水之總鹼度、總二氧化碳與碳-13之垂直分佈以及這些參數在混合層中的季節變化。主要的研究目的，是希望闡明現今影響南海碳化學參數及其碳同位素組成垂直分佈的各項生地化因子，以及控制此些參數在混合層中季節變化的作用機制，以增進吾等對近赤道邊緣海域碳循環之瞭解。以下將先分就海洋碳循環研究之重要性及其研究策略、海洋碳循環之作用機制及其在全球海洋之運作概況、“東南亞時間序列研究”之緣起與目的以及南海的概況等背景課題加以介紹，最後再說明本論文之具體研究目標及其在全球海洋碳循環研究中所扮演的角色。

1.1 海洋碳循環研究之重要性及其研究策略

藉由封存於冰芯中古大氣的研究，科學家發現過去四十二萬年來，大氣中二氧化碳濃度的高低起伏與冰期 - 間冰期的交替有著同步的變化（圖 1.1; Petit et al., 1999）。此種緊密的相關性，意味著大氣中二氧化碳濃度的變化，對於地表溫

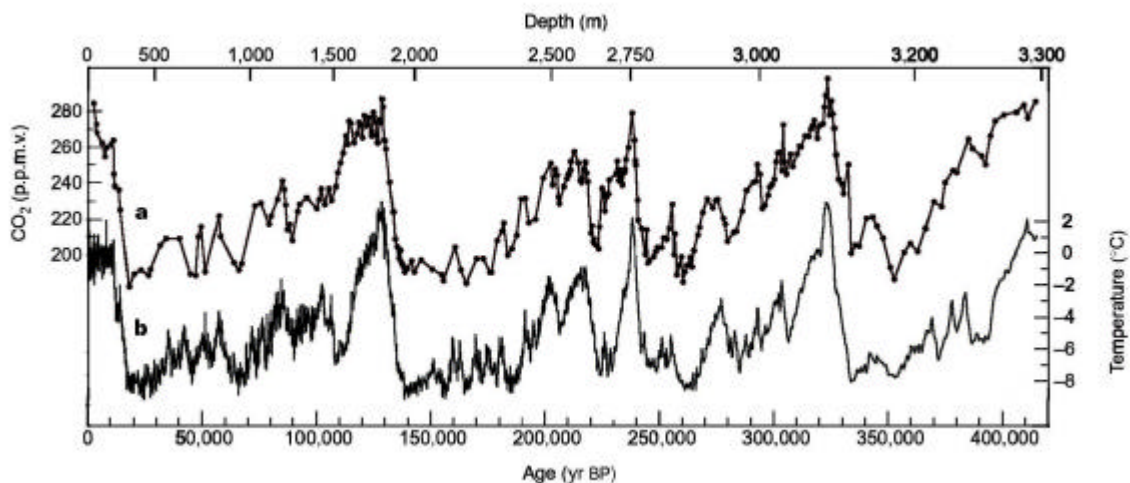


圖 1.1 過去四十二萬年來，南極地區大氣溫度與二氧化碳濃度隨時間之變化圖。

改繪自 Petit et al. (1999)。

度的改變，可能扮演著關鍵性的角色。冰芯中古大氣的研究亦顯示，在工業革命（十九世紀中葉）前的一千年間，大氣二氧化碳的濃度非常穩定，大約維持在 280 ± 10 ppmv 的範圍內（圖 1.2; Indermühle et al., 1999）。易言之，要維持地球氣候系統的穩定，大氣二氧化碳濃度的恆定，很可能是必要的先決條件之一。然而，自工業革命後，由於人類大量使用化石燃料（fossil fuel）及對森林的墾伐，已使得大氣中二氧化碳濃度由工業革命前的 280 ppmv 增加至 2001 年的 371 ppmv（Neftel et al., 1985; Keeling and Whorf, 2004）。在短短不到二百年間，人為活動所造成大氣中二氧化碳濃度的增加幅度（~90ppmv），已超過了過去數十萬年來，自然界中曾經有過的變化。因而，地球氣候系統是否會因人為活動所造成大氣二氧化碳濃度的快速增加，而產生劇烈的變化，遂成為科學家關注的焦點。

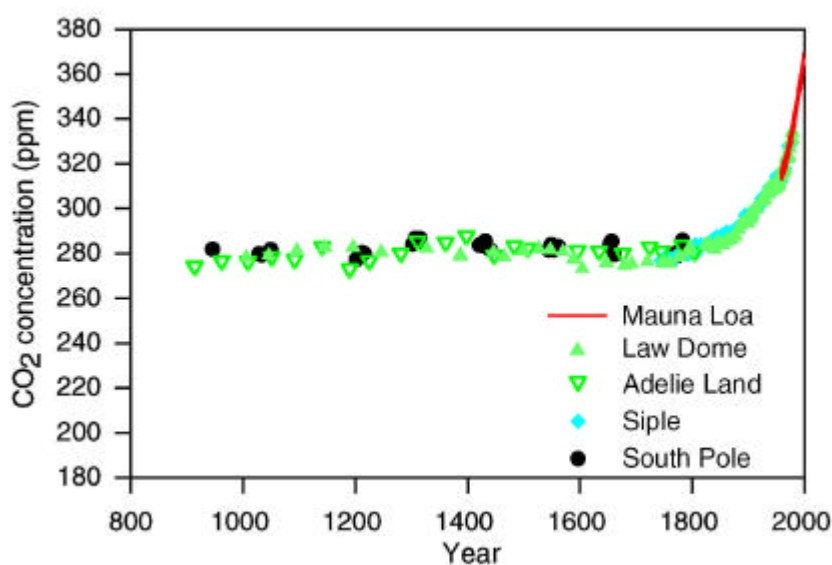


圖 1.2 西元 900 年至 2000 年，大氣二氧化碳濃度隨時間之變化圖。

摘自 Houghton et al. (2001)。

大氣中二氧化碳濃度改變對於地表大氣溫度的影響，主要是透過溫室效應來顯現。溫室效應氣體包括二氧化碳（ CO_2 ）、甲烷（ CH_4 ）、氟氯碳化物（CFCs）、氧化亞氮（ N_2O ）、臭氧（ O_3 ）及水蒸氣等。其中，二氧化碳是最重要的溫室效應氣體，其對地球溫室效應的貢獻度，約佔總溫室效應氣體的 55%。因此，大氣

中二氧化碳濃度逐年的遞增，已使得溫室效應逐漸增強，造成地表平均溫度逐漸升高。根據國際上政府間氣候專家委員會（Intergovernmental Panel on Climate Change, IPCC）的估算，全球地表平均溫度在二十世紀已上升了 $0.6 \pm 0.2^{\circ}\text{C}$ （圖 1.3）。地表溫度的增加，除了會造成極地冰原融化，海平面上升，進而淹沒沿海

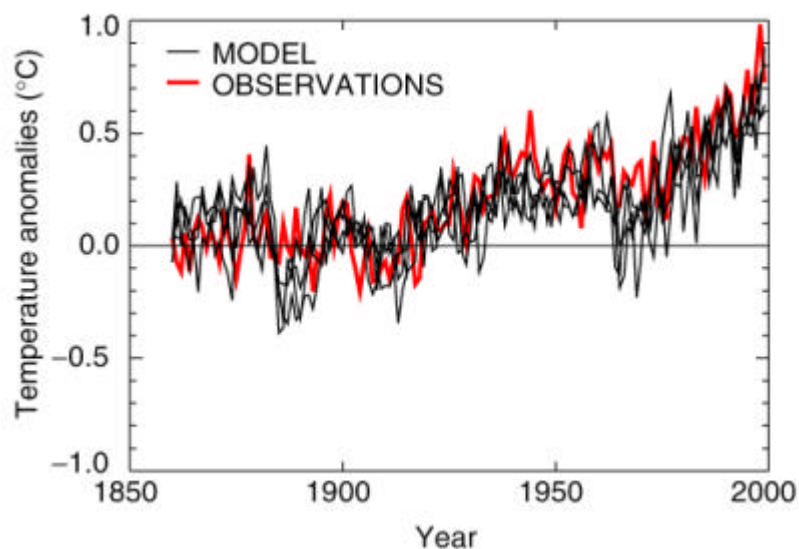


圖 1.3 西元 1850 年至 2000 年，全球地表平均溫度異常隨時間之變化圖。摘自 Houghton et al. (2001)。地表平均溫度異常之參考值，為西元 1880 年至 1920 年間全球地表觀測溫度之平均值。

的都會區外；亦會牽動全球氣候的變遷，導致不正常地暴雨及乾旱現象，衝擊全球的農林漁牧及社經活動。有鑑於溫室效應對人類永續生存所造成的可能威脅，過去數十年來，科學家們不斷努力，希望能夠闡明控制大氣中二氧化碳濃度變化的作用機制，以便能更準確掌握其未來趨勢，進而預測可能發生的氣候變遷。透過科學成果的展現及科學家們的大聲疾呼，世界各國的領袖逐漸意識到溫室效應對人類生存環境所造成可能的危害。終於在 1992 年巴西里約所舉行的「地球高峰會」中，通過了「氣候變化綱要公約」。此公約的終極目標，即是希望將大氣中人為溫室效應氣體的濃度，維持在一個不會危及氣候系統的範圍內。1997 年在日本京都所召開「氣候變化綱要公約」第三次締約國大會，更通過了「京都議定書」（Kyoto Protocol），要求工業化國家訂定由公元 2008 至 2012 年具約束力

的溫室效應氣體排放目標。此議定書的誕生，正式將人類對抗溫室效應的努力，化為具體的行動。

無可置疑，科學研究確認了大氣中二氧化碳濃度增加與全球暖化的相關性，對於「京都議定書」的催生扮演了關鍵性的角色，同時也廣泛的喚起了人們對溫室效應的警覺與重視。然而，以科學研究角度而言，若我們想準確地預測大氣中二氧化碳濃度的變化趨勢，進而評估其對氣候系統所可能造成的衝擊，則只能說「革命尚未成功，同志仍需努力」。IPCC 2001年的評估報告，可說是迄今有關於二氧化碳增加與溫室效應及氣候變遷之關係最權威的一份報告。它總結了過去近二十年來在這個領域中的主要研究成果。其中有關於人為二氧化碳（anthropogenic CO₂）的評估報告指出：人為活動所排放之二氧化碳主要有大氣，海洋及陸地生物圈三個儲存庫。在1980年代中，人為二氧化碳的年平均排放量為 $5.4 \pm 0.4 \text{ Gt C}$ ($1 \text{ GtC} = 10^{15} \text{ g carbon}$)，其中約61% ($3.3 \pm 0.1 \text{ Gt C}$)累積在大氣中，35% ($1.9 \pm 0.6 \text{ Gt C}$)被海洋所吸收，4% ($0.2 \pm 0.7 \text{ Gt C}$)則是儲存於陸地生物圈中。而到1990年代，人為二氧化碳的年平均排放量增為 $6.3 \pm 0.4 \text{ Gt C}$ ，大氣、海洋及陸地生物圈的吸收量分別佔51% ($3.2 \pm 0.1 \text{ Gt C}$)，27% ($1.7 \pm 0.5 \text{ Gt C}$)和22% ($1.4 \pm 0.7 \text{ Gt C}$)。而此報告亦針對1990年代，大氣中每年二氧化碳儲量（inventory）的增加量做進一步的分析。結果發現其並非呈遞增趨勢，而是在1.9到 6.0 GtC yr^{-1} 間波動，年際變化可高達三倍之多（圖1.4）。由於人為二氧化碳的排放量呈逐年遞增的趨勢，因此，大氣中每年二氧化碳儲量之改變，反映了海洋及陸地生物圈對人為二氧化碳吸收量的改變。到目前為止，科學界對為什麼會發生這樣的年際變化，所知極其有限。因此，若想準確推知大氣中二氧化碳濃度的變化趨勢，進而釐清其對全球氣候的影響，勢必對海洋及陸地生物圈的碳循環有更清楚的瞭解。而這其中，又以海洋碳循環的研究最為關鍵，因為大氣、海洋及陸地生物圈這三個儲存庫碳的儲量，分別約為：600、39800及550 Gt C（Siegenthaler and Sarmiento, 1993）顯而易見地，海洋之碳儲量遠較陸地生物圈為大，其微小的變動，便足以牽動大氣中二氧化碳濃度大幅度的改變。

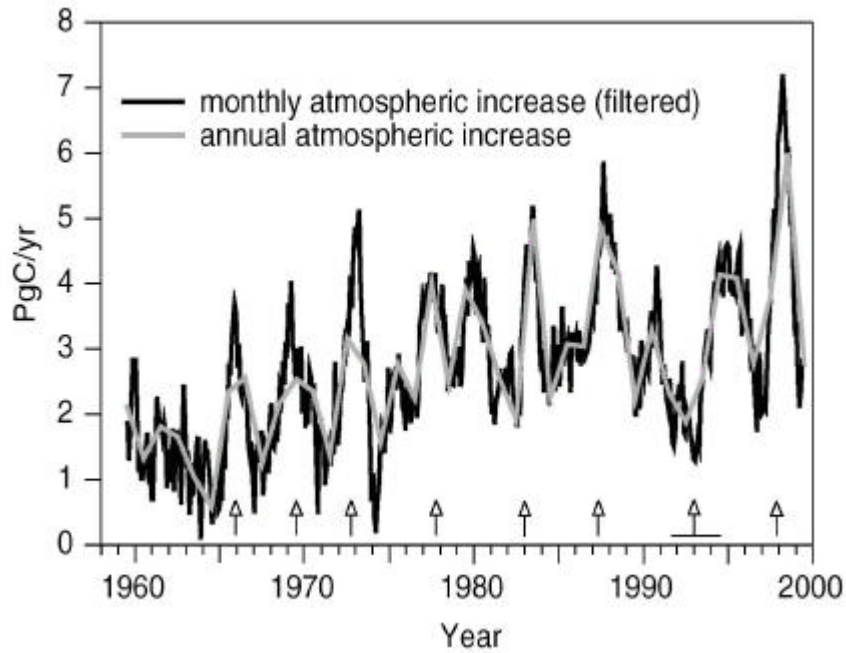


圖 1.4 西元 1960 年至 2000 年，大氣二氧化碳儲量月及年變化圖。

摘自 Houghton et al. (2001)。

有鑑於海洋碳循環的研究，對瞭解大氣中二氧化碳濃度變化的趨勢，扮演著關鍵性的角色。在美國的主導下，全球海洋學家自1988年至2003年，進行了一個史無前例的大規模海洋生地化整合研究：「聯合全球海洋通量研究」；Joint Global Ocean Flux Study，簡稱JGOFS。此研究所揭櫫的主要目標，就是要瞭解全球海洋碳通量的時空變化，並闡明控制此變化之各種生地化機制，進而去預測在人為活動影響下，海洋生地化作用所可能發生的變化，以及此種改變對氣候系統所可能造成的衝擊。為了達成上述目標，JGOFS將海洋碳循環的研究，區分為四大主軸（Buesseler, 2001）：第一、針對各個生地化特性較敏感之代表性海域，進行以作用機制（process studies）為導向的研究，例如，North Atlantic Bloom Experiment, Arabian Sea Process Study..等等，以瞭解海洋生地化作用在人為活動干擾下，所可能發生的變化及其對氣候系統所可能產生的回饋效應。第二、透過在特定海域之定點，進行碳化學與其它生地化及物理參數的長期時間序列觀測（time-series），例如，Hawaii Ocean Time-series (HOT) 和 Bermuda Atlantic

Time-Series Study (BATS) ..等等，以闡明不同時間尺度下，海洋碳循環隨時間之變化特性及其與其它生地化和物理參數變化的相關性。第三、針對全球海域之碳化學與其它相關之生地化參數，進行全面性的調查，以瞭解二氧化碳海氣交換通量以及人為二氧化碳在全球海域之分佈特性。第四、綜合上述三項及其它相關的研究成果，並據以發展模式，以預測海洋碳循環未來的變化趨勢，進而精確的評估其對氣候系統所可能產生的衝擊。綜觀JGOFS所擘劃的研究策略及方法，兼顧了時間和空間上的研究面向，同時亦結合了實測與模式的研究方法，可說是迄今有關於海洋碳循環研究方向最完整且最具前瞻性的規劃，不僅充分展現了人類對瞭解海洋碳循環全貌的強烈企圖心，也提供了現今海洋碳循環研究工作者一個清楚且完整的架構。本論文所要探討的主題為“東南亞時間序列研究”中海水碳化學參數之垂直分佈特徵及其在混合層中的季節變化，顧名思義是屬於這整個海洋碳循環研究大架構下，有關於時間序列研究的分支。

1.2 海洋碳循環之作用機制及其在全球海洋之運作概況

海洋中碳的循環，主要是透過“生物幫浦”（biological pump）及“物理幫浦”（physical pump）等兩種機制來進行（圖 1.5）。所謂的“生物幫浦”，是指浮游植物在透光層中行光合作用時，將溶解於海水中的無機碳，轉化為有機碳。雖然大部分光合作用所生成的有機碳，會在上層海水中再循環使用，但仍有少部分的有機質會沉降至深層水中才分解，甚至被永遠埋藏於沉積物中。因此，透過“生物幫浦”的運轉，碳可被上層海水中之浮游植物所吸收利用，然後向下輸出儲存在深海乃至沉積物中。故其作用之強弱，具有調節大氣中二氧化碳濃度高低的的能力。因此，海洋碳循環研究針對“生物幫浦”之探討重點，乃在於瞭解並量化藉由生物生產作用向深海輸出之碳通量隨時空的變異，及其背後之控制機制。透過沉積物收集器（sediment trap）廣泛地佈放及 ^{234}Th 放射性核種的研究，目前對“生物幫浦”之強度（輸出生產力與基礎生產力的比值）在全球海洋中的分佈概況已

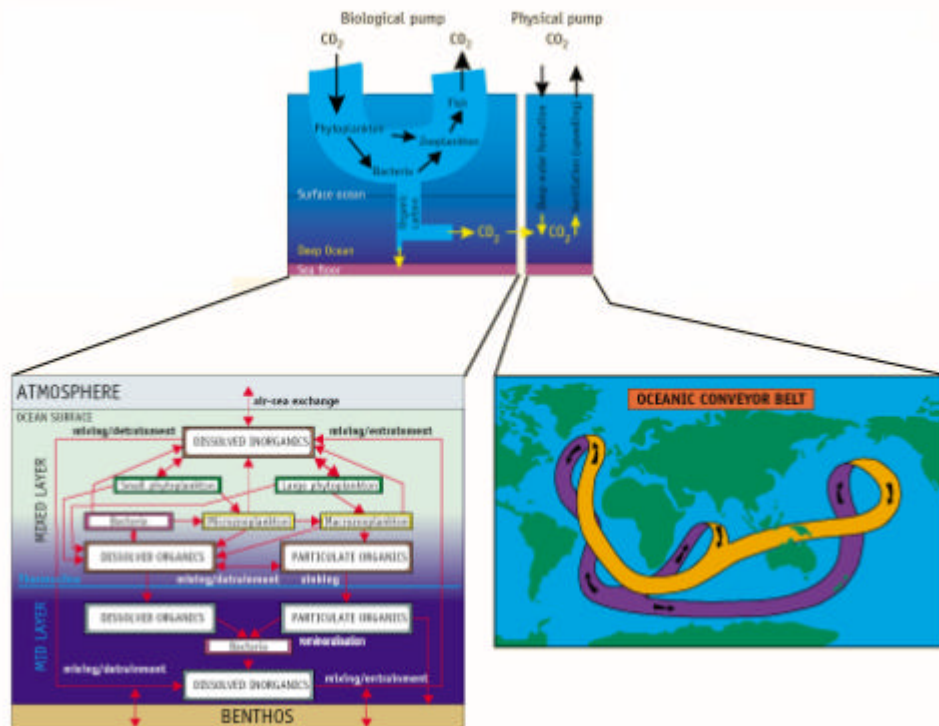


圖 1.5 海洋碳循環運作機制：生物幫浦（biological pump）及物理幫浦（physical）之示意圖。摘自 Baliño et al.(2001)。

有初步瞭解。一般認為在 100m 水深處，“生物幫浦”的強度有較明顯的時空變化，不過其變化，在大多數海域與基礎生產力之變化無關（Buesseler, 1998）。然而在少數海域，“生物幫浦”之增強則與基礎生產力的提高明顯有關，例如，中、高緯度海域春季藻華（bloom）現象發生時，以及阿拉伯海夏季時季風效應所引發之高生產力時期，“生物幫浦”都會顯著增強。此種增強效果與浮游生物族群結構的改變密切相關。在這些高生產力時期，生物族群的結構會以大型之浮游生物為主(例如矽藻)，而這些浮游生物死亡後會有較快的沉降速度，故造成較高的“生物幫浦”強度（Ducklow et al., 2001）。但在深海中（2000m 以下），“生物幫浦”的強度並無明顯的時空變化，全球海域僅在 1% 到 3% 的範圍內變動。總計目前全球海洋每年透過“生物幫浦”向深海輸出之碳通量約為 $0.34 \text{ Gt C yr}^{-1}$ ，約佔基礎生產力的 1%（Berelson, 2001）。此外，近年來的研究亦指出，溶解態有機碳（DOC）可能是“生物幫浦”向深海輸出碳的另一重要形式（Hansell and Carlson, 2001）。

所謂的“物理幫浦”，是指大氣中之二氧化碳可透過海氣交換作用進入表層海水，造成海水中總二氧化碳濃度的增高。再藉由大規模海洋環流的輸送，二氧化碳可被輸出並儲存於深層水中。因此，“物理幫浦”亦具有減緩大氣二氧化碳濃度增加速率的能力。而海洋碳循環研究針對“物理幫浦”之研究重點，乃在於瞭解全球海域表水二氧化碳分壓（ $p\text{CO}_2$ ）之分佈情形，以精確估算海氣二氧化碳之交換通量，同時亦針對全球海域之碳化學參數進行全面性的調查，以瞭解人為二氧化碳在全球海域中之分佈特性，並估算其在海水中之總儲量（inventory）。經過 JGOFS 與 World Ocean Circulation Experiment（JGOFS/WOCE）的合作調查，以及整合過去其它相關研究所取得的數據，目前對全球海洋碳化學參數的分佈概況，已有相當清楚的掌握，大幅增進了我們對“物理幫浦”的瞭解。以下將分別介紹全球海洋表水中二氧化碳分壓、海氣交換通量以及人為二氧化碳 在全球海域之分佈概況，以說明“物理幫浦”在全球海洋的運作情形。

(1) 全球海洋表水中二氧化碳分壓與海氣交換通量之分佈概況

二氧化碳海氣交換通量的多寡，即代表“物理幫浦”作用的強弱。而此通量之大小與海水和大氣二氧化碳之分壓差（ $\Delta p\text{CO}_2 = p\text{CO}_2(\text{海水}) - p\text{CO}_2(\text{大氣})$ ）成正比。由於大氣循環非常快速，故大氣 $p\text{CO}_2$ 在空間上之分佈非常地均勻。然而，表層海水之 $p\text{CO}_2$ 與溫度、生物作用以及海水垂直運動的狀況密切相關，而這些因子在全球海域中的分佈，有極顯著的差異，導致全球表層海水之 $p\text{CO}_2$ 存有相當大的變異（ ~ 150 至 $\sim 750 \mu\text{atm}$; Feely et al., 2001）。因此， $\Delta p\text{CO}_2$ 空間上之分佈特徵，主要是受控於海水 $p\text{CO}_2$ 的分佈型態。故欲瞭解“物理幫浦”在全球海洋之空間分佈，首先必須瞭解 $p\text{CO}_2$ 的在全球海域之分佈型態。

迄今，有關於 $p\text{CO}_2$ 在全球海域之分佈情形最完整的研究，當屬 Takahashi et al. 所發表之一系列論文（Takahashi et al., 1993, 1997, 2002）。其中在 2002 年的研究中，作者匯整了西元 1956 至 2001 年間全球海洋表水 $p\text{CO}_2$ 的分析數據（總計約 940,000 筆），繪製出二月及八月時全球海洋表水 $p\text{CO}_2$ 的分佈圖（圖 1.6）。

由圖中可看出： $p\text{CO}_2$ 的最低值主要出現在南、北半球夏季時的高緯地區：二月時的南大洋（Southern Ocean；圖 1.6 上）及八月時北大西洋的高緯地區（圖 1.6 下）。此 $p\text{CO}_2$ 最低值，一般認為與高緯度海域夏季時旺盛的生物生產作用，大量消耗海水中溶解之二氧化碳有關。 $p\text{CO}_2$ 的次低值主要分佈在南、北兩半球冬季時中緯度的海域。此 $p\text{CO}_2$ 之次低值，主要是由冬季降溫效應所引起。 $p\text{CO}_2$

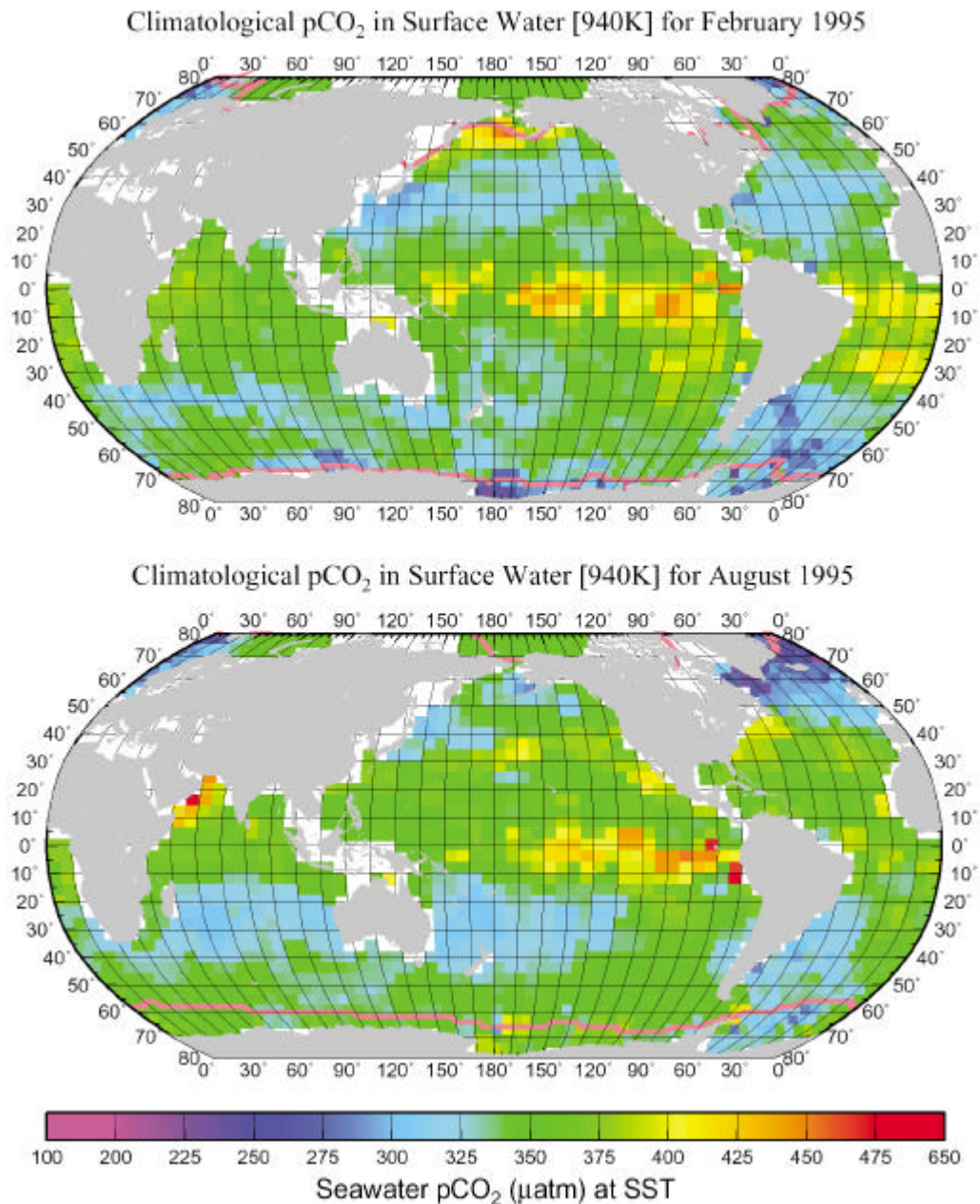


圖 1.6 全球海域表水之二氧化碳分壓($p\text{CO}_2$)在二月及八月時之分佈圖。以 1995 年為參考基準年。摘自 Takahashi et al. (2002)。

的最高值終年出現在東赤道太平洋；而北半球冬季時，西北太平洋副極區，亦有 $p\text{CO}_2$ 的高值出現；此外，北半球夏季時，阿拉伯海亦會出現 $p\text{CO}_2$ 的高值。這些高值皆與海水垂直運動較強有關（湧升或是強烈的垂直混合）。

二氧化碳之海氣交換通量，可以下列方程式計算之：

$$F = K \times \Delta p\text{CO}_2 \dots\dots\dots \text{Eq. 1.1}$$

上式中“F”為二氧化碳之海氣交換通量(Flux)；“K”為二氧化碳交換係數 (CO_2 exchange coefficient)，可由風速資料計算得出；“ $\Delta p\text{CO}_2$ ”為表層海水與大氣之二氧化碳分壓差。 $\Delta p\text{CO}_2$ 之正負控制了二氧化碳海氣交換的方向。當 $\Delta p\text{CO}_2 > 0$ 時，海水中二氧化碳氣體呈過飽和狀態，二氧化碳會由海水向大氣釋放，造成大氣二氧化碳濃度升高，此種海域被稱之為大氣二氧化碳的“源”（source）。反之，若 $\Delta p\text{CO}_2 < 0$ ，海水中二氧化碳氣體呈未飽和狀態，大氣中之二氧化碳會進入海水中，故會使大氣二氧化碳濃度減少，此種海域謂之“匯”（sink）。Takahashi et al. 在 2002 年所發表的文獻中，利用上述全球海域表水 $p\text{CO}_2$ 之分析結果和美國國家環境預測中心（NCEP）全球平均風場之資料，以及美國國家海洋大氣總署（NOAA）所收集大氣 $p\text{CO}_2$ 的數據，估算了每年二氧化碳海氣交換淨通量在全球海域的分佈情況（圖 1.7）。由圖中可清楚的看出，南、北半球之中、高緯度海

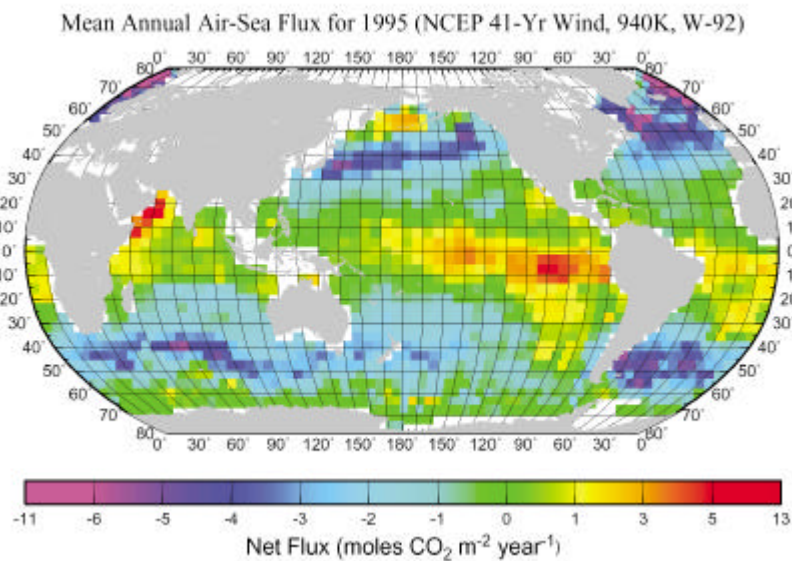


圖 1.7 二氧化碳海氣交換淨通量在全球海域之分佈圖。
摘自 Takahashi et al. (2002)。

域(40°N-60°N 和 40°S-60°S), 是主要“sink”之所在。東赤道太平洋及阿拉伯海的西北海域則是最重要的“source”。此外, 大西洋及印度洋之近赤道海域和西北太平洋的副極區, 亦是明顯“source”之所在。而全球海域所累計海氣二氧化碳之淨交換通量約為每年 2.2 ± 0.2 Gt C。換言之, 透過“物理幫浦”的作用, 全球海洋每年對人為二氧化碳的吸收量約為 2.2 ± 0.2 Gt C。

(2) 人為二氧化碳在全球海域之分佈概況

大氣中之二氧化碳透過海氣交換作用進入表層海水後, 如何透過大規模的海洋環流向深海輸送儲存, 以及究竟有多少人為二氧化碳(指因大氣 $p\text{CO}_2$ 增高, 造成海水中 TCO_2 對應之增加量) 可以透過“物理幫浦”的作用被儲存在全球的海水中? 亦為瞭解海洋“物理幫浦”之運作的研究重點之一。此部分的研究, 傳統上是藉助海水中碳化學參數的研究分析來進行。Feely et al. (2001) 匯整 JGOFS/WOCE 計畫中所收集之碳化學數據, 以 ΔC^* 法 (Gruber, 1996) 計算了三大洋中人為二氧化碳的含量, 完整地描繪出人為二氧化碳在全球海域的分佈特徵 (圖 1.8)。由圖中可清楚看出, 在三大洋中, 都以表水有最高的人為二氧化碳含量, 約介於 40 至 $60 \mu\text{mol kg}^{-1}$ 之間, 此乃因表水可透過海氣交換作用, 持續接受到大氣中人為二氧化碳之影響所致。而隨深度的增加, 海水中人為二氧化碳的濃度逐漸減少, 這是由於愈深之海水, 其出露海平面可進行海氣交換的年代, 距今愈久遠, 因此其受人為二氧化碳的影響程度愈小。同時, 由圖中亦可發現, 人為二氧化碳穿透較深的地方, 亦是深層水形成的區域。例如, 全球人為二氧化碳穿透最深的地方是北大西洋高緯度海域 (其穿透深度可達 4000 公尺), 正是北大西洋深層水 (NADW) 生成的位置。此外, 中層水形成的區域 (南緯 40° - 50°), 人為二氧化碳亦有較大之穿透深度。而人為二氧化碳穿透深度最淺的區域, 則是有強烈湧升作用發生的區域。例如, 赤道太平洋海域。此種緊密的相關性表明, “物理幫浦”在海洋中的運作, 主要是受海洋環流模式所控制。而三大洋深層水中

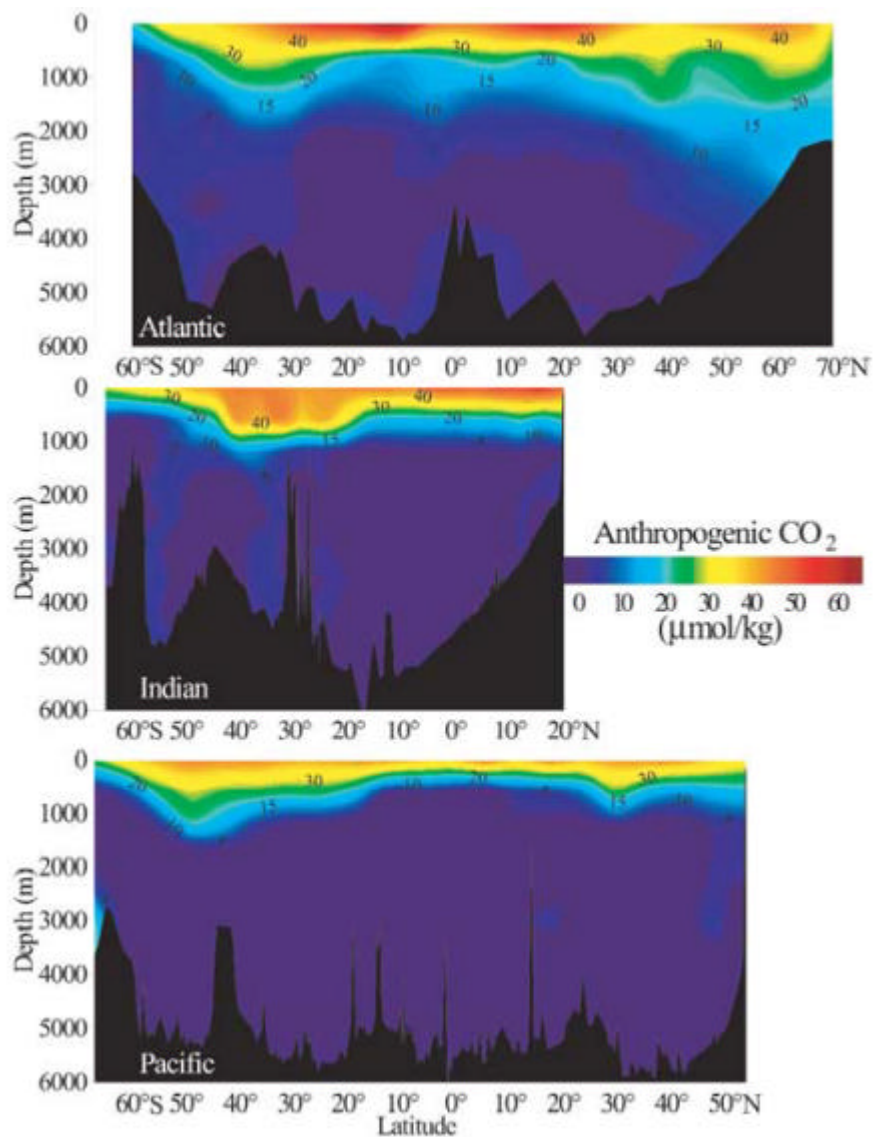


圖 1.8 人為二氧化碳在大西洋（上）、印度洋（中）和太平洋（下）之分佈圖。

摘自 Feely et al. (2001)。

僅大西洋出現了人為二氧化碳的訊號，亦與全球深層水輸送帶模式（conveyor belt）所預期之結果相符，進一步驗證了人為二氧化碳藉由海氣交換作用進入表層海水後，再經由溫鹽環流向深海傳送儲存的作用模式。三大洋累計人為二氧化碳之總儲量約為 $105 \pm 8 \text{ Gt C}$ ，此一結果與模式之計算結果大致相符。這些研究成果不僅大幅增進了我們對“物理幫浦”運作機制的瞭解，也首次以實測資料為基礎，估算了人為二氧化碳在海洋中的總儲量。

1.3 東南亞時間序列研究之緣起與目的

海洋時間序列研究，是 JGOFS 所規劃的四大研究主軸之一，亦是本論文所欲探究之重點所在，故以下將簡要說明“東南亞時間序列研究”之緣起及其研究目的。

海洋時間序列研究之主要目的乃在於探究海洋碳循環在不同時間尺度下，自然背景之變化及其控制機制。因為唯有清楚瞭解自然背景的變化，方能將人為活動所引起海洋碳循環的改變與自然變化之背景值加以區辨，進而評估海洋對人為二氧化碳的吸收能力，以及此種能力在人為活動持續影響下，所可能發生的改變，及其對氣候系統所可能產生的回饋效應。

由於全球海域分佈極其遼闊，不同海域的外在作用營力（如氣溫、風場及流場 .. 等等），在時空的變化上都存在著顯著的差異。因此，不難預期在不同海域，碳的生地化循環可能存在著截然不同的運作模式，且其時序變化的形態亦可能迥然不同。為了增進對全球海域碳循環隨時序變化的瞭解，在世界各國通力合作下，JGOFS 建構了一個由八個時間序列測站所組成的全球海洋時間序列觀測網，這八個時間序列測站分佈在不同海域，各有其代表性（圖1.9；Karl et al., 2003）。而其中唯一一個位於低緯度邊緣海域的測站：東南亞時間序列觀測站

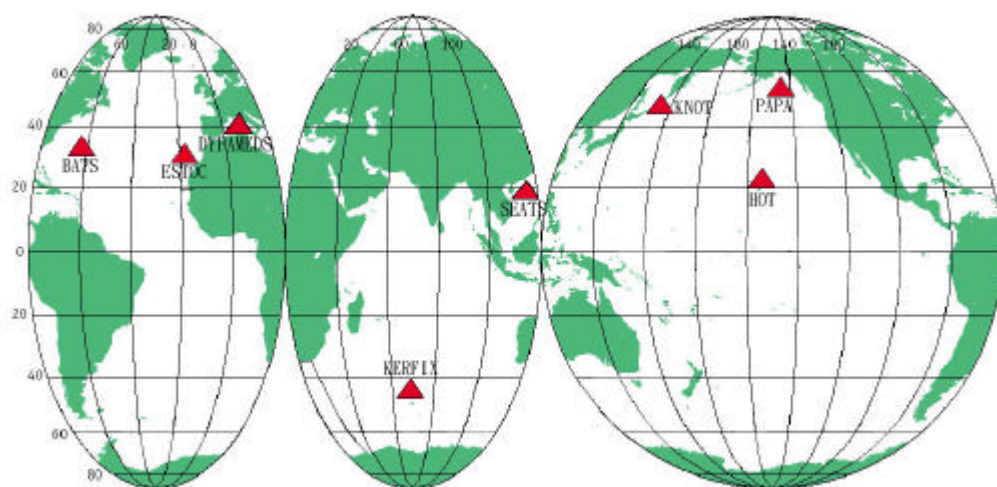


圖1.9 JGOFS海洋時間序列測站分佈圖。改繪自Baliño et al. (2001)。

(South East Asia Time-series Study , 簡稱SEATS) , 位於南海北部 , 是由我國負責其運作。SEATS計畫的緣起 , 是基於身為地球村一員的我們 , 對地球生命體永續發展的關心與體認 , 以及配合政府對海洋事務日漸增加的關懷與重視 , 在國科會的資助下 , 自1998年起由國家海洋科學研究中心 (海科中心) 開始負責執行的一項整合性研究計畫。其具體之研究目標為(Shiah et al., 1999; Karl et al., 2003):

- (1) 瞭解季風交替對南海生地化循環之影響 , 以及ENSO事件所造成季風強度改變時 , 生地化過程所伴隨發生的變化。
- (2) 探討偶發事件 , 例如颱風、中尺度渦漩等 , 對南海生地化循環之影響。
- (3) 利用對現今生地化過程的認識與瞭解 , 嘗試建立保存於沉積物岩心中 , 過去南海生地化過程演變與氣候變遷之相關性。

SEATS計畫深受國際海洋學界所重視 , 除因其為唯一一個位於低緯度邊緣海域的時間序列測站 (其餘之測站大多位於中、高緯度之開放性大洋) , 故適可彌補全球海洋時間序列觀測網中 , 在近熱帶貧營養鹽海域觀測資料不足的缺憾外 , 南海環境的獨特性亦使其明顯有別於其它的時間序列測站 , 其特色保括 : 明顯的季風變化 , 高頻率的颱風經過 , 較淺的混合層等 , 故大氣幫浦效應極可能是混合層中營養鹽循環和相關生地化過程變化主要的驅動力。此外 , 南海也是世界上承受大氣沙塵沉降通量最大的邊緣海之一 (Duce et al., 1991) , 因此對於 “ 鐵假說 ” 的驗證 , 提供了一個絕佳天然試驗場。

1.4 研究區域之背景介紹

1.4.1 南海的地理型態

南海是西北太平洋邊緣海之一，南起卡里馬塔島北岸，以及卡里馬塔島和蘇門答臘島之間的隆起地帶（約南緯 3°）；北以台灣島南端與廣東南澳島的連線與兩廣沿岸為界（約北緯 22°）；西接中南半島及馬來半島東岸（約東經 105°）；東以台灣、呂宋島至巴拉望島的連線為界（約東經 120°），總面積約為 3.5×10^6 平方公里，為世界面積最大之邊緣海。由於四周島陸為鄰，使南海成為一半封閉性的海域，僅藉由各海峽與鄰近海域相通。北有台灣海峽與東海相連；東有巴士、巴林塘、巴布延、明多羅及巴拉巴克等海峽與太平洋與蘇祿海相接；南有卡斯帕、卡里馬塔等海峽通往爪哇海。但這些海峽多半很淺，唯有東北部的巴士海峽，入口深度可達 2200 公尺，寬度達 380 公里，是南海與太平洋海水交換的主要通道（陳，2001）。

南海的外型為呈東北 - 西南走向之尖菱形。其海底地形複雜多樣，平均深度約為 1350m，最深可達 5,567m。主要的地貌單元包括大陸棚、大陸坡、中央盆地以及海盆東部邊緣的海槽、海溝等類型（圖 1.10）。其北、西、南三面是大陸地殼的延伸，自大陸棚到大陸斜坡的底部，是一片廣闊被海水淹沒的亞洲大陸邊緣地區。而南海中央盆地卻有著典型的海洋地殼，其中的深海平原和星棋羅佈的海底火山群，與大洋之深洋盆地地形特徵非常相似。分佈在南海東部的島弧 - 海溝交錯的地形特徵，屬太平洋海板塊隱沒系統的一環，是整個西北太平洋地區共同的構造特徵。綜而觀之，南海北、西、南方的海底是屬於海水淹沒的大陸地形區；而中部及東部的海底，屬大洋型的地形區。這兩類地形區的組合，構成了南海海底地形的基本架構（陳，2001）。

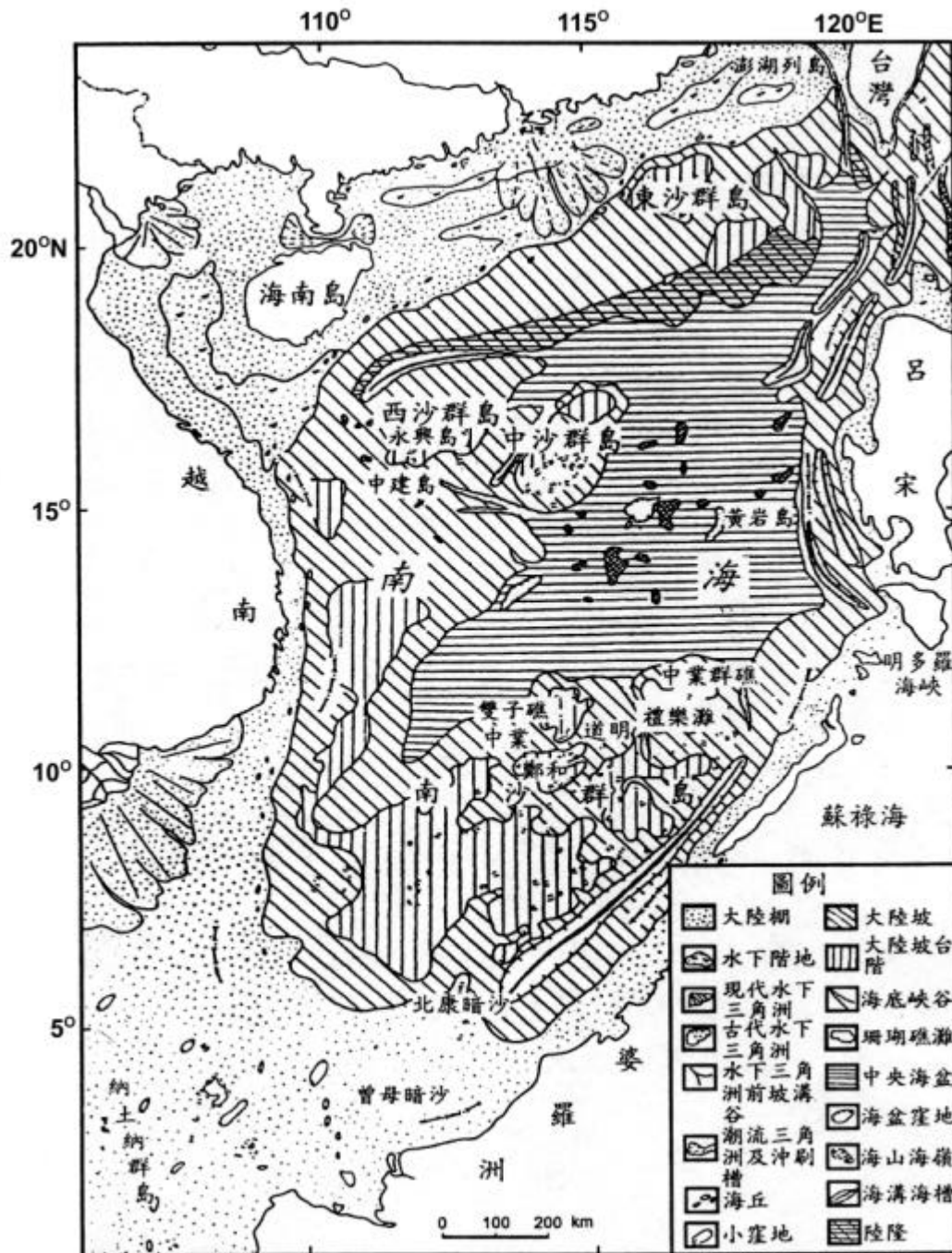


圖 1.10 南海海底地貌圖。摘自陳 (2001)。

1.4.2 南海的氣候概況

南海位於亞洲季風區內，冬季時，大陸冷高壓由北向南流向海洋，但因受地球自轉偏向力的影響，此氣流偏向西，形成東北季風；夏季時則正好相反，形成西南季風。東北季風盛行於 11 月至 3 月，而西南季風盛行於 6 月至 8 月，4 月至 5 月及 9 月至 10 月則為季風切換的時期（圖 1.11；Liang et al., 2000）。東北季風的平均風速約為 9 m/sec，明顯較西南季風時之 6 m/sec 為強（Hu et al., 2000）。東北季風強度之年際變化被認為與 South Oscillation Index (SOI) 有關：當 SOI 較高時 (La niña 年)，會出現較強的東北季風；反之，SOI 較低時 (El Niño 年)，東北季風則會減弱 (Zhang et al., 1997)。

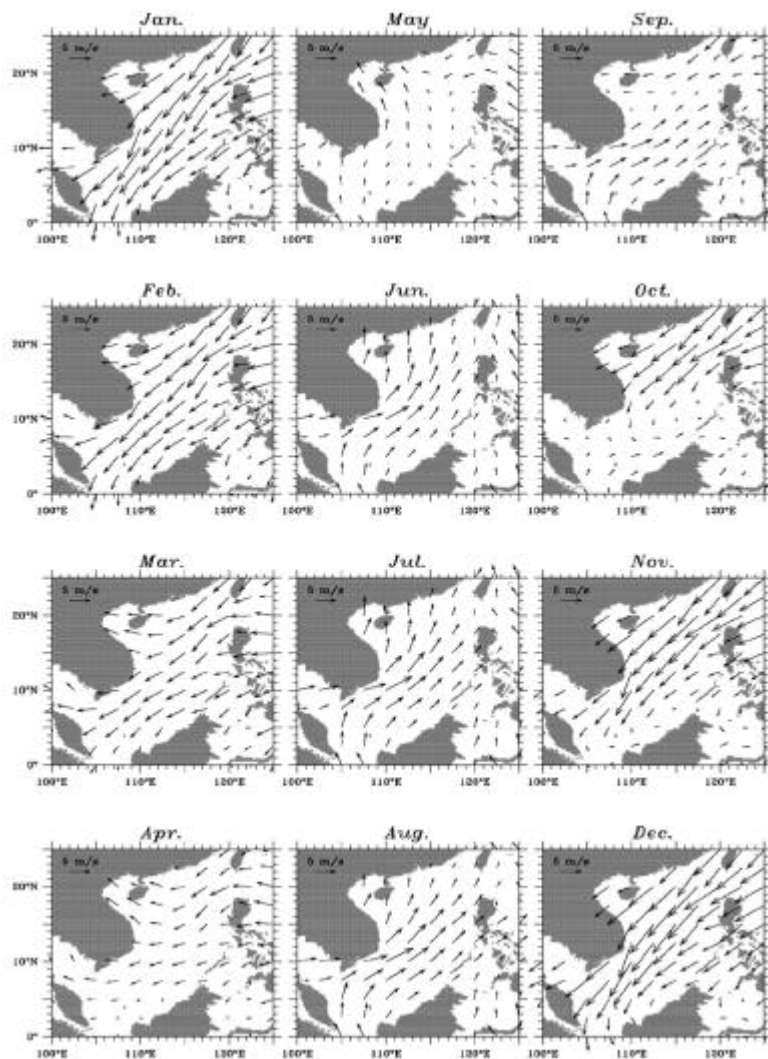


圖 1.11 南海季風風速和風向月平均變化圖。摘自 Liang et al. (2000)。

南海表水溫度之分佈特徵，呈現明顯的季節性變化。冬季時，表水之溫度梯度最大，且等溫線成東北 - 西南走向。以 1 月為例，表水溫度可由海盆南方的 27°C 向北遞減至 21°C，南北溫差可達 6°C (圖 1.12)。而夏季時，整個南海海域表水溫度分佈非常均勻，幾乎沒有溫度梯度的存在，由北到南，表水溫度都維持在 29°C 左右 (Liang et al., 2000)。表水溫度之年際變動，可能亦與

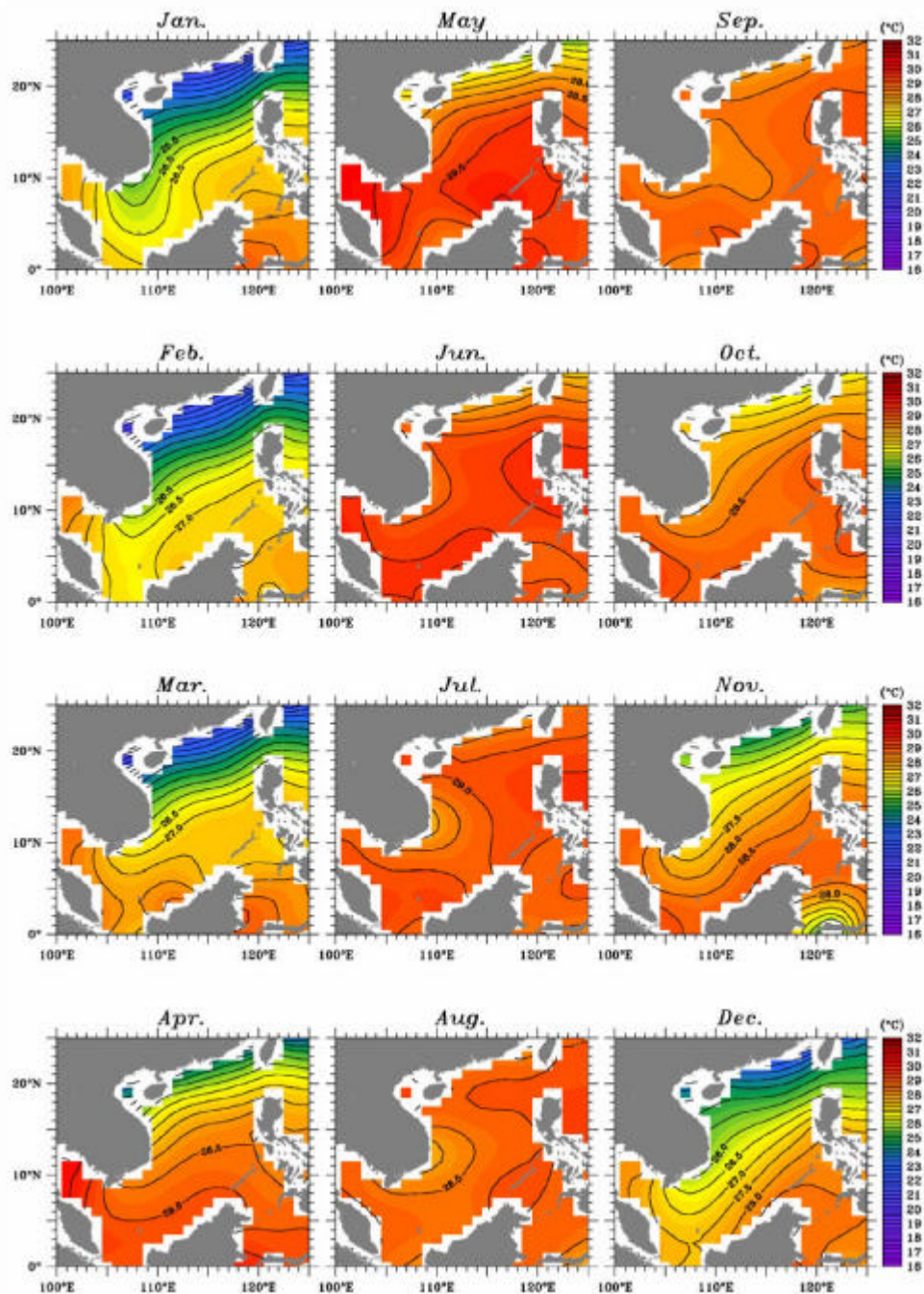


圖 1.12 南海表層海水水溫月平均變化圖。摘自 Liang (2000)。

ENSO 事件有關。在 ENSO 年時，由於冬季季風減弱，造成南海整體之湧升速率減緩，故會有較高的表水溫度 (Chao et al., 1996)。而南海夏季時表水溫度的異常，與前一年冬季時赤道海域之溫度異常有良好的相關性。因此，南海表水溫度的異常可作為季風變異及 ENSO 事件的指標 (Ose et al. 1997)。

1.4.3 南海的環流概況

由於南海位於季風盛行帶上，且其海盆成東北 - 西南走向，長軸方向與盛行風向一致，因此其表面環流形態，主要受季風控制。在東北季風時期，由於強風區位於菱形海盆縱軸略微偏西的位置上，故南海西部形成強大的漂流；而東部海區的風力相對較弱，有利於形成一北上的逆流，該逆流具有補償流的性質，可對南海北部海區進行部分水量的補償。而此西部漂流及東部逆流即構成了冬季時涵蓋整個南海的氣旋式環流系統 (圖 1.13(a); Shaw and Chao, 1994; Hu et al., 2000)。在這整個大環流系統內，南海的東北及西南海域，分別存在二個中尺度氣旋式的渦流 (eddy)。東北部的渦流位於呂宋島的西側，其主要是由於風力及地形效應所造成；西南部的渦流位於中南半島東南外海，其主要是因為西部漂流所輸送相對低溫的海水在此堆積的結果。在西南季風時期，南海的表層環流與冬季的流場大致相反 (圖 1.13 (b))。唯其並未在整個南海形成一大規模的反氣旋式的環流系統。在南海北部，東北向的海流佔絕對的優勢，西南向的逆流僅出現在南部的海域。故此時期，反氣旋的環流系統僅出現在南海南部的海域。另一方面，與東北季風時期相似地，此時期在盤據南海南部的反氣旋環流系統中，亦存在有二個中尺度的渦流。其中位於中南半島東南方的渦流為一反氣旋式的渦流，其形成原因與由巽他陸棚和暹羅灣輸送來之高溫、低鹽水在此幅聚有關。另一渦流位於越南外海，為一氣旋式渦流，其形成原因與離岸風造成之湧升現象所產生的冷渦有關。此外，在南海北部海域，除季風風向外，黑潮的入侵亦對此海域之流場變化有顯著的影響。冬季時，受東北季風影響，黑潮會入侵南海，形成一南海黑

潮分支；夏季時，黑潮則間歇性的入侵南海，且多以套流的形式出現（Wang and Chern, 1987; Shaw, 1991）。另外，在廣東外海水深較深處，終年存在一股由海南島流向台灣海峽的暖流，稱為南海暖流。其流向相當穩定，始終保持東北向，但其流速、流軸和流幅則有相當程度的時空變化。到目前為止，對於南海暖流形成的機制，尚無定論。不過一般認為，應與黑潮入侵、風應力及海面高度差等因素有關（Hu et al., 2000）。

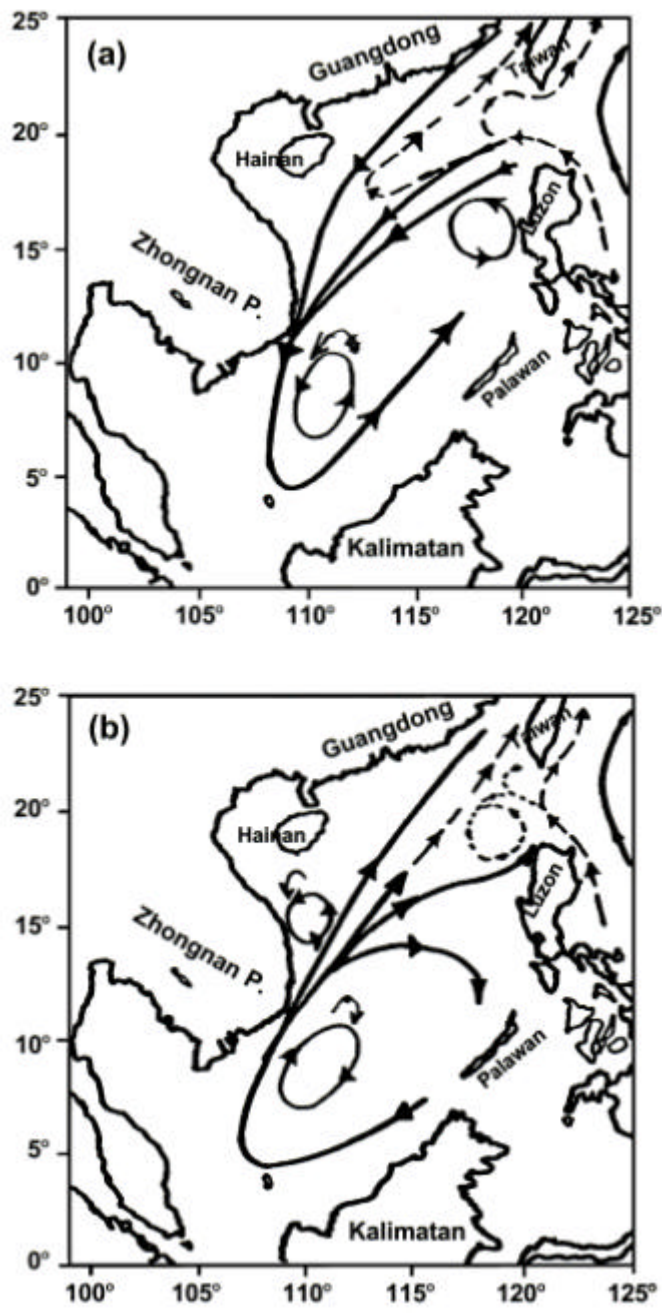


圖 1.13 南海之表面環流系統 (a) 冬季 ,(b) 夏季。改繪自 Hu et al. (2000)。

1.4.4 南海之水文特性

地理的格局及內部強烈的湧升和垂直混合作用是影響南海水文特性最重要的因素。由於南海為一半封閉性的海盆，故其上層海水之水文特性會受到陸源淡水注入及每年近 2,000mm 降雨的影響，其中最顯著的特徵，即為南海表水的鹽度明顯較相鄰之西菲律賓海為低（圖 1.14）。再者，雖然南海四周有為數眾多的海峽與周遭的海域相連，但唯有東北部之巴士海峽夠深且夠寬，可做為南海水與外洋水交換的主要通道。因此，南海表層以下海水之水文特性，深受西菲律賓海海水的影響。例如，西菲律賓海次表層鹽度極大值及中層鹽度極小值的訊號，在南海中亦可觀察到。不過由於南海垂直混合及湧升作用強盛，致使鹽度極值的強度明顯減弱（極大值變小而極小值變大，圖 1.14）。且其極大、極小值出現的深度，都有抬升的現象（Chen and Huang, 1996）。此外，垂直混合及湧升作用，亦造成了南海的次表層水（100-600m）較西菲律賓海同層的水為冷，且其營養鹽、表觀耗氧量（AOU）、pH 值、總二氧化碳及總鹼度的含量均較同一溫度之西菲律賓海水為高的現象（Gong et al., 1992; 王, 1997; Chen and Wang, 1998）。至於南海的深層及底層水，因受巴士海峽海檻深度的限制，其來源均為西菲律賓海 2,200m 左右的海水。故其水文性質非常均勻，幾乎沒有任何的變化，且與西菲律賓海 2,200m 附近水體之水文特性幾乎完全一致。

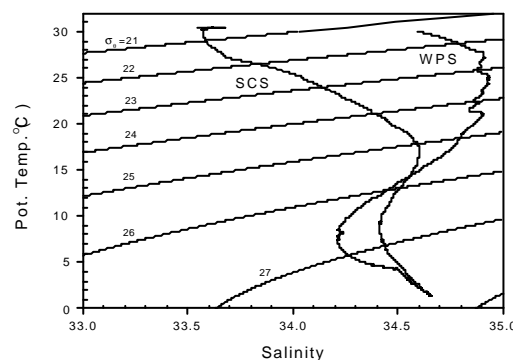


圖 1.14 南海及西菲律賓海之溫鹽圖。南海和西菲律賓海海水之溫鹽資料分別以 ORIII-794 航次 KK1 測站（18°15' N, 115°40' E）與 ORI-650 航次 K5 測站（19° N, 123° E）的溫鹽資料代表之。

1.5 論文目標

碳在海水中可以四種型態存在，分別為顆粒態有機碳、無機碳和溶解態有機碳、無機碳。這其中以溶解態無機碳之含量（total carbon dioxide, TCO_2 ）為最高，其濃度較溶解態有機碳濃度高出 20 倍以上，更遠較顆粒態有機碳、無機碳高出數百倍。因此， TCO_2 可說是瞭解海水碳化學系統最基本的參數。根據熱力學的方法，藉由下列四項參數：pH、 TCO_2 、總滴定鹼度（TA）及二氧化碳分壓（ $f\text{CO}_2$ ），任兩個參數的測量，海水的碳酸鹽系統即可被完整的描述。由於，TA 和 TCO_2 皆具有不隨溫度及壓力改變的特性（Dyrssen and Sillé, 1967），且由其計算所得到之 $f\text{CO}_2$ 與實測結果最為相符（在 $500\mu\text{atm}$ 以內，其偏差僅為 $0.07\pm 0.50\%$ ；Lueker et al., 2000）。故 TA 是除 TCO_2 外，研究海水碳酸鹽系統另一最常被測量的參數。因此，以探討碳通量時序變化為宗旨的海洋時間序列研究計畫，莫不將 TA 和 TCO_2 列為核心的量測項目（core measurements），以求對海水之二氧化碳系統有完整之掌握。大氣二氧化碳濃度持續的增加，透過海氣交換作用的進行，勢必對海水之二氧化碳系統產生衝擊，進而造成碳循環的改變（Riebesell et al., 2000; Zondervan et al., 2001）。因此，對現今海水之二氧化碳系統的瞭解，可說是海洋時間序列研究中最基本的研究課題。故本論文的研究目標之一，就是要探討 TA 及 TCO_2 在 SEATS 測站垂直分佈的特徵，並解析控制其垂直變化的各項生地化因子，以作為日後探討在人為活動影響下，南海碳化學系統所可能發生之變化時的對比依據。

誠如 1-3 節所言，SEATS 是世界海洋時間序列觀測網中，唯一位於低緯度邊緣海域的測站，且南海具有季風交替及大氣沉降鐵通量高等環境特性。而 1.4.4 節亦指出南海之水文特性深受內部湧升作用之影響。前人的研究已指出，由於深水的湧升使南海營養鹽躍層（nutricline）的深度較相鄰的西菲律賓海抬升了 100m 左右（Gong et al., 1992）。而營養鹽躍層的淺化，極可能是南海之葉綠素濃度較西菲律賓海高出一倍之多的原因（Liu et al., 2002）。而較淺的硝酸鹽躍層

(nitracline), 則是南海 *Trichodesmium* 密度較黑潮流域為低的控制因素之一 (Chen et al., 2003)。 Liu et al. (2002) 根據三維物理-生地化耦合模式的研究結果發現, 南海之基礎生產力呈現夏低冬高明顯之季節性變化, 此變化與季風引起湧升狀況的改變有關。 Wong et al. (2002) 亦由上部營養鹽躍層中硝酸鹽異常值 (nitrate anomaly; Gruber and Sarmiento, 1997; Deutsch et al., 2001) 的季節變化, 推論 SEATS 測站上層水體中固氮作用的強弱, 可能受季風切換所造成大氣沉降鐵通量的變化所控制。凡此種種皆說明南海獨特的環境特徵, 使得 SEATS 測站生地化作用之季節變化, 可能明顯有別於其它的時間序列測站。而碳化學參數可說是所有生地化研究中不可或缺的項目之一, 然而到目前為止, 有關於碳化學參數在南海季節變化之研究卻付之闕如。因此, 本論文之另一研究目標為: 瞭解 SEATS 測站混合層中碳化學參數 (TA, TCO₂, fCO₂) 季節變化的情形, 並探討其可能之控制機制, 進而去估算二氧化碳海氣交換通量的季節變化, 以釐清就年的時間尺度而言, SEATS 究竟是大氣二氧化碳的“sink”亦或是“source”? 並將其與其它時間序列測站的研究結果加以比對, 以瞭解在湧升、季風和高鐵沉降通量等因素的影響下, 南海碳循環之季節變化是否有別於其它緯度相近之貧營鹽海域?

此外, 傳統上以實測資料來探討人為二氧化碳在海洋中分佈的方法, 幾乎都以碳化學資料為基礎。然而, 近年來的研究已指出, $\delta^{13}\text{C}_{\text{TCO}_2}$ 是除了碳化學參數外, 另一良好之示蹤劑 (tracer), 可用來追蹤人為二氧化碳在海水中的分佈情形 (Quay et al., 2003)。其應用之基本原理乃在於: 化石燃料及植物之 $\delta^{13}\text{C}$, 遠較大氣中二氧化碳之 $\delta^{13}\text{C}$ 為輕, 因此隨著人類大量使用化石燃料及對森林的墾伐, 人為活動所釋放之二氧化碳不斷的累積在大氣中, 使大氣之 $\delta^{13}\text{C}$ 亦逐年變輕 (Friedli et al., 1986)。而透過海氣交換作用的進行, 這些同位素組成較輕的二氧化碳會進入海水中, 使得海水之 $\delta^{13}\text{C}_{\text{TCO}_2}$ 亦不斷遞減, 故藉由海水 $\delta^{13}\text{C}_{\text{TCO}_2}$ 的研究, 亦能得知人為二氧化碳在海洋中分佈的訊息。不過與碳化學資料相較而言, $\delta^{13}\text{C}_{\text{TCO}_2}$ 在海水中的實測資料可說是少之又少。而碳化學與 $\delta^{13}\text{C}_{\text{TCO}_2}$ 同步量測的資料又更為稀少, 更遑論同時以此兩類不同之方法, 來探究人為二氧化碳在海洋

中的分佈。故本研究與碳化學資料同步量測了 SEATS 測站之 $\delta^{13}\text{C}_{\text{TCO}_2}$ ，進而分別以碳化學及 $\delta^{13}\text{C}_{\text{TCO}_2}$ 的資料，來探討人為二氧化碳在 SEATS 測站的穿透情形。如此，不僅可提供除碳化學以外另一獨立之方法，來探究人為二氧化碳在南海垂直分佈的情形。同時亦能得出在人為二氧化碳影響下，海水中 TCO_2 增加量(ΔTCO_2)與 $\delta^{13}\text{C}_{\text{TCO}_2}$ 減輕量($\Delta\delta^{13}\text{C}_{\text{TCO}_2}$)之相對比值。近年來，根據模式的研究指出，海水中 $\Delta\text{TCO}_2/\Delta\delta^{13}\text{C}_{\text{TCO}_2}$ 的比值可應用於陸地生物圈與大氣二氧化碳可交換碳總儲量的估算上（在全球碳循環的研究中，這個量幾乎無法以實測的方法來求得；Körtzinger et al., 2003）然而到目前為止， $\Delta\text{TCO}_2/\Delta\delta^{13}\text{C}_{\text{TCO}_2}$ 比值在海洋中之實測資料嚴重不足，使其在全球碳循環研究上的應用深受限制。故本論文亦嘗試對南海之 $\Delta\text{TCO}_2/\Delta\delta^{13}\text{C}_{\text{TCO}_2}$ 比值做出估計，以期對瞭解此比值在全球海洋之分佈情況能有所貢獻。

二、研究方法

2.1 研究材料

本論文之研究主題，屬SEATS計畫中的一環。因此，本研究分析 TCO_2 、TA及 $\delta^{13}\text{C}_{\text{TCO}_2}$ 所需之水樣，皆與SEATS計畫中用以測定其它化學水文參數之水樣同步採集。SEATS計畫之水文及生地化參數觀測站（KK1站），位於南海海盆北部（ $18^\circ 15' \text{N}$, $115^\circ 40' \text{E}$ ；圖2.1），水深約為3770公尺。而本文所討論之數據，是由2002年3月至2003年8月間八個SEATS探測航次所取得。各航次之編號、探測日期

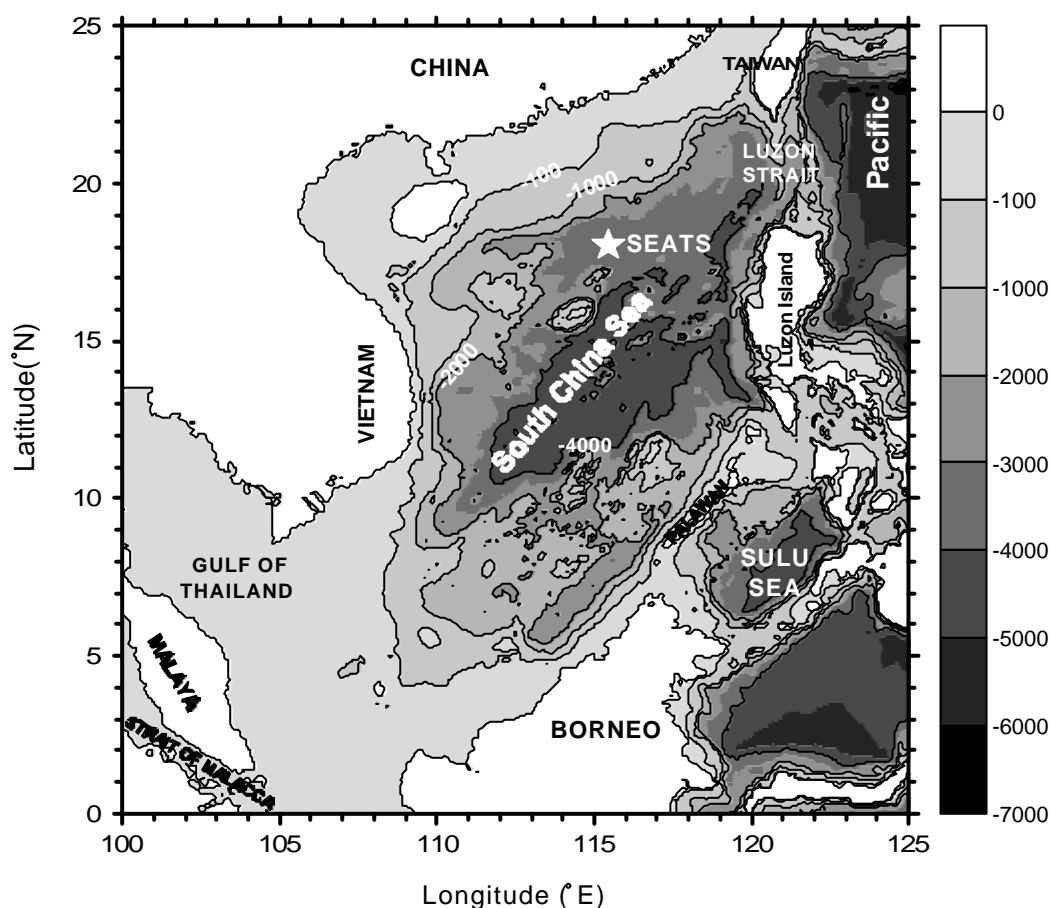


圖2.1 南海之水深等深線及SEATS測站之位置圖。

及採樣深度如表2.1所示。其中ORIII-859航次（2003年4月）為錨定航次，故僅有本實驗室所分析水深150m以內之 TCO_2 、TA及 $\delta^{13}\text{C}_{\text{TCO}_2}$ 的數據。其餘各航次皆為水文暨生地化調查航次，故有完整之化學水文數據的分析以及由淺至深完整之垂

直剖面的採樣。各航次之溫、鹽資料係經由海研一號及三號上SBE 9/11 plus型 (Sea-Bird Electronics Inc.) 溫鹽深儀所取得。溶氧 (DO)、磷酸鹽 (PO_4^{3-}) 及硝酸鹽 (NO_3^-) 的資料, 由台大海科中心所提供。DO之測定方法為希巴辣光度測氧法 (Pai et al., 1993; 白等, 1998), PO_4^{3-} 和 NO_3^- 則是以Trident-223三同步營養鹽測定系統所測定(白和郭, 1995), 其分析之基本原理皆為比色法 (Pai et al., 1990; Pai et al., 1994)。 TCO_2 、TA及 $\delta^{13}\text{C}_{\text{TCO}_2}$ 的分析方法則將於下節中討論。

表 2.1 本研究所參與各航次之編號、探測日期及採樣深度表。

航次編號	探測日期	採水深度
ORI-639	03/19-04/02/2002	5, 10, 20, 40, 60, 80, 100, 125, 150, 200, 300, 350, 400, 500, 600, 700, 800, 900, 1000, 1200, 1400, 1600, 1800, 2000, 2200, 2400, 2600, 2800, 3000
ORIII-794	06/30-07/04/2002	5, 10, 20, 40, 60, 80, 100, 125, 150, 200, 250, 300, 400, 500, 600, 700, 800, 900, 1000, 1200, 1400, 1600, 1800, 2000, 2200, 2400, 2600, 2800
ORI-656	08/31-09/06/2002	5, 10, 20, 40, 60, 80, 100, 125, 150, 200, 300, 350, 400, 500, 600, 700, 800, 900, 1000, 1200, 1400, 1600, 1800, 2000, 2200, 2400, 2600, 2800, 3000
ORI-664	11/09-11/15/2002	5, 10, 20, 40, 60, 80, 100, 150, 200, 400, 350, 400, 600, 800, 1000, 1200, 1500, 2000, 2500, 3000
ORI-673	01/17-01/23/2003	5, 10, 20, 40, 50, 60, 80, 100, 125, 150, 200, 250, 300, 400, 500, 600, 800, 900, 1000, 1200, 1400, 1500, 1600 1800, 2000, 2500, 3000
ORI-674	03/03-03/09/2003	5, 10, 20, 40, 50, 60, 80, 100, 150, 200, 400, 500, 600, 800, 1000, 1500, 2000, 2500, 3000
ORIII-859	04/10-04/14/2003	2, 5, 10, 20, 40, 60, 80, 100, 120, 150
ORI-690	08/05-08/10/2003	5, 10, 20, 40, 50, 60, 70, 80, 90, 100, 125, 150, 200, 300, 400, 500, 600, 700, 800, 900, 1000, 1200, 1500, 2000, 2500, 3000

2.2 實驗方法

2.2.1 海水滴定總鹼度 (TA) 之測定

本研究海水 TA 之分析是採用美國能源部 (DOE) 所訂定之海水二氧化碳系統參數分析手冊 (Handbook of methods for the analysis of the various parameters of the carbon dioxide system in sea water) 中所建議的電位滴定法來進行 (DOE, 1994)。其測量方法簡要說明如下：將一已知量的海水樣品置入一恆溫槽內 (25°C)，以一已知濃度的鹽酸滴定之。滴定過程中，隨時以由玻璃電極與參考電極所組成的 pH 計監測電位的變化。最後根據滴定液 (鹽酸) 消耗量與電位變化之關係，以非線性最小平方法 (non-linear least-squares approach) 來求取海水樣品之 TA (Dickson, 1981; DOE, 1994)。整個滴定系統由 pH 計 (Radiometer pH meter, pHM-85) 可維持恆溫之滴定槽、恆溫水槽及自動滴定儀 (Metrohm 665 Dosimat) 等四部份所組成。滴定用之鹽酸，採用 Merck 公司所生產的 0.1N 標準鹽酸，並加入超純氯化鈉來調整離子強度至 0.68 (與海水近似)，以防止滴定时濃度差異所造成的液體接合電位改變，影響了電位測量的正確性。

2.2.2 海水總二氧化碳 (TCO₂) 之測定

本研究 TCO₂ 之測定亦是採用 DOE 所訂定之海水二氧化碳系統參數分析手冊中所推薦之庫倫電量滴定法 (coulometric titration) 來進行。整個分析過程可概分為兩大步驟：TCO₂ 之萃取以及 TCO₂ 含量之測定。水樣中之 TCO₂ 是使用美國羅德島大學海洋系儀器發展實驗室所研發之 SOMMA 系統 (Single Operator Multiparameter Metabolic Analyzer) 來進行萃取。此系統主要由恆溫槽、定量管 (pipette) 及二氧化碳萃取槽 (stripper) 等三部分組成。首先將海水樣品置入恆溫槽內 (15 °C)，待溫度恆定後，利用空氣將水樣注入定量管內 (約 22 毫升)，接著將定量管內的海水送入二氧化碳萃取槽中，萃取槽底部附有細氣泡孔，當海

水進入後，與先前加入之 2 毫升 8.5 % 的磷酸混合，將海水酸化至酸鹼值小於 2 以下，使海水中碳酸根及碳酸氫根離子全部變為碳酸。此時高純氮氣通過底部氣泡孔所形成之小氣泡會攪動海水，將海水中的碳酸全數趕出。被趕出的二氧化碳氣體，經過水分萃取管路後，會進入“電流法二氧化碳分析儀”，開始進行二氧化碳含量的測定。

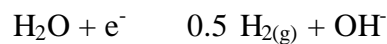
二氧化碳分析儀之主體是一個由光電比色管做終點判定的電解槽。其測定原理簡述如下：當二氧化碳進入電解槽陰極後，會與陰極溶液中所含之乙醇胺 (ethanolamine) 反應生成弱酸 (hydroxyethylcarbamic acid)：



此時，陰極溶液內的酸鹼指示劑 (thymolphthalein)，會由原先不含二氧化碳時的深藍色，變為淺藍或更淺的顏色。光電比色管根據顏色變化的幅度，於陽極(銀電極)釋出銀離子及電子：



而此時陰極會發生水電解反應：



此反應所生成之 OH⁻ 離子可用以平衡陰極溶液吸收二氧化碳後，酸鹼值所產生的改變。待陰極溶液回復到原來不含二氧化碳之深藍色時 (由光電比色管判定)，即為反應終點，最後再依法拉第電解定律將達到反應終點所消耗之總電流量，換算為二氧化碳的莫耳數。“電流法二氧化碳分析儀”並附有輸出串列，可將電量、時間等訊號傳至微電腦，經由軟體直接換算成我們所需的資料型式 (μmol kg⁻¹)。此種方法準確度極高，是目前國際上測定海水 TCO₂ 含量普遍使用的方式，亦是 JGOFS 所指定之標準分析方法。

2.2.3 海水總二氧化碳碳同位素組成 (δ¹³C_{TCO₂}) 之測定

海水 δ¹³C_{TCO₂} 之分析，分為 TCO₂ 萃取及同位素組成分析等兩大步驟。海水

樣品中之 TCO_2 ，是利用一套由真空幫浦及玻璃管件所組成的真空製備系統來進行萃取，其步驟簡述如下：將 2 毫升 85 % 的磷酸滴入反應瓶後，將反應瓶密封並在真空系統內抽為真空（低於 10^{-5} 大氣壓），再以針筒注入 40 毫升的水樣，使其與磷酸反應。此時水樣中碳酸根及碳酸氫根離子會全部轉變為碳酸，以磁攪拌子加以攪拌將海水中的碳酸全數趕出，並以液態氮收集被趕出之二氧化碳，再改以乾冰與酒精之混合液將先前與二氧化碳同時被收集之水氣加以固結。經過此一步驟所產生之二氧化碳必須再通過一乾冰與酒精之混合液所組成的水氣收集器，以確保無殘存的水分在氣體樣品中。最後再以液態氮將二氧化碳氣體固結於 6mm Pyrex 玻璃管中，然後用火焰將玻璃管封住。如此，海水中總溶解態的無機碳，即以氣態二氧化碳的形式被保存於玻璃管中，以待質譜儀進行同位素組成的分析。

二氧化碳氣體之 $\delta^{13}\text{C}$ 是以 VG OPTIMA 穩定同位素比值質譜儀來進行測定。而用以分析 $\delta^{13}\text{C}$ 與 $\delta^{18}\text{O}$ 之工作標準樣（working standard）的 $\delta^{13}\text{C}$ 與 $\delta^{18}\text{O}$ 對 NBS 19 的測值分別為 -3.65 % 及 -15.82 % (vs. PDB)。 $^{12}\text{C}^{17}\text{O}^{17}\text{O}$ 和 $^{13}\text{C}^{17}\text{O}^{16}\text{O}$ 離子的校正，則是根據 Craig (1957) 所提出之校正公式。測得之同位素比值以 per mil (‰) 表示：

$$\delta^{13}\text{C}_{\text{TCO}_2} (\text{‰}) = [(R_{\text{sample}} / R_{\text{standard}}) - 1] \times 1000$$

式中， R 為 $^{13}\text{C}/^{12}\text{C}$ 之值； R_{sample} 及 R_{standard} 分別代表樣品和實驗室所使用之工作標準樣。最後之分析結果以 PDB 國際標準碳酸鹽為比對標準來表示。

2.2.4 TA, TCO_2 和 $\delta^{13}\text{C}_{\text{TCO}_2}$ 分析準確度及精確度的評估

本研究進行期間，TA 及 TCO_2 的分析都會在每 20 個樣品中插入一個標準品（美國加州大學聖地牙哥分校 Scripps 海洋研究所 Dickson 教授所提供），以確保各航次之間的數據，並無系統性偏差的存在。根據這些標準品量測所累積之數據的統計分析結果顯示：TA 和 TCO_2 分析之精確度分別為 $\pm 2.4 \mu\text{mol kg}^{-1}$ ($\pm 1\sigma$ ，

n=15), $\pm 1.7 \mu\text{mol kg}^{-1}$ ($\pm 1\sigma$, n=12); 準確度則分別為0.11%及0.08%。每個標準品之測量值與標定值之差異如圖2.2所示。

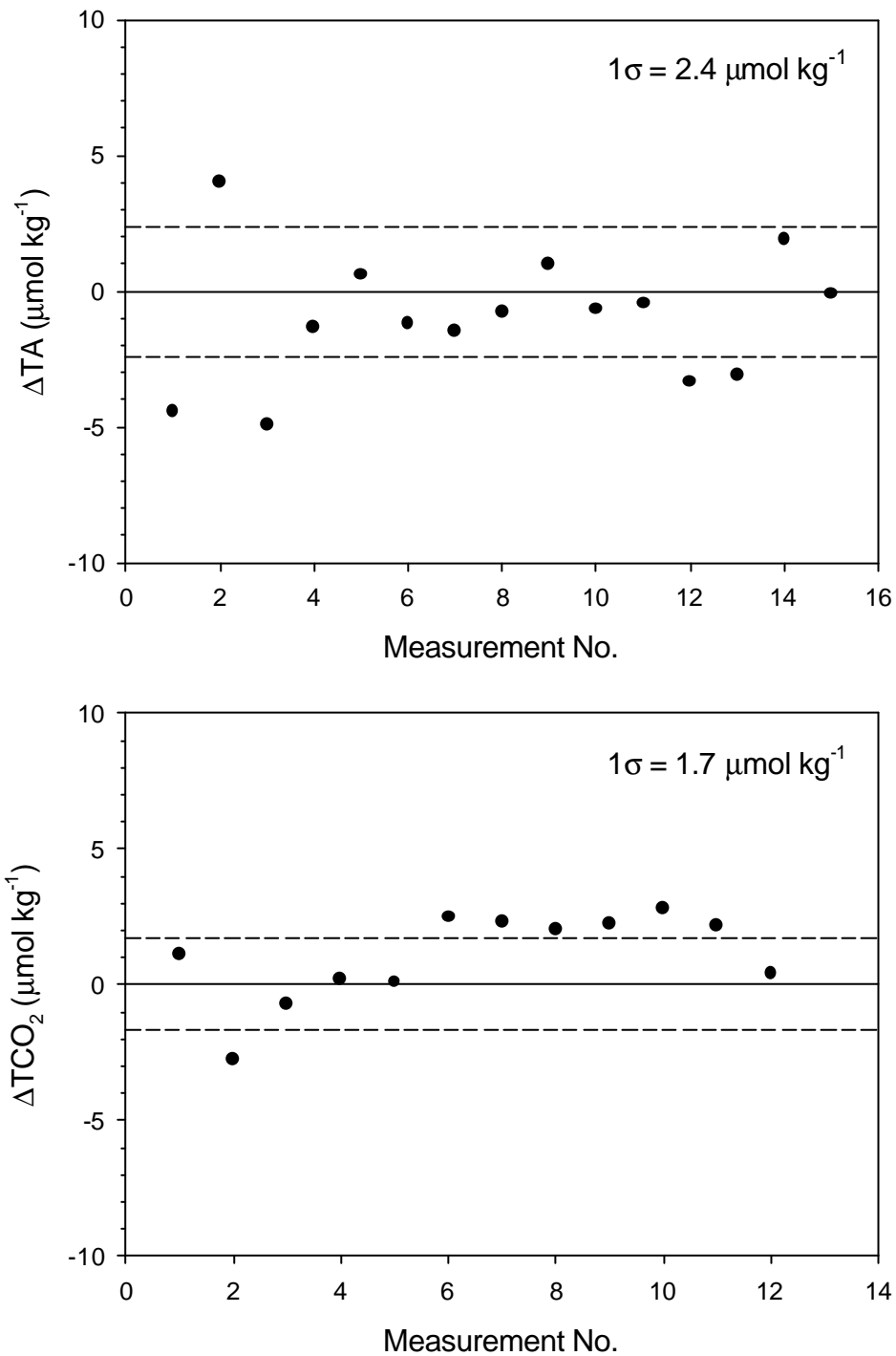


圖2.2 TA (上) 和TCO₂ (下) 標準品測量值與標定值之差異分佈圖。

海水 $\delta^{13}\text{C}_{\text{TCO}_2}$ 分析之精確度為 $\pm 0.06 \text{‰}$ ($\pm 1\sigma$, n=8), 此精確度是由重覆分析8次同一TCO₂標準品之 $\delta^{13}\text{C}_{\text{TCO}_2}$ 後所求得之結果 (表2.2) 由於到目前為止國際間

尚無可供海水 $\delta^{13}\text{C}_{\text{TCO}_2}$ 分析比對用之標準品，故準確度很難評估。為彌補此一缺憾，在本所林慧玲老師協助下，我們委請美國加州大學戴維斯分校Howard Spero教授實驗室與本實驗室同步分析了三個採自南海不同深度的水樣。結果顯示（表2.3），本實驗室之分析結果與Spero教授實驗室之結果相較而言，並無明顯偏輕或偏重的趨勢，代表兩實驗室間應無系統性誤差的存在。若加上精確度的考慮，則兩個實驗室的分析結果可說是極其接近。說明本實驗室 $\delta^{13}\text{C}_{\text{TCO}_2}$ 分析之準確度應與國際上之主流實驗室所得之結果相仿。

表2.2 TCO_2 標準品(Batch 56, Bottle No. 551)重覆分析8次 $\delta^{13}\text{C}_{\text{TCO}_2}$ 之結果(左下表)。

表2.3 本實驗室與Dr. Spero實驗室針對南海2m (1)，400m (2)及1500m (3)水樣 $\delta^{13}\text{C}_{\text{TCO}_2}$ 之分析結果比較表（右下表）。

$\delta^{13}\text{C}_{\text{TCO}_2}$				
1	1.23			
2	1.31			
3	1.32			
4	1.18			
5	1.26			
6	1.23			
7	1.25			
8	1.15			
Average	1.24			
S.D.	0.06			

Sample No.	$\delta^{13}\text{C}_{\text{TCO}_2}$		Difference
	Dr. Spero's Lab	Dr. Sheu's Lab	
1	0.64	0.78	+0.14
2	0.07	0.10	+0.03
3	-0.05	-0.15	-0.10

三、結果與討論

本論文研究所參與八個SEATS探測航次，所測得之鹽度、位溫、 PO_4^{3-} 、 NO_3^- 、DO、TA、 TCO_2 及 $\delta^{13}\text{C}_{\text{TCO}_2}$ 之原始數據收錄於附錄一。這些資料的結果與討論，將分為兩部分來進行：

第一部分：是有關於表面混合層中TA、 TCO_2 和二氧化碳分壓（ fCO_2 ）的季節性變化。此部分之結果，已以“Preliminary investigation on seasonal variability of mixed-layer CO_2 , alkalinity, and fCO_2 at the SEATS time-series site, northern South China Sea”為題，投稿至Deep-Sea Research I，目前正在審稿中。在此僅將該篇論文之重要結論節譯為中文，完整的文章請參閱附錄二。

第二部分：則是針對SEATS測站TA、 TCO_2 、 $\delta^{13}\text{C}_{\text{TCO}_2}$ 以及其它相關生地化參數之垂直分佈特徵，進行討論。以釐清控制這些參數垂直變化的各項生地化因子，以及人為二氧化碳在SEATS測站穿透的情形。此部分之結果亦已完成初稿，題目為“Vertical distributions of alkalinity, TCO_2 , $\delta^{13}\text{C}_{\text{TCO}_2}$ at South East Asia Time-series Study (SEATS) site: controlling processes and anthropogenic CO_2 influence”。故在本論文中，僅將該篇手稿中之討論重點節譯為中文，詳盡的說明與討論，請參見附錄三。

3.1 SEATS測站混合層中滴定總鹼度/標準化鹼度（TA/NTA）、總二氧化碳/標準化總二氧化碳（ $\text{TCO}_2/\text{NTCO}_2$ ）及二氧化碳分壓（ fCO_2 ）季節變化之初探

在正式進入討論前，首先將本研究中對混合層深度、標準化鹼度（Normalized TA, NTA）、標準化總二氧化碳（Normalized TCO_2 , NTCO_2 ）之定義以及 fCO_2 的計算方法說明如下：

混合層深度：位密度（ σ_θ ）與水深10m處之位密度差達 0.1kg m^{-3} 以上時之深度（ $\sigma_\theta - \sigma_\theta \text{ at } 10\text{m} > 0.1$ ）。

$$\text{NTA} = \text{TA} \times (\text{平均鹽度}) \div (\text{實測鹽度})$$

$$\text{NTCO}_2 = \text{TCO}_2 \times (\text{平均鹽度}) \div (\text{實測鹽度})$$

上述兩組方程式之平均鹽度為33.5。將TA和TCO₂標準化至平均鹽度之目的為去除鹽度效應對此二參數之影響。

fCO₂乃根據實測之溫鹽、TA、TCO₂等資料帶入美國能源部所發展之二氧化碳系統計算程式 (Lewis and Wallace, 1998) 運算而得。碳酸之解離常數則選用 Mehrbach et al. 1973年所發表並經 Dickson and Millero (1987) 重新修訂後之解離常數。此常數是目前研究認為以TA及TCO₂資料來計算fCO₂時，最適用之解離常數 (Lee et al., 2000; Lueker et al., 2000)。本研究計算所得之fCO₂值與CO₂現場即時自動測定系統 (underway system) 之實測結果非常吻合，平均差異小於0.5% (私人通信，海科中心曾鈞懋博士)。TA及TCO₂測量不準度所可能造成fCO₂之計算誤差約為±5µatm。

3.1.1 混合層中溫度、鹽度、TANTA、TCO₂/NTCO₂ 及 fCO₂ 季節變化型態

2002年3月至2003年4月間七個航次之混合層深度以及混合層中溫度、鹽度、TANTA、TCO₂/NTCO₂和fCO₂之平均值繪於圖3.1(a)-(f)。如圖3.1(a)所示，受太陽輻射量改變之影響，溫度呈現明顯之季節變化。一如預期，冬季時出現最低溫 (~23.9°C, 2003年1月); 夏季時出現最高溫 (~30.2°C, 2002年7月)。由冬至夏溫度遞增，由夏至冬溫度則逐漸下降。鹽度之季節變化無明顯規律性存在，在觀測期間其波動幅度約為0.34，最大值 (~33.72) 出現在2003年1月; 最小值 (~33.38) 則出現在2002年11月 (圖3.1(b))。混合層深度季節變化最明顯的特徵為，自秋末 (2002年11月) 開始混合層逐漸加深，冬季時達到最大 (約90m; 圖3.1(c))。其餘季節 (春夏及秋初) 則無顯著變化且都相當淺，約介於20至30m之間。秋末及冬季時混合層的深化，應是由下列兩項因素所共同造成：第一、秋冬時溫度下降，海水密度增高，使表層海水之垂直不穩定度加大，故利

於垂直混和作用的發生。第二、每年 10 月起，整個南海籠罩在東北季風的作用下，強勁的風力，亦有助於上層海水所受之擾動向下傳遞，進而促成混合層的深化。由於南海鹽度垂直的變化，在 150m 以上是隨深度的增加而增加（圖 1.14），故冬季時混合層出現最高的鹽度，可能與混合層的深化作用有關。

在整個觀測期間內，TA 隨季節變化的範圍介於 2190 to 2200 $\mu\text{mol kg}^{-1}$ 之間，變化幅度約為 30 $\mu\text{mol kg}^{-1}$ ，其變化起伏幾乎與鹽度同步（圖 3.1(d)）。這表示影響鹽度變化之因子（例如，蒸發、降雨和淡水注入等等），可能亦是控制 TA 變化的主要因素。此種 TA 與鹽度同步變化的趨勢，在 HOT 及 BATS 時間序列測站亦有類似的現象（Winn et al., 1994; Bates et al., 1996）經過鹽度標準化後，NTA 的變化的確明顯變小（圖 3.1(d)），然而其變化幅度仍超過了測量的誤差範圍。此乃表示，除了鹽度外，其它影響 TA 變化的因子：碳酸鈣的生成與溶解，硝酸鹽的吸收與釋放等，可能亦有季節性的差異。

TCO₂ 隨季節變化之特徵為：在冬季時有明顯高值的出現（~1924 $\mu\text{mol kg}^{-1}$ ），其餘季節變化幅度不大，僅介於~1887 到~1898 $\mu\text{mol kg}^{-1}$ 之間波動（圖 3.1(e)）。冬季 TCO₂ 之高值應是混合層深化所造成的結果。此乃因次表層水之 TCO₂ 濃度較高，當混合層深化時，有較多的次表層水可進入混合層中，故可造成混合層中 TCO₂ 濃度的升高。NTCO₂ 的季節變化主要則受混合層深度的改變及生物生產等兩個因素所控制。由春季到秋初這段時期，由於溫度較高，上層海水層化良好，故混合層深度均很淺且相當穩定，因此 NTCO₂ 濃度較高之次表層水不易進入混合層中，故混合層中缺乏 NTCO₂ 的補充，再加上生物生產作用持續消耗掉碳，致使此段時期內 NTCO₂ 呈遞減之趨勢（圖 3.1(e)）。到了秋末，隨著混合層的深化（圖 3.1(c)），NTCO₂ 含量較高之次表層水進入了混合層中，使得混合層 NTCO₂ 的濃度逐漸回升，此種作用在冬季時達到最高峰，於是形成了 NTCO₂ 的最大值。

fCO₂ 的最高值出現在夏季，最低值則出現在冬季。由冬至夏其呈穩定遞增之趨勢；而由夏至冬則呈遞減之趨勢，其與溫度的改變呈現近乎完美的同步變化

(圖 3.1(f)) 此種緊密的相關性，表明了溫度極可能是控制混合層中季節變化最重要的因素。混合層中 $f\text{CO}_2$ 季節變化的控制機制將在下節中做比較深入的討論。

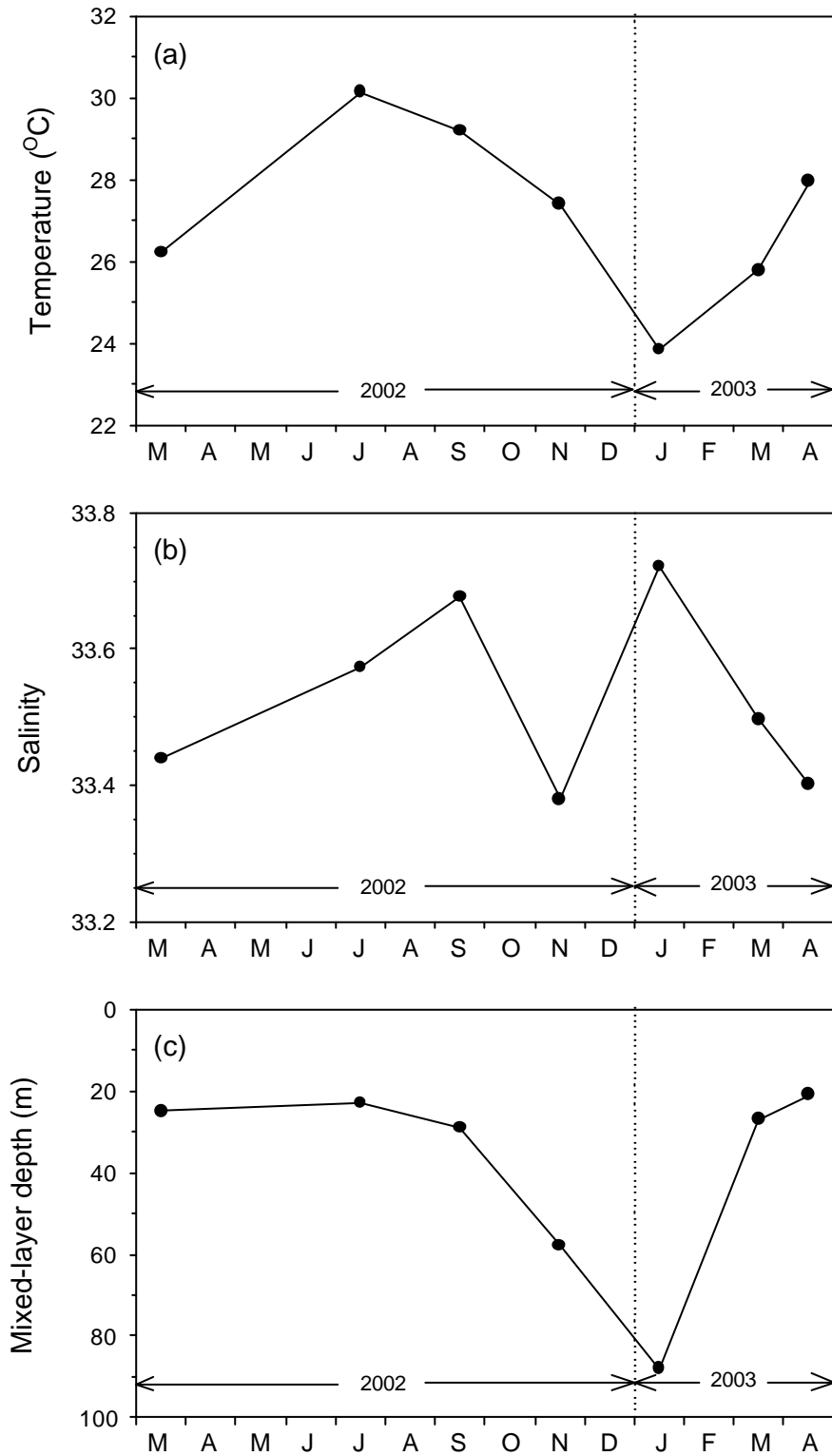


圖 3.1 2002 年 3 月至 2003 年 4 月 SEATS 測站，混合層之 (a) 平均溫度，
(b) 平均鹽度及 (c) 深度 之時間序列變化圖。

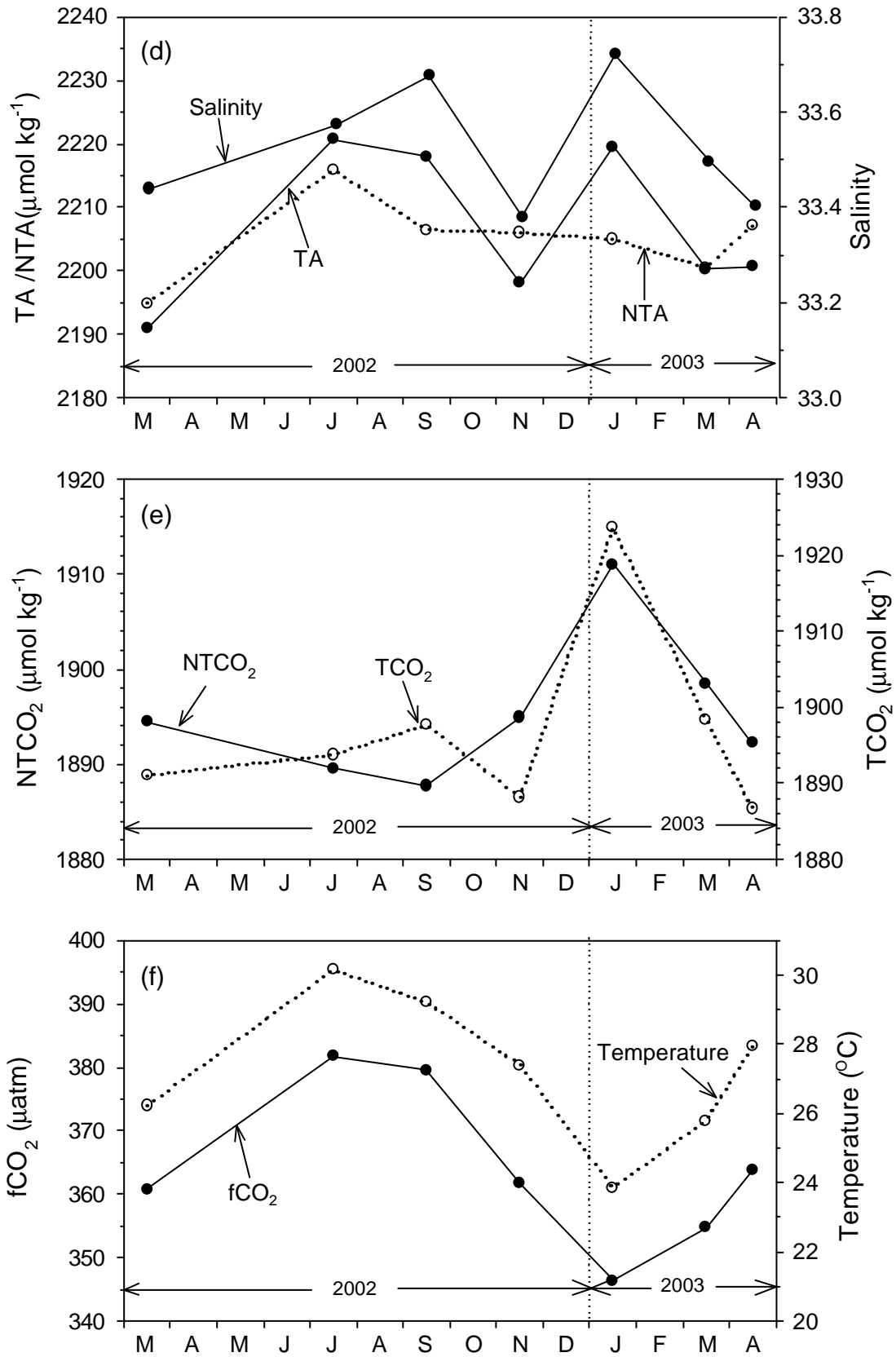


圖 3.1 (續) 2002 年 3 月至 2003 年 4 月 SEATS 測站，混合層之平均 (d)

TA/NTA, (e) TCO₂/NTCO₂ 及 (f) fCO₂ 之時間序列變化圖。

3.1.2 混合層中 $f\text{CO}_2$ 季節變化的控制機制

混合層中 $f\text{CO}_2$ 的增減，受下列四項因素所影響：

- (I) 溫度，二氧化碳在海水中的溶解度隨溫度的增加而減少 (Weiss et al., 1974)，故 $f\text{CO}_2$ 會隨溫度的增高而增大；反之溫度降低會使 $f\text{CO}_2$ 減小 (Takahashi et al., 1993)。
- (II) 生物作用，生物生產作用會消耗掉到海水中之 TCO_2 ， TCO_2 的減少會造成 $f\text{CO}_2$ 的降低。
- (III) 海水垂直運動的狀況，由於次表層水之 TCO_2 濃度較高，故當海水垂直運動加強時，會有較多的次表層水可進入混合層中，造成混合層中 TCO_2 濃度的升高，進而促使 $f\text{CO}_2$ 變大。
- (IV) 海氣交換作用，若一海域為大氣二氧化碳之“source”時，表水中之二氧化碳氣體會向大氣中逸散，造成表水 $f\text{CO}_2$ 的降低。反之，若一海域為大氣二氧化碳之“sink”時，大氣中之二氧化碳氣體會進入表水中，使得 $f\text{CO}_2$ 的升高。

由於這四種作用機制，在不同海域隨季節變化的情形不盡相同。因此，全球不同海域 $f\text{CO}_2$ 季節變化的形態有非常顯著的差異。為瞭解 SEATS 測站 $f\text{CO}_2$ 之季節變化形態與其它時間序列測站的異同，本節中首先將介紹全球不同海域 $f\text{CO}_2$ 季節變化的特徵，然後再針對 SEATS 測站混合層中 $f\text{CO}_2$ 季節變化的控制因子進行分析，最後再與其它時間序列測站的研究結果加以比較。

(1) 北大西洋副極區海域 (Subarctic North Atlantic)

圖 3.2 是冰島附近海域 (63°N-68°N) 表水溫度與 $p\text{CO}_2$ (未考慮氣體分子與分子之間作用力時，氣體分壓之表達方式；在表層海水的二氧化碳分壓範圍內， $p\text{CO}_2$ 與 $f\text{CO}_2$ 的差異極小，幾可相等視之) 隨季節之變化圖。由圖中可看出，一月至五月該海域表水之溫度及 $p\text{CO}_2$ 並無顯著之變化，但伴隨春末夏初藻華現象 (spring blooms) 之發生， $p\text{CO}_2$ 快速減少至一年中的最低值。此乃因生物生產大

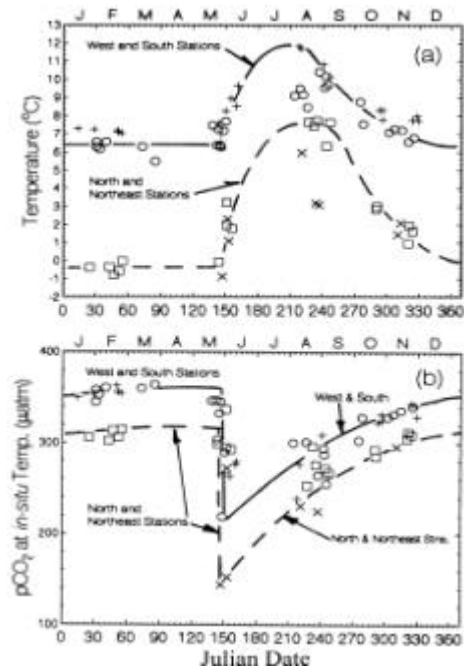


圖 3.2 北大西洋高緯地區（冰島附近海域）表水溫度及 $p\text{CO}_2$ 之季節變化圖。摘自 Takahashi et al. (1993)。

量消耗海水中溶解之二氧化碳所致。由夏初到秋初，受海水溫度持續升高的影響， $p\text{CO}_2$ 亦呈現逐漸升高的趨勢。由秋初到冬末，雖然水溫變冷有降低 $p\text{CO}_2$ 的效果，但在這段時期內，次表層海水的湧升作用增強，其對 $p\text{CO}_2$ 增高之效果較溫度降低對 $p\text{CO}_2$ 所造成之減少效果更為顯著，故 $p\text{CO}_2$ 持續增加，到冬末達到一年之中的最高值。

(2) 北大西洋副熱帶海域 (Subtropical North Atlantic)

此處以 BATS 時間序列測站及 European Station for Time Series in the Ocean at the Canary Islands (ESTOC; 29° 10' N, 15° 30' W; 圖 1.9) 測站之觀測結果，分別來代表西北和東北大西洋副熱帶貧營養鹽海域表水 $p\text{CO}_2$ 之季節變化特性。圖 3.3 (上) 及 (下) 分別是 BATS 測站 1996 年至 1998 年及 ESTOC 測站 1996 年至 2000 年混合層中溫度及 $p\text{CO}_2$ 的時序變化圖。由圖中可清楚發現，兩個測站 $p\text{CO}_2$ 皆呈現非常規則的季節性變化：冬季時（溫度最低時）出現極小值，夏季（溫度最高時）出現極大值。由冬至夏變暖的過程中， $p\text{CO}_2$ 呈遞增的趨勢。反

之，由夏至冬變冷的過程中， $p\text{CO}_2$ 呈遞減的趨勢。換言之，在此海域 $p\text{CO}_2$ 與溫度的變化呈現良好的對應關係。此種良好對應關係形成之機制，簡要說明如下：在海水逐漸暖化的過程中，由於海水層化現象加強，表層海水中缺乏營養鹽的補充，基礎生產力偏低。故海水增溫對 $p\text{CO}_2$ 增加之效果超過了生物生產對 $p\text{CO}_2$ 降低的效果。因此，隨著溫度的增高， $p\text{CO}_2$ 亦逐漸增高。當水溫逐漸變冷的時期，雖然混合層深度會加深，但在副熱帶海域中，混合層深度之季節性變化幅度，一般皆遠較高緯度海域為小，故混合層深化造成表水 $p\text{CO}_2$ 增加之效果，不及降溫及生物生產對 $p\text{CO}_2$ 降低加總後的效果，故可觀察到 $p\text{CO}_2$ 伴隨溫度降低而減少的現象。

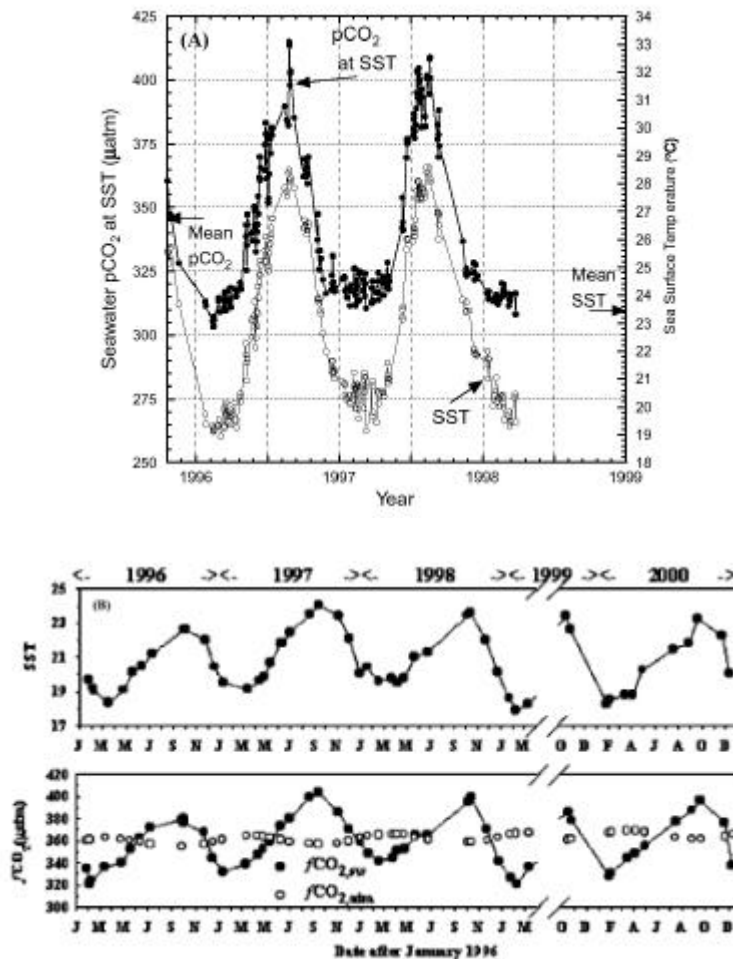


圖 3.3 BATS (上) 及 ESTOC (下) 時間序列測站混合層中溫度及 $p\text{CO}_2$ 的時序變化圖。上、下兩圖分別摘自 Takahashi et al. (2002)和 González-Dávila et al. (2003)。

(3) 西北太平洋副極區海域 (Northwestern subarctic Pacific)

Kyodo western North Pacific Ocean Time-series study (KNOT; 44°N, 155°E, 圖 1.9) 時間序列測站之研究結果, 在此被用來代表西北太平洋高緯度海域表水 $f\text{CO}_2$ 之季節變化。圖 3.4 是 KNOT 測站由 1998 年至 2000 年表水 $f\text{CO}_2$ 的時序變化圖。雖然資料的密度稍嫌不足, 不過仍可明顯看出表水 $f\text{CO}_2$ 夏天低、冬天高的基本特徵。此種季節性變化的特性, 與副熱帶海域之研究結果呈相反的趨勢 (BATS 和 ESTOC)。Tsurushima et al. (2002) 認為這是由於夏季之高基礎生產力大量消耗二氧化碳造成 $f\text{CO}_2$ 快速降低且其效果超越了溫度增高對 $f\text{CO}_2$ 增加的效果, 所以形成夏天的低值。而冬季時表水溫度降低, 水層垂直不穩定度加大, 混合層大幅深化, 造成二氧化碳含量較高之次表層水進入了混合層中, 使 $f\text{CO}_2$ 遽增, 故出現冬季之高值。

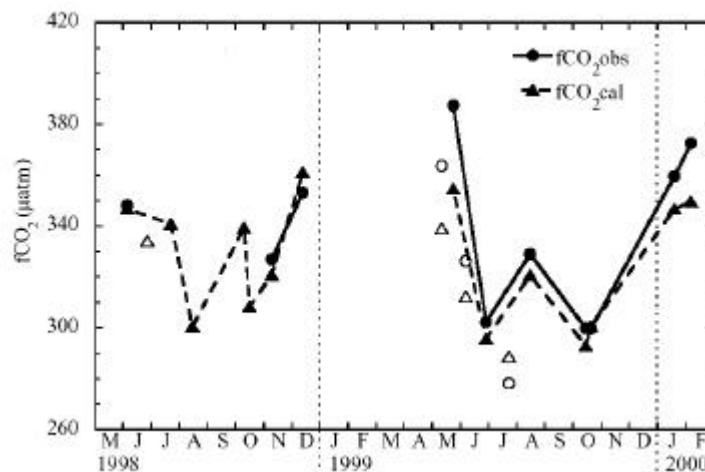


圖 3.4 KNOT 時間序列測站 1998 年至 2000 年表水 $p\text{CO}_2$ 的時序變化圖。

摘自 Tsurushima et al. (2002)。

(4) 東北太平洋副極區海域 (Northeastern subarctic Pacific)

東北太平洋高緯度海域表水 $p\text{CO}_2$ 之季節變化特性, 以 Ocean Weather Station P (OSP; 50°N, 145°W, 圖 1.9) 時間序列測站之探測結果代表之。圖 3.5 為 OSP 測站混合層內 $p\text{CO}_2$ 及溫度在一年內隨時序變化的情形。與其它所有海域相似, 溫度呈現夏高冬低典型之季節性變化。然而, 由圖中不難發現與其它海域相較,

OSP 測站 $p\text{CO}_2$ 之季節性的變化並不顯著，且一年之中 $p\text{CO}_2$ 的波動幅度遠較大西洋及西北太平洋高緯度海域為小。Wong and Chan (1991) 將此一現象，歸因於各個影響 $p\text{CO}_2$ 升降因子相互抵消的結果。在春、夏溫度漸增的時期，基礎生產力亦較高，此時溫度升高對 $p\text{CO}_2$ 增加的效果與海水中二氧化碳因生物生產被消耗對 $p\text{CO}_2$ 的減少效果幾乎相仿，故夏季並無明顯之 $p\text{CO}_2$ 極大值或極小值的出現。而秋、冬溫度漸減的時期，由於此海域次表層水之湧升速率遠較西北太平洋海域為小，故其造成混合層中 $p\text{CO}_2$ 升高之效果與溫度下降及生物生產對 $p\text{CO}_2$ 降低之加總效果相去不遠。因此，冬季亦無明顯之 $p\text{CO}_2$ 極大或極小值的形成。

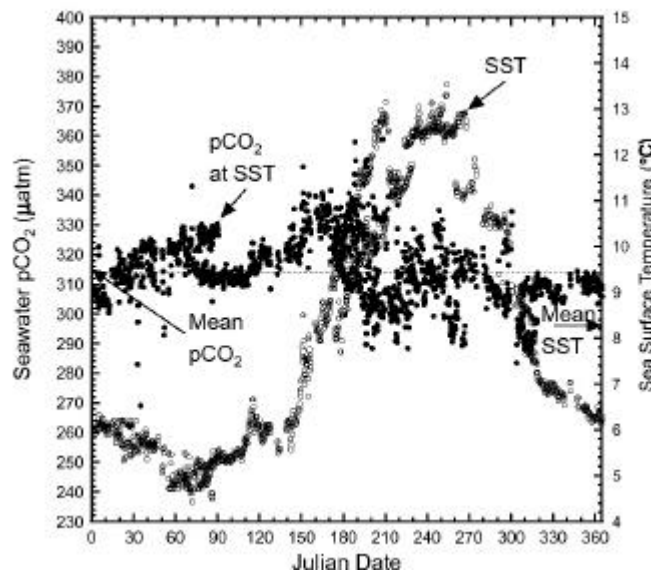


圖 3.5 OSP 時間序列測站混合層內 $p\text{CO}_2$ 及溫度之年時序變化圖。摘自 Takahashi et al. (2002)。

(5) 北太平洋副熱帶海域 (Subtropical North Pacific)

北太平洋副熱帶海域表水 $f\text{CO}_2$ 之季節變化特徵，以 HOT 時間序列測站所得之結果代表之。圖 3.6 為 1989 年底至 1992 年 HOT 測站上層海水溫度與 $f\text{CO}_2$ 的時序變化圖。由圖中可發現，此海域與北大西洋副熱帶海域 (BATS 及 ESTOC 測站) 相同， $f\text{CO}_2$ 與溫度幾成同步的變化。這表明儘管分屬兩個不同大洋，在副熱帶貧營鹽的海域中，控制 $f\text{CO}_2$ 季節變化之機制的運作方式應非常相似。意即在海水增溫的階段，受限於營養鹽的缺乏，基礎生產力偏低，使海水增溫對

fCO₂ 增加之效果超過了生物生產對 fCO₂ 降低的效果，故 fCO₂ 隨溫度增高而增加。在海水降溫的過程，雖然混合層深化有造成 fCO₂ 增加的效果，但其造成表水 fCO₂ 增加之幅度，不若降溫及生物生產對 fCO₂ 降低加總後的效果，故 fCO₂ 隨溫度降低而減少。

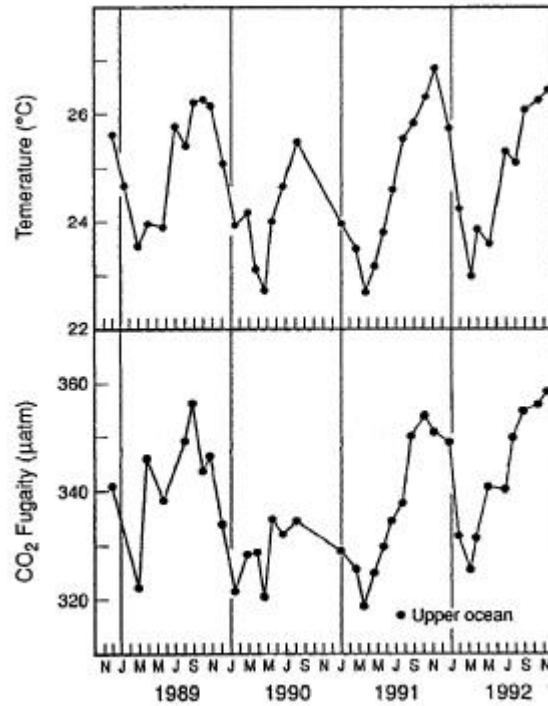


圖 3.6 HOT 時間序列測站 1988 年底至 1992 年上層海水溫度與 pCO₂ 的時序變化圖。摘自 Winn et al. (1994)。

由上述文獻的回顧可發現，SEATS 測站 fCO₂ 之季節變化型態與 BATS、ESTOC 和 HOT 等位於副熱帶貧營養鹽海域的時間序列測站非常相似。這表示儘管南海有季風交替，內部湧升強等與其它海域不同之環境特徵，但控制 SEATS 測站 fCO₂ 季節變化各項因素的運作方式，應與上述各時間序列測站極為類似。為進一步釐清各項因子對 fCO₂ 變化的貢獻，本研究根據 Takahashi et al.(2002)所提出的兩組公式，分別評估溫度及非溫度因素對 fCO₂ 的影響程度：

$$fCO_{2\text{mean}} \text{ corrected for } \Delta T = (\text{Mean annual } fCO_2) \times \exp[0.0423 \times (T_{\text{obs}} - T_{\text{mean}})] \dots\dots\dots \text{Eq. 3.1}$$

$$fCO_2 \text{ at } T_{\text{mean}} = fCO_{2\text{obs}} \times \exp[0.0423 \times (T_{\text{mean}} - T_{\text{obs}})]. \dots\dots\dots \text{Eq. 3.2}$$

T_{obs} ：溫度之觀測值

Mean annual $f\text{CO}_2$ ：測量期間 $f\text{CO}_2$ 的平均值 ($364\mu\text{atm}$)

T_{mean} ：測量期間溫度的平均值 (27)

$f\text{CO}_{2\text{obs}}$ ： $f\text{CO}_2$ 之觀測值

Eq. 3.1 之計算結果，代表溫度變化對 $f\text{CO}_2$ 的影響大小；Eq. 3.2 之計算結果，代表非溫度因素對 $f\text{CO}_2$ 變化的影響效果。“ $f\text{CO}_{2\text{mean}}$ corrected for ΔT ”、“ $f\text{CO}_2$ at 27 ”和 $f\text{CO}_2$ 觀測值隨時間之變化，繪於圖 3.7。由圖中可發現，雖然“ $f\text{CO}_{2\text{mean}}$ corrected for ΔT ”與 $f\text{CO}_2$ 實測值有相同的變化趨勢，然而前者的波動幅度遠較後者為大。而“ $f\text{CO}_2$ at 27 ”則呈現與“ $f\text{CO}_{2\text{mean}}$ corrected for ΔT ”相反的變化趨勢。這表示溫度改變所造成 $f\text{CO}_2$ 變化的效果，有部分被其它非溫度因素之加總效果所抵銷。但非溫度因素對 $f\text{CO}_2$ 影響之加總效果始終較溫度效應為小，故仍可觀察到 $f\text{CO}_2$ 與溫度同步變化，但其波動幅度較預期為小的現象。

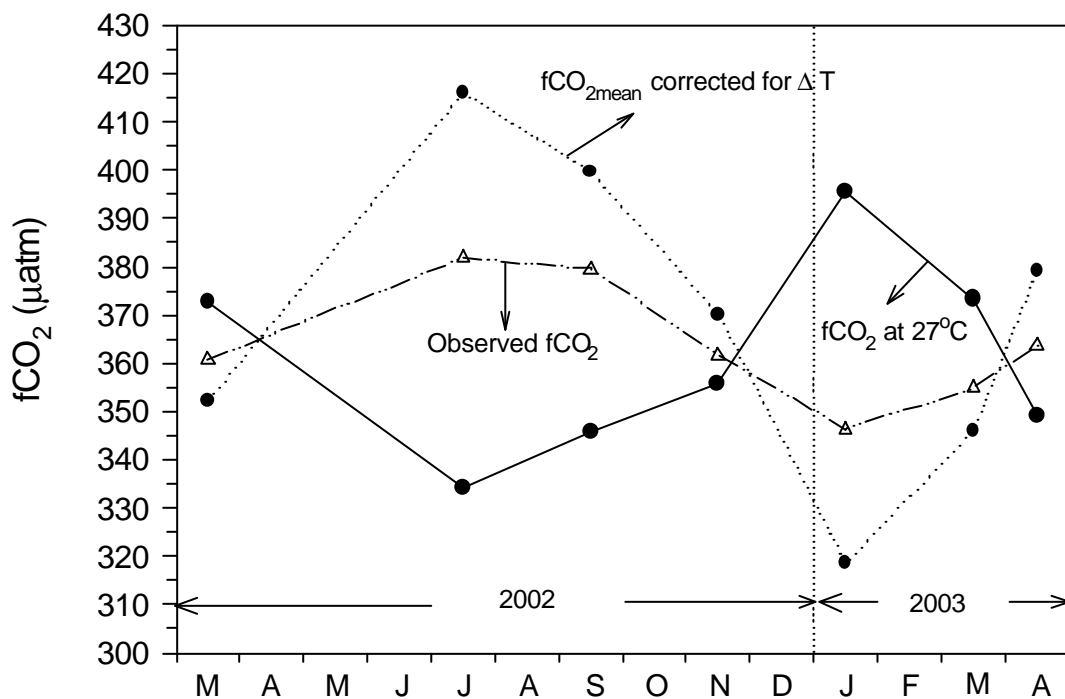


圖 3.7 “ $f\text{CO}_{2\text{mean}}$ corrected for ΔT ”、“ $f\text{CO}_2$ at 27 ”以及 $f\text{CO}_2$ 觀測值 (Observed $f\text{CO}_2$) 之時序變化圖。“ $f\text{CO}_{2\text{mean}}$ corrected for ΔT ”和“ $f\text{CO}_2$ at 27 ”的定義，請參見本文。

“fCO₂ at 27 °C”的變化代表生物作用、次表層水的加入以及海氣交換等三項非溫度因子加總後對混合層中 fCO₂ 變化的影響效果，但在由冬至夏溫度漸增的時期，由於上層海水層化作用逐漸加強，故次表層水進入混合層中的影響應可忽略。而此段時期內，海氣交換之淨通量極小（見下節討論），故可暫不予考慮。因此，“fCO₂ at 27 °C”由冬至夏遞減的趨勢，主要可歸因於生物生產作用消耗 TCO₂ 所致。若假設 2003 年 1 月和 2002 年 7 月的“fCO₂ at 27 °C”和 TCO₂ 為冬季及夏季之代表值，則由冬至夏“fCO₂ at 27 °C”和 TCO₂ 的減少量（圖 3.1(d)）分別為 60 μatm 和 30 μmol kg⁻¹。根據 Takahashi(1993)所提出之公式：

$$(\partial fCO_2 / \partial TCO_2) / (TCO_2 / fCO_2) = 10. \dots\dots\dots Eq. 3.3$$

計算結果顯示，此段時間內 TCO₂ 減少所造成 fCO₂ 對應之減少量約為 55 μatm，與“fCO₂ at 27 °C”之變化量大致相符，說明 TCO₂ 的減少是“fCO₂ at 27 °C”減少的主因。“fCO₂ at 27 °C”在由夏至冬溫度遞減的時期，呈現逐漸增加的趨勢。此段時期海氣交換之淨通量亦不大，故此項因素亦暫不予考慮，而生物生產作用會造成“fCO₂ at 27 °C”的減少，所以此時期“fCO₂ at 27 °C”之遞增趨勢，必然是由於富含 TCO₂ 之次表層水加入混合層中所造成。在此，我們假設由夏至冬和由冬至夏生物作用對“fCO₂ at 27 °C”減少的效果相等（~-60μatm），而溫度引起 fCO₂ 的改變量約為-90μatm，fCO₂ 觀測值的變化量約為-30μatm，故次表層水加入混合層中對這個時期 fCO₂ 變化的貢獻約為+120μatm。因此，當海水降溫的時期，次表層水進入混合層中，對 fCO₂ 變化的貢獻大於溫度的效應。

綜上所述，SEATS 測站 fCO₂ 季節變化之控制機制可概述如下：在由冬至夏溫度回暖的時期，fCO₂ 的變化主要由溫度及生物生產作用所控制。但後者對 fCO₂ 之減少效果（~-60μatm）較前者對 fCO₂ 之增加效果（~+90μatm）為小，故可觀察到 fCO₂ 隨溫度增加而增加之趨勢。在由夏至冬變冷的時期中，由於混合層深化，次表層水的加入大幅提高了混合層中的 fCO₂（~+120μatm），但其增加效果不若溫度降低（~-90μatm）與生物生產（~-60μatm）加總對 fCO₂ 的減少效果，故仍可觀察到 fCO₂ 隨溫度遞減的現象。

為了進一步探討控制 SEATS 測站 $f\text{CO}_2$ 季節變化作用之機制與其它時間序列站的異同，本研究根據 Takahashi et al. (2002) 所提出的方法，分別計算溫度及生物效應對各時間序列測站 $f\text{CO}_2$ 季節變化之相對重要性。雖然海水垂直運動狀況亦對 $f\text{CO}_2$ 的變化有重要的影響，但此部分之影響效果很難精確評估，故不在比較討論之列。

根據 Takahashi et al. (2002)的定義，溫度及生物效應對 $f\text{CO}_2$ 變化的相對影響程度，可以 (T/B) 或 (T-B) 表示之。其定義以方程式表示如下：

$$T / B = [(\Delta f\text{CO}_2)_{\text{temp}} / (\Delta f\text{CO}_2)_{\text{bio}}] \dots\dots\dots \text{Eq. 3.4}$$

$$T - B = [(\Delta f\text{CO}_2)_{\text{temp}} - (\Delta f\text{CO}_2)_{\text{bio}}] \dots\dots\dots \text{Eq. 3.5}$$

Eq. 3.4 和 Eq. 3.5 中 $(\Delta f\text{CO}_2)_{\text{temp}}$ 代表一年之中“ $f\text{CO}_2$ mean corrected for ΔT ”最大值與最小值的差； $(\Delta f\text{CO}_2)_{\text{bio}}$ 則是一年之中“ $f\text{CO}_2$ at T_{mean} ”最大值與最小值的差。當 (T/B) > 1 或 (T-B) > 0 時，代表該海域溫度效應對 $f\text{CO}_2$ 季節變化之影響大於生物效應；反之，當 (T/B) < 1 或 (T-B) < 0 時，表示該海域生物效應大於溫度效應；當 (T/B) = 1 或 (T-B) = 0 時，代表兩者對 $f\text{CO}_2$ 變化之影響呈勢均力敵之勢。

SEATS、HOT、BATS、KNOT 和 OSP 等五個時間序列測站之 (T/B) 及 (T-B) 列於表 3.1。由表中可看出，SEATS 與另二個位於低緯度貧營養鹽海域的測站 (HOT 和 BATS) 相同，溫度效應對 $f\text{CO}_2$ 變化的影響都較生物作用為大。而位於高緯海域的 KNOT 和 OSP 測站，則是生物效應較溫度效應為重要。這主要是因為，一般而言高緯度海域透光層中，營養鹽的含量都遠較低緯度貧營養鹽海域為高，故當環境條件適合時 (通常為春末夏初海水溫度迅速回升之際)，可造成遠較低緯度貧營養鹽海域為高的基礎生產力。故生物效應取代溫度效應成為主導 $f\text{CO}_2$ 變化的因素。此外，由表 3.1 中可發現另一令人意外的結果：HOT 是與 SEATS 緯度最相近之測站，而兩者同樣位於副熱帶貧營養鹽海域中，且兩者之混合層深度之季節變化幅度非常相似 (HOT 混合層深度之季節變動約介於 20 到 100m 之間；Neuer et al., 2002)。故可預期兩者之溫度和生物效應對 $f\text{CO}_2$ 之影響應非常

表 3.1 SEATS 與 HOT、BATES、KNOT 和 OSP 等時間序列測站，溫度及生物效應對 fCO₂ 季節變化之相對重要性比較表。溫度效應（Temperature effect）及生物效應（Biological effect）的定義請參見本文。

	Location and Oceanic regime represented	Temperature effect / Biological effect	Temperature effect - Biological effect	References
SEATS	18° 15' N, 115° 35' E South China Sea, the largest subtropical marginal sea	1.6 (97/62 μatm)	+35 μtam	This study
HOT	22° 45' N, 158° W North Pacific subtropical gyre	2.6 (59/23 μatm)	+36 μtam	Calculated based on Winn et al. (1994)
BATS	31° 50' N, 64° 10' W Western North Atlantic subtropical gyre	2.7 (150/55 μatm)	+95 μtam	Bates et al. (2001) Takahashi et al. (2002)
KNOT	44° N, 155° E Northwestern subarctic Pacific Ocean	0.8 (174/228 μatm)	-54 μtam	Calculated based on Tsurushima et al. (2002)
OSP	50° N, 145° W Northeastern subarctic Pacific Ocean	0.9 (100/115 μatm)	-10 μtam	Wong and Chan (1991) Takahashi et al. (2002)

相近。然而，實際結果卻顯示無論是溫度（97 vs. 59 μ atm）還是生物效應（62 vs. 23 μ atm），SEATS 都明顯較 HOT 為大。推測此種差異可能與南海內部湧升作用強烈有關。由於湧升作用較強，南海之溫躍層、營養鹽躍層、二氧化碳躍層都較位於太平洋中間之 HOT 測站為淺（圖 3.8）。在此種情況下，儘管混合層深層之季節變化幅度相仿，但 SEATS 測站在混合層深化時，加入混合層中之次表層水可能具有溫度較低，營養鹽及 TCO₂ 濃度較高等特點。因此，形成了溫度及生物效應都較 HOT 測站為大的現象。

3.1.3 二氧化碳海氣交換通量之季節變化

二氧化碳海氣交換通量的大小，代表海洋對人為二氧化碳吸收的能力。因此，二氧化碳海氣交換通量隨時間之變化，是所有時間序列研究中必定探討的主題之一。故本節將針對 SEATS 測站二氧化碳海氣交換通量之季節變化進行分析，並據以判斷就年的時間尺度而言，SEATS 究竟是大氣二氧化碳的“sink”還是“source”？最後再與 HOT 及 BATS 的結果加以比較。

二氧化碳海氣交換通量可以 Eq. 1.1 計算之。其中 $\Delta f\text{CO}_2$ 代表表層海水與大氣二氧化碳分壓的差。由於本研究並未同步測量大氣二氧化碳分壓。因此，大氣二氧化碳濃度是取自夏威夷 Mauna Loa Observatory 的觀測資料（Keeling and Whorf, 2004），並以溫度 27、鹽度 33.5 為條件修正水蒸氣壓後所得（DOE, 1994）。 $\Delta f\text{CO}_2$ 隨時間之變化繪於圖 3.9。由於我們假定大氣二氧化碳分壓在研究期間為一定值，故 $\Delta f\text{CO}_2$ 之季節變化型態與混合層中 $f\text{CO}_2$ 之變化型態一致：最大值出現在夏季，最小值出現在冬季，由夏至冬遞減，由冬至夏遞增。由圖 3.9 可發現，SEATS 測站在夏季及秋初明顯是大氣二氧化碳的“source”，冬季時則扮演“sink”的角色，春季及秋末大致呈現海氣平衡的狀態。

計算二氧化碳海氣交換通量時所需之氣體交換係數，通常由風速資料推導。然而不同經驗公式所求出之氣體交換係數有相當大的差異（Bates et al.,

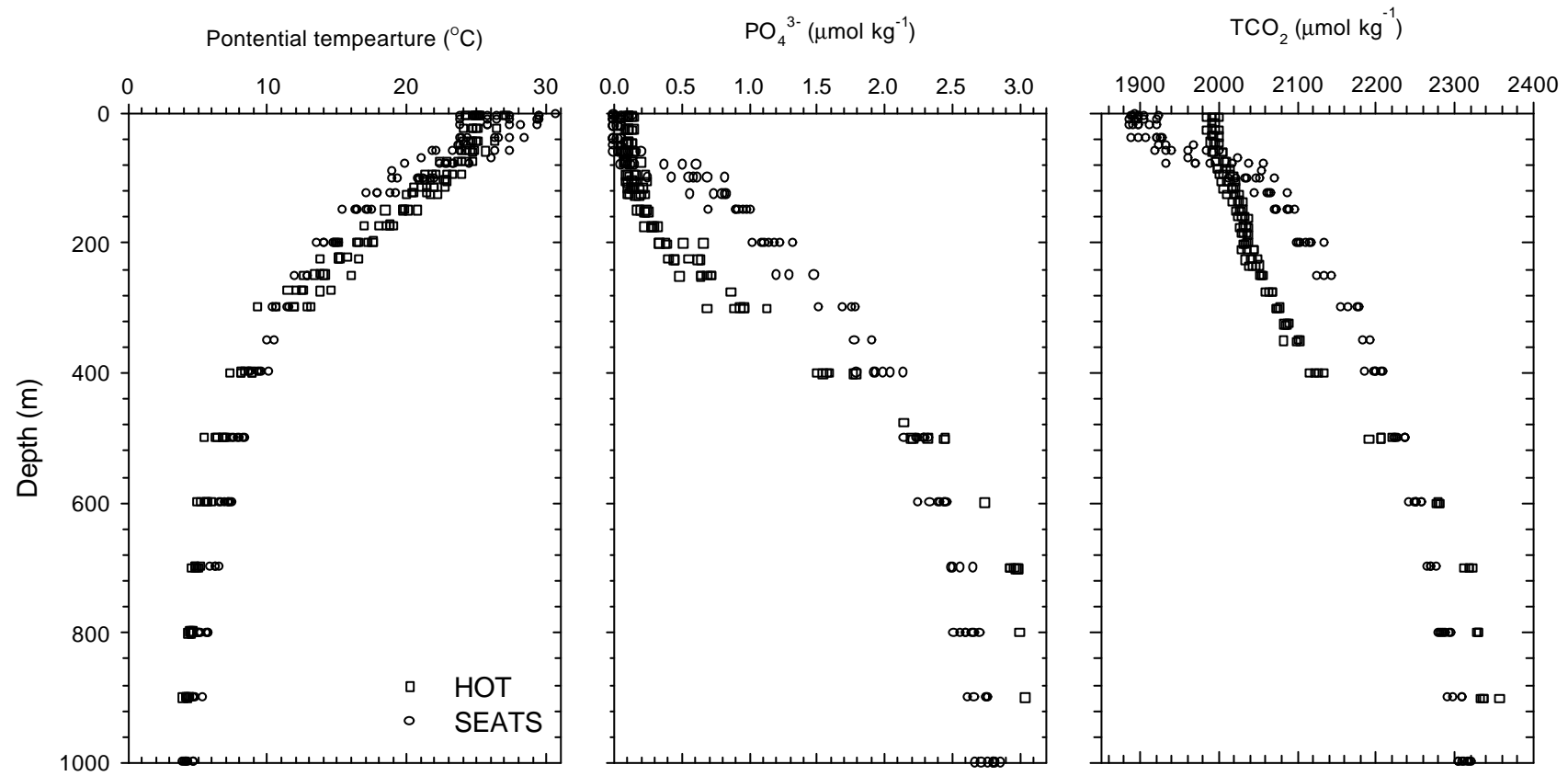


圖 3.8 SEATS 和 HOT 時間序列測站位溫、磷酸鹽與總二氧化碳濃度之垂直分佈比較圖。

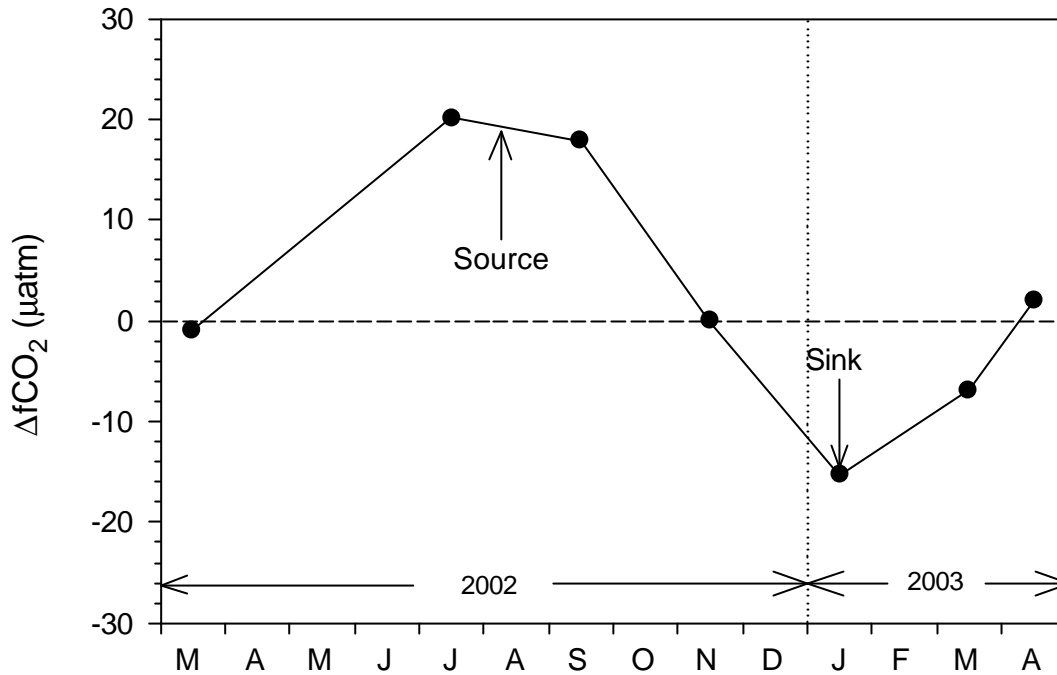


圖 3.9 $\Delta f\text{CO}_2$ 之時序變化圖。 $\Delta f\text{CO}_2$ 為表層海水與大氣 $f\text{CO}_2$ 的差。

1996)。為界定不同之經驗公式所求出二氧化碳海氣交換通量差異的範圍，本研究採用了三組文獻中常見的經驗公式（Liss and Merlivat, 1986; Tans et al., 1990; Wanninkhof, 1992）來計算氣體交換係數。而風速資料則是取自歐洲中尺度氣象預報中心（ECMWF）所模擬 1985 到 1999 年在 18°N , 116°E 海平面 10m 高處之月平均風速（海軍官校梁文德教授提供）。2002 年及 2003 年 3 月與 2003 年 4 月之 $\Delta f\text{CO}_2$ 的平均值作為春季（3, 4, 5 月） $\Delta f\text{CO}_2$ 之代表值；2002 年 7 月之 $\Delta f\text{CO}_2$ 作為夏季（6, 7, 8 月）之代表值；2002 年 9 月和 11 月之平均值作為秋季（9, 10, 11 月）之代表值；冬季（12, 1, 2 月）之 $\Delta f\text{CO}_2$ 則以 2003 年 1 月之 $\Delta f\text{CO}_2$ 代表之。依據上述資料，SEATS 測站春、夏、秋、冬四季之二氧化碳海氣交換通量之計算結果分別為：春季， $-0.03 \pm 0.07 \sim -0.25 \pm 0.64 \text{ gC m}^{-2} \text{ yr}^{-1}$ ；夏季， $0.30 \pm 0.07 \sim 2.77 \pm 0.68 \text{ gC m}^{-2} \text{ yr}^{-1}$ ；秋季， $2.10 \pm 1.16 \sim 5.36 \pm 2.97 \text{ gC m}^{-2} \text{ yr}^{-1}$ ；冬季， $-7.47 \pm 2.44 \sim -17.04 \pm 5.57 \text{ gC m}^{-2} \text{ yr}^{-1}$ （表 3.2）。由上述結果可發現，儘管夏季時海水與大氣二氧化碳之分壓差最大，但由於冬季時東北季風之風速較夏季西南季風風速高出了近二倍，使得冬季時之二氧化碳海氣交換通量遠大於其它的季節，因此使

SEATS 測站每年之淨交換通量為負值，成為大氣二氧化碳的“sink”。

SEATS 測站每年之二氧化碳海氣交換通量介於 -1.28 ± 0.94 至 -2.73 ± 2.20 $\text{gC m}^{-2} \text{yr}^{-1}$ ，明顯較 HOT 的 -2.84 $\text{gC m}^{-2} \text{yr}^{-1}$ (Winn et al., 1994) 以及 BATS 的 -3.0 至 -7.2 $\text{gC m}^{-2} \text{yr}^{-1}$ 為小 (Bates et al., 1998)。推測這可能是由於 SEATS 測站所處緯度最低，故其平均溫度較 HOT 及 BATS 為高，溫度高不利海洋對大氣二氧化碳的吸收，故可能造成 SEATS 測站有較低之海氣交換通量。此外，南海內部較強的湧升作用，亦不利大氣二氧化碳的吸收，故亦有可能是 SEATS 測站每年對大氣二氧化碳吸收量較 BATS 和 HOT 為低的原因。若將 SEATS 測站所得之結果，外插到整個南海 (3.5×10^6 km^2)，則整個南海每年對大氣二氧化碳之吸收量為 4.5 ± 3.3 到 9.6 ± 7.7 Tg C yr^{-1} ($1\text{Tg}=10^{12}\text{g}$) 之間。此量約佔全球海洋吸收量的 0.20% 到 0.44% 之間。然而，以面積比例而言，南海約佔全球海洋的 0.97%。故南海對大氣二氧化碳之吸收能力，明顯低於世界海洋之平均值。

3.1.4 基礎生產力的估算

在 3.1.1 和 3.1.3 節的討論中，混合層溫度由冬轉夏漸增的這段期間， NTCO_2 和“ $f\text{CO}_2$ at 27

 ”的遞減，被歸因於生物生產作用消耗掉水中溶解之無機碳所致。若此推論為真，則此段時期混合層中 NTCO_2 的減少量即可視為是基礎生產力與再生生產力的差（此即為新生產力）。假設 2002 年 7 月及 2003 年 1 月之 NTCO_2 為夏季及冬季之代表值，則此段時期 NTCO_2 的減少量約為 $21\mu\text{mol kg}^{-1}$ 。混合層平均深度假設為 50m，則此段時期內，混合層內消耗之總溶解無機碳量約為 1.05 ± 0.20 mole C m^{-2} 。由於這僅代表了半年（1 月至 7 月）碳的消耗量。在假設後半年生物作用對碳之消耗速率不變的條件下，則 SEATS 全年之新生產力約為 2.10 ± 0.40 mole C m^{-2} 。Chen et al. (2004)報導 SEATS 測站附近之 f-ratio（新生產力與基礎生產力之比）介於 0.19 到 0.39 之間。根據上述之碳消耗量及 f-ratio，SEATS 測站全年混合層中基礎生產力應介於 177 ± 34 到 363 ± 69 $\text{mgC m}^{-2} \text{day}^{-1}$

表 3.2 SEATS 測站春、夏、秋、冬四季以及年平均二氧化碳海氣交換通量之估算結果表。二氧化碳氣體交換係數 (K) 共使用 Liss and Merlivat (1986) , Tans et al. (1990)和 Wanninkhof (1992)三組不同的經驗公式計算之。ΔfCO₂ 不準度所可能造成通量估算之誤差，以ΔfCO₂ 觀測值加減 5 μatm 來估計之。

	ΔfCO ₂ (μatm)	Wind speed (m s ⁻¹)	CO ₂ flux (F, gC m ⁻² yr ⁻¹) and exchange coefficient (K, gC m ⁻² year ⁻¹ μatm ⁻¹)					
			Liss and Merlivat (1986)		Tans et al. (1990)		Wanninkhof (1992)	
			K	F	K	F	K	F
Spring	-1.9 ± 5	3.1	0.016	-0.03 ± 0.07	0.019	-0.04 ± 0.07	0.129	-0.25 ± 0.64
Summer	20.1 ± 5	3.2	0.015	0.30 ± 0.07	0.038	0.77 ± 0.18	0.139	2.77 ± 0.68
Fall	9.0 ± 5	6.1	0.220	2.10 ± 1.16	0.595	5.36 ± 2.97	0.501	4.50 ± 2.50
Winter	-15.3 ± 5	8.8	0.488	-7.47 ± 2.44	1.114	-17.04 ± 5.57	1.043	-15.93 ± 5.20
Yearly Average				-1.28 ± 0.94		-2.73 ± 2.20		-2.23 ± 2.26

之間。此結果與Liu et al. (2002)以三維數值模式及SeaWiFs水色資料所估算南海基礎生產力之平均值的變動範圍 (280-350 mgC m² day⁻¹), 以及Chen et al.(2004)在SEATS附近實測之基礎生產力之結果 (2000及2001年三月時, 基礎生產力分別為180和330 mgC m² day⁻¹) 大致吻合。故支持生物生產作用的確是形成由冬轉夏期間, 混合層NTCO₂和“fCO₂ at 27 ”遞減趨勢的主要原因。

3.1.5 碳氮消耗不平衡的現象

由上節的討論得知, 生物生產作用應是由冬到夏混合層中 NTCO₂ 遞減的主因。若生物生產作用對碳、氮之消耗依 Redfield-ratio 之碳、氮比 (C:N=106:16 ; Redfield et al., 1963) 來進行, 則此一時期 NTCO₂ 的減少量 (21μmol kg⁻¹) 所對應硝酸鹽之消耗量應為 3.2 μmol kg⁻¹。然而, 此一時期所觀測到硝酸鹽之減少量僅約 0.4 μmol kg⁻¹。換言之, 此段時期內僅有約 12.5% 生物生產所需的氮是由硝酸鹽所提供, 其餘 87.5% 的氮則必須有另外的來源。雖然, 近年來的研究已指出, 在氮限制的情況下, 浮游植物體內的碳、氮比會較 Redfield-ratio 為高 (此現象被稱為“carbon overconsumption”; Toggweiler, 1993; Sambrotto et al., 1993), 但即使在此種情況下, 浮游植物體內的碳、氮組成最多也不會超過 Redfield-ratio 的兩倍 (Copin-Montégut, 2000; Michales et al., 2001)。因此, 縱然在最極端的情形下 (碳、氮比假定為 Redfield-ratio 的 3 倍), 在 SEATS 測站, 仍有 62% 左右的氮並非直接由硝酸鹽所提供。近來最常被提及用來解釋此一碳、氮不平衡現象的機制為固氮作用 (Karl et al., 1997)。雖然, 南海符合所有固氮作用發生所需之環境條件 (高溫, 缺乏硝酸鹽, 水體分層良好和充足鐵的供應), 且 Wong et al. (2002) 根據硝酸鹽異常值的計算, 認為 SEATS 測站在秋、冬兩季應有明顯固氮作用的發生。然而, Chen et al. (2003, 2004) 調查 *Trichodesmium* sp. 和 *R. intracellularis* 在南海的分佈指出, 此二類固氮藍綠藻 (nitrogen-fixing cyanobacteria) 的分佈都很稀疏, 其對新生產力的貢獻不超過 3%。Wu et al. (2003) 認為, 由於可供鐵鍵結之

有機配位基 (iron-binding organic ligands) 的缺乏，使得南海雖然有很高的大氣鐵沉降通量，但海水中真正可供生物使用之溶解態鐵的濃度卻很低，因此限制了 *Trichodesmium* 的生長。是故，固氮作用可能亦無法完全解釋氮不足的現象。

綜言之，根據現有的資料判斷，在 SEATS 測站，即使考慮了“carbon overconsumption”的因素，硝酸鹽還是無法完全提供生物生長所需的氮。而受限於溶解態鐵濃度的不足，固氮作用可能亦無法完全說明的氮不足。因此，欲揭開 SEATS 測站“mysterious carbon draw-own”的謎底，勢必對溶解態有機氮 (DON) 的循環，浮游動物垂直運動對營養鹽輸送所扮演的角色以及其它固氮生物可能之貢獻. 等等的機制，作進一步詳細的研究。

3.2 SEATS測站標準化鹼度 (NTA) 標準化總二氧化碳 (NTCO₂) 及總二氧化碳同位素組成 ($\delta^{13}\text{C}_{\text{TCO}_2}$) 之垂直分佈特徵:控制機制及人為二氧化碳影響之探討

大氣二氧化碳濃度持續的升高，勢必造成海水碳化學系統的變化，進而使碳循環發生改變。為提供日後探討南海碳化學系統變化時，可供對比之基準。本節中將針對現今控制SEATS測站NTA，NTCO₂以及 $\delta^{13}\text{C}_{\text{TCO}_2}$ 垂直變化的機制進行探討，同時亦將分別利用碳化學及 $\delta^{13}\text{C}_{\text{TCO}_2}$ 的資料來估算人為二氧化碳目前在SEATS測站垂直分佈的狀況。

3.2.1 磷酸鹽 (PO_4^{3-}) 硝酸鹽 (NO_3^-) 表觀溶氧消耗量 (AOU) NTA、NTCO₂ 和 $\delta^{13}\text{C}_{\text{TCO}_2}$ 之垂直分佈

在正式進入討論前，首先說明表觀溶氧消耗量 (AOU) 之定義，以及本節中NTA與NTCO₂之計算方式：

表觀溶氧消耗量 (Apparent oxygen utilization; AOU): 為溶氧理論飽和值與實測值的差。溶氧理論飽和值是根據各水樣之溫鹽資料帶入Benson and Krause (1984)的公式所求出。

$$\text{NTA} = \text{TA} \times (35) \div (\text{實測鹽度})$$

$$\text{NTCO}_2 = \text{TCO}_2 \times (35) \div (\text{實測鹽度})$$

此處是以 35 為鹽度校正之基準，而非混合層中之平均鹽度 (33.5)。此項調整，仍因在討論整個水層碳化學參數變化時，基於水團來源之複雜性，一般而言，文獻中都將鹽度之標準化基準訂為 35，在此我們採用相同之標準，以方便與其它研究之比較。

根據前人的研究，海水碳化學參數以及 $\delta^{13}\text{C}_{\text{TCO}_2}$ 的垂直變化與營養鹽及AOU等參數的變化密切相關 (Kroopnick et al., 1972; Kroopnick, 1985; Lin et al., 1999)。故本節首先將就上述這些相關參數在 SEATS 測站垂直變化的狀況做比

較。圖 3.10 是 2002 年 3 月至 2003 年 8 月間七個 SEATS 水文及生地化調查航次所測得之 PO_4^{3-} 、 NO_3^- 、AOU、NTA、 NTCO_2 和 $\delta^{13}\text{C}_{\text{TCO}_2}$ 的垂直分佈圖。由圖中可發現 PO_4^{3-} 、 NO_3^- 和 AOU 三者之垂直分佈非常相似，其濃度在表水幾乎都為零，而後一直到 1000m 左右，三者的濃度均隨深度增加而快速增加，1000m 以下則幾乎保持不變。此三者垂直變化高度的相似性乃預期中的結果。因 PO_4^{3-} 和 NO_3^- 隨深度的增加，主要是由於有機質分解將營養鹽重新釋放回海水中所造成，而有機質分解會同時消耗掉溶氧，故造成 AOU 與營養鹽同步增加的趨勢。NTA 及 NTCO_2 之垂直分佈亦呈現隨深度遞增的趨勢。然而，其變化趨勢與前述三者有所不同：NTA 在 150m 以上並無明顯變化 ($\sim 2300\mu\text{mol kg}^{-1}$)，而後隨深度增加而增加，此增加趨勢一直持續到 1600m 左右，1600m 以下則幾乎維持不變； NTCO_2 之垂直變化趨勢雖與營養鹽及 AOU 較為相似，但其隨深度遞增的趨勢，一直持續到約 1400m 為止，亦明顯有別於營養鹽及 AOU 的 1000m。此種差異表明了雖然 NTA 及 NTCO_2 與營養鹽及 AOU 相似，其濃度都隨深度的增加而增加，但控制其垂直變化的機制，應與營養鹽及 AOU 有所不同。由於 NTA 及 NTCO_2 是瞭解海水碳化學系統以及探討人為二氧化碳影響的基礎，故其垂直變化之控制機制，將於下節中做較完整的討論。 $\delta^{13}\text{C}_{\text{TCO}_2}$ 之垂直變化，幾乎與營養鹽及 AOU 的變化完全相反，意即隨深度增加而遞減。而此種緊密的相關性，代表 $\delta^{13}\text{C}_{\text{TCO}_2}$ 之垂直變化，主要可能亦是受到有機質分解作用所控制。而之所以會呈現相反的變化趨勢，乃因浮游植物行光和作用時，傾向使用較輕的 ^{12}C ，故有機質之 $\delta^{13}\text{C}$ 會較海水的 $\delta^{13}\text{C}_{\text{TCO}_2}$ 為輕。當有機質分解釋放營養鹽並消耗溶氧的同時，亦會釋放較輕的 ^{12}C 回到海水中使 $\delta^{13}\text{C}_{\text{TCO}_2}$ 變輕，於是形成營養鹽和 AOU 與 $\delta^{13}\text{C}_{\text{TCO}_2}$ 反向同步變化的趨勢。雖然， $\delta^{13}\text{C}_{\text{TCO}_2}$ 之垂直變化，主要應受控於有機質的分解作用，但誠如 1.5 節所言， $\delta^{13}\text{C}_{\text{TCO}_2}$ 會受到人為二氧化碳的影響，故其垂直變化的控制機制，將於下節中與 NTA 及 NTCO_2 之垂直變化的控制機制一併再做深入的討論。以作為探討人為二氧化碳影響之基礎。

由 PO_4^{3-} 、 NO_3^- 、AOU 垂直變化的相似性，不難推知此三者兩兩之間應有良

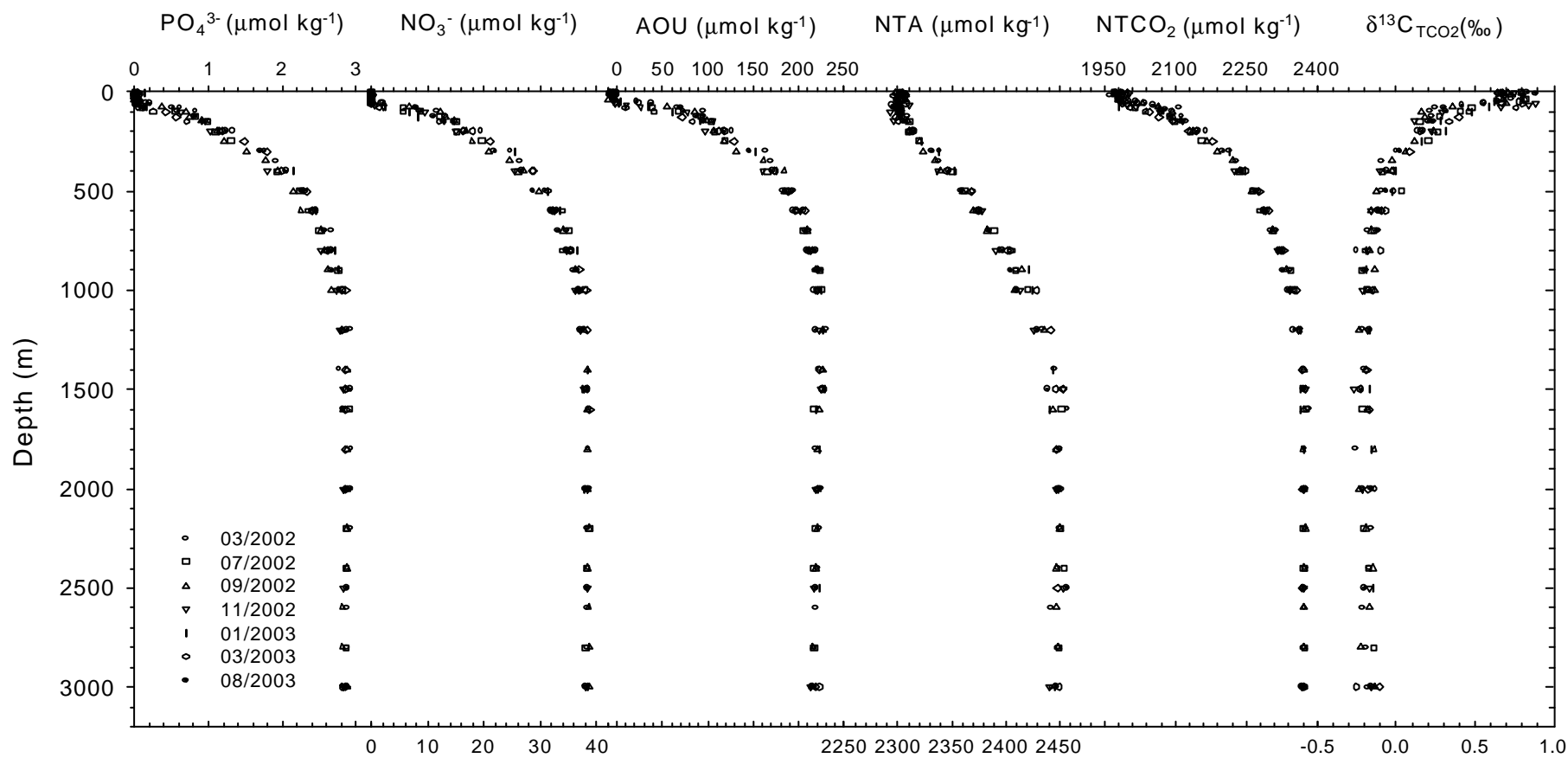


圖 3.10 2002 年 3 月至 2003 年 8 月間七個 SEATS 水文及生地化調查航次所測得之 PO_4^{3-} 、 NO_3^- 、AOU、NTA、 NTCO_2 和 $\delta^{13}\text{C}_{\text{TCO}_2}$ 的垂直分佈圖。

好的線性相關，且可預期此線性關係之斜率，應與 Redfield-ratio 相近（本研究引用之 Redfield-ratio 為 Anderson and Sarmiento (1994)所發表的比值）。然而，由圖 3.10 (a)-(c)可發現，無論是 PO_4^{3-} 對 AOU (P/AOU)、 NO_3^- 對 AOU (N/AOU) 還是 NO_3^- 對 PO_4^{3-} (N/P) 作圖的結果都顯示：水深 100m 以上的資料（圖 3.11 之實心三角形）大致皆與 Redfield-ratio 所預期之結果相符，但 100m 以下之資料（圖 3.11 之實心圓），雖然三者的確都呈現良好之線性相關，然而其斜率卻明顯與 Redfield-ratio 不同，其中 P/AOU 和 N/AOU 之斜率較 Redfield-ratio 為大， N/P 則較 Redfield-ratio 為小。 P/AOU 和 N/AOU 之斜率較 Redfield-ratio 為大的現象，主要應是營養鹽與 AOU 起始值（preformed value，指該水樣出露海平面時所具有的值）的差異所造成。一般而言，全球表水營養鹽濃度之分佈有隨溫度降低而增加的趨勢，故隨著深度的增加，溫度亦隨之降低，其具有營養鹽之起始濃度就愈高。但溶氧在全球表水中幾乎都呈現飽和的狀態，因此不同深度的水其 AOU 的起始值，應該都非常接近於零。在此種營養鹽起始值隨深度增加，而 AOU 不變的情況下，便形成了愈深的水其 P/AOU 和 N/AOU 與 Redfield-ratio 所代表之理論關係線偏差量愈大的現象，也因此形成了 P/AOU 和 N/AOU 的斜率較 Redfield-ratio 為高的現象。而 100m 以上，由於營養鹽起始值的差異並不明顯，故尚能大致維持與 Redfield-ratio 所預期相符之結果。為了檢驗上述推論的正確性，本研究根據 Chen et al. (1986)所發表太平洋表水 PO_4^{3-} 起始值和 NO_3^- 起始值與位溫之關係式，計算出每個水樣之 PO_4^{3-} 和 NO_3^- 的起始濃度，而後以 PO_4^{3-} 和 NO_3^- 之實測濃度減去起始濃度，即可得出因有機質分解作用所產生之再生性 PO_4^{3-} (P_{Rg}) 和再生性 NO_3^- (N_{Rg}) 的濃度。 P_{Rg} 和 N_{Rg} 對 AOU 之作圖結果顯示（圖 3.11 之空心正方形）， P_{Rg} 與 AOU 之關係已大致回到 Redfield-ratio 所預期的理論關係線上，顯示起始值的差異的確是造成 P/AOU 的斜率較 Redfield-ratio 為高的主因。然而， N_{Rg} 與 AOU 之關係卻仍與 Redfield-ratio 所應有之關係模式有相當程度的偏差（圖 3.11(b) 之空心正方形），在 AOU 濃度小於 $130\mu\text{mol kg}^{-1}$ 時， $\text{N}_{\text{Rg}}/\text{AOU}$ 的比都較 Redfield-ratio 為大；反之，當 AOU 濃度大於 $130\mu\text{mol kg}^{-1}$

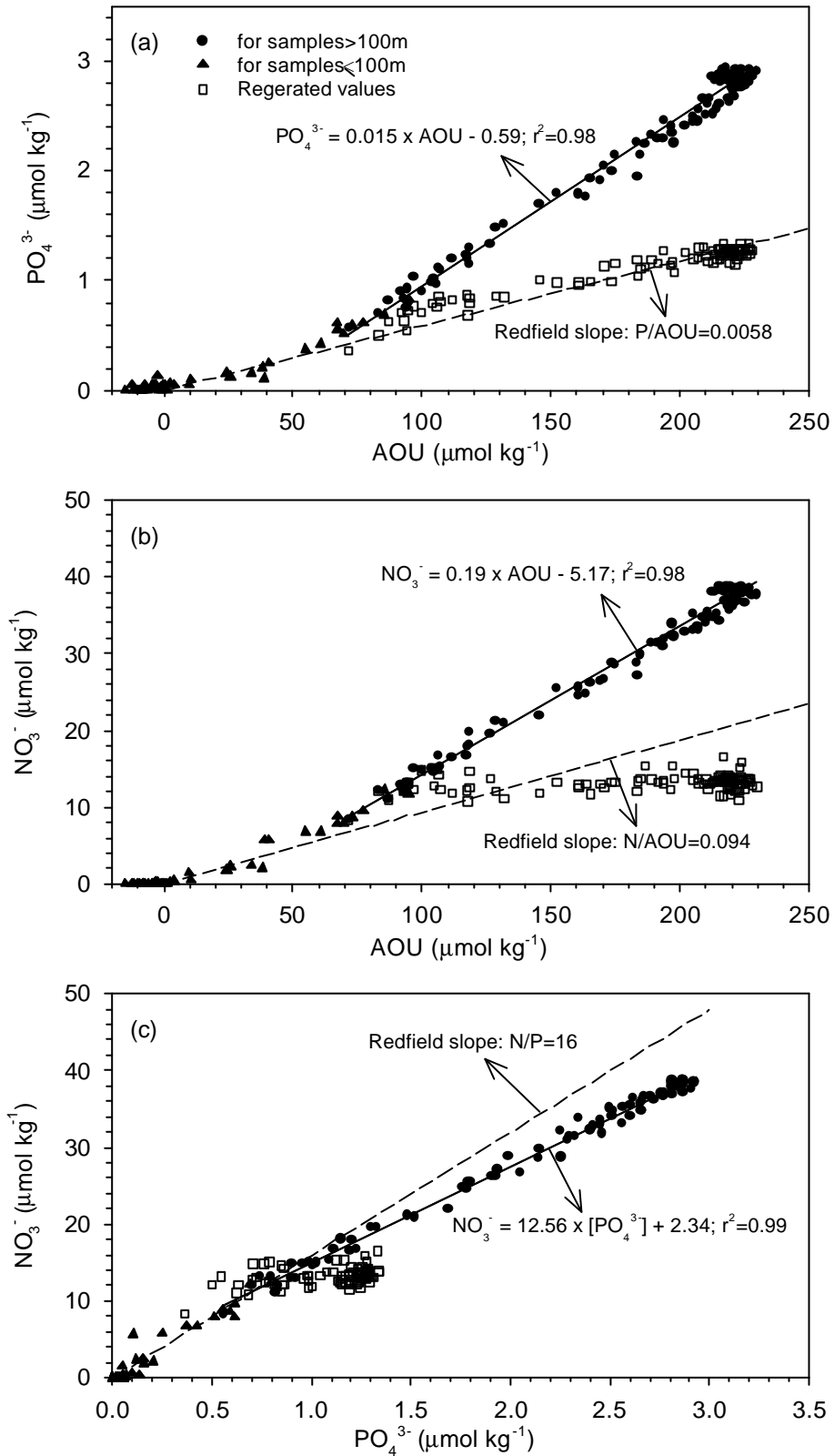


圖 3.11 SEATS 測站(a) PO_4^{3-} 對 AOU , (b) NO_3^- 對 AOU 和(c) NO_3^- 對 PO_4^{3-} 之關係圖。實心三角形代表 100m 以上水樣之測值，實心圓形代表 100m 以下水樣之測值，空心正方形代表再生性 PO_4^{3-} 和 NO_3^- 的值。

時， N_{Rg}/AOU 的比都較 Redfield-ratio 為小。 N_{Rg}/P_{Rg} 亦有類似的情況（圖 3.11(c) 之空心正方形），在 PO_4^{3-} 濃度低於 $0.8\mu\text{mol kg}^{-1}$ 時， N_{Rg}/P_{Rg} 的比都較 Redfield-ratio 為大；反之，當 PO_4^{3-} 濃度高於 $0.8\mu\text{mol kg}^{-1}$ 時， N_{Rg}/P_{Rg} 的比都較 Redfield-ratio 為小。推測此種趨勢的形成，可能與固氮及脫硝作用有關。為探討固氮和脫硝作用對 N_{Rg}/AOU 及 N_{Rg}/P_{Rg} 比可能之影響。本研究進一步計算了硝酸鹽異常值（nitrate anomaly, N^* ） N^* 的定義如下（Gruber and Sarmiento, 1997; Deutsch et al., 2001）：

$$N^* = N - 16P + 2.90$$

N^* 為一相對性之指標，當 $N^* > 0$ 時，代表該水體與全球海水平均值相較而言，固氮作用對氮循環之影響超過了脫硝作用；反之，當 $N^* < 0$ 時，代表脫硝作用對氮循環之影響超過了固氮作用。由圖 3.12 可發現在 SEATS 測站水深 200m 以下 N^* 皆 < 0 ，表明了 200m 以下的水體的確可能經歷了脫硝作用，進而造成次表層以下之水體， N_{Rg}/AOU 及 N_{Rg}/P_{Rg} 比較 Redfield-ratio 為小的現象。水深 200m 以上 N^* 皆 > 0 ，代表 SEATS 測站極可能有固氮作用在進行。然而，3.1.5 節的討論已指出，雖然南海符合所有固氮作用發生所需之環境條件，但 *Trichodesmium sp.* 和 *R. intracellularis* 二類固氮藍綠藻的濃度卻很低，故此 N^* 的高值，是否為固氮作用所造成尚有疑問。此外，南海為一半封閉性之邊緣海，河川輸入之影響並不能完全忽略。而南海周遭河川之 N/P 比遠高於 Redfield-ratio (~ 86 ; Chen et al., 2001)，亦是形成 N^* 高值的可能原因。總之，在固氮作用對南海氮循環所扮演之角色徹底被釐清之前，並無法確定此 N^* 高值是由固氮作用所造成。

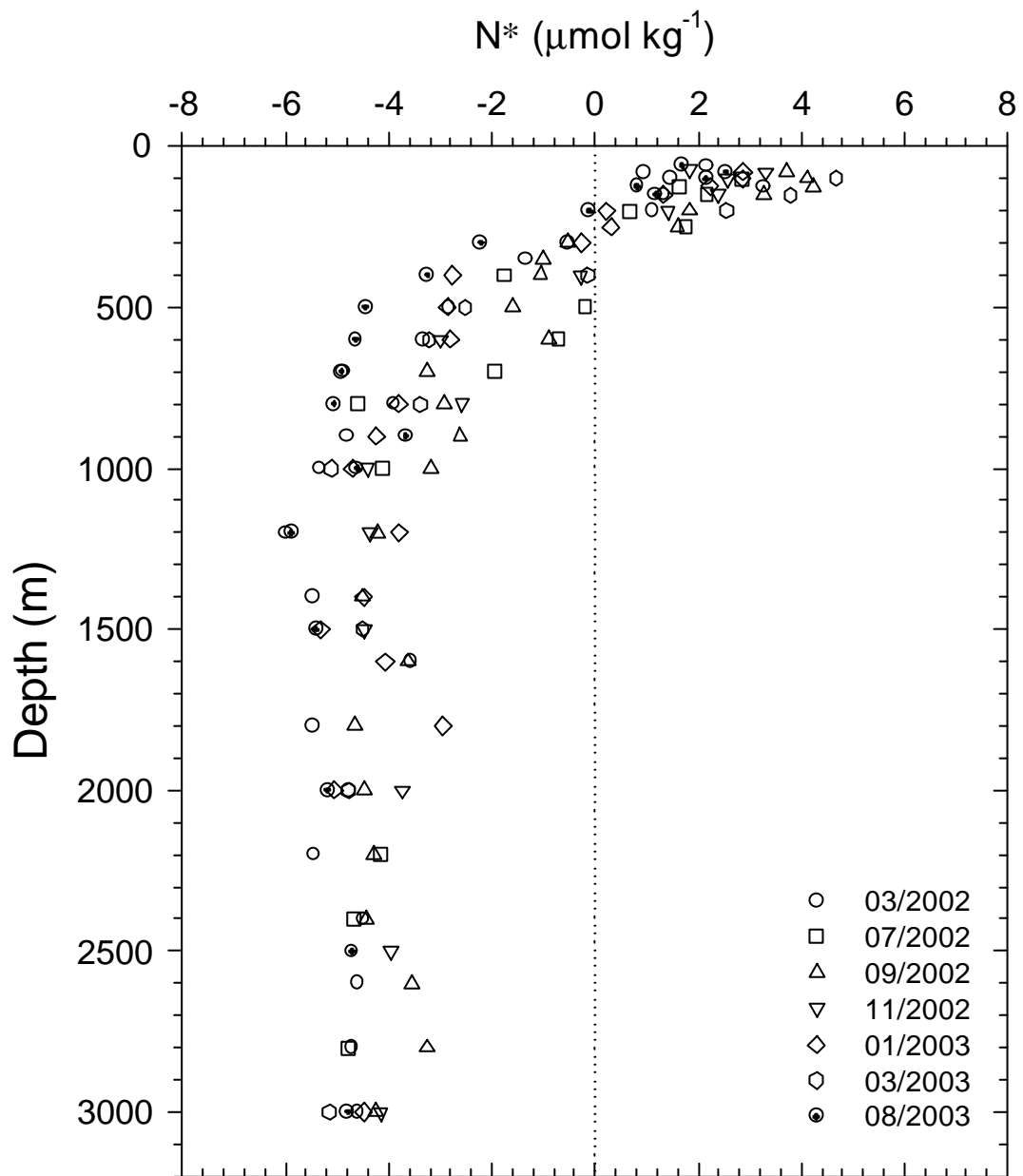


圖 3.12 SEATS 測站硝酸鹽異常值 (nitrate anomaly, N^*) 之垂直分佈圖。

3.2.2 NTA、NTCO₂ 和 δ¹³C_{TCO₂} 垂直變化之控制機制

對任一水樣而言，我們所量測到 NTA、NTCO₂ 和 δ¹³C_{TCO₂} 的值，都可視為是下列三項因子加總的結果(Chen and Millero, 1979; Kroopnick, 1985; Feely et al., 2002): (1) 起始值，指該水樣出露海表面時所具有的值；(2) 有機質分解作用所造成之變動量；(3) 碳酸鈣溶解作用所造成之變動量。上述之關係可以方程式表達如下：

$$\text{NTA}^{\text{meas}} = \text{NTA}^{\text{pre}} + \text{TA}^{\text{org}} + \text{TA}^{\text{carb}} \dots\dots\dots \text{Eq. 3.1}$$

$$\text{NTCO}_2^{\text{meas}} = \text{NTCO}_2^{\text{pre}} + \text{TCO}_2^{\text{org}} + \text{TCO}_2^{\text{carb}} \dots\dots\dots \text{Eq. 3.2}$$

$$\delta^{13}\text{C}^{\text{meas}} = \delta^{13}\text{C}^{\text{pre}} + \delta^{13}\text{C}^{\text{org}} + \delta^{13}\text{C}^{\text{carb}} \dots\dots\dots \text{Eq. 3.3}$$

Eq. 3.1 – Eq. 3.3 中上標之縮寫 meas, pre, org 和 carb 分別代表實測值，起始值，有機質分解作用所造成之變動量以及碳酸鈣溶解作用所造成之變動量。由上述之說明可知，NTA、NTCO₂ 和 δ¹³C_{TCO₂} 在垂直方向之變化，是由上述三項因子之消長變化所共同形成。以下將分別針對此三項因子對 NTA、NTCO₂ 和 δ¹³C_{TCO₂} 垂直變化之相對貢獻程度進行分析，以瞭解現今控制這些參數垂直變化之作用機制由淺至深變化的情形。

(I) NTA

如 Eq. 3.1 所示，NTA^{meas} 是由 NTA^{pre}、TA^{org} 和 TA^{carb} 等三個部分加總而成。由於全球表水之 TA 通常與溫鹽等守恆性示蹤劑 (conservative tracers) 有良好之相關性，且大氣二氧化碳濃度的增加，並不會直接造成 TA 的改變。故在假設由過去到現在 TA 與這些守恆性示蹤劑之關係不變的條件下，可將各水樣之溫、鹽 .. 等等資料帶入其與現今 TA 之回歸方程式，即可求出各水樣之 NTA^{pre}。本研究採用 Sabine et al.(2002a)根據 WOCE/JGOFS 資料所建立之太平洋 TA 與溫、鹽及 PO (PO = DO + 170 x [PO₄³⁻]) 等參數之複回歸方程式：

$$\text{TA}^{\text{pre}} = 148.7 + (61.36 \times S) + (0.00941 \times \text{PO}) - (0.0582 \times \theta)$$

來計算 SEATS 測站不同深度之 NTA^{pre}。結果顯示 NTA^{pre} 由表層之 2305 μmol kg⁻¹

左右，隨深度逐漸增加，到 1500m 處約為 $2353 \mu\text{mol kg}^{-1}$ 。1500m 以下則幾乎保持不變（圖 3.13 空心正方形）。由此分佈趨勢可知， NTA^{meas} 隨深度遞加之趨勢有部分是由於 NTA^{pre} 隨深度增加所造成的結果。若就整個垂直剖面之增加量而言， NTA^{pre} 增加對 NTA^{meas} 的貢獻量約佔 33.3%（50/150）。

有機質進行氧化分解反應時，會釋放質子造成 TA 的減少（Brewer and Goldman, 1976; Chen et al., 1982）。此部分 TA 之減少量，可由 AOU 的資料換算求出，其關係如下（Feely et al., 2002）：

$$\text{TA}^{\text{org}} = -0.019 \times \text{AOU}$$

由於 TA^{org} 是由 AOU 的資料所求出，故有機質分解所造成 TA 之減少量（圖 3.13，空心正方形與三角形的差）應與 AOU 的變化相同，意即隨深度增加而增加。

碳酸鈣溶解時會釋放碳酸根離子（ CO_3^{2-} ），造成鹼度的增加。此溶解效應所造成 TA 的增加量可由 NTA^{meas} 減去（ $\text{NTA}^{\text{pre}} + \text{TA}^{\text{org}}$ ）後求出（圖 3.13，空心圓與三角形的差）。結果顯示， TA^{carb} 亦呈現隨深度增加而增加的趨勢，說明碳酸鈣溶解量的增加，亦是造成 TA^{meas} 隨深度遞增的原因之一。

綜上所述，控制 SEATS 測站 NTA^{meas} 垂直變化的機制之作用概況可歸納如下：由表層至 150m 的深度範圍內，由於 NTA^{pre} 之增加量與 TA^{org} 之減少量相互抵銷，且此深度範圍內，碳酸鈣尚處於過飽和狀態，還無須考慮其溶解作用。故 NTA^{meas} 在此深度範圍內大致保持不變。150m 以下， NTA^{meas} 隨深度增加而增加的趨勢一直持續到 1600m 左右。此一增加趨勢是由 NTA^{pre} 及 TA^{carb} 增加所共同造成的結果，在 500m 以上 NTA^{pre} 的貢獻較 TA^{carb} 為大；500m 以下 TA^{carb} 則是造成 NTA^{meas} 隨深度遞增最重要的因素。 TA^{org} 在此深度範圍內，雖然仍會造成 NTA^{meas} 的減少，但其重要性遠不及 NTA^{pre} 及 TA^{carb} 對 NTA^{meas} 的增加效果，故其僅扮演減緩 NTA^{meas} 之垂直增加梯度的角色。

(II) NTCO_2

如 Eq. 3.2 所示， $\text{NTCO}_2^{\text{meas}}$ 是 $\text{NTCO}_2^{\text{pre}}$ 、 $\text{TCO}_2^{\text{org}}$ 和 $\text{TCO}_2^{\text{carb}}$ 等三個部分加總的結果。其中 $\text{TCO}_2^{\text{org}}$ 可依 Redfield-ratio 之 C/AOU 比（117/170; Anderson and

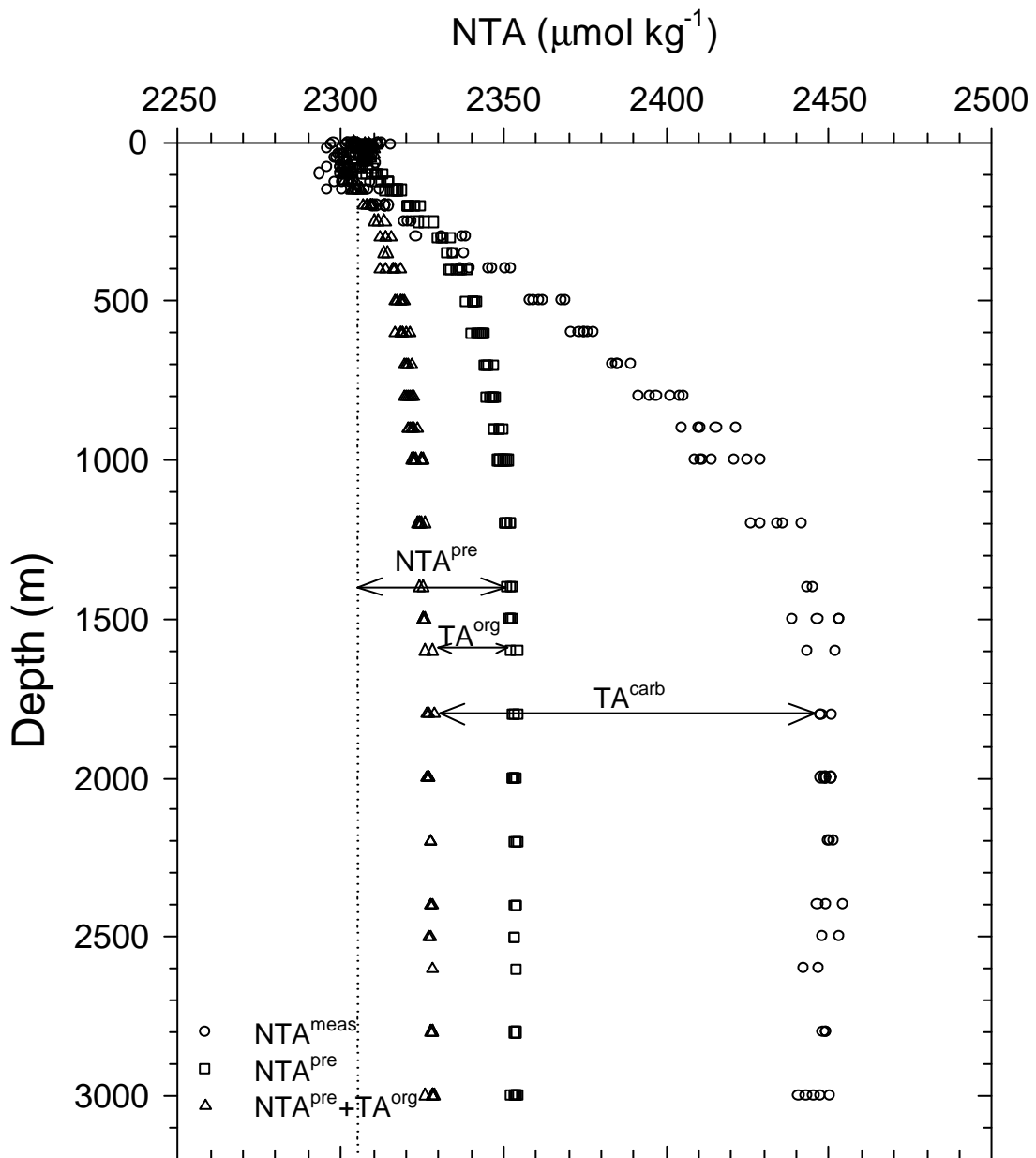


圖 3.13 SEATS 測站 NTA 實測值 (NTA^{meas})、NTA 起始值 (NTA^{pre}) 和 NTA 起始值 + 有機質分解所造成 TA 之變化量 ($NTA^{pre} + TA^{org}$) 之垂直分佈圖。

Sarmiento, 1994), 帶入 AOU 的資料而求出, 以方程式表示如下:

$$\text{TCO}_2^{\text{org}} = 117/170 \times \text{AOU}$$

由於碳酸鈣溶解時, 造成 TA 及 TCO_2 增加之莫耳數比為 2:1, 故 $\text{TCO}_2^{\text{carb}}$ 可由 TA^{carb} 的資料計算而得, 以方程式表示如下:

$$\begin{aligned}\text{TCO}_2^{\text{carb}} &= 0.5 \times \text{TA}^{\text{carb}} = 0.5 \times (\text{NTA}^{\text{meas}} - \text{NTA}^{\text{pre}} - \text{TA}^{\text{org}}) \\ &= 0.5 \times (\text{NTA}^{\text{meas}} - \text{NTA}^{\text{pre}}) + 0.0593 \times \text{AOU}\end{aligned}$$

一旦 $\text{TCO}_2^{\text{org}}$ 和 $\text{TCO}_2^{\text{carb}}$ 由上列兩組方程式求出後, $\text{NTCO}_2^{\text{pre}}$ 即可由 $\text{NTCO}_2^{\text{meas}}$ 減去 ($\text{TCO}_2^{\text{org}} + \text{TCO}_2^{\text{carb}}$) 求得。

$\text{NTCO}_2^{\text{pre}}$ 、 $\text{TCO}_2^{\text{org}}$ 和 $\text{TCO}_2^{\text{carb}}$ 之計算結果繪於圖 3.14。由圖中可發現 $\text{NTCO}_2^{\text{pre}}$ (正方形)、 $\text{TCO}_2^{\text{org}}$ (三角形與正方形的差) 和 $\text{TCO}_2^{\text{carb}}$ (圓形與三角形的差) 大致上都呈現隨深度漸增之趨勢, 由此可見起始值、有機質分解量及碳酸鈣溶解量之增加, 對形成 $\text{NTCO}_2^{\text{meas}}$ 隨深度遞增之趨勢皆有貢獻。此三者之相對貢獻隨深度變化的情況概述如下: 水深 400m 以上, $\text{NTCO}_2^{\text{meas}}$ 隨深度的增加主要是由 $\text{NTCO}_2^{\text{pre}}$ 和 $\text{TCO}_2^{\text{org}}$ 的增加所造成, 且兩者之貢獻比例大約相等。而 $\text{TCO}_2^{\text{carb}}$ 在此深度範圍內, 對 $\text{NTCO}_2^{\text{meas}}$ 的增加並無明顯貢獻, 主因碳酸鈣在此深度範圍內仍處於過飽和狀態, 故不易發生溶解。400m 以下, $\text{TCO}_2^{\text{carb}}$ 的訊號開始出現, 然而, 其對 $\text{NTCO}_2^{\text{meas}}$ 增加的貢獻度, 仍明顯小於 $\text{NTCO}_2^{\text{pre}}$ 和 $\text{TCO}_2^{\text{carb}}$ 。若就整個垂直剖面的增加量而言, $\text{NTCO}_2^{\text{pre}}$ 、 $\text{TCO}_2^{\text{org}}$ 和 $\text{TCO}_2^{\text{carb}}$ 三者所佔百分比分別約為 40%, 40% 和 20%。

由於碳酸鈣溶解會造成 TA 的增加, 進而增強海洋對大氣二氧化碳之吸收能力。而有機質的分解則會造成 TCO_2 增加, 使海洋對大氣二氧化碳之吸收能力減弱。因此, 海水中 IC/OC 比 (碳酸鈣溶解所造成 TCO_2 之增加量與有機質分解所造成 TCO_2 之增加量的比, 即 $\text{TCO}_2^{\text{carb}}/\text{TCO}_2^{\text{org}}$ 比) 是瞭解海水對大氣二氧化碳吸收能力的關鍵參數之一, 同時 IC/OC 比亦可應用於 TCO_2 輸入機制的研究, 故其亦為探討海水碳化學系統特徵, 最重要的參數之一。SEATS 測站 IC/OC 隨深度之變化繪於圖 3.15。如圖所示, IC/OC 在 200m 以上皆為 0 左右, 而後 IC/OC

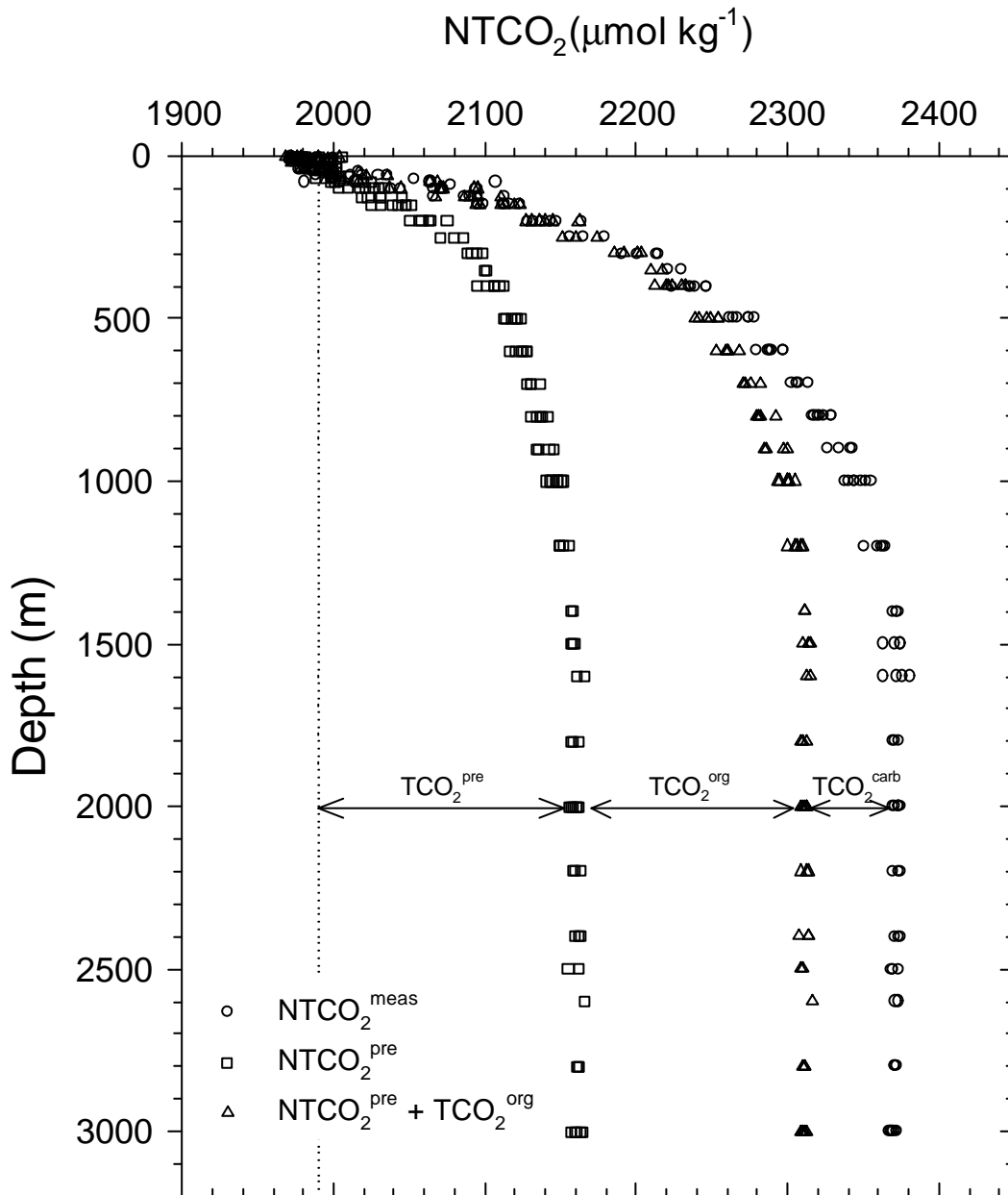


圖 3.14 SEATS 測站 NTCO_2 實測值 ($\text{NTCO}_2^{\text{meas}}$)、 NTCO_2 起始值 ($\text{NTCO}_2^{\text{pre}}$) 和 NTCO_2 起始值 + 有機質分解所造成 TCO_2 之變化量 ($\text{NTCO}_2^{\text{pre}} + \text{TCO}_2^{\text{org}}$) 之垂直分佈圖。

比隨深度之增加而漸加，1500m 以下則維持不變 (~0.4)。IC/OC 比此種隨深度遞增之趨勢，顯示海水中 TCO_2 增加來自於碳酸鈣溶解之貢獻比例隨深度增加而漸增。此種現象主要是由於碳酸鈣之溶解度隨深度遞增所造成。整個垂直剖面中 IC/OC 比最大值約為 0.4，代表即使在最多的情況下，碳酸鈣溶解對 TCO_2 增加的貢獻百分比，亦僅約 29%。由此可見，不論對任何深度而言，有機質的分解作用才是造成海水中 TCO_2 增加的主要因素。本研究之計算結果顯示，SEATS 測站水深 1500m 以下碳酸鈣溶解佔 TCO_2 增加之百分比 (~29%) 與太平洋 1000m 以下的比例非常接近 (~26%到~29%; Tsunogai, 1972; Kroopnick, 1974; Chen, 1990)，支持南海深層及底層水之來源為太平洋深層水且其駐留時間不長的論點。

為了瞭解碳酸鈣溶解作用隨深度變化的情形，本研究利用 Lewis and Wallace (1998)所發展之海水二氧化碳系統計算程式，計算了所有水樣之霏石 (aragonite) 及方解石 (calcite) 的飽和度 ($\Omega = [\text{Ca}^{2+}] \times [\text{CO}_3^{2-}]/K_{sp}$)。一如 IC/OC 比所預期的結果，霏石及方解石的飽和度都呈現隨深度遞減的趨勢，其化學飽和深度 ($\Omega = 1$) 分別為 600m 及 2500m(圖 3.16)。此外，為了進一步探究碳酸鈣溶解所造成 TCO_2 之增加量與霏石及方解石飽和程度之相關性，圖 3.16 將此三個參數一起對深度作圖。結果顯示，在霏石化學飽和深度(約 600m)之上，即出現了 $\text{TCO}_2^{\text{carb}}$ 的訊號。換言之，碳酸鈣在其化學飽和深度之上即發生了溶解的現象。此現象顯然與傳統上認為碳酸鈣的溶解，僅能發生在化學飽和深度以下的認知不相符。然而，近年來有愈來愈多的研究指出，碳酸鈣極有可能在其化學飽和深度之上，就發生了顯著的溶解。例如，Milliman et al. (1999) 分析全球沉積物收集器的資料後，認為高達 60-80% 表水所生產之碳酸鈣，在水深 500m 至 1000m 的範圍內就已溶解。Feely et al. (2002) 和 Sabine et al. (2002b) 計算太平洋及印度洋之超量 TA (Excess TA，與本文之 TA^{carb} 的定義相同) 時亦發現，在霏石及方解石的化學飽和深度以上，就出現了 Excess TA 的訊號，作者亦將此現象歸因於碳酸鈣的溶解。本研究 $\text{TCO}_2^{\text{carb}}$ 和霏石與方解石飽和度之計算結果，似乎也支持此項論點。

到目前為止，被認為可能使碳酸鈣在其化學飽和深度以上就發生溶解之作

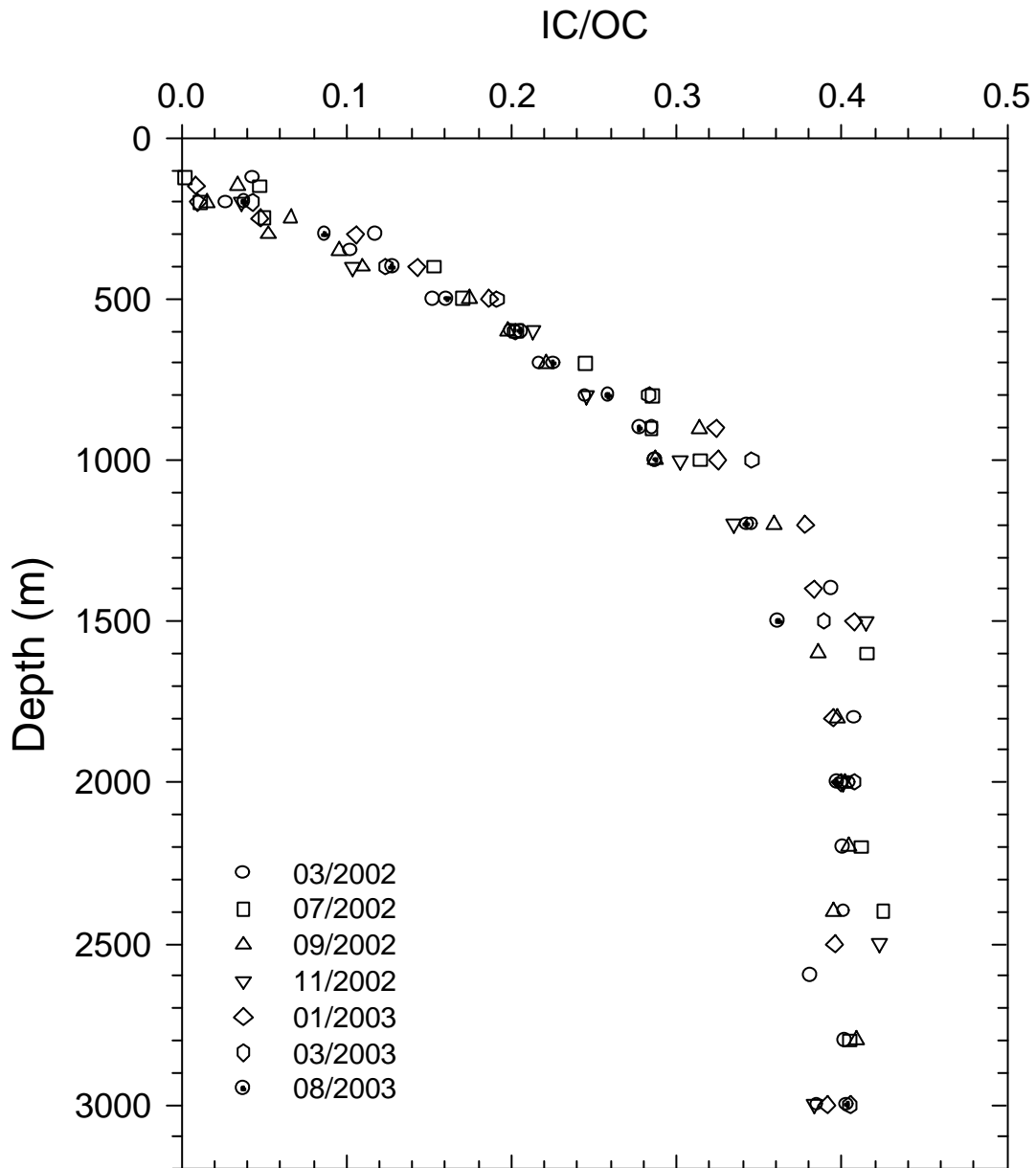


圖 3.15 SEATS 測站碳酸鈣溶解所造成 TCO_2 之增加量 (IC) 與有機質分解所造成 TCO_2 之增加量 (OC) 比值 (IC/OC) 之垂直分佈圖。

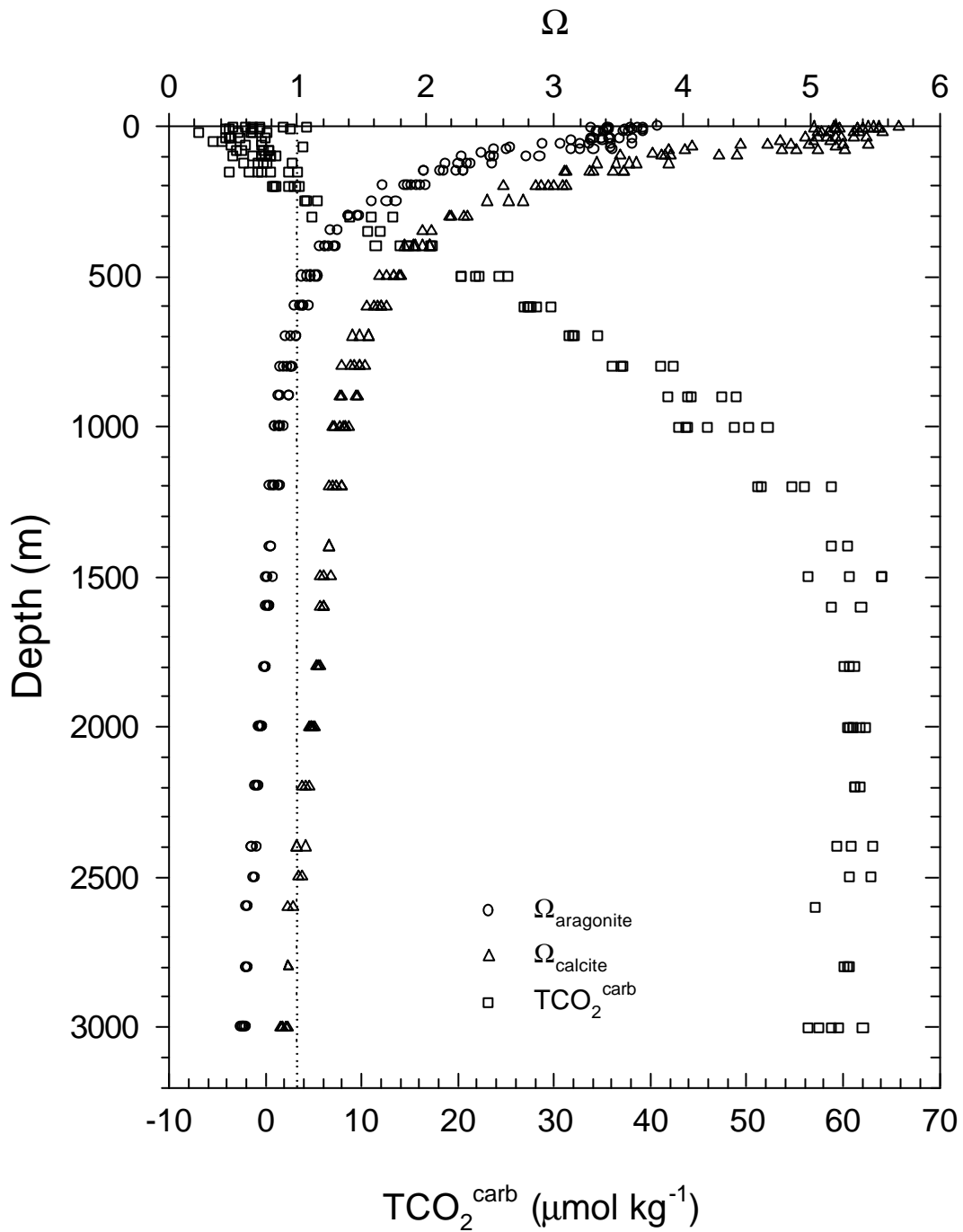


圖 3.16 SEATS 測站霰石與方解石飽和度 ($\Omega_{\text{aragonite}}$, Ω_{calcite}) 和碳酸鈣溶解所造成 $\text{TCO}_2^{\text{carb}}$ 之增加量 ($\text{TCO}_2^{\text{carb}}$) 之垂直分佈圖。

用機制包括 (Milliman et al., 1999): 碳酸鈣被浮游動物攝食後, 在其腸胃道中溶解; 細菌在分解有機質時, 可形成低 pH 值之微環境, (microenvironments) 造成碳酸鈣的分解; 海洋中存在有其它較霰石更易溶解之碳酸鹽類。上述這些機制, 都尚未獲得充分的證實。故碳酸鈣是否在其化學飽和深度以上就發生溶解? 目前尚存在著極大的爭論。此外, Chen (2002) 指出碳酸鈣溶解並非大洋中 TA 唯一的來源, 陸棚沉積物中有機質在還原環境下的分解作用, 亦會釋放出大量的 TA 向外洋傳送。故利用 TA 變化來計算碳酸鈣溶解量之結果應視為上限, 因為此類的計算中, 並未將沉積物中有機質在還原環境下分解所產生之 TA 考慮在內, 故可能高估了碳酸鈣溶解作用的貢獻。

(III) $\delta^{13}\text{C}_{\text{TCO}_2}$

為求出各水樣 $\delta^{13}\text{C}_{\text{TCO}_2}$ 之起始值以及有機質及碳酸鈣分解所造成 $\delta^{13}\text{C}_{\text{TCO}_2}$ 之變動量 ($\delta^{13}\text{C}^{\text{org}}$, $\delta^{13}\text{C}^{\text{carb}}$)。依質量平衡原理, 可將 Eq. 3.3 改寫成以下形式:

$$\delta^{13}\text{C}^{\text{meas}} \times \text{TCO}_2^{\text{meas}} = \delta^{13}\text{C}^{\text{pre}} \times \text{TCO}_2^{\text{pre}} + \delta^{13}\text{C}^{\text{org}'} \times \text{TCO}_2^{\text{org}} + \delta^{13}\text{C}^{\text{carb}'} \times \text{TCO}_2^{\text{carb}}$$

上式中 $\delta^{13}\text{C}^{\text{meas}}$ 和 $\delta^{13}\text{C}^{\text{pre}}$ 分別代表水樣 $\delta^{13}\text{C}_{\text{TCO}_2}$ 之實測值及起始值; $\delta^{13}\text{C}^{\text{org}'}$ 和 $\delta^{13}\text{C}^{\text{carb}'}$ 則分別代表有機質及碳酸鈣之 $\delta^{13}\text{C}$ 。

如前所述, 由於浮游植物行光和作用時, 傾向使用較輕的 ^{12}C , 故有機質之 $\delta^{13}\text{C}$ 會遠較海水之 $\delta^{13}\text{C}_{\text{TCO}_2}$ 為輕。Georiche and Fry (1994) 的研究指出在中、低緯度的海域內, 浮游植物之 $\delta^{13}\text{C}$ 僅在 -18 至 -22 ‰ 的範圍內變動, 故本研究取其平均值, 將有機質之 $\delta^{13}\text{C}$ 假定為 -20‰ 而浮游生物碳酸鈣殼體形成時, 碳同位素的分化作用極小, 故其 $\delta^{13}\text{C}$ 與海水 $\delta^{13}\text{C}_{\text{TCO}_2}$ 之差異多在 ± 1 ‰ 的範圍內 (Bonneau et al., 1980), 本研究將碳酸鈣之 $\delta^{13}\text{C}$ 假定為 +2‰ (約為全球表水之平均值)。由於 $\text{TCO}_2^{\text{pre}}$ 、 $\text{TCO}_2^{\text{carb}}$ 和 $\text{TCO}_2^{\text{org}}$ 等參數俱已在上節中求出, 故將上述兩個假定值帶入上述之質量平衡方程式, 即可求出 $\delta^{13}\text{C}^{\text{pre}}$ 。

計算結果顯示 (圖 3.17, 正方形), $\delta^{13}\text{C}^{\text{pre}}$ 由表層至水深 500m 隨深度增加而逐漸變重 (+0.7 至 +1.2‰)。此種變化趨勢極可能與不同深度的水, 受人為二氧化碳影響程度不同有關。一般而言, 愈深的水其出露海平面可與大氣進行海氣交換的年代距今愈久遠, 故其所受人為二氧化碳之影響應愈小, 而其 $\delta^{13}\text{C}^{\text{pre}}$ 應愈重。由於海氣交換平衡的程度及生物作用的差異亦會影響 $\delta^{13}\text{C}^{\text{pre}}$, 故 $\delta^{13}\text{C}^{\text{pre}}$ 隨深度遞增之趨勢, 並不能完全代表受人為二氧化碳影響的差異。下節中將再針對 $\delta^{13}\text{C}^{\text{meas}}$ 受人為二氧化碳之影響程度做更深入討論。

若暫時將碳酸鈣溶解對海水 $\delta^{13}\text{C}_{\text{TCO}_2}$ 之影響效應忽略不計, 則有機質分解所造成 $\delta^{13}\text{C}_{\text{TCO}_2}$ 之變化量可以下列方程式估算之:

$$\delta^{13}\text{C}^{\text{org}} = [(\delta^{13}\text{C}^{\text{pre}} \times \text{TCO}_2^{\text{pre}}) + (-20 \times \text{TCO}_2^{\text{org}}) / (\text{TCO}_2^{\text{pre}} + \text{TCO}_2^{\text{carb}}) - \delta^{13}\text{C}^{\text{pre}}$$

結果顯示, $\delta^{13}\text{C}^{\text{pre}}$ 加上有機質分解效應修正後, $(\delta^{13}\text{C}^{\text{pre}} + \delta^{13}\text{C}^{\text{org}})$ (圖 3.17 三角形) 即與 $\delta^{13}\text{C}^{\text{meas}}$ 非常接近, 表示 $\delta^{13}\text{C}^{\text{meas}}$ 隨深度遞減的趨勢, 主要是由於有機質分解所形成。換言之, 碳酸鈣溶解對海水 $\delta^{13}\text{C}_{\text{TCO}_2}$ 的垂直變化幾乎沒有影響。此種結果可歸因於下列兩項因素: 第一, 如前段所言, 有機質之 $\delta^{13}\text{C}$ 與海水 $\delta^{13}\text{C}_{\text{TCO}_2}$ 之差異遠較碳酸鈣之 $\delta^{13}\text{C}$ 與海水之 $\delta^{13}\text{C}_{\text{TCO}_2}$ 的差異為大。第二, 由上節 IC/OC 比的計算可知, 有機質分解對海水中 TCO_2 增加的效果遠較碳酸鈣的貢獻為大。因此, 有機質的分解, 同時兼具了同位素分化效應大及貢獻量多等兩個特點, 故其主導了海水中 $\delta^{13}\text{C}_{\text{TCO}_2}$ 垂直遞減趨勢的形成。

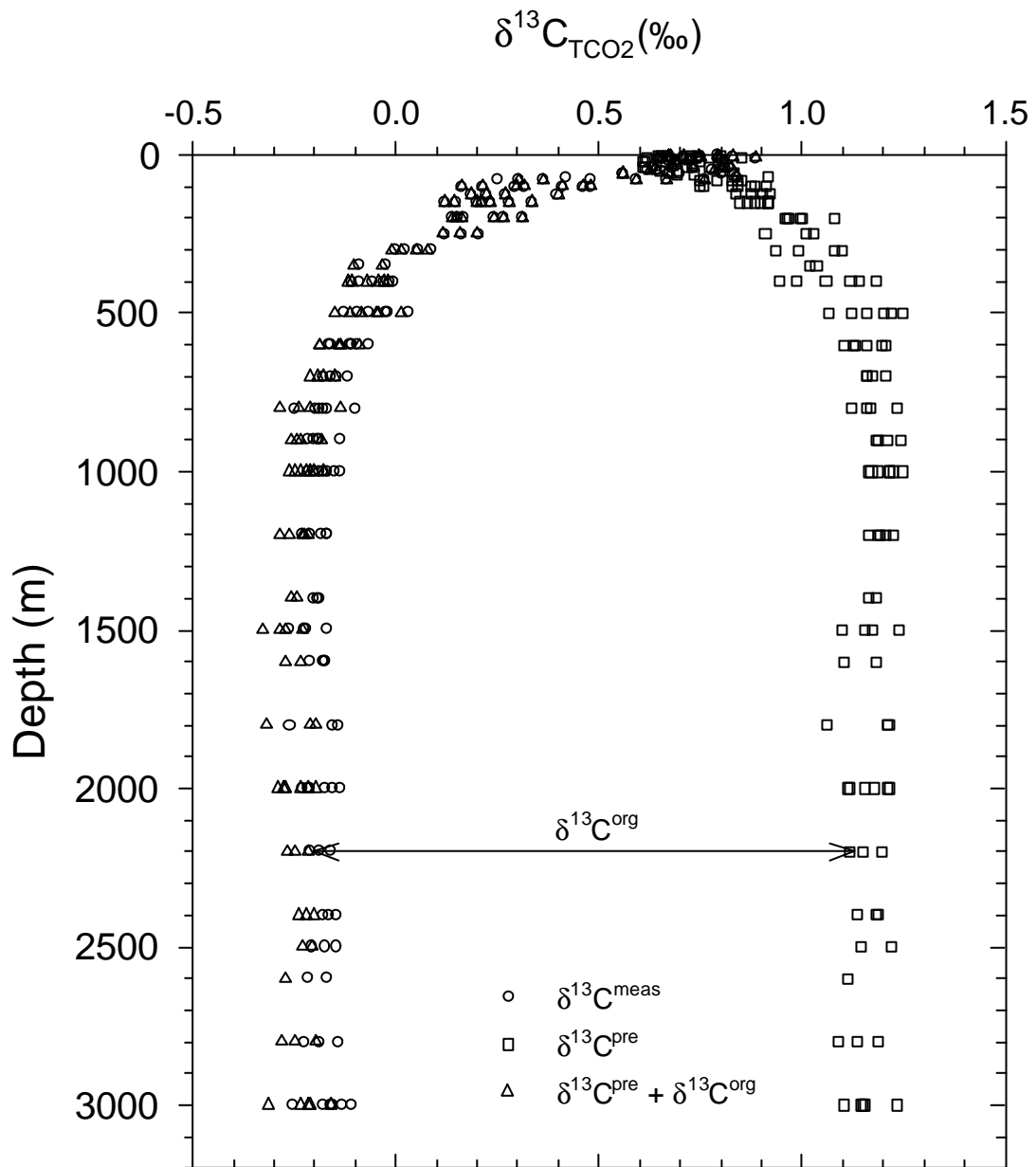


圖 3.17 SEATS 測站 $\delta^{13}\text{C}_{\text{TCO}_2}$ 實測值 ($\delta^{13}\text{C}^{\text{meas}}$) $\delta^{13}\text{C}_{\text{TCO}_2}$ 起始值 ($\delta^{13}\text{C}^{\text{pre}}$) 和 $\delta^{13}\text{C}_{\text{TCO}_2}$ 起始值 + 有機質分解所造成 $\delta^{13}\text{C}_{\text{TCO}_2}$ 之變化量 ($\delta^{13}\text{C}^{\text{pre}} + \delta^{13}\text{C}^{\text{org}}$) 之垂直分佈圖。

3.2.3 人為二氧化碳之影響

大氣中二氧化碳濃度的增高，會使得 $\Delta f\text{CO}_2$ 在二氧化碳的“source”區域變小，故海洋向大氣釋放之二氧化碳通量會減小；反之，在“sink”區域 $\Delta f\text{CO}_2$ 則會增大，因此大氣向海洋輸入之二氧化碳通量會增加。這一減一增，使得全球海洋對人為二氧化碳之吸收能力，會隨著大氣 $f\text{CO}_2$ 的增加而增加，也因此造成了海水中 TCO_2 逐漸地增高。而此因大氣二氧化碳濃度增高，造成海水中 TCO_2 對應之增加量，即稱為海水中之人為二氧化碳（anthropogenic CO_2 ）。由於大氣 $f\text{CO}_2$ 是由西元1750年左右，開始呈現明顯逐年遞增的趨勢。因此，海水中人為二氧化碳的濃度可視為其起始值（ $\text{TCO}_2^{\text{pre}}$ ）與1750年時 TCO_2 起始值的差（Wallace et al., 2001）。如1.5節所言，目前以實測資料來探討海水中人為二氧化碳分佈的方法，可分為以碳化學資料為基礎以及以 $\delta^{13}\text{C}_{\text{TCO}_2}$ 資料為基礎等兩大類。本節將分別利用此兩種方法，來探討SEATS測站人為二氧化碳垂直分佈的情況，並就其結果加以比較。

(I) 以碳化學資料為基礎之估算結果

1970年代末期Brewer (1978)和Chen and Millero (1979)，幾乎同時首先提出了以碳化學資料來計算海水中人為二氧化碳含量的方法。此兩種方法都是運用“反算法”(back-calculation)的觀念，以AOU及TA的資料扣除了有機質和碳酸鈣之分解效應後，求出一水樣之 TCO_2 起始值（ $\text{TCO}_2^{\text{pre}}$ ，參見3.2.2節）。一旦水樣之 $\text{TCO}_2^{\text{pre}}$ 求出後，Brewer的方法是將人為活動干擾前大氣二氧化碳濃度定為 $280\mu\text{atm}$ ，在假設海氣平衡的條件下，即可利用 $f\text{CO}_2$ 及 TA^{pre} 的資料，依熱力學的方法求出該水樣在工業革命前 TCO_2 的濃度（ TCO_2^{280} ）。 $\text{TCO}_2^{\text{pre}}$ 與 TCO_2^{280} 的差，即為該水樣人為二氧化碳的濃度（圖3.18）。Chen及Millero的方法則是根據各海域 NTCO_2 與位溫都有良好之線性關係，故可利用位溫的資料求出一水樣

現今在其起源地之 NTCO_2 起始值 ($\text{NTCO}_2^{\text{pre-present}}$)。 $\text{NTCO}_2^{\text{pre-present}}$ 與 $\text{NTCO}_2^{\text{pre}}$ 的差即代表該水樣受人為二氧化碳的影響程度。

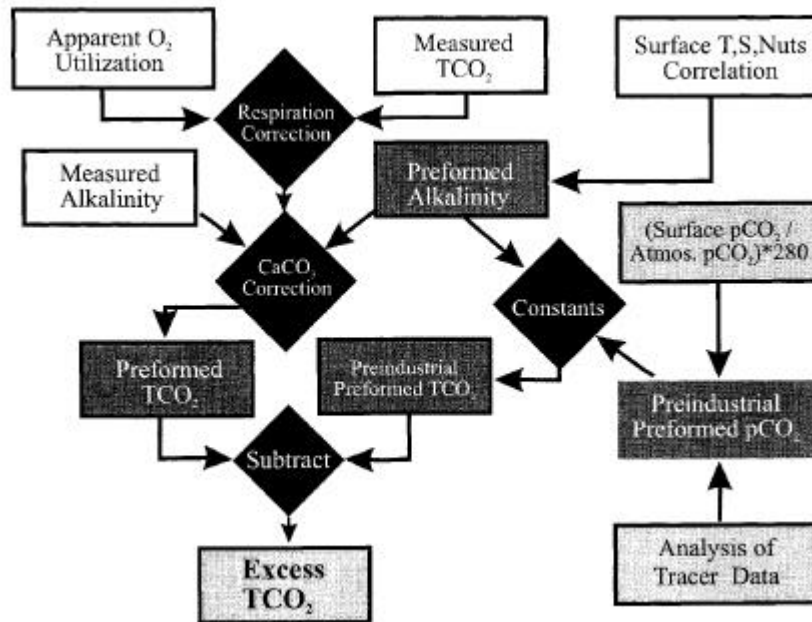


圖 3.18 以“反算法”計算海水中人為二氧化碳含量之觀念流程圖。摘自 Wallace (2001)。

本研究採用 Chen 和 Millero 所提出之方法來計算 SEATS 測站人為二氧化碳垂直分佈的情形。 $\text{TCO}_2^{\text{pre}}$ 的計算已於 3.2.2 節中說明， $\text{NTCO}_2^{\text{pre-present}}$ 之計算公式說明如下：

由於南海鹽度極小值的水源自於北太平洋西北海域，故鹽度極小值以上之水層（水深 500m 以上）， $\text{NTCO}_2^{\text{pre-present}}$ 之計算是使用 Chen and Huang (1995) 所提出之北太平洋表水的起始方程式，並考量採樣時間之差異後修正而得（假設位溫與 NTCO_2 斜率不變，將原始方程式之截距加 20），

$$\text{NTCO}_2^{\text{pre-present}} = 2262 - 12.08 \times \theta (\pm 18)$$

南海深層水來自於北太平洋深層水，而北太平洋深層水又來自於南極，故深層水（2000m 以下） $\text{NTCO}_2^{\text{pre-present}}$ 之計算，是採用 Chen et al. (1986) 所提出之 50°S 以南表水的起始方程式，並考量採樣時間之差異後修正而得（假設位溫與 NTCO_2

斜率不變，將原始方程式之截距加 20)，

$$\text{NTCO}_2^{\text{pre-present}} = 2239 - 11 \times \theta (\pm 16)$$

介於鹽度極小值和深層水之間的水層，則根據位溫資料求出水團混合比例後，帶入上述兩組方程式計算其 $\text{NTCO}_2^{\text{pre-present}}$ 。100m 以上的水層，由於缺乏適當之 $\text{NTCO}_2^{\text{pre-present}}$ 與位溫之迴歸方程式，故採用 Brewer 的方法來計算人為二氧化碳的含量。

計算結果顯示，表水有最高之人為二氧化碳含量，其濃度約介於 $50\text{-}60\mu\text{mol kg}^{-1}$ 之間，而後人為二氧化碳濃度隨深度的增加而漸減，1200m 以下濃度幾乎為 $0\mu\text{mol kg}^{-1}$ (圖 3.19)，代表人為二氧化碳在 SEATS 測站之穿透深度約在 1200m 左右。表水之人為二氧化碳濃度較 Sabine et al.(2002a)根據 JGOFS/WOCE 資料，所估算在北太平洋副熱帶海域的濃度 ($40\text{-}50\mu\text{mol kg}^{-1}$)，高出了 $10\mu\text{mol kg}^{-1}$ 左右。此差異主要應是由於本研究之採樣時間較 JGOFS/WOCE (1990 年代初期) 晚了 10 年左右，故其受人為二氧化碳之影響較大所造成。人為二氧化碳濃度隨深度遞減的趨勢，則是由於愈深的水其出露海平面可進行海氣交換的年代距今愈久遠，故其受人為二氧化碳的影響愈小所造成。若以 1200m 為界，人為二氧化碳對深度的積分結果約為 18mol m^{-2} ，略小於 1990 年代初西北太平洋相同緯度之值 (20mol m^{-2} , Sabine et al., 2002a)。推測這可能是由於南海內部有較強的湧升作用，使其對人為二氧化碳之儲存能力較相鄰之西北太平洋為低。若將 SEATS 測站之結果套用於整個南海，則南海 人為二氧化碳之總儲量約為 0.5 至 0.6Gt C，此量約佔全球海洋人為二氧化碳總儲量的 0.5%。以面積而言，南海約佔全球海洋的 0.97%。故南海對人為二氧化碳之儲存能力亦低於全球海洋的平均值。如前所述，這可能是由於南海內部較強的湧升作用所造成。

(II) 以 $\delta^{13}\text{C}_{\text{TCO}_2}$ 資料為基礎之估算結果

利用 $\delta^{13}\text{C}_{\text{TCO}_2}$ 資料來探討人為二氧化碳在海洋中分佈的原理，簡要說明如下：由 3.2.2 節中的討論已知， $\delta^{13}\text{C}_{\text{TCO}_2}$ 垂直分佈的特徵與營養鹽相似，主要都

是受有機質分解作用所控制。因此，若無其它作用的影響，海水中營養鹽的濃度應與 $\delta^{13}\text{C}_{\text{TCO}_2}$ 成完美之線性關係。根據 Broecker and Maier-Reimer (1992) 的研

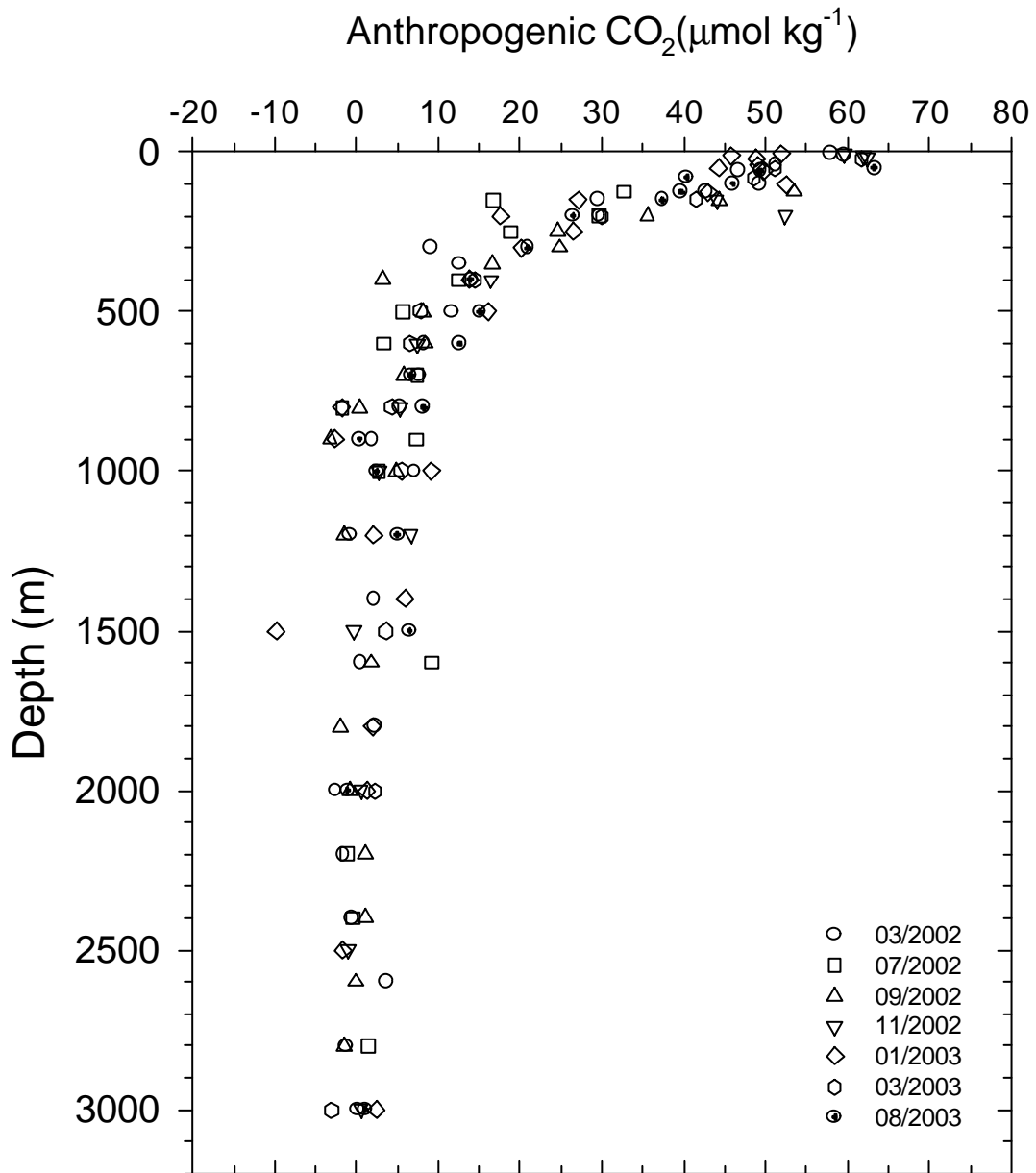


圖 3.19 SEATS 測站人為二氧化碳濃度之垂直分佈圖。

究，對磷酸鹽而言，此一線性關係之斜率應為-1.1 ($\Delta\delta^{13}\text{C}_{\text{TCO}_2}/\Delta\text{PO}_4 = -1.1$ (‰ $(\mu\text{mol kg}^{-1})^{-1}$)。在相同的研究中，作者根據 GEOSECS 在東印度洋及太平洋水深大於 2000 公尺之量測資料，得到 $\delta^{13}\text{C}_{\text{TCO}_2}$ 與 PO_4^{3-} 之線性關係為： $\delta^{13}\text{C}_{\text{TCO}_2} = 2.7 - 1.1 \times [\text{PO}_4^{3-}]$ ，驗證了上述斜率的正確性，同時將此關係稱為全球海水平均 $\delta^{13}\text{C}_{\text{TCO}_2}$ 之生物關係模式 (mean ocean biological trend, 圖 3.20 之點線)。然而，在真實的海洋中，海水中的碳可透過海氣交換作用與大氣二氧化碳進行交換，而營養鹽的循環，基本上與海氣交換作用無關。此種差異，往往使得實際海水中所觀測到營養鹽濃度和 $\delta^{13}\text{C}_{\text{TCO}_2}$ 的線性關係與“mean ocean biological trend”產生偏移 (Mackensen et al., 1996)。海氣交換作用對 $\delta^{13}\text{C}_{\text{TCO}_2}$ 的影響效應，可以實測值與“mean ocean biological trend”的差計算之 (Lynch-Stieglitz et al., 1995)：

$$\delta^{13}\text{C}_{\text{as}} = \delta^{13}\text{C}^{\text{meas}} + 1.1 \times [\text{PO}_4^{3-}] - 2.7$$

“ $\delta^{13}\text{C}_{\text{as}}$ ”即代表海氣交換作用對 $\delta^{13}\text{C}_{\text{TCO}_2}$ 的影響大小。海氣交換作用對 $\delta^{13}\text{C}_{\text{TCO}_2}$ 的影響主要包括熱力學效應及人為二氧化碳等兩部分。在熱力學效應方面，大氣二氧化碳與海水 TCO_2 之間的同位素分化係數為溫度之函數。根據 Mook et al. (1974) 和 Zhang et al. (1995) 的研究，溫度每升高一度，會使海水之 $\delta^{13}\text{C}_{\text{TCO}_2}$ 變輕 0.1 ‰。故較低的海氣交換作用溫度，傾向使 $\delta^{13}\text{C}_{\text{as}}$ 變為正值；反之，較高的海氣交換作用溫度，傾向使 $\delta^{13}\text{C}_{\text{as}}$ 變為負值。在人為二氧化碳的影響方面，主要是透過“Suess effect”來顯現。所謂的“Suess effect” (Friedli et al., 1986) 是指：由於化石燃料及植物之 $\delta^{13}\text{C}$ ，遠較大氣中二氧化碳之 $\delta^{13}\text{C}$ 為輕，因此隨著人為二氧化碳不斷在大氣中累積，大氣中二氧化碳之 $\delta^{13}\text{C}$ 亦逐年變輕。此種大氣中二氧化碳之 $\delta^{13}\text{C}$ ，受人為活動影響逐漸變輕的現象，謂之“Suess effect”。而透過海氣交換作用的進行，這些 $\delta^{13}\text{C}$ 較輕的二氧化碳進入海水中，亦會使 $\delta^{13}\text{C}_{\text{TCO}_2}$ 和營養鹽濃度的關係偏離“mean ocean biological trend”。Keir et al. (1998) 及 Ortiz et al. (2000) 認

為藉由重建一海域中人為二氧化碳影響前營養鹽及 $\delta^{13}\text{C}_{\text{TCO}_2}$ 應有的關係模式，可將熱力學及“Suess effect”對 $\delta^{13}\text{C}_{\text{TCO}_2}$ 影響效應加以分離，進而區辨出人為二氧化碳的訊號。

本研究參照 Keir et al. (1998) 及 Oritz et al. (2000) 所提出之方法，根據下列兩項假設，建立了 SEATS 測站在未受人為二氧化碳影響前， $\delta^{13}\text{C}_{\text{TCO}_2}$ 與 PO_4^{3-} 應有的關係模式(Pre-anthropogenic model) 假設一，水深大於 2000m 的深層水，未受到人為二氧化碳的影響。故取水深大於 2000m 水樣 $\delta^{13}\text{C}_{\text{TCO}_2}$ 與 PO_4^{3-} 測值之平均 ($\delta^{13}\text{C}_{\text{TCO}_2} = -0.18\text{‰}\text{PO}_4^{3-} = 2.86 \mu\text{mol kg}^{-1}$) 作為深層水端點。由於南海深層水唯一的來源為太平洋深層水，而太平洋深層水為全球年齡最老的海水，故其出露海水面的時間早於工業革命之前，應為合理之假設。假設二，SEATS 測站混合層內之 $\delta^{13}\text{C}_{\text{TCO}_2}$ (平均為 0.73 ‰) 自工業革命後至採樣時，由於 Suess effect 的影響，已減輕了 1.0 ‰，故未受人為二氧化碳影響前，表水之 $\delta^{13}\text{C}_{\text{TCO}_2}$ 約為 1.73 ‰，並以此值作為 Pre-anthropogenic model 的表水端點。1.0 ‰的減輕量是由 0.8 與 0.2 ‰相加所得。其中 0.8 ‰是參考 Keir et al. (1998) 的假設，此假設代表工業革命以後至 1992 年表水 $\delta^{13}\text{C}_{\text{TCO}_2}$ 變輕的量，其主要是根據加勒比海(Caribbean Sea) 海棉 (demosponge) 的碳酸鈣骨骼中所記錄由到十九世紀初期到 1992 年間 $\delta^{13}\text{C}$ 之變化量所推得 (Böhm et al. , 1996)。而 0.2 ‰之變輕量，則是考慮本研究的採樣時間介於 2002 至 2003 年間，因此必須對 1992 年至採樣時之 Suess effect 進行修正，0.2 ‰之修正值是根據 Sonnerup et al.(1999)所發表之北太平洋 16°N 至 34.5°N 之 Suess effect ($-0.02 \text{‰yr}^{-1} \times 10 = -0.20 \text{‰}$) 所得出。將表水及深水兩端點連結為一直線：

$$\delta^{13}\text{C}_p = -0.67 \times [\text{PO}_4^{3-}] + 1.73$$

此直線即代表 SEATS 測站未受人為二氧化碳影響前，海水中 PO_4^{3-} 與 $\delta^{13}\text{C}_{\text{TCO}_2}$ 應有之關係模式 (圖 3.20 之實線)。 $\delta^{13}\text{C}_p$ 則代表由 PO_4^{3-} 濃度所計算得出工業革命前應有之 $\delta^{13}\text{C}_{\text{TCO}_2}$ 。 $\delta^{13}\text{C}_{\text{TCO}_2}$ 實測值與 $\delta^{13}\text{C}_p$ 的差 (圖 3.20 實心圓至實線之距離) 即代表一水樣受人為二氧化碳的影響大小，以方程式表示如下：

$$\Delta\delta^{13}\text{C}_{\text{a-p}} = \delta^{13}\text{C}^{\text{meas}} - \delta^{13}\text{C}_{\text{p}}$$

上式中 $\Delta\delta^{13}\text{C}_{\text{a-p}}$ 代表人為二氧化碳對 $\delta^{13}\text{C}_{\text{TCO}_2}$ 影響的指標。 $\delta^{13}\text{C}^{\text{meas}}$ 為實測值； $\delta^{13}\text{C}_{\text{p}}$ 為根據未受人為二氧化碳干擾前 PO_4^{3-} 與 $\delta^{13}\text{C}_{\text{TCO}_2}$ 關係模式之推算值。

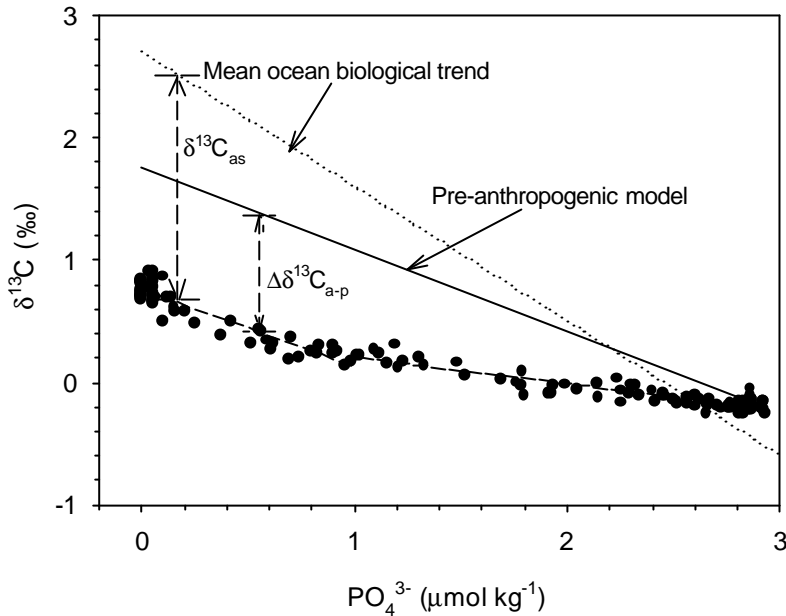


圖 3.20 SATS 測站 $\delta^{13}\text{C}_{\text{TCO}_2}$ 對 PO_4^{3-} 關係圖。點線為全球海水平均 $\delta^{13}\text{C}_{\text{TCO}_2}$ 之生物關係模式 (mean ocean biological trend) ; 實線代表未受人為二氧化碳影響前, $\delta^{13}\text{C}_{\text{TCO}_2}$ 與 PO_4^{3-} 應有之關係模式 (Pre-anthropogenic model)

$\Delta\delta^{13}\text{C}_{\text{a-p}}$ 之計算結果繪於圖 3.21。由圖中可發現, $\Delta\delta^{13}\text{C}_{\text{a-p}}$ 之垂直分佈趨勢與“人為二氧化碳”濃度之變化(圖 3.19)非常相似, 都呈現隨深度漸減的趨勢。至 1200m 左右 $\Delta\delta^{13}\text{C}_{\text{a-p}}$ 即趨近於 0, 顯示人為二氧化碳在 SEATS 測站之穿透深度應在 1200m 左右, 此一結果亦與以碳化學資料為基礎之估算結果非常吻合。

碳化學及 $\delta^{13}\text{C}_{\text{TCO}_2}$ 資料估算結果高度的相似性, 可進一步用來計算, 在人為二氧化碳影響下, 海水中 TCO_2 增加量 (ΔTCO_2)與 $\delta^{13}\text{C}_{\text{TCO}_2}$ 減輕量 ($\Delta\delta^{13}\text{C}_{\text{TCO}_2}$)的相對比值。Keir et al. (1998)及 Körtzinger et al. (2003)的研究指出, $\Delta\delta^{13}\text{C}_{\text{TCO}_2}/\Delta\text{TCO}_2$ 之比值在全球碳循環的研究中, 可用來探討陸地生物圈與大氣二氧化碳可交換碳的總儲量。但由於碳化學參數和 $\delta^{13}\text{C}_{\text{TCO}_2}$ 同步測量的資料並不多見, 故此比值在全球海域中之實測資料相當稀少, 使其在全球碳循環研究的應

用上深受限制。到目前為止，文獻中所發表之 $\Delta\delta^{13}\text{C}_{\text{TCO}_2}/\Delta\text{TCO}_2$ 比，彙整如下：
 南大洋(Southern Ocean): 介於-0.007 至-0.015 ‰($\mu\text{mol kg}^{-1}$)⁻¹ 之間(McNeill et al.,

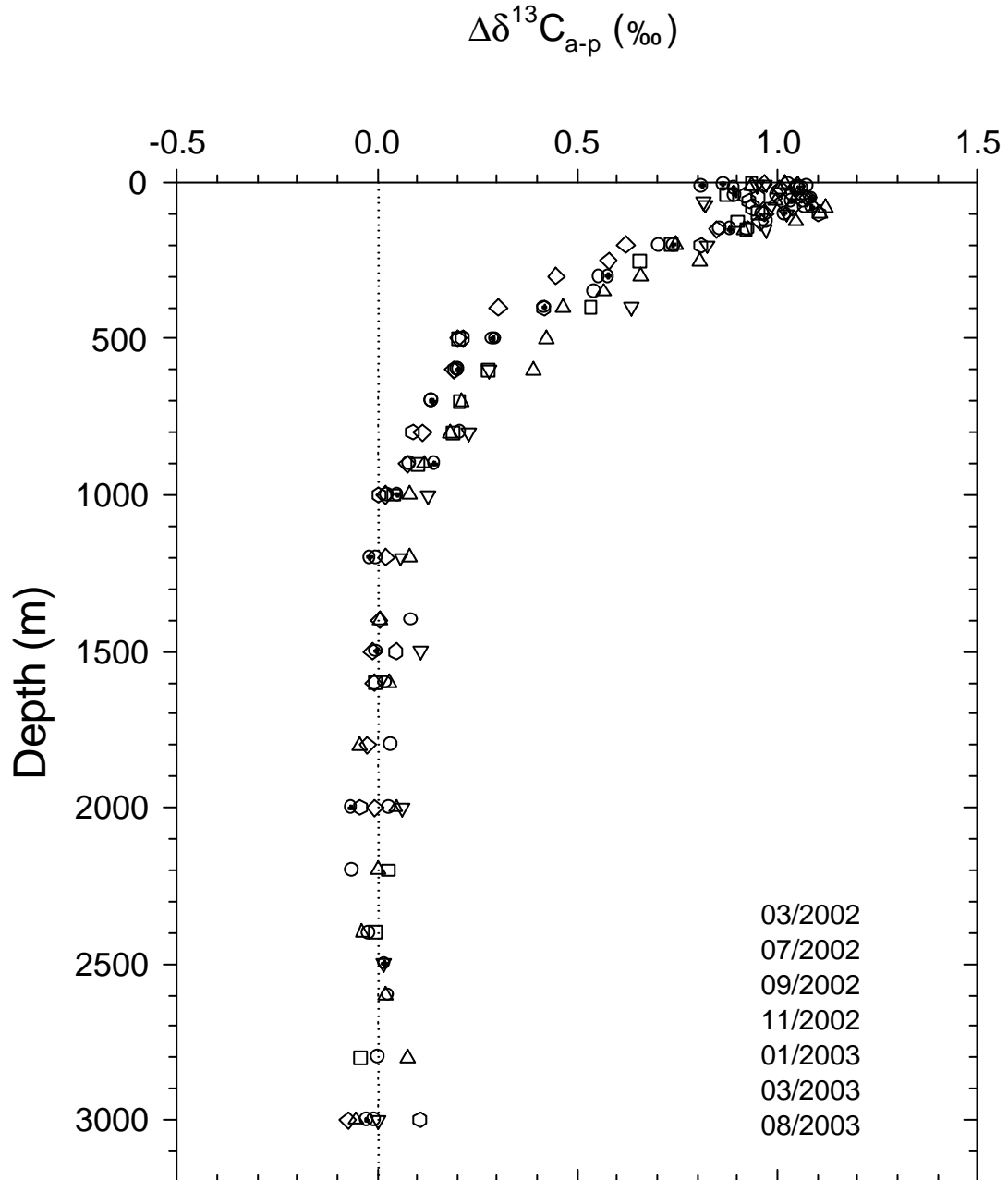


圖 3.21 SEATS 測站 $\Delta\delta^{13}\text{C}_{\text{a-p}}$ 之垂直分佈圖。 $\Delta\delta^{13}\text{C}_{\text{a-p}}$ 為判斷 $\delta^{13}\text{C}_{\text{TCO}_2}$ 受“人為二氧化碳”影響之指標，其定義及計算方式請參閱本文。

2001)；東北大西洋為 $-0.016 \text{ ‰}(\mu\text{mol kg}^{-1})^{-1}$ (Keir et al., 1998)；整個北大西洋為 $-0.024 \text{ ‰}(\mu\text{mol kg}^{-1})^{-1}$ (Körtzinger et al., 2003)；HOT 之觀測結果為 $-0.024 \text{ ‰}(\mu\text{mol kg}^{-1})^{-1}$ (Winn et al., 1994; Gruber et al., 1999)。而根據前述 SEATS 測站人為二氧化碳濃度及 $\Delta\delta^{13}\text{C}_{\text{a-p}}$ 的計算結果，將整個垂直剖面所累積之人為二氧化碳及 $\Delta\delta^{13}\text{C}_{\text{a-p}}$ 的總儲量（分別為 $\sim 18000(\mu\text{mol kg}^{-1}) \text{ m}$ ； $\sim 435 \text{ ‰m}$ ）相除，可得出 SEATS 測站 $\Delta\delta^{13}\text{C}_{\text{TCO}_2}/\Delta\text{TCO}_2$ 之比值約為 $-0.024 \text{ ‰}(\mu\text{mol kg}^{-1})^{-1}$ ，與北大西洋及 HOT 的結果相同。由上述的比較可發現， $\Delta\delta^{13}\text{C}_{\text{TCO}_2}/\Delta\text{TCO}_2$ 比在空間分佈上有顯著之差異，故欲運用此一比值來探討陸地生物圈與大氣二氧化碳可交換碳的總儲量，仍存有相當大的不確定性。同時也彰顯了，對於海水 $\delta^{13}\text{C}_{\text{TCO}_2}$ 時空變化之控制機制，有必要進行更為深入的研究。

四、結論

本研究分析了 2002 年 3 月至 2003 年 8 月間八個 SEATS 探測航次所採得水樣之 TA、 TCO_2 及 $\delta^{13}\text{C}_{\text{TCO}_2}$ 。根據這些數據及其它相關之水文和化學參數的資料，探討了碳化學參數在 SEATS 測站混合層中季節變化的特性，以及控制 NTA、 NTCO_2 和 $\delta^{13}\text{C}_{\text{TCO}_2}$ 垂直變化的作用機制。這兩項研究主要的目的，是希望瞭解在獨特的環境條件影響下，南海碳化學參數之季節性變化以及二氧化碳之海氣交換通量是否與其它海域有所差異？同時希望闡明現今控制碳化學參數及 $\delta^{13}\text{C}_{\text{TCO}_2}$ 垂直變化的各項因子，以作為日後探討在人為活動影響下，南海碳化學系統所可能發生之變化時的對比依據。所得結果分別總結如下：

(一) 碳化學參數在混合層中之季節變化

NTCO_2 在混合層中之季節變化主要受混合層深度改變及生物生產等兩個因素所控制。由春季到秋初 NTCO_2 呈遞減之趨勢，此乃因這段時期表水溫度較高海水層化良好，故 NTCO_2 濃度較高之次表層水不易進入混合層中，加上生物生產作用持續消耗掉碳，致使此段時期內混合層中之 NTCO_2 呈遞減之趨勢。秋末開始，隨著混合層的深化， NTCO_2 含量較高之次表層水進入了混合層中，使得 NTCO_2 的濃度逐漸升高，此種作用在冬季時達到最高峰，於是形成了 NTCO_2 的最大值。由混合層中冬、夏兩季 NTCO_2 之濃度差所推算出全年之平均基礎生產力介於 177 ± 34 到 $363 \pm 69 \text{ mgC m}^{-2} \text{ day}^{-1}$ 之間，此結果與模式估算及實測之基礎生產力的結果均非常相近，故支持生物生產作用為由冬至夏混合層中 NTCO_2 遞減主因之推論。

$f\text{CO}_2$ 的最高值出現在夏季，最低值則出現在冬季。由冬至夏呈遞增之趨勢；由夏至冬則呈遞減之趨勢，其與溫度之季節性波動呈現近乎完美的同步變化。此種變化趨勢與其它位於副熱帶貧營養鹽海域之時間序列測站（HOT, BATS,

ESTCO) 所得之結果相仿。透過“ $f\text{CO}_{2\text{mean}}$ corrected for ΔT ” (代表溫度對 $f\text{CO}_2$ 之影響效應) 和“ $f\text{CO}_2$ at 27 °C” (代表非溫度因子對 $f\text{CO}_2$ 之影響效應) 的計算分析, $f\text{CO}_2$ 季節變化之控制機制可歸納如下: 在由冬至夏溫度回暖的時期, $f\text{CO}_2$ 的變化主要由溫度及生物生產作用所控制。但後者對 $f\text{CO}_2$ 之減少效果較前者對 $f\text{CO}_2$ 之增加效果為小, 故 $f\text{CO}_2$ 仍呈現隨溫度增加而增加之趨勢。由夏至冬變冷的時期中, 由於混合層深化, 次表層水的加入大幅提高了混合層中的 $f\text{CO}_2$, 但其增加效果不若溫度降低與生物生產加總對 $f\text{CO}_2$ 的減少效果, 故 $f\text{CO}_2$ 仍呈現隨溫度遞減的現象。

利用 Takahashi et al.(2002)所提出之方法, 本研究比較了 SEATS、HOT、BATS、KNOT 和 OSP 等五個時間序列測站溫度及生物效應對 $f\text{CO}_2$ 變化的相對影響程度。結果顯示, 位於低緯度貧營養鹽海域的測站 (SEATS, HOT, BATS), 溫度效應對 $f\text{CO}_2$ 變化的影響都較生物效應為大。而位於高緯海域的測站(KNOT, OSP), 則是生物效應較為重要。此種差異應與高緯度海域通常在春末夏初海水溫度迅速回升之際, 有極高之生產力有關。此外, SEATS 與 HOT 皆位於低緯度貧營養鹽海域中, 且兩者之混合層深度之季節變化幅度非常相似。然而, 無論是溫度還是生物效應, SEATS 都明顯較 HOT 為大。推測此種差異可能是由於南海內部湧升作用強烈, 故溫躍層、營養鹽躍層和二氧化碳躍層可能都較 HOT 測站為淺所造成。

由 $\Delta f\text{CO}_2$ 之季節變化得知, SEATS 測站在夏季及秋初明顯是大氣二氧化碳的“source”, 冬季時為“sink”, 春季及秋末則大致呈現海氣平衡的狀態。春、夏、秋、冬四季二氧化碳海氣交換通量之計算結果分別為: 春季, $-0.03 \pm 0.07 \sim -0.25 \pm 0.64 \text{ gC m}^{-2} \text{ yr}^{-1}$; 夏季, $0.30 \pm 0.07 \sim 2.77 \pm 0.68 \text{ gC m}^{-2} \text{ yr}^{-1}$; 秋季, $2.10 \pm 1.16 \sim 5.36 \pm 2.97 \text{ gC m}^{-2} \text{ yr}^{-1}$; 冬季, $-7.47 \pm 2.44 \sim -17.04 \pm 5.57 \text{ gC m}^{-2} \text{ yr}^{-1}$ 。冬季時有最高之二氧化碳海氣交換通量, 此乃因冬季季風之風速遠較其它季節為強所致。全年累計之淨交換通量介於 -1.28 ± 0.94 至 $-2.73 \pm 2.20 \text{ gC m}^{-2} \text{ yr}^{-1}$ 之間, 說明 SEATS 測站應是大氣二氧化碳的“sink”。 此年通量較 HOT 及 BATS 測站之估算

結果為小。推測這可能是由於 SEATS 測站所處緯度最低，故其平均溫度較高，以及南海內部較強的湧升作用所共同造成的結果。若將 SEATS 測站所得之結果外插到整個南海，則整個南海每年對大氣二氧化碳之吸收量為 4.5 ± 3.3 到 $9.6 \pm 7.7 \text{ Tg C yr}^{-1}$ ($1\text{Tg}=10^{12}\text{g}$) 之間。此量約佔全球海洋吸收量的 0.20% 到 0.44% 之間。然而，以面積比例而言，南海約佔全球海洋的 0.97%。故南海對大氣二氧化碳之吸收能力，明顯低於世界海洋之平均值。

由冬夏之間混合層中硝酸鹽及 NTCO_2 的消耗量來看，此段時間內硝酸鹽僅提供了少部分新生產力所需之氮鹽。雖然，南海符合所有固氮作用發生所需之環境條件，但前人研究顯示固氮作用對新生產力之貢獻亦很小。故 SEATS 測站氮的循環仍是一項極待釐清的課題。

(二) NTA 、 NTCO_2 和 $\delta^{13}\text{C}_{\text{TCO}_2}$ 垂直變化之控制機制

SEATS 測站 PO_4^{3-} 、 NO_3^- 和 AOU 之垂直分佈非常相似，其濃度在表水幾乎都為零，而後均隨深度增加而快速增加，至 1000m 以下則幾乎保持不變。此三者垂直分佈高度的相似性乃預期中的結果。因 PO_4^{3-} 和 NO_3^- 隨深度的增加，主要是由於有機質分解將營養鹽重新釋放回海水所致，而有機質分解會同時消耗掉溶氧，故造成 AOU 與營養鹽同步增加的趨勢。 PO_4^{3-} 與 AOU 、 NO_3^- 與 AOU 和 NO_3^- 與 PO_4^{3-} 的關係，在水深 100m 以上大致與 Redfield-ratio 所預期之結果相符，但 100m 以下三者線性關係之斜率卻明顯偏離了 Redfield-ratio。經營營養鹽起始值差異修正後，發現 PO_4^{3-} 和 AOU 之線性關係即與 Redfield-ratio 相符，代表 100m 以下 PO_4^{3-} 和 AOU 線性關係之斜率與 Redfield-ratio 的偏離，可由不同深度水樣 PO_4^{3-} 起始值的差異所解釋。然而，對 NO_3^- 和 AOU 以及 NO_3^- 和 PO_4^{3-} 之線性關係而言，即使經過起始值差異的修正，仍與 Redfield-ratio 有相當程度的偏移。顯示水樣可能受到了固氮及脫硝等作用的影響。 N^* 之計算結果顯示，200m 以下的水體的確可能經歷了脫硝作用，進而造成 NO_3^- 和 AOU 以及 NO_3^- 和 PO_4^{3-} 線性關係之斜率較 Redfield-ratio 為小的現象。200m 以上 N^* 的高值，則可能是受固氮作用及陸源淡水輸入之影響所致。

本研究參照前人之研究成果，將 NTA、 NTCO_2 和 $\delta^{13}\text{C}_{\text{TCO}_2}$ 的測量值拆解為起始值、有機質分解作用所造成之變動量及碳酸鈣溶解作用所造成之變動量等三個部分，並針對此三項因子對 NTA、 NTCO_2 和 $\delta^{13}\text{C}_{\text{TCO}_2}$ 垂直變化之相對貢獻進行分析。分析結果顯示：NTA 由表層至 150m 的深度範圍內，由於起始值之增加量與有機質分解作用所造成之減少量相互抵銷，故其濃度在此深度範圍內大致保持不變。水深 150m 至 1600m 的深度範圍內，NTA 隨深度遞增之趨勢是由起始值之增加及碳酸鈣溶解所造成 TA 之增加共同造成，在 500m 以上起始值增加的貢獻較碳酸鈣溶解作用重要；500m 以下碳酸鈣溶解的重要性則超過起始值的增加。

NTCO_2 隨深度漸增之趨勢是由起始值、有機質分解量及碳酸鈣溶解量的增加所共同造成。水深 400m 以上， NTCO_2 隨深度之增加主要是由起始值和有機質分解量的增加所造成，且兩者之貢獻比例大致相等。而在此深度範圍內由於碳酸鈣尚處於過飽和狀態，故其對 NTCO_2 的增加並無明顯貢獻。400m 以下，碳酸鈣溶解的訊號開始出現，惟其對 NTCO_2 隨深度增加之貢獻，仍明顯較起始值和有機質分解量之增加為小。起始值、有機質分解量及碳酸鈣溶解量之增加對整個垂直剖面 NTCO_2 增加量之貢獻百分比分別約為 40%，40% 和 20%。IC/OC 比之計算結果顯示，在整個垂直剖面中其最大值約為 0.4，代表對任一水樣而言，即使在最多的情況下，碳酸鈣溶解對 TCO_2 增加的貢獻百分比亦不會超過 29%。由此可見，不論對任何深度而言，有機質的分解作用才是造成海水中 TCO_2 增加的主要因素。本研究亦計算了霰石及方解石之飽和度，其化學飽和深度分別為 600m 及 2500m。然而，根據 TA 所計算之碳酸鈣溶解量的結果卻顯示，碳酸鈣在霰石及方解石化學飽和深度之上即出現了溶解訊號。惟碳酸鈣溶解並非大洋中 TA 唯一的來源，陸棚沉積物中有機質在還原環境下的分解作用，亦會釋放出大量的 TA 向外洋傳送。故碳酸鈣是否在其化學飽和深度之上即發生溶解？有待進一步的研究加以釐清。

$\delta^{13}\text{C}_{\text{TCO}_2}$ 隨深度遞減的趨勢，主要是由於有機質分解量的增加所造成，此種

結果可歸因於 $\delta^{13}\text{C}_{\text{TCO}_2}$ 起始值之差異並不顯著，且有機質分解與碳酸鈣溶解作用相較而言，同時兼具了同位素分化效應大及貢獻量多等兩個特點。使有機質之分解作用主導了海水中 $\delta^{13}\text{C}_{\text{TCO}_2}$ 垂直遞減趨勢的形成。而此結論亦可由 $\delta^{13}\text{C}_{\text{TCO}_2}$ 之垂直變化幾乎與營養鹽及 AOU 的變化成完美的鏡像獲得證實。

有關於人為二氧化碳在 SEATS 測站垂直分佈的情形，本研究利用了以碳化學及 $\delta^{13}\text{C}_{\text{TCO}_2}$ 資料為基礎等兩類不同的方法進行估算。兩個方法所獲致的結果非常類似，都顯示人為二氧化碳的濃度隨著深度的增加而減少，而其穿透深度約為 1200m。整個垂直剖面所累積人為二氧化碳之總儲量約為 18mol m^{-2} ，略小於西北太平洋相同緯度海域之儲量。推測這可能是由於南海內部有較強的湧升作用，降低了其對人為二氧化碳之儲存能力。若將 SEATS 測站之結果套用於整個南海，則南海 人為二氧化碳之總儲量約為 0.5 至 0.6Pg C，此量約佔全球海洋人為二氧化碳總儲量的 0.5%。顯示南海對人為二氧化碳之儲存能力亦低於全球海洋的平均值。如前所述，這可能與南海內部較強的湧升作用有關。大氣二氧化碳濃度增加所造成海水中 TCO_2 之增加量 (ΔTCO_2) 與 $\delta^{13}\text{C}_{\text{TCO}_2}$ 減輕量 ($\Delta\delta^{13}\text{C}_{\text{TCO}_2}$) 的相對比值，可用來探討陸地生物圈與大氣二氧化碳可交換碳的總儲量。SEATS 測站 $\Delta\delta^{13}\text{C}_{\text{TCO}_2}/\Delta\text{TCO}_2$ 之比值約為 $-0.024 \text{‰}(\mu\text{mol kg}^{-1})^{-1}$ ，與北大西洋及 HOT 測站所得之結果相同，但明顯較南大洋及東北大西洋為高，到目前為止對為何 $\Delta\delta^{13}\text{C}_{\text{TCO}_2}/\Delta\text{TCO}_2$ 比在空間分佈上會有如此顯著之差異的原因尚不清楚，故欲運用此一比值來探討陸地生物圈與大氣二氧化碳可交換碳的總儲量之前，有必要對控制海水 $\delta^{13}\text{C}_{\text{TCO}_2}$ 時空變化的作用機制進行更為廣泛且深入的研究。

參考文獻

中文部份

- 王樹倫，1997，西北太平洋邊緣海二氧化碳之研究，國立中山大學海洋地質及化學研究所研究所博士論文，共 226 頁。
- 白書禎、郭廷瑜，1995，Trident-223三同步營養鹽測定系統（九五版）之設計與操作，國科會海研一號貴儀中心技術手冊，共26頁。
- 白書禎、郭廷瑜、鍾仕偉、蘇宗德，1998，疊氮修正希巴辣光度測氧法及其在環境監測上的應用，化學，第56卷第三期，173-185頁。
- 陳鎮東，2001，南海海洋學，渤海堂出版社，共 506 頁。

英文部份

- Anderson, L.A., Sarmiento, J.L., 1994. Redfield ratios of remineralization determined by nutrient data analysis. *Global Biogeochemical Cycles* 8, 65-80.
- Baliño, B.M., Fasham, M.J.R., Bowles, M.C., 2001. *Ocean Biogeochemistry and Global Change*. IGBP Science Series No. 2., ICSU, Stockholm, Sweden, 32pp.
- Bates, N.R., Michaels, A.F., Knap, A.H., 1996. Seasonal and interannual variability of oceanic carbon dioxide species at the U.S. JGOFS Bermuda Atlantic-series Study (BATS) site. *Deep-Sea Research II* 43, 347-383.
- Bates, N.R., Takahashi, T., Chipman, D.W., Knap, A.H., 1998. Variability of pCO₂ on diel to seasonal timescales in the Sargasso Sea. *Journal of Geophysical Research* 103, 15567-15585.
- Bates, N.R., 2001. Interannual variability of oceanic CO₂ and biogeochemical properties in the Western North Atlantic subtropical gyre. *Deep-Sea Research II*

48, 1507-1528.

- Benson, B.B., Krause, D., 1984. The concentration and isotopic fractionation of oxygen dissolved in freshwater and seawater in equilibrium with the atmosphere. *Limnology and Oceanography* 29, 620-632.
- Berelson, W.M., 2001. The flux of particulate organic carbon into the ocean interior: a comparison of four U.S. JGOFS regional studies. *Oceanography* 14, 59-67.
- Böhm, F., Joachimski, M.M., Lehnert, H., Morgenroth, G., Kretschmer, W., Vacelet, J., Dullo, W.C., 1996. Carbon isotope records from extant Caribbean and South Pacific sponges: Evolution of $\delta^{13}\text{C}$ in surface water DIC. *Earth and Planetary Science Letters* 139, 291-303.
- Bonneau, M.C., Bergnaud-Grazzini, C., Berger, W.H., 1980. Stable isotope fractionation and differential dissolution in recent planktonic foraminifera from Pacific box cores. *Oceanologica Acta* 3, 377-382.
- Broecker, W.S., Maier-Reime, E., 1992. The influence of air and sea exchange on the carbon isotope distribution in the sea. *Global Biogeochemical Cycles* 6, 315-320.
- Buesseler, K.O., 2001. Ocean biogeochemistry and the global carbon cycle: an introduction to the U.S. Joint Global Ocean Flux Study. *Oceanography* 14, 5.
- Brewer, P.G., Goldman, J.C., 1976. Alkalinity changes generated by phytoplankton growth. *Limnology and Oceanography* 21, 108-117.
- Brewer, P.G., 1978. Direct measurement of the oceanic CO_2 increase. *Geophysical Research Letters* 5, 997-1000.
- Buesseler, K.O., 1998. The decoupling of production and particulate export in the surface ocean. *Global Biogeochemical Cycles* 12, 297-310.
- Chen, C.T.A., 1990. Rates of calcium carbonate dissolution and organic carbon decomposition in the North Pacific Ocean. *Journal of the Oceanographic Society of Japan* 46, 201-210.

- Chen, C.T.A., 2002. Shelf-vs. dissolution-generated alkalinity above the chemical lysocline. *Deep Sea Research II* 49, 5365-5375.
- Chen, C.T.A., Millero, F.J., 1979. Gradual increase of oceanic CO₂. *Nature* 277, 205-206.
- Chen, C.T.A., Pytkowicz, R.M. Olson, E.J., 1982. Evaluation of the calcium problem in the South Pacific. *Geochemical Journal* 16, 1-10.
- Chen, C.T.A., Rodmam, M.R., Wei, C.L., Olson, E.J., Feely, R.A., 1986. Carbonate Chemistry of the North Pacific Ocean. US Department of Energy Technical Report, DOE/NBB-0079, p. 176.
- Chen, C.T.A., Huang, M.H., 1995. Carbonate chemistry and the anthropogenic CO₂ in the South China Sea. *Acta Oceanologica Sinica* 14, 47-57.
- Chen, C.T.A., Huang, M.H., 1996. A mid-depth front separating the South China Sea Water and the Philippine Sea Water. *Journal of Oceanography* 52, 17-25.
- Chao, S.Y., Shaw, P.T., Wu, S.Y., 1996. El Niño modulation of the South China Sea circulation. *Progress in Oceanography* 38, 51-93.
- Chen, C.T.A., Wang, S.L., 1998. Influence of intermediate water in the western Okinawa Trough by the outflow from the South China Sea. *Journal of Geophysical Research* 103, 12,683- 12, 688.
- Chen, C.T.A., Wang, S.L., Wang, B. J., Pai, S.C., 2001. Nutrient budgets for the South China Sea basin. *Marine Chemistry* 75, 281- 300.
- Chen, Y.L., Chen, H.Y., Lin, Y.H., 2003. Distribution and downward flux of *Trichodesmium* in the South China Sea as influenced by the transport from the Kuroshio Current. *Marine Ecology Progress Series* 259, 47-57.
- Chen, Y.L., Chen, H.Y., Karl, D.M., Takahashi, M., 2004. Nitrogen modulates phytoplankton growth in spring in the South China Sea. *Continental Shelf Research* 24, 527-541.

- Copin-Montégut, C., 2000. Consumption and production on scales of a few days of inorganic carbon, nitrate and oxygen by the planktonic community: results of continuous measurements at the Dyfamed station in the northwestern Mediterranean Sea (May 1995). *Deep-Sea Research I* 47, 447-477.
- Craig, H., 1957. Isotopic standards for carbon and oxygen and correction factors for mass-spectrometric analysis of carbon dioxide. *Geochimica et Cosmochimica Acta* 12, 133-149.
- Deutsch, C., Gruber, N., Key, R.M., Samiento, J.L., Ganachaud, A., 2001. Denitrification and N₂ fixation in the Pacific Ocean. *Global Biogeochemical Cycles* 15, 483-506.
- Dickson, A.G., 1981. An exact definition of total alkalinity and a procedure for the estimation of alkalinity and total inorganic carbon from titration data. *Deep-Sea Research* 28A, 609-623.
- Dickson, A.G., Millero, F.J., 1987. A comparison of the equilibrium constants for the dissociation of carbonic acid in seawater media. *Deep-Sea Research I* 34, 1733-1743.
- DOE, 1994. Handbook of methods for the analysis of the various parameters of the carbon dioxide system in seawater. In: Dickson A.G., Goyet C. (Eds), U.S. Department of Energy CO₂ science Team Report, version 2, (unpublished manuscript).
- Duce, R.A., Tindale, N.W., 1991. Atmospheric transport of iron and its deposition in the ocean. *Limnology and Oceanography* 36, 1715-1726.
- Ducklow, H.W., Steinberg, D.K., Buesseler, K.O., 2001. Upper ocean carbon export and the biological pump. *Oceanography* 14, 50-58.
- Dyrssen, D., Sillén, L.G., 1967. Alkalinity and total carbonate in sea water: A plea for *p*-*T* independent data. *Tellus* 19, 113-120.

- Feely, R.A., Sabine, C.L., Takahashi, T., Wanninkhof, R., 2001. Uptake and storage of carbon dioxide in the ocean: the global CO₂ survey. *Oceanography* 14, 18-32.
- Feely, R.A., Sabine C.L., Lee, K., Millero, F.L., Lamb, M.F., Greeley, D., Bullister, J.L., Key, R.M., Peng, T.H., Kozyr, A., Ono, T., Wong, C.S., 2002. In situ calcium carbonate dissolution in the Pacific Ocean. *Global Biogeochemical Cycles* 16, doi:10.1029/2002GB001866.
- Friedli, H., Löttscher, H., Oeschger, H., Siegenthaler, U., Stauffer, B., 1986. Ice core record of the ¹³C/¹²C ratio of atmospheric CO₂ in the past two centuries. *Nature* 324, 237-238.
- Goericke, R., Fry, B., 1994. Variations of marine plankton δ¹³C with latitude, temperature, and dissolved CO₂ in the world ocean. *Global Biogeochemical Cycles* 8, 85-90.
- Gong, G.C., Liu, K.K., Liu, C.T., Pai, S.C., 1992. The chemical hydrography of the South China Sea west of Luzon and a comparison with the West Philippine Sea. *Terrestrial, Atmospheric and Oceanic Sciences* 3, 587-602.
- González-Dávila M., Santana-Casiano, J.M., Rueda, M.-J, Llinás, O., González-Dávila, E.-F., 2003. Seasonal and interannual variability of sea-surface carbon dioxide species at the European Station for Time Series in the Ocean at the Canary Islands(ESTOC) between 1996 and 2000. *Global Biogeochemical Cycles* 17, doi:10.1029/2002GB001993.
- Gruber, N., Sarmiento, J.L., Stocker, T.F., 1996. An improved method for detecting anthropogenic CO₂ in the oceans. *Global Biogeochemical Cycles* 10, 809-837.
- Gruber, N., Sarmiento J.L., 1997. Global patterns of marine nitrogen fixation and denitrification. *Global Biogeochemical Cycles* 11, 235-256.
- Gruber, N., Keeling, C.D., Bacastow, R.B., Guenther, P.R., Lueker, T.J., Wahlen, M.,

- Meijer, H.A.J., Mook, W.G., Stocker, T.F., 1999. Spatiotemporal patterns of carbon-13 in the global surface oceans and the oceanic Suess effect. *Global Biogeochemical Cycles* 13, 307-335.
- Hansell, D.A., Carlson, C.A., 2001. Marine dissolved organic matter and the carbon cycle. *Oceanography* 14, 41-49.
- Houghton J.T., Ding, Y., Griggs, D.J., Noguer, M., van der Linden, P.J., Xiaosu, D., 2001. *Climate Change 2001: The Scientific Basis* contribution of working group I to the third assessment report of the Intergovernmental Panel on Climate Change. Cambridge Univ. Press, Cambridge, 944pp.
- Hu, J.Y., Kawamura, H., Hong, H., Qi, Y.Q., 2000. A review on the currents in the South China Sea: seasonal circulation, South China Sea Warm Current and Kuroshio intrusion. *Journal of Oceanography* 56, 607-624.
- Indermühle, A., Stocker, T.F., Joos, F., Fischer, H., Smith, H.J., Wahlen, M., Deck, B., Mastroianni, D., Tschumi, J., Blunier, T., Meyer, R., Stauffer, B., 1999. Holocene carbon-cycle dynamics based on CO₂ trapped in ice at Taylor Dome, Antarctica. *Nature* 398, 121-126.
- Karl, D.M., Letelier, L., Tupas, L., Dore, J., Christian, J., Hebel, D., 1997. The role of nitrogen fixation in biogeochemical cycling in the subtropical north Pacific ocean. *Nature* 386, 533-538.
- Karl, D.M., Bates, N.R., Emerson, S., Harrison, P.J., Jeandel, C., Llinás, O., Liu, K.K., Marty, J-C, Michaels, A.F., Miquel, J.C., Neuer, S., Nojiri, Y., Wong, C.S., 2003. Temporal studies of biogeochemical processes determined from ocean time-series observations during the JGOFS era. In: Fasham, M.J.R. (Ed), *Ocean Biogeochemistry: the role of the ocean carbon cycle in global change*. Springer, Berlin, pp. 239-267.
- Keeling, C.D., Whorf, T.P., 2004. Atmospheric CO₂ records from sites in the SIO air

- sampling network. In Trends: A Compendium of Data on Global Change. Carbon Dioxide Information Analysis Center, Oak Ridge National Laboratory, U.S. Department of Energy, Oak Ridge, Tenn.
- Keir, R., Rehder, G., Suess, E., 1998. The $\delta^{13}\text{C}$ anomaly in the Northeastern Atlantic. *Global Biogeochemical Cycles* 12, 467-477.
- Körtzinger, A., Quay, P.D., Sonnerup, R.E., 2003. Relationship between anthropogenic CO_2 and ^{13}C Suess effect in the North Atlantic Ocean. *Global Biogeochemical Cycles* 17, doi:10.1029/2001GB001427.
- Kroopnick, P., 1974. The dissolved O_2 - CO_2 - ^{13}C system in the eastern equatorial Pacific. *Deep-Sea Research* 21, 211-227.
- Kroopnick, P. M., 1985. The distribution of ^{13}C of ΣCO_2 in the world oceans. *Deep Sea Research* 32, 57-84.
- Kroopnick, P., Weiss, R.F., Chaig, H., 1972. Total CO_2 , ^{13}C , and dissolved oxygen- ^{18}O at GEOSECS II in the North Atlantic. *Earth and Planetary Science Letters* 16, 103-110.
- Lee, K., Millero, F.J., Byrne, R.H., Feely, R.A., Wanninkhof, R., 2000. The recommended dissociation constants for carbonic acid in seawater. *Geophysical Research Letters* 27, 229-232.
- Lewis, E., Wallace, D.W.R., 1998. Program developed for CO_2 system calculations, Carbon Dioxide Information Analysis Center, Report ORNL/CDIAC-105, Oak Ridge National Laboratory, Oak Ridge, Tenn.
- Liang, W.D., Jan, J.C., Tang, T.Y., 2000. Climatological wind and upper ocean heat content in the South China Sea. *Acta Oceanographica Taiwanica* 38, 91-114.
- Lin, H.L., Wnag, L.W., Wang, C.H., Gong, G.C., 1999. Vertical distribution of $\delta^{13}\text{C}$ of dissolved inorganic carbon in the Northeastern South China Sea. *Deep-Sea Research I* 46, 757-775.

- Liss, P.S., Merlivat, L., 1986. Air-sea gas exchange rates: introduction and synthesis. In: Buat-Menard, P. (Ed), The role of air-sea exchange in geochemical cycling, NATO ASI Series C: Mathematical and Physical Sciences, vol. 185, pp. 113-128.
- Liu, K.K., Chao, S.Y., Shaw, P.T., Gong, G.C., Chen, C.C., Tang, T.Y., 2002. Monsoon-forced chlorophyll distribution and primary production in the South China Sea: observations and a numerical study. *Deep-Sea Research I* 49, 1387-1412.
- Lueker, T.J., Dickson, A.G., Keeling, C.D., 2000. Ocean pCO₂ calculated from dissolved inorganic carbon, alkalinity, and equations for K₁ and K₂: validation based on laboratory measurements of CO₂ in gas and seawater at equilibrium. *Marine Chemistry* 70, 105-119.
- Lynch-Stieglitz, J., Stocker, T.F., Broecker, W.S., Fairbanks, R.G., 1995. The influence of air-sea exchanges on the isotopic composition of oceanic carbon: Observations and modeling. *Global Biogeochemical Cycles* 9, 653-666.
- Mackensen, A., Hubberten, H.W., Scheele, N., Schlitzer, R., 1996. Decoupling of $\delta^{13}\text{C}_{\text{TCO}_2}$ and phosphate in Recent Weddell Sea deep and bottom water: Implications for glacial Southern Ocean paleoceanography. *Paleoceanography* 11, 203-215.
- McNeill, B.I., Matear, R.J., Tilbrook, B., 2001. Does carbon 13 track anthropogenic CO₂ in the Southern Ocean? *Global Biogeochemical Cycles* 15, 597-614.
- Mehrbach, C., Culberson, C.H., Hawley, J.E., Pytkowicz, R.M., 1973. Measurement of the apparent dissociation constants of carbonic acid in seawater at atmospheric pressure. *Limnology and Oceanography* 18, 897-907.
- Michaels, A.F., Karl, D.M., Capone, D.G., 2001. Element stoichiometry, new production and nitrogen fixation. *Oceanography* 14, 68-77.
- Milliman, J.D., Troy, P.J., Balch, W.M., Adams, A.K., Li, Y.H., Mackenzie, F.T., 1999.

- Biological mediated dissolution of calcium carbonate above the chemical lysocline. *Deep Sea Research I* 46, 1653-1669.
- Mook, W.G., Bommerson, J.C., Staverman, W.H., 1974. Carbon isotope fractionation between dissolved bicarbonate and gaseous carbon dioxide. *Earth and Planetary Science Letters* 22, 169-176.
- Neftel, A., Moor, E., Oeschger, H., Stauffer, B., 1985. Evidence from polar ice cores for the increase in atmospheric CO₂ in the past two centuries. *Nature* 315, 45-47.
- Neuer, S., Davenport, R., Freudenthal, T., Wefer, G., Llinás, O., Rueda, M.J., Steinberg, D.K., Karl, D.M., 2002. Differences in the biological carbon pump at three subtropical ocean sites. *Geophysical Research Letters* 29, doi:10.1029/2002GL015393.
- Ortiz, J.D., Mix, A.C., Wheeler, P.A., Key, R.M., 2000. Anthropogenic CO₂ invasion into the northeast Pacific based on concurrent $\delta^{13}\text{C}_{\text{DIC}}$ and nutrient profiles from the California Current. *Global Biogeochemical Cycles* 14, 917-929.
- Ose, T., Song, Y.K., Kitoh, A., 1997. Sea surface temperature in the South China Sea-an index for the Asian monsoon and ENSO system. *Journal of Meteorological Society of Japan* 75, 1091-1107.
- Pai, S.C., Yang, C.C., Riley, J.P., 1990. Effects of acidity and molybdate concentration on the kinetics of the formation of the phosphoantimonymolybdenum blue complex. *Analytica Chimica Acta* 229, 115-120.
- Pai, S.C., Gong, G.C., Liu, K.K., 1993. Determination of dissolved oxygen in seawater by direct spectrophotometry of total iodine. *Marine Chemistry* 41, 343-351.
- Pai, S.C., Riley, J.P., 1994. Determination of nitrate in the presence of nitrite in natural waters by flow injection analysis with a non-quantitative on-line cadmium

- reductor. *Internal Journal Environmental Analysis Chemistry* 57, 263-277.
- Petit, J.R., Jouzel, J., Raynaud, D., Barkov, N.I., Barnola, J.M., Basile, I., Bender, M., Chappellaz, J., Davis, M., Delaygue, G., Delmotte, M., Kotlyakov, V.M., Legrand, M., Lipenkov, V.Y., Lorius, C., Pépin, L., Ritz, C., Saltzman, E., Stievenard, M., 1999. Climate and atmospheric history of the past 420,000 years from the Vostok ice core, Antarctica. *Nature* 399, 429-436.
- Quay, P., Sonnerup, R., Westby, T., Stutsman, J., McNichol, A., 2003. Changes in the $^{13}\text{C}/^{12}\text{C}$ of dissolved inorganic carbon in the ocean as a tracer of anthropogenic CO_2 uptake. *Global Biogeochemical Cycles* 17, doi:10.1029/2001GB001817.
- Redfield, A.C., Ketchum, B.H., Richards, F.A., 1963. The influence of organisms on the composition of sea water. In : Hill, M.N. (Ed), *The Sea*, vol. 2. Interscience, New York, pp. 26-77.
- Riebesell, U., Zondervan, I., Rost, B., Tortell, P.D., Zeebe, R.E., Morel, F.M.M., 2000. Reduced calcification of marine plankton in response to increased atmospheric CO_2 . *Nature* 407, 364-367.
- Sabine, C.L., Feely, R.A., Key, R.M., Bullister, J.L., Millero, F.L., Lee, K., Peng, T.H., Tilbrook, B., Wong, C.S., 2002a. Distribution of anthropogenic CO_2 in the Pacific Ocean. *Global Biogeochemical Cycles* 16, doi:10.1029/2001GB001639.
- Sabine, C.L., Key, R.M., Feely, R.A., Greeley, D., 2002b. Inorganic carbon in the Indian Ocean: distribution and dissolution processes. *Global Biogeochemical Cycles* 16, doi:10.1029/2002GB001869.
- Sambrotto, R.N., Savidge, G., Robinson, C., Boyd, P., Takahashi, T., Karl, D.M., Langdon, C., Chipman, D., Marra, J., Codispoti, L., 1993. Elevated consumption of carbon relative to nitrogen in the surface ocean. *Nature* 363, 248-249.
- Shaw, P.T., 1991. The seasonal variation of the intrusion of the Philippine Sea Water into the South China Sea. *Journal of Geophysical Research* 96, 821-827, 1991.

- Shaw, P.T., Chao, S.Y., 1994. Surface circulation in the South China Sea. *Deep-Sea Research I* 41, 1663-1683.
- Shiah, F.K., Liu, K.K., Tang, T.Y., 1999. South East Asia Time-series Station established in South China Sea. *US JGOFS Newsletter* 10, 8-9.
- Siegenthaler, U., Samiento, J.L., 1993. Atmospheric carbon dioxide and the ocean. *Nature* 365, 119-125.
- Sonnerup, R.E., Quay, P.D., McNichol, A.P., Bullister, J.L., Westby, T.A., Anderson, H.L., 1999. Reconstructing the oceanic ^{13}C Suess effect. *Global Biogeochemical Cycles* 13, 857-872.
- Takahashi, T., Olafsson, J., Goddard, J.G., Chipman, D.W., Sutherland, S.C., 1993. Seasonal variation of CO_2 and nutrients in the high-latitude surface oceans: a comparative study. *Global Biogeochemical Cycles* 7, 843-878.
- Takahashi, T., Feely, R.A., Weiss, R., Wanninkhof, R.H., Chipman, D.W., Sutherland, S.C., Takahashi, T.T., 1997. Global air-sea flux of CO_2 : an estimate based on measurements of sea-air pCO_2 difference. *Proceedings of the National Academy of Science* 94, 8292-8299.
- Takahashi, T., Sutherland, S.C., Sweeney, C., Poisson, A., Metzl, N., Tilbrook, B., Bates, N.R., Wanninkhof, R., Feely, R.A., Sabine, C., Olafsson, J., Nojiri, Y., 2002. Global sea-air CO_2 flux based on climatological surface ocean pCO_2 , and seasonal biological and temperature effects. *Deep-Sea Research II* 49, 1601-1622.
- Tans, P.P., Fung, I.Y., Takahashi, T., 1990. Observational constraints on the global atmospheric CO_2 budget. *Science* 247, 1431-1438.
- Toggweiler, J.R., 1993. Carbon overconsumption. *Nature* 363, 210-211.
- Tsunogai, S., 1972. An estimate of the rate of decomposition of organic matter in the deep water of the Pacific Ocean. In: Takenouti, Y., Shoten, I. (Eds), *Biological Oceanography of the Northern North Pacific Ocean*, Tokyo, pp. 517-533.

- Tsurushima, N., Nojiri, Y., Imai, K., Watanabe, S., 2002. Seasonal variations of carbon dioxide system and nutrients in the surface mixed layer at station KNOT (44° N, 155° E) in the subarctic western North Pacific. *Deep-Sea Research II* 49, 5377-5394.
- Wallace, D.W.R., 2001. Introduction to special section: Ocean measurements and models of carbon sources and sinks. *Global Biogeochemical Cycles* 15, 3-10.
- Wang, J., Chern, C.S., 1987. The warm-core eddy in the northern South China Sea, I. Preliminary observations on the warm-core eddy. *Acta Oceanographica Taiwanica* 18, 92-103.
- Wanninkhof, R., 1992. Relationship between wind speed and gas exchange over the ocean. *Journal of Geophysical Research* 97, 7373-7382.
- Weiss, R.F., 1974. Carbon dioxide in water and seawater: The solubility of a non-ideal gas. *Marine Chemistry* 2, 203-215.
- Winn, C.D., Mackenzie, F.T., Carrillo, C.J., Sabine, C.L., Karl, D.M., 1994. Air-Sea carbon dioxide exchange in the North Pacific Subtropical Gyre: Implications for the global carbon budget. *Global Biogeochemical Cycles* 8, 157-163.
- Wong, C.S., Chan, Y.H., 1991. Temporal variations in the partial pressure and flux of CO₂ at ocean Station P in the subarctic northeast Pacific Ocean. *Tellus* 43B, 206-223.
- Wong, G.T.F., Chung, S.W., Shiah, F.K., Chen, C.C., Wen, L.S., Liu, K.K., 2002. Nitrate anomaly in the upper nutrientcline in the northern South China Sea—Evidence for nitrogen fixation. *Geophysical Research Letters* 29, doi:10.1029/2002GL015796.
- Wu, J., Chung, S.W., Wen, L.S., Liu, K.K., Chen, Y.L., Chen, H.Y., Karl, D.M., 2003. Dissolved inorganic phosphorus, dissolved iron, and Trichodesmium in the oligotrophic South China Sea. *Global Biogeochemical Cycles* 17, doi:10.1029/2002GB001924.

- Zhang, J., Quay, P.D., Wilbur, D.O., 1995. Carbon isotope fractionation during gas-water exchange and dissolution of CO₂. *Geochimica et Cosmochimica Acta* 59, 107-114.
- Zhang, Y., Sperber, K.R., Boyle, J.S., 1997. Climatology and interannual variation of the East Asian winter monsoon: results from the 1979-95 NCEP/NCAR reanalysis. *Monthly Weather Review* 125, 2605-2619.
- Zondervan, I., Zeebe, R.E., Rost, B., Riebesell, U., 2001. Decreasing marine biogenic calcification: A negative feedback on rising atmospheric pCO₂. *Global Biogeochemical Cycles* 15, 507-516.

附錄一

各航次鹽度 (Salinity) 位溫 (P. Temp.) 磷酸鹽 (PO_4^{3-}) 硝酸鹽 (NO_3^-) 溶氧 (DO) 總滴定鹼度 (TA) 總二氧化碳 (TCO_2) 及總二氧化碳碳同位素 ($\delta^{13}\text{C}_{\text{TCO}_2}$) 數據。

ORI-639 (3/19 - 4/2/2002)

Depth (m)	Salinity (psu)	P. Temp. (°C)	PO_4^{3-} (μM)	NO_3^- (μM)	DO (μM)	TA (μM)	TCO_2 (μM)	$\delta^{13}\text{C}_{\text{TCO}_2}$ (‰)
5	33.29	26.47	0.05	0.00	204.3	2192.1	1890.8	0.67
10	33.31	26.45	0.00	0.00	204.7	2195.3	1894.0	0.66
20	33.72	25.82	0.00	0.00	204.5	2186.5	1890.9	0.67
40	33.93	24.38	0.00	0.00	212.6	2229.3	1927.8	0.73
60	34.40	22.19	0.16	1.83	193.4	2260.7	1985.1	0.56
80	34.50	20.74	0.61	7.85	147.0	2275.9	2057.0	0.25
100	34.61	18.93	0.83	11.77	135.7	2275.5	2071.4	0.22
125	34.60	17.11	0.80	13.17	143.8	2282.9	2089.3	0.23
150	34.59	15.47	1.01	14.59	141.6	2277.9	2098.3	0.20
200	34.53	13.56	1.33	19.47	129.4	2283.1	2135.5	0.14
300	34.44	10.71	1.76	24.74	108.2	2301.2	2179.2	0.00
350	34.43	9.96	1.91	26.31	106.8	2300.1	2193.6	-0.09
400	34.43	9.18	*2.34	*31.97	*110.0	*2345.6	*2264.2	*-0.09
500	34.42	7.97	2.29	30.90	94.7	2319.3	2237.0	-0.10
600	34.44	6.96	2.45	32.97	89.7	2336.7	2259.7	-0.11
700	34.47	5.91	2.66	34.74	90.6	2348.5	2278.4	-0.18
800	34.49	5.15	2.65	35.66	88.3	2360.1	2295.3	-0.25
900	34.52	4.67	2.77	36.61	85.6	2377.2	2309.2	-0.20
1000	34.54	4.15	2.82	36.88	97.8	2379.1	2313.5	-0.18
1200	34.57	3.35	2.91	37.68	91.1	2404.4	2335.4	-0.21
1400	34.59	2.90	2.76	35.84	101.4	2416.7	2344.5	-0.20
1600	34.61	2.61	2.82	38.64	*88.79	2423.9	2348.3	-0.18
1800	34.61	2.43	2.93	38.52	110.0	2423.8	2347.2	-0.26
2000	34.62	2.34	2.86	38.10	105.0	2424.1	2348.2	-0.21

2200	34.62	2.25	2.92	38.42	107.7	2423.7	2348.0	-0.16
2400	34.62	2.18	2.87	38.53	109.5	2422.8	2348.8	-0.17
2600	34.63	2.16	2.87	38.42	112.3	2416.1	2347.8	-0.22
2800	34.63	2.14	2.87	38.30	112.7	2422.1	2345.8	-0.19
3000	34.63	2.12	2.87	38.42	113.6	2417.0	2344.3	-0.18

ORIII-794 (6/30 - 7/4/2002)

Depth (m)	Salinity (psu)	P. Temp. (°C)	PO ₄ ³⁻ (μM)	NO ₃ ⁻ (μM)	DO (μM)	TA (μM)	TCO ₂ (μM)	δ ¹³ C _{TCO2} (‰)
2	33.61	30.73	0.00	0.00	*155.0	2220.7	1893.7	0.79
10	33.63	30.52	n.d.	n.d.	197.0	*2256.5	*2009.6	*0.49
20	33.61	29.38	*0.54	*6.71	*197.0	*2301.8	*2149.2	*0.26
40	33.76	26.56	0.05	0.00	215.5	2219.0	1907.0	0.82
60	34.09	24.33	n.d.	n.d.	211.0	2256.4	n.d.	0.90
80	34.24	22.86	0.10	5.69	176.7	*2270.4	1970.5	0.48
100	34.42	20.78	0.55	8.81	156.0	2261.5	2036.1	0.41
125	34.59	17.96	0.83	12.06	141.9	2276.4	2062.2	0.27
150	34.59	16.51	0.99	15.08	137.4	2285.0	2075.0	0.15
200	34.57	14.88	1.09	15.25	141.9	2281.2	2105.6	0.27
250	34.50	12.90	1.30	19.67	141.0	2286.5	2125.0	0.20
300	34.45	11.56	n.d.	n.d.	131.0	2298.1	n.d.	0.12
400	34.42	9.30	1.93	26.14	114.8	2311.5	2199.2	-0.09
500	34.42	7.85	2.24	32.71	102.5	2322.6	2226.0	0.03
600	34.43	7.28	2.34	33.86	95.8	2334.5	2242.4	-0.11
700	34.45	6.26	2.50	35.11	94.4	2351.6	2270.0	-0.14
800	34.48	5.31	2.60	34.14	90.8	2369.8	2286.8	-0.20
900	34.51	4.67	2.76	39.89	87.2	2376.2	2310.6	-0.21
1000	34.53	4.22	2.81	37.95	89.0	2388.2	2317.2	-0.19
1200	34.55	3.55	*2.65	*34.31	95.0	n.d.	n.d.	-0.13
1400	34.59	2.86	n.d.	n.d.	100.0	2423.9	n.d.	-0.19
1600	34.60	2.64	2.91	*41.22	109.8	2423.9	2349.0	-0.21
1800	34.60	2.46	*2.65	*35.03	103.0	2423.2	n.d.	-0.20
2000	34.61	2.36	2.75	*34.49	106.0	n.d.	n.d.	-0.23
2200	34.61	2.27	2.86	38.74	111.6	2424.0	2343.5	-0.21
2400	34.61	2.21	2.86	38.21	114.3	2427.3	2344.7	-0.18
2600	34.61	2.17	*2.65	*33.63	117.0	n.d.	n.d.	-0.20
2800	34.62	2.14	2.86	38.12	113.4	2422.2	2346.0	-0.14

ORI-656 (8/31 - 9/6/2002)

Depth (m)	Salinity (psu)	P. Temp. (°C)	PO ₄ ³⁻ (μM)	NO ₃ ⁻ (μM)	DO (μM)	TA (μM)	TCO ₂ (μM)	δ ¹³ C _{TCO2} (‰)
5	33.68	29.58	0.00	0.00	202.0	2217.1	1897.8	0.71
10	33.67	29.40	0.00	0.00	202.0	2209.5	1897.5	0.79
20	33.67	29.39	0.00	0.00	209.2	2219.0	1897.6	0.73
40	33.63	28.39	0.00	0.00	206.5	2214.1	1898.8	0.68
60	33.82	26.35	0.05	0.00	203.3	2241.9	1961.1	0.70
80	34.22	22.44	0.37	6.77	162.2	2251.0	2017.5	0.36
100	34.33	21.18	0.69	12.24	136.4	2258.6	2053.2	0.16
125	34.50	19.19	0.74	13.21	135.5	2267.9	2065.9	0.19
150	34.59	17.51	0.90	14.82	136.9	2281.0	2088.5	0.21
200	34.57	15.10	1.11	16.76	141.4	2281.9	2110.8	0.24
250	34.49	12.85	1.20	17.96	141.9	2287.2	2134.1	0.12
300	34.46	11.58	1.52	20.87	134.6	2287.1	2156.1	0.06
350	34.43	10.50	1.78	24.58	112.0	2296.3	2184.2	-0.03
400	34.42	9.67	1.94	27.03	94.0	2300.7	2197.9	-0.03
500	34.41	8.45	2.15	29.85	100.7	2321.3	2223.4	-0.13
600	34.42	7.30	2.25	32.22	94.9	2331.5	2249.3	-0.16
700	34.44	6.35	2.51	34.05	89.0	2345.5	2270.4	-0.16
800	34.47	5.62	2.57	35.21	89.9	n.d.	2285.0	-0.17
900	34.49	4.87	2.62	36.37	90.3	2380.3	2299.7	-0.14
1000	34.51	4.39	2.67	36.64	91.7	2375.4	2311.3	-0.14
1200	34.55	3.47	2.81	37.90	93.1	2404.7	2331.9	-0.23
1400	34.57	3.00	2.87	38.44	96.7	*2426.8	2343.7	-0.19
1600	34.59	2.66	2.81	38.48	104.4	2414.5	2343.8	-0.18
1800	34.59	2.44	2.87	38.30	108.0	2419.1	2341.9	-0.14
2000	34.60	2.33	2.87	38.48	108.4	2421.2	2345.8	-0.23
2200	34.60	2.25	2.87	38.66	109.8	2422.1	2348.3	-0.19
2400	34.61	2.20	2.87	38.52	111.6	2419.0	2346.4	-0.15
2600	34.61	2.16	2.81	38.57	n.d.	2419.2	2344.9	-0.17

2800	34.61	2.13	2.81	38.84	114.8	2421.5	2344.3	-0.22
3000	34.61	2.11	2.87	38.70	115.7	n.d.	2343.8	-0.13

ORI-664 (11/9 -11/15/2002)

Depth (m)	Salinity (psu)	P. Temp. (° C)	PO ₄ ³⁻ (μM)	NO ₃ ⁻ (μM)	DO (μM)	TA (μM)	TCO ₂ (μM)	δ ¹³ C _{TCO2} (‰)
5	33.37	27.37	0.02	0.00	204.1	2203.9	1888.8	0.75
10	33.37	27.37	0.05	0.00	205.4	2198.5	1887.4	0.75
20	33.37	27.37	0.03	0.00	204.9	2197.7	1887.7	*0.33
40	33.37	27.37	0.03	0.00	204.7	2176.6	1888.7	*0.53
60	33.40	27.39	0.03	0.00	202.6	2235.9	1919.0	0.89
70	34.34	26.09	0.10	0.53	194.8	2267.0	1961.5	0.84
80	34.54	24.53	0.12	2.32	185.4	2269.8	1989.3	0.67
100	34.46	22.04	0.62	9.54	144.7	2258.0	2034.9	0.29
150	34.57	17.08	0.96	14.85	131.2	2268.0	2090.5	0.12
200	34.56	15.06	1.03	14.94	151.4	2284.5	2102.0	0.22
400	34.42	10.16	1.80	25.57	114.3	2297.9	2186.6	-0.11
600	34.42	7.45	2.41	32.72	90.3	2338.0	2251.1	-0.16
800	34.45	5.82	2.52	34.78	89.4	2354.1	2280.8	-0.18
1000	34.50	4.71	2.72	36.23	90.3	2379.3	2306.6	-0.22
1200	34.54	3.70	2.77	37.09	96.2	2394.0	2328.2	-0.18
1500	34.57	2.85	2.82	37.80	99.8	2423.1	2345.6	-0.26
2000	34.59	2.37	2.82	38.54	108.0	2419.2	2345.4	-0.22
2500	34.60	2.17	2.82	38.33	112.7	2425.3	2346.0	-0.17
3000	34.60	2.11	2.82	38.13	115.2	2413.1	2340.4	-0.16

ORI-673 (1/17 - 1/23/2003)

Depth (m)	Salinity (psu)	P. Temp. (°C)	PO ₄ ³⁻ (μM)	NO ₃ ⁻ (μM)	DO (μM)	TA (μM)	TCO ₂ (μM)	δ ¹³ C _{TCO2} (‰)
5	33.69	23.90	0.15	0.47	214.9	2217.8	1925.0	0.67
10	33.69	23.89	0.05	0.38	216.0	2228.4	1923.2	0.65
20	33.69	23.85	0.05	0.43	216.0	2221.0	1922.9	0.69
40	33.70	23.84	0.05	0.45	215.8	2218.9	1922.4	0.64
50	33.80	23.84	0.05	0.36	208.8	2220.4	1924.5	0.62
60	33.88	23.85	0.07	0.29	210.1	2227.6	1933.4	0.67
80	34.17	23.39	0.15	2.47	179.8	2248.0	1933.9	0.59
100	34.60	20.93	0.42	6.92	161.8	2274.8	2021.8	0.48
125	34.65	18.88	0.56	8.52	159.0	2275.1	2045.0	0.40
150	34.62	16.53	0.90	13.15	149.3	2282.2	2072.1	0.28
200	34.54	14.11	1.19	16.83	141.4	2280.6	2100.2	0.31
250	34.45	11.94	1.48	21.64	136.0	2285.6	2144.5	0.16
300	34.41	10.41	1.79	26.09	121.1	2297.7	2176.2	0.09
400	34.40	8.83	2.14	29.36	108.0	2312.1	2208.2	-0.01
500	34.40	7.63	2.32	32.19	101.4	2327.6	2239.0	-0.02
600	34.43	6.69	2.45	34.34	90.0	n.d.	2259.4	-0.10
800	34.47	5.17	2.70	37.46	*72.3	2365.4	2294.4	-0.19
900	34.51	4.40	2.76	37.92	93.1	2387.1	n.d.	-0.19
1000	34.52	3.97	2.86	39.12	92.0	2391.9	2323.0	-0.20
1200	34.55	3.29	2.81	39.21	95.3	2410.6	2333.7	-0.17
1400	34.57	2.85	2.86	39.34	101.6	2413.7	2340.5	-0.19
1500	34.58	2.68	2.86	38.42	98.0	2423.5	2335.3	-0.17
1600	34.58	2.53	2.86	39.77	108.9	2412.0	2335.4	-0.17
1800	34.59	2.41	2.86	40.92	105.3	2419.1	2343.2	-0.16
2000	34.59	2.32	2.86	38.77	108.0	2420.1	2342.1	-0.17
2500	34.60	2.16	n.d.	n.d.	107.5	2420.3	2342.0	-0.15
3000	34.60	2.11	2.86	39.35	112.5	2417.7	2341.8	-0.11

ORI-674 (3/3 -3/9/2003)

Depth (m)	Salinity (psu)	P. Temp. (°C)	PO ₄ ³⁻ (μM)	NO ₃ ⁻ (μM)	DO (μM)	TA (μM)	TCO ₂ (μM)	δ ¹³ C _{TCO2} (‰)
5	33.50	25.84	0.00	0.00	*191.1	2199.6	1898.4	n.d.
10	33.50	25.84	0.00	0.00	214.2	2203.5	n.d.	0.68
20	33.50	25.80	0.00	0.00	216.4	2197.6	1898.2	0.68
40	33.94	24.02	0.00	0.00	*180.7	2231.2	1922.3	0.81
50	34.08	23.69	0.00	0.00	224.6	2238.0	1933.4	0.78
60	34.17	23.37	0.00	0.00	*152.7	2252.8	1941.7	0.80
80	34.40	22.77	0.05	1.44	206.1	2260.4	1970.2	0.76
100	34.56	21.75	0.25	5.77	178.5	2273.8	2012.3	0.46
150	34.65	17.24	0.70	12.09	154.5	2277.7	2074.2	0.34
200	34.57	14.69	1.15	18.05	131.5	2285.0	2117.2	0.15
400	34.42	8.74	1.99	28.82	109.8	2306.8	2209.6	-0.02
500	34.43	7.53	2.30	31.34	99.8	2330.1	2237.5	-0.02
600	34.44	6.62	2.40	32.27	100.7	2336.6	2251.2	-0.07
800	34.48	5.13	2.60	35.37	96.7	2368.7	2289.3	-0.10
1000	34.54	4.07	2.81	36.92	95.8	2396.8	2320.4	-0.15
1500	34.60	2.72	2.86	38.34	99.4	2418.5	2347.4	-0.23
2000	34.62	2.32	2.86	38.07	108.4	2423.7	2347.6	-0.14
2500	34.62	2.17	*2.71	*36.21	*98.0	*2403.7	*2324.5	n.d.
3000	34.62	2.11	2.81	36.88	108.0	2423.8	2346.6	-0.25

ORIII-859 (4/10 - 4/14/2003)

Depth (m)	Salinity (psu)	P. Temp. (°C)	PO ₄ ³⁻ (μM)	NO ₃ ⁻ (μM)	DO (μM)	TA (μM)	TCO ₂ (μM)	δ ¹³ C _{TCO2} (‰)
2	33.40	28.35	n.d.	n.d.	n.d.	2200.3	n.d.	0.65
5	33.40	28.20	n.d.	n.d.	n.d.	2202.9	1887.3	0.61
10	33.40	28.04	n.d.	n.d.	n.d.	2198.7	1886.0	0.62
20	33.41	27.92	n.d.	n.d.	n.d.	2215.5	1894.1	0.60
40	33.94	26.05	n.d.	n.d.	n.d.	2248.6	1979.9	0.83
60	34.33	23.59	n.d.	n.d.	n.d.	2247.6	1946.4	0.89

80	34.66	21.09	n.d.	n.d.	n.d.	2255.6	1996.6	0.57
100	34.75	19.19	n.d.	n.d.	n.d.	2272.3	2047.7	0.33
120	34.81	17.79	n.d.	n.d.	n.d.	2273.6	2072.3	0.19
150	34.70	16.13	n.d.	n.d.	n.d.	2280.7	2086.8	0.14

ORI-690 (8/5 - 8/10/2003)

Depth (m)	Salinity (psu)	P. Temp. (°C)	PO ₄ ³⁻ (μM)	NO ₃ ⁻ (μM)	DO (μM)	TA (μM)	TCO ₂ (μM)	δ ¹³ C _{TCO2} (‰)
5	33.77	29.57	0.05	0.00	197.9	2221.1	1904.7	0.83
10	33.84	29.49	0.05	0.00	197.9	2225.3	1905.9	0.88
20	33.87	28.21	0.05	0.00	205.1	2226.2	1913.9	0.80
40	33.97	26.30	0.05	0.00	207.9	2231.6	1928.5	0.80
50	34.19	24.36	n.d.	n.d.	n.d.	2247.4	1969.6	0.64
60	34.43	21.89	0.20	2.06	180.7	2263.8	2002.7	0.56
70	34.51	21.03	n.d.	n.d.	n.d.	2262.8	2024.8	0.42
80	34.56	19.93	0.51	7.84	156.8	2266.7	2039.3	0.30
90	34.61	19.01	n.d.	n.d.	n.d.	2273.5	2054.7	0.32
100	34.60	19.33	0.59	8.68	155.9	2277.0	2047.8	0.32
125	34.62	17.97	0.82	11.03	147.7	2277.8	2067.4	0.17
150	34.60	16.39	0.92	13.03	147.3	2278.9	2088.3	0.23
200	34.54	14.16	1.23	16.66	135.5	2284.6	2119.3	0.17
300	34.45	11.42	1.69	21.94	122.0	2294.6	2165.7	0.02
400	34.41	9.48	2.05	26.63	108.4	2307.1	2200.8	-0.06
500	34.41	8.23	2.25	28.72	103.5	2319.6	2228.4	-0.07
600	34.43	7.24	2.46	31.80	99.4	2337.1	2251.0	-0.11
700	34.44	6.56	2.56	33.17	90.3	2346.7	2266.1	-0.12
800	34.47	5.78	2.66	34.66	94.0	2360.7	2283.0	-0.09
900	34.49	5.33	2.66	36.05	87.2	2369.6	2292.1	-0.19
1000	34.51	4.77	2.77	36.74	87.9	2376.6	2305.0	-0.17
1200	34.55	3.74	2.87	37.11	99.4	2397.8	2320.9	-0.17
1500	34.58	3.01	2.92	38.41	96.7	2409.6	2342.9	-0.22
2000	34.60	2.55	2.92	38.63	103.5	2421.3	2344.2	-0.16
2500	34.61	2.38	2.87	38.29	110.2	2430.1	2343.4	-0.20
3000	34.61	2.35	2.87	38.21	113.8	2420.4	2341.7	-0.16

*: data questionable; n.d.: not determined

附錄二

(Submitted to Deep-Sea Research I)

Preliminary investigation on seasonal variability of mixed-layer CO₂,
alkalinity, and fCO₂ at the SEATS time-series site,
northern South China Sea

W.C. Chou^a, D.D., Sheu^{a,*}, C.T.A. Chen^a, S.L. Wang^b and C.M. Tseng^c

^aInstitute of Marine Geology and Chemistry, National Sun Yat-Sen University,
Kaohsiung 804, Taiwan, Republic of China.

^bDepartment of Marine Environmental Engineering, National Kaohsiung Institute of
Marine Technology, Kaohsiung 811, Taiwan, Republic of China.

^cNational Center for Ocean Research, P.O. Box 23-13, Taipei 106, Taiwan, Republic
of China.

*Address: Institute of Marine Geology and Chemistry, National Sun Yat-Sen
University, Kaohsiung 804, Taiwan, Republic of China

Email: ddsheu@mail.nsysu.edu.tw

Tel: + 886-7-525-5148

Fax: + 886-7-525-5348

Abstract

Analyses of total carbon dioxide (TCO_2) and titration alkalinity (TA) in the mixed-layer was performed approximately bimonthly at the SEATS time series site ($18^\circ 15' \text{N}$, $115^\circ 35' \text{E}$) in the northern South China Sea (SCS) from March 2002 to April 2003. These measurements and the calculated- fCO_2 were then used to estimate the annual air-sea flux of CO_2 at the site. Results show that the normalized TCO_2 ($\text{NTCO}_2 = \text{TCO}_2 \times 33.5/\text{S}$) fluctuates seasonally between ~ 1888 and $\sim 1910 \mu\text{mol kg}^{-1}$, with the highest value in winter. The decline of NTCO_2 in spring-summer mainly results from *in situ* biological utilization, while the resurgence of NTCO_2 in fall-winter is due to entrainment of the CO_2 -rich subsurface waters from below. TA varies from ~ 2190 to $\sim 2220 \mu\text{mol kg}^{-1}$ in tandem with salinity, suggesting the oscillation of prime control of physical processes. fCO_2 increases progressively from spring to summer, reaches the maximum in July ($\sim 382 \mu\text{atm}$), then decreases from fall to winter to the minimum ($\sim 347 \mu\text{atm}$) in January with an amplitude of $\sim 35 \mu\text{atm}$. The seasonal variability of fCO_2 is in phase with temperature changes but is inversely correlated with the fluctuation of NTCO_2 , suggesting that the fCO_2 seasonality is primarily controlled by temperature changes, though other factors have compensated partially to yield the observed low amplitude of its variability. ΔfCO_2 ($\text{fCO}_{2(\text{seawater})} - \text{fCO}_{2(\text{atmosphere})}$) increases gradually from spring to summer followed by

a progressive decrease to fall and winter. The maximal positive and negative $\Delta f\text{CO}_2$ occurs in summer ($\sim +20\mu\text{tam}$; July 2002) and winter ($\sim -15\mu\text{tam}$; January 2003), respectively. Throughout the year, the annual sea-to-air CO_2 flux is estimated to be $-1.28\pm 0.94 \sim -2.73\pm 2.20 \text{ gC m}^{-2} \text{ year}^{-1}$. Furthermore, although the drawdown of NTCO_2 from winter to summer ($21\mu\text{M}$) implies a primary production of $177\pm 34 \sim 363\pm 69 \text{ mgC m}^{-2} \text{ day}^{-1}$ in the mixed layer at the SEATS site, other sources of nitrogen required to sustain the new production remain elusive.

(Key words: carbon dioxide, air-sea flux, time-series, South China Sea)

1. Introduction

For the past two decades, enormous research efforts have been made in an attempt to better quantify the spatial and temporal variability of CO₂ fluxes between the atmosphere and the oceans. One of the most direct methods to measure the fluxes is to carry out long-term time-series measurements in the world oceans. In the late 1980s, the Bermuda Atlantic Time-series Study (BATS; 31° 50' N, 64° 10' W) and the Hawaii Ocean Time-series program (HOT; 22° 45' N, 158° 00' W) were established in the subtropical Atlantic and Pacific, respectively. Results from these long-term oceanic time-series observations have greatly improved our knowledge of processes modulating the CO₂ exchange between the atmosphere and the upper oceans (Winn et al., 1994; 1998; Bates et al., 1996; Bates, 2001; Gruber et al., 2002; Dore et al., 2003). The general consensus has been that the temperate and polar oceans of both hemispheres are major sinks for atmospheric CO₂, while the equatorial oceans are major sources for CO₂ (Takahashi et al., 1997; 2002). However, in order to gain a better air-sea CO₂ flux scenario on a global scale, time-series observations from other key regions in the world oceans is required (Feely et al., 2001; Karl et al., 2001; Quay, 2002). Among these, the South East Asia Time-series Study (SEATS; 18° 15' N, 115° 35' E; Fig. 1) in the northern South China Sea (SCS), a semi-enclosed marginal sea off the Asian continent in the western Pacific, is critical (Shiah et al.,

1999).

This study reports the first observations of the carbon system in the mixed-layer at the SEATS site from March 2002 to April 2003. Although the results are based on just a little over a year's measurements, the observed seasonality and the processes controlling its variability are believed to be representative and thus contribute to a better synthesis of the oceanic CO₂ flux on a global basis.

2. Methods

2.1. Sampling and analysis

During the course of this study, the SEATS site has been investigated aboard the *R/V Ocean Research I* and *III* in March, July, September, and November 2002, as well as January, March, and April 2003. On board, temperature and salinity were recorded with a CTD (SeaBird Inc. model 911 plus). All raw data and other pertinent measurements are kept on file in the SEATS time-series database of the NCOR (National Center for Ocean Research). Interested readers should contact Dr. C. M. Tseng at the NCOR for data requests. Discrete water samples at depths of 5, 10, 20, 40, 60, 80, 100, 125, 150, and 200 m were sampled and transferred into 250 ml BOD bottles from Go-Flo bottles mounted onto a Rosette sampling assembly (General Oceanic Inc.). All water samples are poisoned with 50 µl saturated HgCl₂

solution immediately after sampling and stored at 5°C in darkness to prevent biological alteration (DOE, 1994).

Determinations of TCO₂ and TA follow the standard operating procedures described in DOE (1994). For TCO₂ analysis, the single operator multiparameter metabolic analyzer (SOMMA) system was used to control the pipetting system and extraction of CO₂ from seawater samples. The CO₂ gas was then measured by a coulometric detector (UIC, Coulometric Inc., model 5011) (Johnson et al., 1993). TA was determined by the potentiometric titration method (Bradshaw et al., 1981; Millero et al., 1993; DOE, 1994). The set-up of the titration system is composed of a Radiometer pH meter (pHM-85), a GK 2041C combination electrode, an autoburette (Metrohm 665 Dosimat), an open titration cell, and a temperature-controlled water bath at 25±0.05°C. A specific amount of seawater (~150g) was first dispensed into the cell, and then titrated with hydrochloric acid by passing the carbonic acid endpoint. The acid titrant, approximately 0.1 N hydrochloric acid, was prepared in a NaCl solution with an ionic strength similar to that of seawater of 0.68. Titration data passing the carbonic acid endpoint (~4.5 pH) were used to calculate TA, using a proton condition to define TA (Dickson, 1981; 1992; Butler, 1992). TCO₂ and TA were normalized to the averaged surface water salinity of the SCS (33.5) in order to eliminate the evaporation/precipitation effect,

and are denoted as NTCO_2 and NTA , respectively.

Seawater references (batch number #51) prepared and provided by A. G. Dickson are used throughout this study for assessing the accuracy of our TCO_2 and TA measurements. Differences between the certified values (2050.28 ± 0.03 and $2269.86 \pm 0.78 \mu\text{mole kg}^{-1}$ for TCO_2 and TA respectively) and our measurements are less than $2 \mu\text{mol kg}^{-1}$ and $3 \mu\text{mol kg}^{-1}$ for TCO_2 and TA, respectively. Precisions of the TCO_2 and TA analyses, estimated by repeated measurements of deep-water samples from 2000-3000m on each cruise, are better than $\pm 2 \mu\text{mol kg}^{-1}$ and $\pm 2.5 \mu\text{mol kg}^{-1}$, respectively. Finally, the fugacity of CO_2 ($f\text{CO}_2$) is computed from temperature, salinity, TCO_2 , TA, phosphate, and silicate data for samples collected from each cruise using the software program of Lewis and Wallace (1998), in which the carbonic dissociation constants are adopted from Mehrbach et al. (1973) and refitted by Dickson and Millero (1987). It is worth mentioning, however, that phosphate and silicate are almost undetectable at μmolar levels in the mixed-layer at SEATS site. The error of the calculated $f\text{CO}_2$ is less than $\pm 5 \mu\text{atm}$.

2.2. Correction for temperature effect on $f\text{CO}_2$

In this study, the extent of temperature effect is assessed using the equation of Takahashi et al. (2002):

$$f\text{CO}_2 \text{ at } T_{\text{obs}} = (\text{Mean annual } f\text{CO}_2) \times \exp[0.0423(T_{\text{obs}} - T_{\text{mean}})] \quad (1)$$

where T is temperature in $^{\circ}\text{C}$, and the subscripts “mean” and “obs” stand for the annual average and observed values, respectively. In our calculations, we use the averaged values of $f\text{CO}_2$ ($364 \mu\text{atm}$) and temperature (27°C) measured throughout the period of this study as the mean. The resultant $f\text{CO}_2$, designated as “ $f\text{CO}_{2\text{mean}}$ corrected for ΔT ”, are the expected $f\text{CO}_2$ values that are only affected by temperature if a parcel of water with a $f\text{CO}_2$ value of $364 \mu\text{atm}$ are subjected to seasonal temperature changes (the difference between observed and annual mean temperature) under constant TA and TCO_2 . Moreover, in order to further discern other factors besides temperature that may affect $f\text{CO}_2$ changes, we normalized the observed $f\text{CO}_2$ to a constant temperature using the following equation (Takahashi et al., 2002):

$$f\text{CO}_2 \text{ at } T_{\text{mean}} = (f\text{CO}_2)_{\text{obs}} \times \exp[0.0423(T_{\text{mean}} - T_{\text{obs}})] \quad (2)$$

where T and the subscripts “mean” and “obs” are defined as the same as those in Eq. (1).

2.3. Calculation of $Df\text{CO}_2$ and air-sea CO_2 exchange flux

Since there are no direct measurements of atmospheric $f\text{CO}_2$ at SEATS, we

adopted 361.7 μatm as the atmospheric $f\text{CO}_2$ in our calculations. The value is modified from the average value of 370.89 ppmv reported at Mauna Loa Observatory for 2001 (Keeling and Whorf, 2002) after corrections for the equilibrium water vapor pressure at the temperature of 27 °C and a salinity of 33.5 (i.e. the annual mean temperature and salinity of the surface water at SEATS). Values of $\Delta f\text{CO}_2$ in different seasons are derived as follows: spring (March, April and May) value is the mean $\Delta f\text{CO}_2$ of the observed data in March 2002 and 2003 as well as April 2003; summer (June, July and August) value is the observed $\Delta f\text{CO}_2$ in July 2002; fall (September, October and November) value is the average of $\Delta f\text{CO}_2$ in September and November 2002; winter (December, January, February) value is the observed $\Delta f\text{CO}_2$ in January 2003. The net sea-to-air CO_2 flux, F , is then computed using the following equation:

$$F = K \times (\Delta f\text{CO}_2) \quad (3)$$

where K is the CO_2 gas exchange coefficient, and $\Delta f\text{CO}_2$ is $f\text{CO}_{2(\text{seawater})} - f\text{CO}_{2(\text{atmosphere})}$. The seasonal wind-speed data at a 10m height are computed from monthly average values for 1985-1999 from the ECMWF database (Liang, et al., 2000). Furthermore, results calculated from formulations of Liss and Merlivat (1986), Tans et al. (1990), and Wanninkhof (1992) are compared to show the range and uncertainty of the CO_2 flux estimates.

3. Results and discussion

3.1 The seasonal hydrography at the SEATS site

The relationships between potential temperature and salinity from different cruises at the SEATS site are depicted in Fig. 2. They are consistent with the general features reported previously for the South China Sea water (Gong et al., 1992; Chen and Huang, 1996; Shaw et al., 1996; Lin et al., 1999; Chen et al., 2001; Wong et al., 2002), and have been used frequently to distinguish them from other water masses (e.g. the Western Philippine Sea water) upon mixing. As shown in Fig. 2, the SCS waters are characteristic of both a distinct shallow salinity maximum ($S > 34.6$; $\sigma_\theta = \sim 24.5$) at approximately 150 m and a pronounced minimum ($S = \sim 34.4$; $\sigma_\theta = \sim 26.8$) at about 350m. The former is indicative of the North Pacific Tropical Water, while the later fingerprints the core of the North Pacific Intermediate Water (Nitani, 1972). Below 15° C (which corresponds to a depth of about 200m), data from the seven cruises are indistinguishable from each other throughout the year. On a closer examination, Fig. 2 further shows sea surface temperature is moderately high ($\sim 26^\circ\text{C}$) in March 2002, increases gradually to a maximum of $\sim 30^\circ\text{C}$ in July 2002, then decreases to a minimum of $\sim 24^\circ\text{C}$ in January 2003, and rebounds back to $\sim 28^\circ\text{C}$ in April 2003, giving a total range of $\sim 6^\circ\text{C}$ year-round. In the meantime, salinities

fluctuate between 33.4 and 33.7 with higher values in summer and winter and lower values in spring and fall. Thus, the seasonal variability of temperature and salinity at the SEATS site appears to be confined within the upper 200m of the water column and characterized by the summer heating and winter cooling.

3.2 The seasonal patterns of $TCO_2/NTCO_2$, TA/NTA and fCO_2 in the mixed-layer

In this study, depths of mixed-layer and data of $TCO_2/NTCO_2$, TA/NTA , and the calculated- fCO_2 from each cruise are averaged to depict their overall seasonality in the mixed-layer at the SEATS site (Fig. 3a-f). As seen in Fig. 3a, the mixed-layer depth, defined as “ $(\sigma_q$ at the bottom of mixed-layer - σ_q at 10 m) > 0.1 kg m³”, remains relatively constant between 20-30m until late fall (November), then reaches the maximal depth of ~90 m in January. The deepening of mixed-layer from late fall to winter is caused by the vigorous vertical mixing induced by the winter cooling and increased wind stress as a much stronger northeast (winter) monsoon prevails in the SCS during this season (Liu et al., 2002). A similar monsoon-induced temperature forcing and convective mixing during northeast monsoon and inter-monsoon seasons are also observed in the central Arabian Sea (Goyet et al., 1998; Sarma et al., 1998; 2000).

TCO_2 remains fairly constant from ~1887 to ~1898 $\mu\text{mol kg}^{-1}$ throughout the

period of this study except for the highest value of $\sim 1925 \mu\text{mol kg}^{-1}$ in winter (Fig. 3b). The TCO_2 maximum thus coincides with the deepening of the mixed-layer (Fig. 3a) and the winter cooling. Such a close association suggests that the strong northeast monsoon not only causes vigorous downward mixing to deepen the mixed-layer but also brings in more cold, CO_2 -rich subsurface waters from the deep. The drawdown of NTCO_2 in spring-summer (Fig. 3c) manifests the biological uptake in the mixed-layer. Similar observations were also reported previously at time-series stations of BATS (Bates et al., 1996) and HOT (Winn et al., 1994).

Fig. 3d shows the seasonal variability of TA measured in the mixed-layer at SEATS site. TA values vary from ~ 2190 to $\sim 2220 \mu\text{mol kg}^{-1}$ with higher values in January, July and September and lower values in March, April and November. The observed seasonal oscillation of TA is thus controlled primarily by the same factors affecting salinity. A similar relationship between TA and salinity is also documented at BATS and HOT sites (Winn et al., 1994; Bates et al., 1996). However, as revealed in Fig. 3e, NTA remains varying throughout the year, suggesting the potential contribution of the formation and/or dissolution of CaCO_3 and the consumption and/or remineralization of nitrate to the observed NTA variability.

A strong seasonality with an amplitude of $\sim 35 \mu\text{atm}$ during the yearly cycle is

found in the mixed-layer $f\text{CO}_2$ at the SEATS site (Fig. 3f). The $f\text{CO}_2$ increases progressively in spring to summer with the maximum in July ($\sim 382 \mu\text{atm}$) followed by a decrease in fall to winter with the minimum ($\sim 347 \mu\text{atm}$) in January. The seasonal changes of $f\text{CO}_2$ are closely in phase with temperature (Fig. 3f) but are inversely correlated with NTCO_2 (Fig. 3c). These relationships suggest that the variation in $f\text{CO}_2$ at SEATS is controlled ultimately by seawater temperature change, and will be examined in detail in the following sections.

3.3 Processes controlling the mixed-layer $f\text{CO}_2$ at the SEATS site

Fig. 4 depicts graphically the seasonal variability of “ $f\text{CO}_{2\text{mean}}$ corrected for ΔT ”, the observed $f\text{CO}_2$, and “ $f\text{CO}_2$ at 27°C ” at the SEATS site. As can be seen, the magnitude of seasonal variation of the “ $f\text{CO}_{2\text{mean}}$ corrected for ΔT ” is greater than the observed seasonal $f\text{CO}_2$ fluctuation, and the “ $f\text{CO}_2$ at 27°C ” and the “ $f\text{CO}_{2\text{mean}}$ corrected for ΔT ” are inversely correlated. These relationships imply that the temperature effect on the seasonal variability of $f\text{CO}_2$ must have been compensated in part by other factors to yield the observed smaller amplitude.

These factors other than temperature include biological processes, air-sea exchanges of CO_2 and vertical transport of subsurface waters. Although it is difficult to discern their respective effects on the seasonal $f\text{CO}_2$ oscillations, the

decrease in “fCO₂ at 27° C” from winter to summer (the warming period) can be attributed chiefly to biological effects because both the upward transport of subsurface waters and the air-sea CO₂ exchange are minimal during this period of time. The shoaling of the mixed-layer during warming period (Fig. 3a) results in a stronger stratification that, in turn, prevents subsurface waters underneath the mixed-layer from moving upward. To further estimate the extent of biological effects on the mixed-layer fCO₂, we will use the “fCO₂ at 27° C” in January 2003 and July 2002 as winter and summer values, respectively, in the following discussion. Accordingly, the decline of “fCO₂ at 27° C” from winter to summer is ~60 μatm (Fig. 4), yet the drawdown of TCO₂ is only about one-half of that figure (~30 μmol kg⁻¹; Fig. 3c). Using a Revelle factor of 10 (Takahashi et al., 1993), the observed drop in TCO₂ is calculated to be equivalent to a decrease of fCO₂ of ~55 μatm. The close agreement between the measured difference and the hypothetical value (60 vs. 55 μatm) thus confirms the aforementioned biological utilization responsible for the decrease of “fCO₂ at 27° C” during the warming period.

On the other hand, the increase of “fCO₂ at 27° C” from summer to winter (the cooling period) mainly results from the entrainment of subsurface water from the deep. Assuming the biological effect is as same as that of the warming period (i.e. ~ -60 μatm) and the effect of air-sea exchange is negligible on the fCO₂ variation

during the cooling period, a simple mass-balance calculation shows that the entrainment of the subsurface water will lead to an increase of $f\text{CO}_2$ of $+120 \mu\text{atm}$ in the mixed-layer during this period, providing that the temperature effect on the $f\text{CO}_2$ change is about $-90 \mu\text{atm}$ (i.e. the difference of “ $f\text{CO}_{2\text{mean}}$ corrected for ΔT ” between July 2002 and January 2003; Fig. 4) and the observed $f\text{CO}_2$ change is about $-30 \mu\text{atm}$.

3.4 Assessing the relative importance of the biological and temperature effects on seasonal $f\text{CO}_2$ variability at the SEATS site

The relative importance of the temperature and biological effects on surface-water $f\text{CO}_2$ can be evaluated in terms of (T/B) and/or (T-B), in which (T/B) = $[(\Delta f\text{CO}_2)_{\text{temp}} / (\Delta f\text{CO}_2)_{\text{bio}}]$ and/or (T-B) = $[(\Delta f\text{CO}_2)_{\text{temp}} - (\Delta f\text{CO}_2)_{\text{bio}}]$ (Takahashi et al., 2002). According to the authors, the biological effect, $(\Delta f\text{CO}_2)_{\text{bio}}$, on the surface-water $f\text{CO}_2$ can be represented by the seasonal amplitude of “ $f\text{CO}_2$ at T_{mean} ”, i.e. $(\Delta f\text{CO}_2)_{\text{bio}} = (f\text{CO}_2 \text{ at } T_{\text{mean}})_{\text{max}} - (f\text{CO}_2 \text{ at } T_{\text{mean}})_{\text{min}}$, while the temperature effect, $(\Delta f\text{CO}_2)_{\text{temp}}$, can be estimated from the seasonal magnitude of the “ $f\text{CO}_{2\text{mean}}$ corrected for ΔT ”, i.e. $(\Delta f\text{CO}_2)_{\text{temp}} = (f\text{CO}_{2\text{mean}} \text{ corrected for } \Delta T)_{\text{max}} - (f\text{CO}_{2\text{mean}} \text{ corrected for } \Delta T)_{\text{min}}$. In any given oceanic regime, if the effect of temperature exceeds the biological effect, the (T/B) ratio is greater than 1 and the (T-B) is positive, whereas in areas where the biological effect appears to surpass the temperature effect, the (T/B)

ratio varies from 0 to 1, and the (T-B) is negative. In areas where the two effects are equally important and cancel each other out, the (T/B) ratio is 1 and (T-B) is 0.

Fig. 4 shows that the maximum and minimum of “fCO₂ at 27° C” at the SEATS site are ~395 and ~333 μatm, respectively, while the maximum and minimum of the “fCO_{2mean} corrected for ΔT” are ~415 and ~318 μatm. The maximal changes of (ΔfCO₂)_{bio} and (ΔfCO₂)_{temp}, therefore, are ~62 μatm and ~97 μatm, respectively. Accordingly, the (T/B) ratio and the (T-B) difference are calculated to be 1.6 and 35 μatm, respectively. The results thus indicate that temperature overwhelms the biological effect on regulating the mixed-layer fCO₂ at the SEATS site.

A comparison of our results with those from other time-series stations (e.g. HOT, BATS, KNOT and OSP) is shown in Table 1. It is evident that the effect of temperature surpasses the biological effect at all of the subtropical time-series stations (SEATS, HOT and BATS), while the opposite is evident for stations located at high latitudes (KNOT and OSP). The contrast is attributed to the fact that the nutrient-rich surface waters in high latitudes usually are high in biological production and tend to reinforce the biological effect on regulating the fCO₂ in the mixed-layer. It should be noted that both temperature (97 vs. 59 μatm) and biological (62 vs. 23 μatm) effects on the fCO₂ in the mixed-layer at the SEATS site are greater than those at HOT, despite the fact that both sites are situated at similar latitudes in the

oligotrophic oceanic regime, and are constrained presumably by similar temperature and biological effects (Table 1). The discrepancy may be attributed to the vigorous vertical mixing during strong winter monsoon in the South China Sea as cold, nutrient-laden, CO₂-rich subsurface waters entrains from deep to cause a greater amplitude of temperature and biological effects on the surface water fCO₂.

3.5 The seasonal pattern of $\Delta f\text{CO}_2$ and air-sea exchange of CO₂ at the SEATS site

Fig. 5 shows the seasonal variability of $\Delta f\text{CO}_2$ at SEATS site, in which the maximum positive and negative $\Delta f\text{CO}_2$ occur in summer ($\sim +20\mu\text{tam}$; July 2002) and in winter ($\sim -15\mu\text{tam}$; January 2003), respectively. In other words, there has been an efflux of CO₂ from the SCS in summer and fall but an influx of CO₂ into the surface SCS in winter. The seasonal variability also reveals that the $\Delta f\text{CO}_2$ increases gradually from spring to summer, and then decreases progressively from fall to winter. Values of the calculated sea-to-air CO₂ flux at the SEATS site using different formulations (see method section) are listed in Table 2. As seen, they vary remarkably in different seasons and depend on which formula is used in calculations, ranging from -0.03 ± 0.07 to -0.25 ± 0.64 (spring), $+0.30\pm 0.07$ to $+2.77\pm 0.68$ (summer), $+2.10\pm 1.16$ to $+5.36\pm 2.97$ (fall), and -7.47 ± 2.44 to -17.04 ± 5.57 (winter) gC m⁻² year⁻¹. It further shows that the annual sea-to-air CO₂ flux is dominated by the influx of CO₂

from the atmosphere onto the surface waters in winter. It is worth pointing out that despite of the positive $\Delta f\text{CO}_2$ in summer, the modest wind speed results in a relatively small CO_2 efflux. In contrast, the high wind speed in winter gives rise to higher CO_2 influx regardless of the smaller $\Delta f\text{CO}_2$. The annual sea-to-air CO_2 flux at the SEATS site is estimated to be around -1.28 ± 0.94 to $-2.73 \pm 2.20 \text{ gC m}^{-2} \text{ year}^{-1}$ (Table 2), and is in good agreement with that reported previously by Takahashi et al. (2002) in the SCS region (~ 0 to $-4.8 \text{ gC m}^{-2} \text{ year}^{-1}$).

Similar seasonal patterns have also been documented at BATES and HOT (Winn et al., 1994; Bates, 1996). Our estimates, however, are less than $-8.4 \text{ gC m}^{-2} \text{ year}^{-1}$ found at HOT (Winn et al., 1994) or -3.0 to $-7.2 \text{ gC m}^{-2} \text{ year}^{-1}$ found at BATS (Bates et al., 1998). The lower values at SEATS can be attributed to the higher sea surface temperature at SEATS, which increases $f\text{CO}_2$ in the surface water and depresses the capacity for CO_2 uptake, and the general upwelling circulation in the SCS (Chao et al., 1996; Chen et al., 2001). Finally, if the estimated annual sea-to-air CO_2 flux at SEATS are extrapolated to the entire SCS ($3.5 \times 10^6 \text{ km}^2$), it could take up $4.5 \pm 3.3 \sim 9.6 \pm 7.7 \text{ Tg C}$ per year, i.e. only about 0.20 ± 0.15 to $0.44 \pm 0.35\%$ of the total CO_2 uptake by the global oceans ($\sim 2.2 \text{ Pg C yr}^{-1}$; Takahashi et al., 2002). These values are small, considering the SCS' s share that occupies 0.97 % of the total ocean area. The small fraction of CO_2 uptake estimated for the SCS in this study, however,

is consistent with the small percentage of CO₂ inventory reported by C.T.A. Chen et al. (2004), in which the SCS contains 0.6±0.1 Pg C of anthropogenic CO₂, while the global ocean inventory is about 100 Pg C.

3.6 Estimate of net community production and the “mysterious carbon drawdown”

In our previous discussion, we attributed the decrease of NTCO₂ and the drawdown of “fCO₂ at 27° C” from winter to summer to the biological uptake. The net amount of NTCO₂ consumed biologically in the euphotic zone during this period can be regarded as the difference between primary and regenerated productions, i.e. new production. The observed magnitude of ΔNTCO₂ between winter and summer at SEATS during the period of this study is about 21 μM (Fig. 3c). Assuming a mean mixed-layer depth of 50m, the net biological CO₂ utilization in the mixed-layer can be calculated to be about 1.05±0.20 mole C m⁻². Since this value only represents the phytoplankton growth over the first six months in a year, the annual new productivity would be about 2.1±0.40 mole C m⁻² yr⁻¹. In a thorough investigation of the roles of nitrogen in modulating phytoplankton growth in the SCS, Y.L. Chen et al. (2004) note a great variability of primary production between 180 and 330 mgC m⁻² day⁻¹ in March 2000 and 2001, respectively, whereas the new production remains constant at 60-70 mgC m⁻² day⁻¹. On the basis of these values,

the authors further report an *f*-ratio of 0.39 and 0.19 in March 2000 and 2001, respectively. Taking these *f*-ratios and the above annual new production rate of 2.1 mole C m² yr⁻¹, the primary productivity are calculated to range from 177±34 to 363±69 mgC m² day⁻¹. Using a modeling result and the data from SeaWiFS ocean color images, Liu et al. (2002) reported an annual mean primary productivity in the SCS of 280-354 mgC m² day⁻¹. Our estimated primary productivity using carbon data in this study is thus consistent with their results, and confirms the importance of biological utilization in controlling the observed seasonal drawdown of “fCO₂ at 27° C” and NTCO₂ from winter to summer at the SEATS site in the South China Sea.

Nonetheless, nitrate concentrations in the mixed-layer at SEATS site are undetectable except a trace of 0.5 μmol kg⁻¹ found in January during the course of this study. The observation of no measurable nitrate in the mixed-layer during spring and summer is also reported by Wong et al. (2002) and Y.L. Chen et al. (2004). The continuous decrease of NTCO₂ in the absence of measurable nitrate, the so-called “mysterious carbon drawdown”, observed in this study has also been observed at BATS and HOT time-series stations (Michaels et al., 1994; Bates et al., 1996; Karl et al., 1997). A recent global ocean analysis further shows that such a phenomenon is a common feature for all tropical and subtropical marine habitats (Lee et al., 2001). Moreover, it has been shown that in seawaters of low-nitrate

concentrations the C:N ratio utilized by marine organisms be very different from the conventional Redfield (Copin-Montégut, 2000; Michaels et al. 2001). Assuming a C:N ratio of 16 (ref. Copin-Montégut, 2000), the utilization of 0.5 μM nitrate can only sustain 8 μM of NTCO_2 drawdown, i.e. only 38% of the overall drawdown of NTCO_2 (21 μM ; Fig. 3c) measured between winter and summer.

It thus appears that other sources of nitrogen from processes such as the nitrogen fixation, riverin inputs, vertical migration of zooplankton, utilization of the dissolved organic nitrogen, vertical diffusion of nutrients from deep, horizontal advection and atmospheric deposition are required to compensate for the deficit. For instance, the nitrogen fixation has been the most frequently mentioned in literature and shown to be as a new production pathway in the nutrient-depleted waters (Karl et al., 1997; Michaels et al., 2000). In fact, Wong et al. (2002) report high values of nitrate anomaly up to 2.5 μM at the SEATS site from the fall through early spring during the northeast monsoon, indicating that the remineralization of nitrogen-rich organic matter formed by nitrogen fixation have played an important role in the nutrient dynamics in the northern SCS. However, as shown by Y.L. Chen et al. (2004), the nitrogen-fixing cyanobacteria, *Trichodesmium* sp. and *R. intracellularis*, are both sparsely distributed in the mixed layer during spring, and constitute less than 3% of the new production. The dichotomy between rates of nitrogen fixation measured

directly by biological techniques and inferred from geochemical data in the North Atlantic has been thoroughly investigated by Bates and Hansell (2004) and Hansell et al. (2004). Further studies, therefore, are necessary to elucidate the sources of nitrogen in the mixed layer at SEATS site in the northern SCS.

4. Conclusions

A better assessment of seasonal and inter-annual variability of CO₂ fluxes in different oceanic regimes is a premise for adequately quantifying the global oceanic CO₂ uptake. However, our present knowledge from time-series studies has been largely achieved by studies in the open ocean (e.g. BATS and HOT), with scant attention to the marginal seas. In this study, we report the first observation of the carbon system in the mixed-layer at the SEATS time-series site in the northern South China Sea. Results show that the seasonal pattern of NTCO₂ in the mixed-layer is characterized by a progressive decline from spring to early fall and by a subsequent increase in fall and winter. This seasonal variability of NTCO₂ is mainly due to biological utilization in spring-summer, and to strong vertical mixing in fall-winter, respectively. The seasonal changes of fCO₂, however, are nearly opposite to that of NTCO₂. The observed fCO₂ augmentation in spring-summer appears to be primarily the result of temperature increases, despite the fact that about 60% of such a

temperature effect is compensated by biological utilization. In the fall and winter, the temperature effect dominates over the combined effects of subsurface water entrainment and biological production, giving rise to the diminishing $f\text{CO}_2$ during the cooling period.

By comparison, our data show that the stronger wind-induced vertical mixing at SEATS has resulted in a greater extent of biological and temperature effects on $f\text{CO}_2$ variations than at HOT. According to the seasonal $f\text{CO}_2$ distributions, surface waters at the SEATS site act as an atmospheric CO_2 sink in winter, yet a source in summer and fall. Throughout the year, however, a net annual sea-to-air CO_2 flux is estimated to be -1.28 ± 0.94 to -2.73 ± 2.20 $\text{gC m}^{-2} \text{ year}^{-1}$. In response to the observed NTCO_2 drawdown, an estimated primary productivity of $177 \pm 34 \sim 363 \pm 69$ $\text{mgC m}^{-2} \text{ day}^{-1}$ in the mixed-layer is obtained. The continuous spring-summer drawdown of NTCO_2 with the absence of nitrate, however, suggests other sources of nitrogen are required to support the observed new production.

Acknowledgments

We are grateful to the Captains, crew and technicians of *R/V Ocean Research I* and *III* for assistance with deck operations and shipboard sampling, and to F. S. Lee and S. G. Lin for laboratory assistance. We thank K. K. Liu, L. S. Wen, F. K. Shiah,

and the staff of the National Center for Ocean Research (NCOR) for cruise participation and logistic support during the course of this research, Y. L. Chen for constructive discussion on the nitrogen fixation, and B. S. Lee for providing the TCO_2 and TA data of March 2002. We also thank three anonymous reviewers for their constructive comments and suggestions on the early version of this manuscript. This work was supported by the National Science Council grants (NSC90-2611-M-110-008-OP1 and NSC91-2611-M-110-003) to D. D. Sheu. The study is a contribution to the SEATS (South East Asia Time-series Study) program sponsored by NCOR, National Science Council, Republic of China.

References

- Bates, N.R., Michaels, A.F., Knap, A.H., 1996. Seasonal and interannual variability of oceanic carbon dioxide species at the U.S. JGOFS Bermuda Atlantic-series Study (BATS) site. *Deep-Sea Research II* 43, 347-383.
- Bates, N.R., Takahashi, T., Chipman, D.W., Knap, A.H., 1998. Variability of pCO_2 on diel to seasonal timescales in the Sargasso Sea. *Journal of Geophysical Research* 103, 15567-15585.
- Bates, N.R., 2001. Interannual variability of oceanic CO_2 and biogeochemical properties in the Western North Atlantic subtropical gyre. *Deep-Sea Research II*

48, 1507-1528.

Bates, N.R., Hansell, D.A., 2004. Temporal variability of excess nitrate in the subtropical mode water of the North Atlantic Ocean. *Marine Chemistry* 84, 225-241.

Bradshaw, A.L., Brewer, P.G., Shafer, D.K., William, R.T., 1981. Measurement of total carbon dioxide and alkalinity by potentiometric titration in the GEOSECS program. *Earth and Planetary Science Letters* 55, 99-115.

Butler, J.N., 1992. Alkalinity titration in seawater: how accurately can the data be fitted by an equilibrium model? *Marine Chemistry* 38, 251-282.

Chao, S.Y., Shaw, P.T., Wu, S.Y., 1996. Deep water ventilation in the South China Sea. *Deep-Sea Research I* 43, 445-466.

Chen, C.T.A., Huang, M.H., 1996. A mid-depth front separating the South China Sea Water and the Philippine Sea Water. *Journal of Oceanography* 52, 17-25.

Chen, C.T.A., Wang, S.L., Wang, B.J., Pai, S.C., 2001. Nutrient budgets for the South China Sea basin. *Marine Chemistry* 75, 281-300.

Chen, C.T.A., Wang, S.L., Wang, B.J., Liu, C.L., 2004. Carbonate chemistry of the South China Sea. (in preparation)

Chen, Y.L., Chen, H.Y., Karl, D.M., Takahashi, M., 2004. Nitrogen modulates phytoplankton growth in spring in the South China Sea. *Continental Shelf*

Research 24, 527-541.

Copin-Montégut, C., 2000. Consumption and production on scales of a few days of inorganic carbon, nitrate and oxygen by the planktonic community: results of continuous measurements at the Dyfamed station in the northwestern Mediterranean Sea (May 1995). *Deep-Sea Research I* 47, 447-477.

Dickson, A.G., 1981. An exact definition of total alkalinity and a procedure for the estimation of alkalinity and total inorganic carbon from titration data. *Deep-Sea Research* 28A, 609-623.

Dickson, A.G., Millero, F.J., 1987. A comparison of the equilibrium constants for the dissociation of carbonic acid in seawater media. *Deep-Sea Research I* 34, 1733-1743.

Dickson, A.G., 1992. The development of alkalinity concept in marine chemistry. *Marine Chemistry* 40, 49-63.

DOE, 1994. Handbook of methods for the analysis of the various parameters of the carbon dioxide system in seawater. In: Dickson A.G. and Goyet C. (Eds), U.S. Department of Energy CO₂ science Team Report, version 2, (unpublished manuscript).

Dore, J.E., Lukas, R., Sadler, D.W., Karl, D.M., 2003. Climate-driven changes to the atmospheric CO₂ sink in the subtropical North Pacific Ocean. *Nature* 424, 754-757.

- Feely, R.A., Sabine, C.L., Takahashi, T., Wanninkhof, R., 2001. Uptake and storage of carbon dioxide in the ocean: The Global CO₂ survey. *Oceanography* 14, 18-32.
- Gong, G.C., Liu, K.K., Liu, C.T., Pai, S.C., 1992. The chemical hydrography of the South China Sea west of Luzon and a comparison with the west Philippine Sea. *Terrestrial, Atmospheric and Oceanic Science* 3, 587-602.
- Goyet, C., Millero, F.J., O' Sullivan, D.W., Eiseheid, G., McCue, S.J., Bellerby, R.G.J., 1998. Temporal variations of pCO₂ in surface seawater of the Arabian Sea in 1995. *Deep-Sea Research I* 45, 609-623.
- Gruber, N., Keeling, C.D., Bates, N.R., 2002. Interannual variability in the North Atlantic ocean carbon sink. *Science* 298, 2374-2378.
- Hansell, D.A., Bates, N., Olson, D.B., 2004. Excess nitrate and nitrogen fixation in the North Atlantic Ocean. *Marine Chemistry* 84, 243-265.
- Johnson, K.M., Wills, K.D., Butler, D.B., Johnson, W.K., Wong, C.S., 1993. Coulometric total carbon dioxide analysis for marine studies: maximizing the performance of an automated gas extraction system and coulometric detector. *Marine Chemistry* 44, 167-188.
- Karl, D.M., Letelier, L., Tupas, L., Dore, J., Christian, J., Hebel, D., 1997. The role of nitrogen fixation in biogeochemical cycling in the subtropical north Pacific ocean. *Nature* 386, 533-538.

Karl, D.M., Dore, J.E., Lukas, R., Michaels, A.F., Bates, N.R., Knap, A., 2001.

Building the long-term picture: the U.S. JGOFS Time-series Programs.

Oceanography 14, 6-17.

Keeling, C.D., Whorf, T.P., 2002. Atmospheric CO₂ records from sites in the SIO air

sampling network. In: Trends: A compendium of data on global change. carbon

dioxide information analysis center, Oak Ridge national laboratory, Department of

Energy, Tenn., U.S.

Lee, K., Karl, D.M., Wanninkhof, R., Zhang, J.Z., 2001. Global estimates of net

carbon production in the nitrate-depleted tropical and subtropical oceans.

Geophysical Research Letters 29, 13-1-13-4.

Lewis, E., Wallace, D.W.R., 1998. Program developed for CO₂ system calculations,

Carbon Dioxide Information Analysis Center, Report ORNL/CDIAC-105, Oak

Ridge National Laboratory, Oak Ridge, Tenn., U.S.

Liang, W.D., Jan, J.C., Tang, T.Y., 2000. Climatological wind and upper ocean heat

content in the South China Sea. Acta Oceanographica Taiwanica 38, 91-114.

Lin, H.L., Wang, L.W., Wang, C.H., Gong, G.C., 1999. Vertical distribution of $\delta^{13}\text{C}$

of dissolved inorganic carbon in the Northeastern South China Sea. Deep-Sea

Research I 46, 757-775.

Liss, P.S., Merlivat, L., 1986. Air-sea gas exchange rates: introduction and synthesis.

- In: Buat-Menard, P. (Ed), The role of air-sea exchange in geochemical cycling, NATO ASI Series C: Mathematical and Physical Sciences, vol. 185, pp. 113-128.
- Liu, K.K., Chao, S.Y., Shaw, P.T., Gong, G.C., Chen, C.C., Tang, T.Y., 2002. Monsoon-forced chlorophyll distribution and primary production in the South China Sea: observations and a numerical study. *Deep-Sea Research I* 49, 1387-1412.
- Mehrbach, C., Culbertson, C.H., Hawley, J.E., Pytkowicz, R.M., 1973. Measurement of the apparent dissociation constants of carbonic acid in seawater at atmospheric pressure. *Limnology and Oceanography* 18, 897-907.
- Michaels, A.F., Bates, N.R., Bueseler, K.O., Carlson, C.A., Knap, A.H., 1994. Carbon-cycle imbalances in the Sargasso Sea. *Nature* 372, 537-540.
- Michaels, A.F., Karl, D.M., Knap, A.H., 2000. Temporal studies of biogeochemical dynamics in oligotrophic oceans. In: Hanson, R.B., Ducklow, H.W., Field, J.G. (Eds), *The Changing Ocean Carbon Cycles*, Cambridge University Press, Cambridge, pp. 393-413.
- Michaels, A.F., Karl, D.M., Capone, D.G., 2001. Element stoichiometry, new production and nitrogen fixation. *Oceanography* 14, 68-77.
- Millero, F.J., Zhang, J.Z., Lee, K., Campelle, D., 1993. Titration alkalinity of seawater. *Marine Chemistry* 44, 269-280.

- Nitani, H., 1972. Beginning of the Kuroshio. In: Stommel, H., Yoshida, K. (Eds),
Kuroshio, University of Washington Press, Seattle, pp. 129-163.
- Quay, P., 2002. Ups and downs of CO₂ uptake. *Science* 298, 2344.
- Sarma, V.V.S.S., Dileep Kumar, M., George, M.D., 1998. The central and eastern
Arabian Sea as a perennial source of atmospheric carbon dioxide. *Tellus* 50B,
179-184.
- Sarma, V.V.S.S., Dileep Kumar, M., Gauns, M., Madhupratap, M., 2000. Seasonal
controls on surface pCO₂ in the central and eastern Arabian Sea. *Proceedings
Indian Academy of Science* 109, 471-479.
- Shaw, P.T., Chao, S.Y., Liu, K.K., Pai, S.C., Liu, C.T., 1996. Winter upwelling off
Luzon in the north-eastern South China Sea. *Journal of Geophysical Research* 101,
16435-16448.
- Shiah, F.K., Liu, K.K., Tang, T.Y., 1999. South East Asia Time-series Station
established in South China Sea. *US JGOFS Newsletter* 10, 8-9.
- Takahashi, T., Olafsson, J., Goddard, J.G., Chipman, D.W., Sutherland, S.C., 1993.
Seasonal variation of CO₂ and nutrients in the high-latitude surface oceans: a
comparative study. *Global Biogeochemical Cycles* 7, 843-878.
- Takahashi, T., Feely, R.A., Weiss, R.A., Wanninkhof, R., Chipman, R.H., Sutherland,
D.W., Takahashi, T.T., 1997. Global air-sea flux of CO₂: an estimate based on

measurements of sea-air pCO₂ difference. *Proceedings of the National Academy of Science* 94, 8292-8299.

Takahashi, T., Sutherland, S.C., Sweeney, C., Poisson, A., Metz, N., Tilbrook, B., Bates, N.R., Wanninkhof, R., Feely, R.A., Sabine, C., Olafsson, J., Nojiri, Y., 2002. Global sea-air CO₂ flux based on climatological surface ocean pCO₂, and seasonal biological and temperature effects. *Deep-Sea Research II* 49, 1601-1622.

Tans, P.P., Fung, I.Y., Takahashi, T., 1990. Observational constraints on the global atmospheric CO₂ budget. *Science* 247, 1431-1438.

Tsurushima, N., Nojiri, Y., Imai, K., Watanabe, S., 2002. Seasonal variations of carbon dioxide system and nutrients in the surface mixed layer at station KNOT (44° N, 155° E) in the subarctic western North Pacific. *Deep-Sea Research II* 49, 5377-5394.

Wanninkhof, R., 1992. Relationship between wind speed and gas exchange over the ocean. *Journal of Geophysical Research* 97, 7373-7382.

Winn, C.D., Mackenzie, F.T., Carrillo, C.J., Sabine, C.L., Karl, D.M., 1994. Air-Sea carbon dioxide exchange in the North Pacific Subtropical Gyre: Implications for the global carbon budget. *Global Biogeochemical Cycles* 8, 157-163.

Winn, C.D., Li, Y.H., Mackenzie, F.T., Karl, D.M., 1998. Rising surface ocean dissolved inorganic carbon at the Hawaii Ocean Time-series site. *Marine*

Chemistry 60, 33-47.

Wong, C.S., Chan, Y.H., 1991. Temporal variations in the partial pressure and flux of CO₂ at ocean Station P in the subarctic northeast Pacific Ocean. *Tellus* 43B, 206-223.

Wong, G.T.F., Chung, S.W., Shiah, F.K., Chen, C.C., Wen, L.S., Liu, K.K., 2002. Nitrate anomaly in the upper nutrientline in the northern South China Sea-Evidence for nitrogen fixation. *Geophysical Research Letters* 29, 12-1-12-4.

FIGURE CAPTIONS

- Fig. 1. Bathymetric map showing the location of the SEATS (South East Asia Time-series Study) time-series site ($18^{\circ}15'N$, $115^{\circ}35'E$) at a water depth of $\sim 3770m$ in the northern South China Sea.
- Fig. 2. T-S diagram showing the distinct shallow salinity maximum ($S > 34.6$; $\sigma_{\theta} = \sim 24.5$) at approximately 150 m and the pronounced salinity minimum ($S = \sim 34.4$; $\sigma_{\theta} = \sim 26.8$) at about 350m, a typical feature of the South China Sea waters. (NPTW: North Pacific Tropical Water; NPIW: North Pacific Intermediate Water)
- Fig. 3. Seasonal fluctuations of (a) the mixed-layer depth, (b) TCO_2 , (c) $NTCO_2$ (solid line) and potential temperature (dash line), (d) TA (solid line) and salinity (dash line), (e) NTA and (f) fCO_2 (solid line) and potential temperature (dash line) in the mixed-layer at the SEATS site from March 2002 to April 2003. The data points represent the averaged values of all samples measured in the mixed-layer from each cruise.
- Fig. 4. Seasonal variability of “ fCO_{2mean} corrected for ΔT ” (open circle), “ fCO_2 at $27^{\circ}C$ ” (filled circle), and observed fCO_2 (open triangle) in the mixed layer at the SEATS site from March 2002 to April 2003. (See text for details in the definitions and calculations of “ fCO_{2mean} corrected for ΔT ” and “ fCO_2 at $27^{\circ}C$ ”.)
- Fig. 5. Seasonal variations of ΔfCO_2 (surface seawater fCO_2 - atmospheric fCO_2) in the mixed layer at SEATS site from March 2002 to April 2003.

Fig. 1

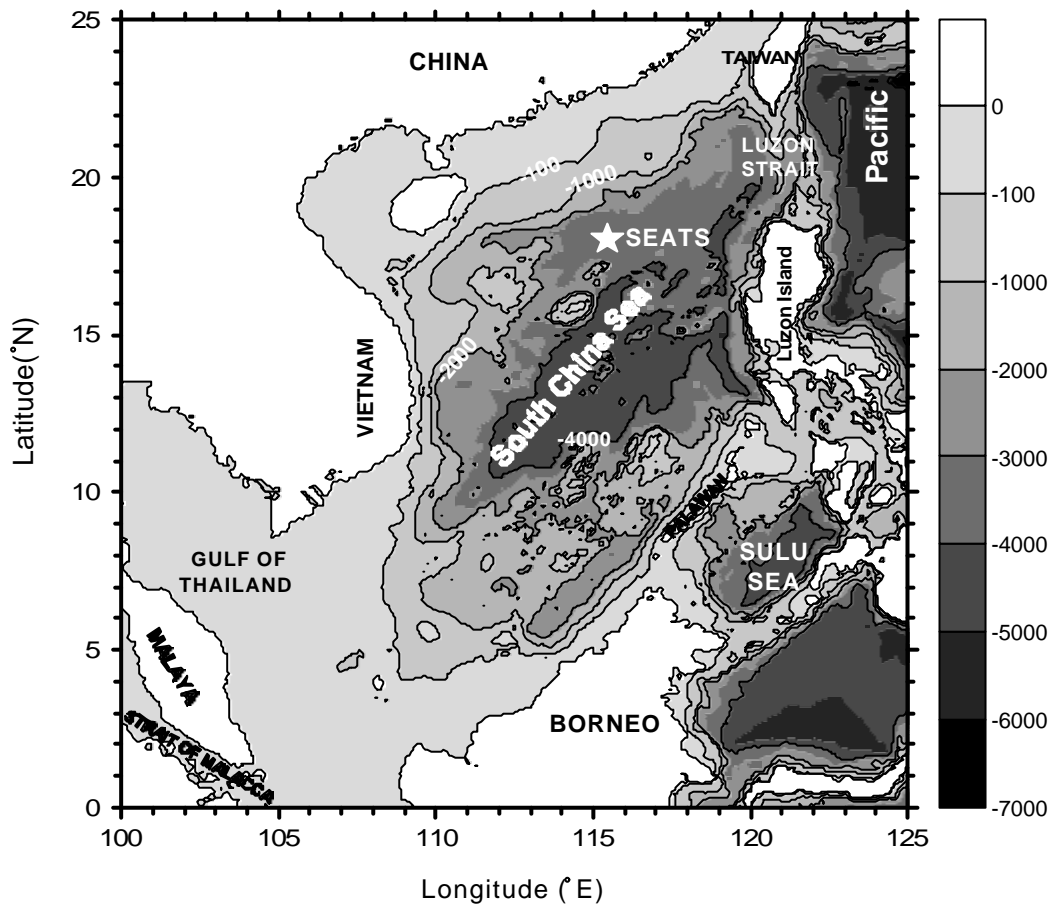


Fig. 2

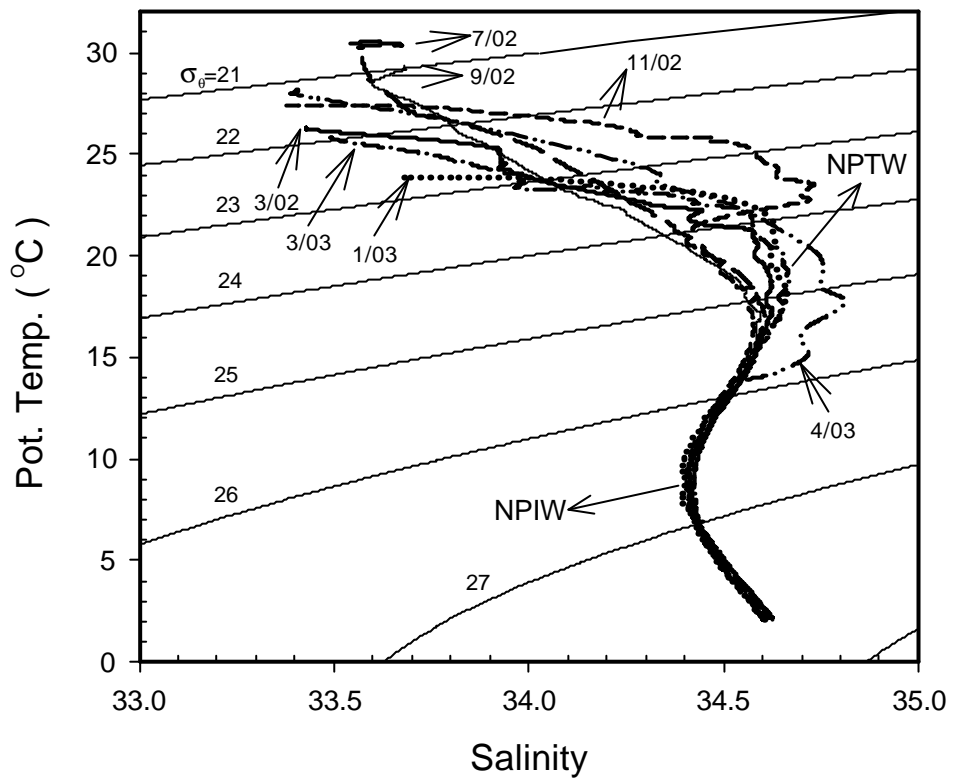


Fig. 3

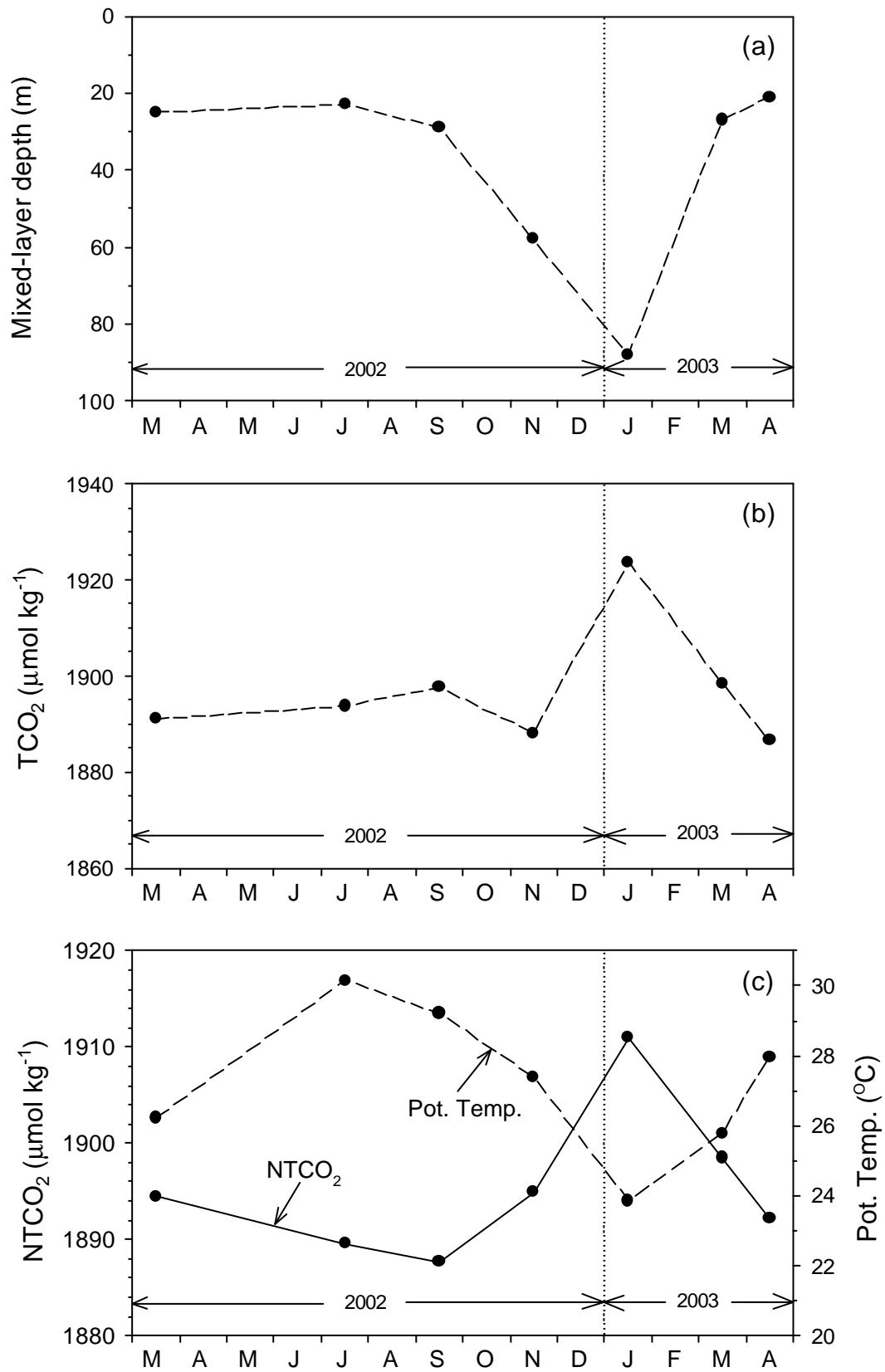


Fig. 3 (continued)

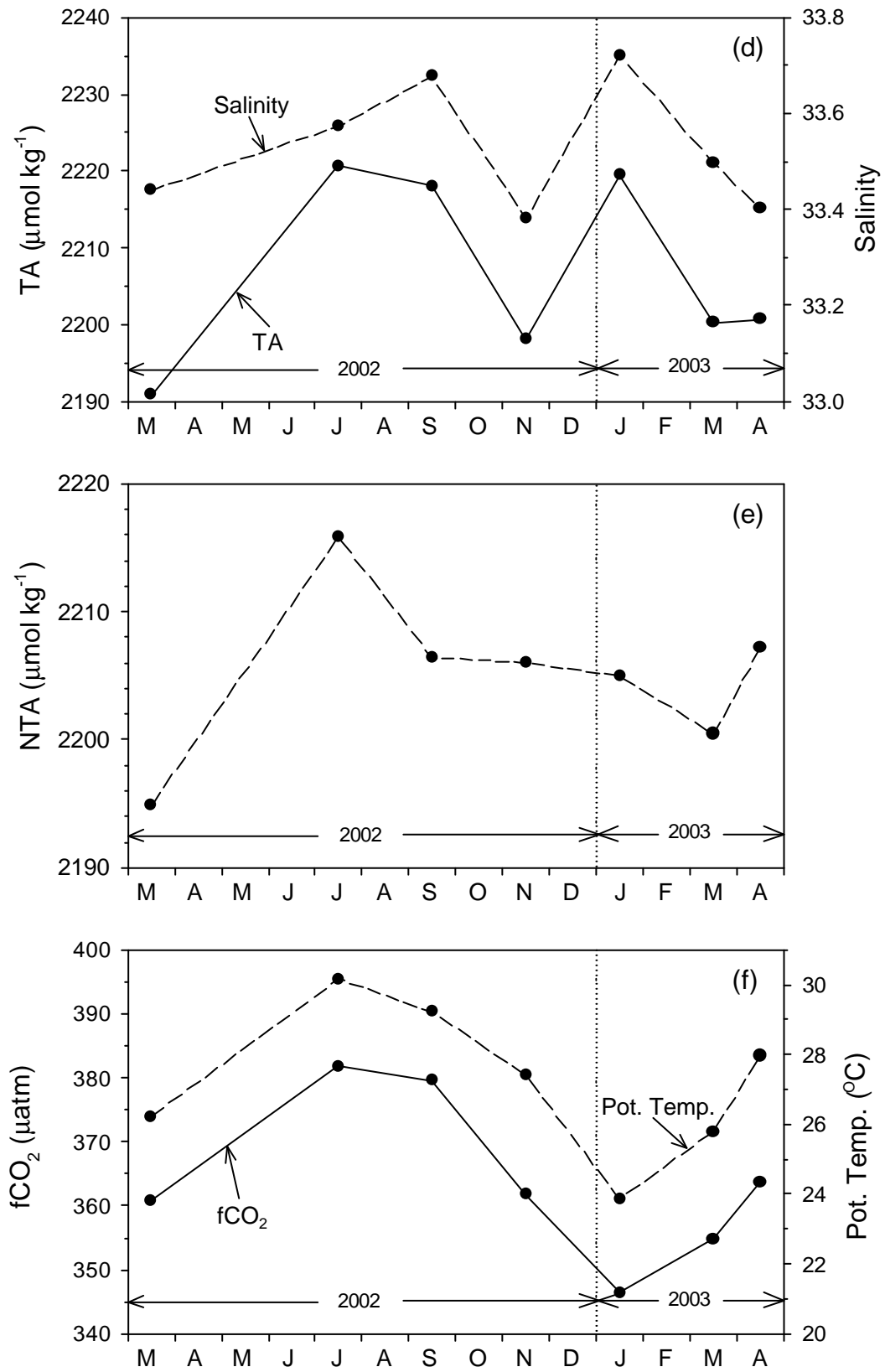


Fig. 4

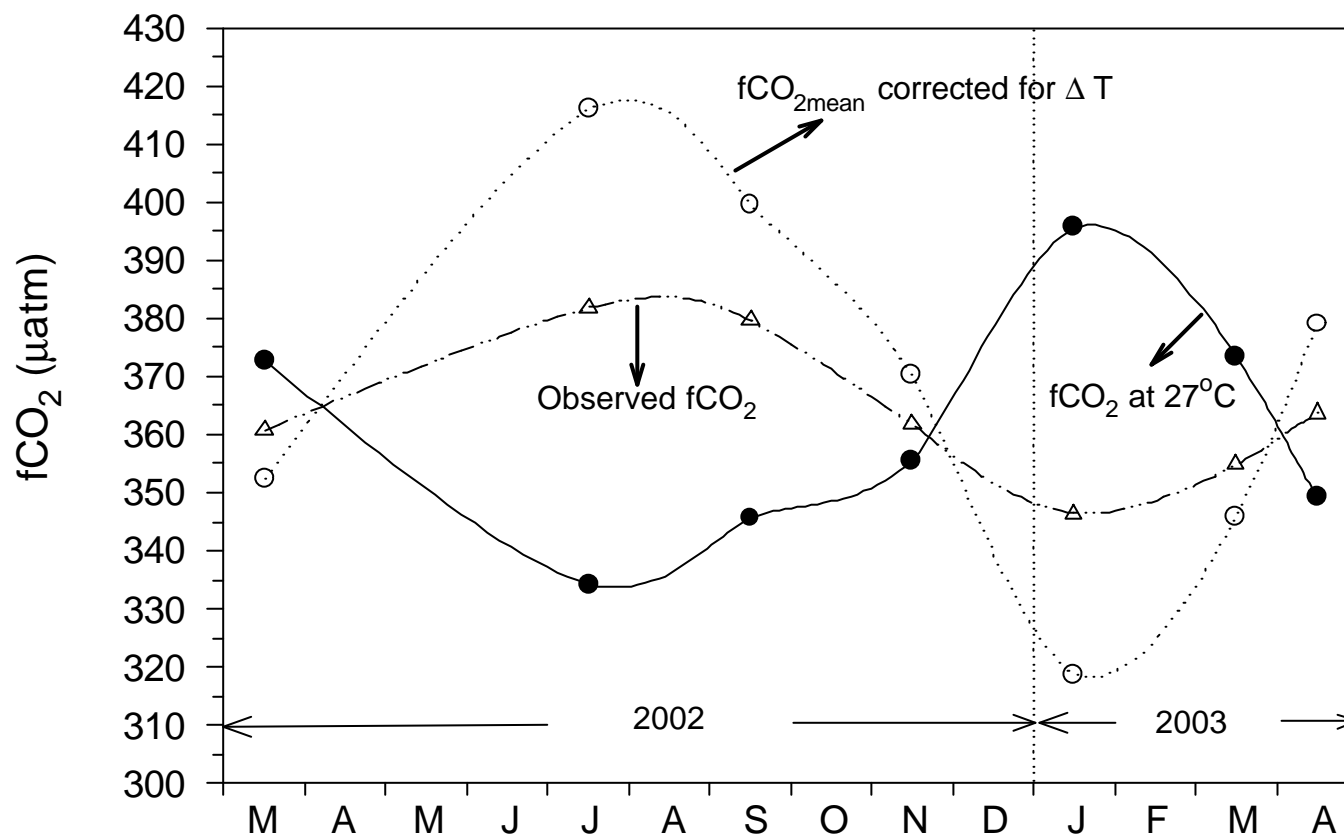


Fig. 5

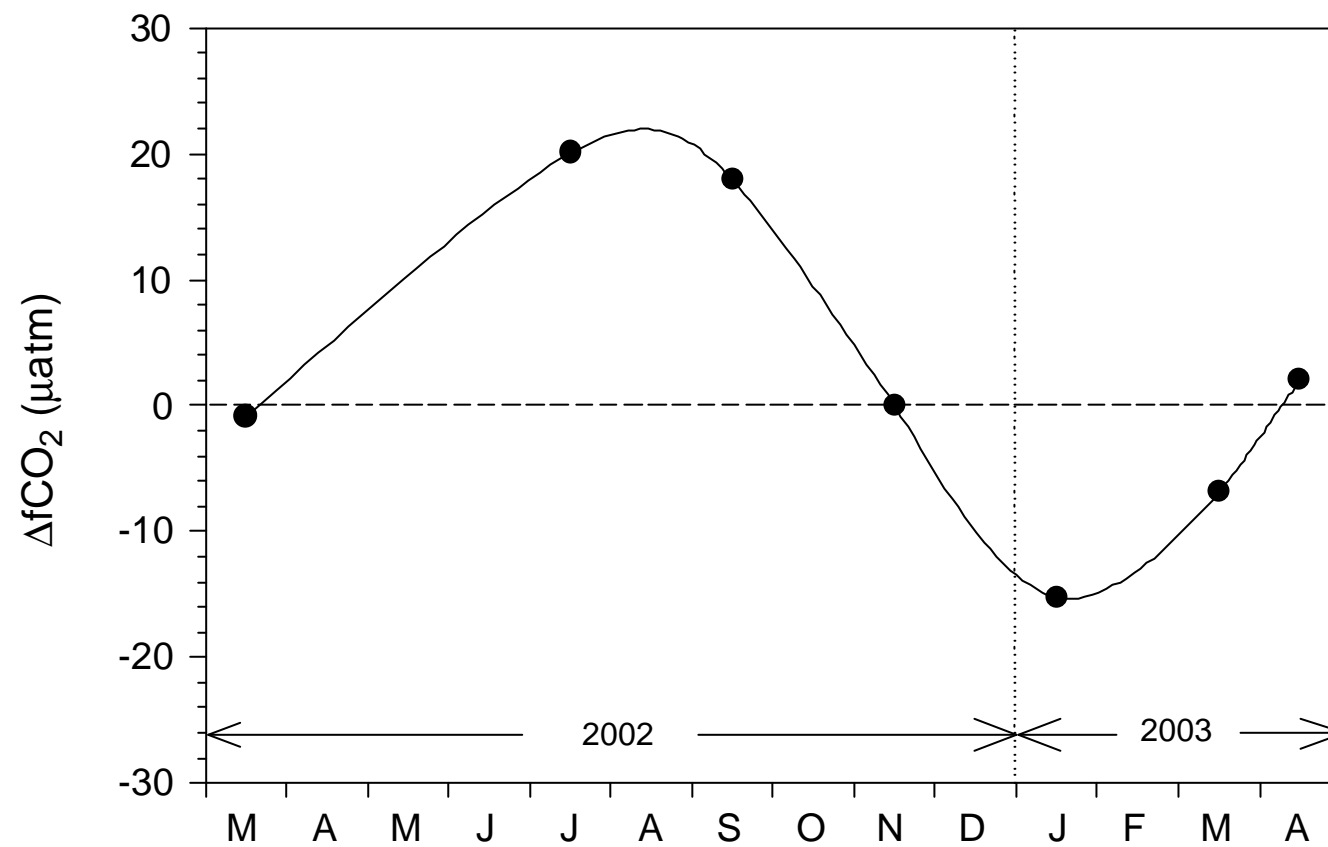


Table 1. Comparison of the relative importance of temperature and biological effects on fCO₂ variations at the SEATS site with those at HOT, BATS, KNOT and OSP time-series stations.

	Location and Oceanic regime represented	Temperature effect / Biological effect	Temperature effect - Biological effect	References
SEATS	18° 15' N , 115° 35' E South China Sea, the largest subtropical marginal sea	1.6 (97/62 μatm)	+35 μtam	This study
HOT	22° 45' N, 158° W North Pacific subtropical gyre	2.6 (59/23 μatm)	+36 μtam	Calculated based on Winn et al. (1994)
BATS	31° 50' N, 64° 10' W Western North Atlantic subtropical gyre	2.7 (150/55 μatm)	+95 μtam	Bates et al. (2001) Takahashi et al. (2002)
KNOT	44° N, 155° E Northwestern subarctic Pacific Ocean	0.8 (174/228 μatm)	-54 μtam	Calculated based on Tsurushima et al. (2002)
OSP	50° N, 145° W Northeastern subarctic Pacific Ocean	0.9 (100/115 μatm)	-10 μtam	Wong and Chan (1991) Takahashi et al. (2002)

Table 2. Estimates of seasonal CO₂ flux at the SEATS site using formulations of Liss and Merlivat (1986), Tans et al. (1990), and Wanninkhof (1992). The seasonal wind speed data are calculated from monthly averaged values for 1985-1999 from the ECMWF database (Liang et al. 2000).

	$\Delta f\text{CO}_2$ (μatm)	Wind speed (m s^{-1})	CO ₂ flux (F, $\text{gC m}^{-2} \text{ yr}^{-1}$) and exchange coefficient (K, $\text{gC m}^{-2} \text{ year}^{-1} \mu\text{atm}^{-1}$)					
			Liss and Merlivat (1986)		Tans et al. (1990)		Wanninkhof (1992)	
			K	F	K	F	K	F
Spring	-1.9 ± 5	3.1	0.016	-0.03 ± 0.07	0.019	-0.04 ± 0.07	0.129	-0.25 ± 0.64
Summer	20.1 ± 5	3.2	0.015	0.30 ± 0.07	0.038	0.77 ± 0.18	0.139	2.77 ± 0.68
Fall	9.0 ± 5	6.1	0.220	2.10 ± 1.16	0.595	5.36 ± 2.97	0.501	4.50 ± 2.50
Winter	-15.3 ± 5	8.8	0.488	-7.47 ± 2.44	1.114	-17.04 ± 5.57	1.043	-15.93 ± 5.20
Yearly Average				-1.28 ± 0.94		-2.73 ± 2.20		-2.23 ± 2.26

附錄三

(First draft)

Depth distributions of alkalinity, TCO_2 and $\delta^{13}\text{C}_{\text{TCO}_2}$ at SEATS time-series site, northern South China Sea

Wen-Chen Chou¹, David D., Sheu^{1*}, C. T. Arthur Chen¹, and C. M. Tseng²

¹Institute of Marine Geology and Chemistry, National Sun Yat-Sen University,
Kaohsiung 804, Taiwan, Republic of China.

²National Center for Ocean Research, P.O. Box 23-13, Taipei 106, Taiwan, Republic
of China

*Address: Institute of Marine Geology and Chemistry, National Sun Yat-Sen
University, Kaohsiung 804, Taiwan, Republic of China

Email: ddsheu@mail.nsysu.edu.tw

Tel: + 886-7-525-5148

Fax: + 886-7-525-5348

Abstract

Profiles of titration alkalinity (TA), total carbon dioxide (TCO_2), $\delta^{13}\text{C}$ of TCO_2 ($\delta^{13}\text{C}_{\text{TCO}_2}$) and other pertinent data (phosphate, nitrate and apparent oxygen utilization, AOU) throughout the water column at SEATS time-series station, northern South China Sea (SCS), collected from seven separate cruises between March 2002 and August 2003 are thoroughly investigated in this study to better understand their controlling processes and the influence of anthropogenic CO_2 on their depth distributions.

Results show that phosphate, nitrate, AOU, NTA (normalized TA = TA x 35/salinity) and NTCO_2 (normalized TCO_2 = TCO_2 x 35/salinity) all increase, while $\delta^{13}\text{C}_{\text{TCO}_2}$ decreases, with increasing depth. The vertical distributions thus are similar to those generally observed in the open ocean except that they all lack a prominent maximum or minimum in the water column. The discrepancy is attributed to the fact that deep waters in SCS is originated entirely from the adjacent West Philippine Sea deep waters and the characteristically short turnover time (~40 yrs) of SCS deep waters that may have diminished any appreciable excursion in water columns.

A close examination on processes controlling their variations further reveals

that the increasing trend of NTA is resulted mainly from higher preformed-NTA and carbonate dissolution at deep, while organic oxidation and greater preformed-NTCO₂ are responsible for the observed increase in NTCO₂. The decrease in $\delta^{13}\text{C}_{\text{TCO}_2}$ with depths, however, is principally owing to the decomposition of organic matter. Moreover, carbonate dissolution accounts for approximately 30% of TCO₂ production in the SCS deep waters, and it may have taken place at depths well above aragonite and calcite saturation depths at 600 m and 2500 m, respectively, in the SCS. Furthermore, the penetration depth of anthropogenic CO₂ at the SEATS site is estimated to be slightly deeper than 1000 m. The ratio of the decrease of $\delta^{13}\text{C}_{\text{TCO}_2}$ to TCO₂ increase, i.e. $\Delta\delta^{13}\text{C}_{\text{TCO}_2}/\Delta\text{TCO}_2$, due to the uptake of anthropogenic CO₂ is about $-0.024\text{‰}(\mu\text{mol kg}^{-1})^{-1}$. Results from this study thus document for the first time a complete set of background data necessary for future assessment of both temporal variability of carbon system and the fate of anthropogenic CO₂ in SCS.

1. Introduction

It has long been recognized that variations of TCO_2 , TA and $\delta^{13}\text{C}_{\text{TCO}_2}$ in seawater constitute a direct and reliable means to investigate the penetration and storage of anthropogenic CO_2 in the ocean [Wallace, 2001; Quay et al., 2003]. Pioneer works have been conducted in several research programs such as World Ocean Circulation Experiment (WOCE) and the Joint Global Ocean Flux Study (JGOFS).

To better understand the oceanic uptake of anthropogenic CO_2 , one of the most straightforward means is to carry out long-term time-series observations, which is designed to examine temporal variability in oceanic carbon system and the mechanisms controlling its variability. Since the JGOFS era (i.e. late 1980s), eight ocean time-series programs: Bermuda Atlantic Time-series Study (BATS), European Station for Time-series in the ocean, Canary Islands (ESTOC), Dynamique des Flux Atmosphériques Méditerranée (DYFAMED), Hawaii Ocean Time-series (HOT), Kerguelen Point Fixe (KERFIX), Kyodo Northwest Pacific Ocean Time-series (KNOT), Ocean Station Papa (OSP) and the Southeast Asia Time-series (SEATS) programs, have been established in order to better understand processes that control the oceanic carbon cycles in different oceanic regimes [Karl et al., 2003]. During

the past decade, results from these programs have provided enormously valuable information on the understanding of biogeochemical processes in the sea and have been used to constrain models of the carbon cycles in the ocean [Wong and Chan, 1991; Sabine et al., 1995; Winn et al., 1998; Bates, 2001; Gruber et al., 2002; Tsurushima et al., 2002; Dore et al., 2003; González-Dávila et al., 2003].

As one of recognized oceanic time-series stations by the JGOFS program, the SEATS station is located in the northern South China Sea (SCS; 18° 15' N, 115° 35' E; Fig. 1), which is a semi-enclosed marginal sea off the Asian continent in the West Pacific, and thus represents an oceanic regime of “subtropical marginal sea”. The seasonal variability of the carbon system within the mixed layer and the air-sea CO₂ exchange have recently been reported for the SEATS site [Chou et al., 2004]. The objectives of this study is to examine processes controlling the distribution of NTA (normalized TA = TA x 35/salinity), NTCO₂ (normalized TCO₂ = TCO₂ x 35/salinity) and $\delta^{13}\text{C}_{\text{TCO}_2}$ throughout the water column, and provides the background information necessary for future evaluations of temporal variability in the carbon system below the mixed layer at the SEATS site. In particular, since we focus on the current status of anthropogenic CO₂ distributions in the water column, results from this study can be used as the “baseline” for future comparison.

2. Methods

During the course of this study, the SEATS site had been investigated seven times between March 2002 and August 2003 aboard either *R/V Ocean Research I* or *III* in March, July, September, and November 2002, as well as January, March, and August 2003. Discrete water samples for TCO_2 , TA and $\delta^{13}\text{C}_{\text{TCO}_2}$ analyses were transferred into 250 ml BOD bottles from Go-Flo bottles mounted onto a Rosette sampling assembly (General Oceanic Inc.). All water samples were poisoned with 50 μl saturated HgCl_2 solution immediately after collection and stored at 5°C in darkness to prevent biological alteration [DOE, 1994]. The sub-samples for nitrate (NO_3^-) and phosphate (PO_4^{3-}) measurements were frozen immediately with liquid nitrogen and kept frozen until they were analyzed in laboratory.

In this study, TCO_2 and TA were determined following the standard operating procedures described in DOE [1994]. The coulometric method was used for TCO_2 measurements with a precision of 0.1%. The single operator multiparameter metabolic analyzer (SOMMA) system was used to extract CO_2 from acidified seawater samples and then measured by a coulometric detector (UIC, coulometric Inc., model 5011) [Johnson et al., 1993]. TA was determined by the potentiometric titration method with a precision of 0.15% (Bradshaw et al., 1981; Millero et al.,

1993). The titration data passing the carbonic acid endpoint (~ 4.5 pH) were calculated to obtain TA using the mass and charge balance method developed by Butler [1992]. Seawater references prepared and provided by A. G. Dickson were used throughout this study for calibration and accuracy assessment. The difference between the certified values and our measurements was less than $2 \mu\text{mol kg}^{-1}$ and $3 \mu\text{mol kg}^{-1}$ for TCO_2 and TA, respectively.

Nitrate plus nitrite was measured by reducing nitrate to nitrite that was identified by means of the pink azo dye method using a flow injection analyzer with an on-line Cd coil [Strickland and Parsons, 1972; Pai et al., 1990a; Pai and Riley, 1994]. Nitrate was calculated by subtracting nitrite from nitrate plus nitrite. Precision of this method was approximately 1% at $40 \mu\text{mol kg}^{-1}$ and 3% at $1 \mu\text{mol kg}^{-1}$, respectively. Phosphate was measured by the molybdenum blue method using a flow injection analyzer [Murphy and Riley, 1962; Pai et al., 1990b] with a precision of $\pm 0.5\%$ ($0.1\text{-}3.0 \mu\text{M}$). Dissolved oxygen was measured directly by a spectrophotometer with a flow injection analyzer [Pai et al., 1993] with a precision $\pm 0.5 \mu\text{M}$. AOU was calculated using Benson and Krause's formula [1982].

For $\delta^{13}\text{C}_{\text{TCO}_2}$ analysis, 40 ml of sample was injected into a pre-evacuated vessel and then reacted with 2 ml 85% H_3PO_4 to liberate TCO_2 . The evolved CO_2 was

trapped in a 6-mm glass finger using liquid nitrogen after complete removal of water vapor and other condensable gases by a slurry of dry ice and alcohol mixture, and then torch sealed [McNichol and Druffel, 1992; Sheu et al., 1996; Lin et al., 1999]. Isotopic analysis was performed with a VG Optima mass spectrometer. Results of isotopic measurement were expressed with the conventional δ notation and reported as per mil (‰) difference relative to the PDB standard [Craig, 1957]. The overall procedural error for $\delta^{13}\text{C}_{\text{DIC}}$ analyses was better than ± 0.05 ‰

3. Results and Discussion

3.1 Depth profiles of phosphate, nitrate, AOU, NTA, NTCO_2 and $\delta^{13}\text{C}_{\text{TCO}_2}$

Results of phosphate, nitrate, AOU, NTA, NTCO_2 and $\delta^{13}\text{C}_{\text{TCO}_2}$ measurements from seven cruises between March 2002 and August 2003 are plotted in Figure 2 to demonstrate their general distributions in the water column at the SEATS station. As can be seen, phosphate, nitrate, AOU, NTA and NTCO_2 all increase gradually with increasing depth, whereas $\delta^{13}\text{C}_{\text{TCO}_2}$ exhibits a mirror image of the other parameters. Thus, the increasing trends of phosphate, nitrate, AOU, NTA, and NTCO_2 at SEATS station coincide with the typical nutrient-type profiles that are normally observed in open oceans, i.e. low at surface and high at deep. The decrease of $\delta^{13}\text{C}_{\text{TCO}_2}$ with depth is due to the preferential uptake of ^{12}C by

microorganisms during photosynthetic utilization in surface waters and subsequent oxidation of organic remains, which are settling through the water column and are enriched in ^{12}C , at deep.

On a close examination, however, unlike those observed in the open ocean where phosphate, nitrate, AOU, NTA, and NTCO_2 show a maximum and $\delta^{13}\text{C}_{\text{TCO}_2}$ exhibits a minimum in the water column [Kroopnick et al., 1972; Kroopnick, 1985], the profiles at SEATS site are without these prominent features. Such a discrepancy has been reported previously in Gong et al. (1992), Chen and Huang (1996), Chen and Wang (1998), and Chen et al. (2001) and attributed collectively to the short turnover time of the deep waters in SCS. Since SCS is a semi-closed marginal sea, the only sill that is deep enough to allow the deep water flow into the SCS is the Luzon Strait with a maximal depth of ~2200 m (Fig. 1). As a consequence, the physical and chemical properties below 2200 m in the SCS bear the similar characteristics of the deep waters in the West Philippine Sea at depth of ~2200m [Gong et al., 1992; Chen and Huang, 1996]. The turnover time of the deep waters in SCS is only ~40 years [Chen and Wang, 1998; Chen et al., 2001] so that the intermediate, deep, and bottom waters in SCS basin are effectively well mixed and are nearly the same age. As a result, any appreciable excursion of the profiles in water column is diminished readily in the SCS.

The linear plots of PO_4^{3-} vs. AOU, NO_3^- vs. AOU, and NO_3^- vs. PO_4^{3-} are depicted respectively in Fig. 3. As shown, the data from waters at a depth above 100 m follow the hypothetical Redfield trend fairly well. In contrast, data from waters deeper than 100 m depart appreciably from the expected Redfield slopes [Redfield et al., 1963; Anderson and Samiento, 1994] despite they are well correlated. Moreover, the $\text{PO}_4^{3-}/\text{AOU}$ and NO_3^-/AOU ratios are higher but the $\text{NO}_3^-/\text{PO}_4^{3-}$ ratio is lower than the Redfield ratios. The good correlation and agreement with the hypothetical Redfield ratios in the upper 100 m waters imply that values of preformed phosphate and nitrate in the surface waters are similar, and regeneration of the particulate organic matters mainly takes place within this layer. On the contrary, deep waters in SCS, which was flowing from the West Philippine Sea deep waters and originated from their source regions in high latitude, are characteristic of higher preformed nutrient values and a very low preformed AOU [Emerson, 1987; Jenkins, 1985; Gruber, et al., 1996]. Subsequent mixing of these waters would therefore lead to the observed departure of phosphate and nitrate from the expected Redfield trend as well as the steeper slopes of P/AOU and N/AOU in waters below 100 m in SCS.

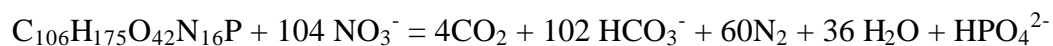
The low N/P values (Fig. 3c) for deep waters observed at the SEATS site in this study are not uncommon and have been reported in many other regions [Peng and Brocker, 1987; Minster and Boulahdid, 1987; Boulahdid and Minster, 1989]. After

a sophisticated analysis of global nutrients data, Anderson and Sarmiento [1994] concluded that denitrification might have played an important role in the observed nitrate deficit in the intermediate waters of the Atlantic, Indian, and Pacific Oceans. Here, we further test whether denitrification is also responsible for the observed low N/P in SCS deep waters using the quasi-conservative tracer N^* [Gruber and Sarmiento, 1997; Deutsch et al., 2001], which is defined as:

$$N^* (\mu\text{mol kg}^{-1}) = N - 16P + 2.90,$$

where the constant of $2.90 \mu\text{mol kg}^{-1}$ is derived by forcing the global mean of N^* to 0.

In principle, remineralization of organic matter releases nitrate and phosphate in a molar ratio of 16:1 [Redfield et al., 1963; Takahashi et al., 1985; Anderson and Sarmiento, 1994], while organic matters produced by nitrogen fixers are characterized by a high N/P ratio [Karl et al., 1992]. Denitrification, on the other hand, consumes nitrate and releases phosphate at a ratio of 104, provided the stoichiometry of Anderson [1995]:



Thus, N^* signifies the nitrate deviation from the normal organic decomposition as a result of the sum of the effects of denitrification and nitrogen fixation. Accordingly,

a positive N^* implies nitrogen fixation being dominant over denitrification, whereas a negative N^* indicates the opposite.

In this study, we have calculated N^* only for samples whose nitrate and phosphate concentrations are higher than 1 and $0.1 \mu\text{mol kg}^{-1}$, respectively, because of the inherent uncertainty in N^* estimates using low N and P data. Results show that all N^* values in waters below 200 m are negative with a minimum of approximately $-6 \mu\text{mol kg}^{-1}$ (Fig. 4). The calculated N^* values thus suggest that the denitrification indeed can account for the low N/P ratios observed in waters below 200 m in SCS. Nonetheless, it should point out that the negative N^* does not necessarily mean that denitrification is taking place in the water column at SEATS site, instead it may represent signals integrated over the course of formation of these waters. In other words, denitrification may have happened in the oxygen minimum zones in other locations or in sediments in SCS and then carries to the SEATS site.

In contrast, N^* values in the upper 200 m waters are positive with a maximum up to about $5 \mu\text{mol kg}^{-1}$. These values are among the highest values reported in the Pacific [Deutsch et al., 2001]. As indicated previously in Wong et al. [2002], the northern SCS meets all environmental conditions required for occurrence of nitrogen fixation, e.g. a temperature greater than 20°C , an absence of inorganic combined

nitrogen, a stratified water column, and availability of iron [Karl et al., 1997]. The positive N^* seen in surface waters at SEATS station thus suggests the presence of active nitrogen fixation. This interpretation is further supported by the observations of seasonal variations of dissolved inorganic carbon and nitrate in the mixed-layer at the SEATS site [Chou et al., 2004]. In that study, the authors found that the seasonal nitrate change could not sustain the corresponding dissolved inorganic carbon drawdown, and the nitrogen fixation must have to occur to account for the discrepancy. Our results also agree with that of Deutsch et al. [2001], in which they suggested that the western part of the northern Pacific might be the most important regions for nitrogen fixation in the entire Pacific Ocean.

3.2. Factors controlling the changes of NTA, $NTCO_2$ and $\delta^{13}C$ in the water column at SEATS station

It has been well known that variations in NTA, $NTCO_2$, and $\delta^{13}C$ (hereafter, unless specified otherwise, $\delta^{13}C$ stands for $\delta^{13}C_{TCO_2}$) in seawaters can be attributed to changes in their preformed values, i.e. values at surface outcrops of a water mass at the time of its formation and subsequent organic production/oxidation and carbonate formation/dissolution at various depths in oceans [Chen and Millero, 1979; Kroopnick, 1985; and Feely et al. 2002], and can be represented respectively by the

following equations:

$$\text{NTA}^{\text{meas}} = \text{NTA}^{\text{pre}} + \text{TA}^{\text{org}} + \text{TA}^{\text{carb}} \quad (1)$$

$$\text{NTCO}_2^{\text{meas}} = \text{NTCO}_2^{\text{pre}} + \text{TCO}_2^{\text{org}} + \text{TCO}_2^{\text{carb}} \quad (2)$$

$$\delta^{13}\text{C}^{\text{meas}} = \delta^{13}\text{C}^{\text{pre}} + \delta^{13}\text{C}^{\text{org}} + \delta^{13}\text{C}^{\text{carb}} \quad (3)$$

where the superscripts “meas”, “pre”, “org” and “carb” stand for the measured, preformed, organic oxidation and carbonate dissolution, respectively. In this study, we have applied these equations separately to assess the relative contribution of these processes to the depth profiles observed at SEATS station.

3.2.1. NTA

The preformed TA equation of Sabine et al. [2002a] is used to calculate the NTA^{pre} values,

$$\text{TA}^{\text{pre}} = 148.7 + (61.36 \times S) + (0.00941 \times \text{PO}) - (0.0582 \times \theta) \quad (4)$$

where S is salinity, PO is a quasi-conservative tracer (PO = dissolved oxygen + 170 x phosphate; after Broecker, 1974), and θ is the potential temperature. The reason for choosing this equation lies in the fact that it is derived from the WOCE/JGOFS data in the surface water (0-60 m) of entire Pacific and, as mentioned earlier, that the water below the surface in the SCS is originated from the West Philippine Sea deep

waters. Also, the physical uptake of anthropogenic CO₂ has been shown to not change the TA concentration of the waters [Millero et al., 1998; Gruber et al., 1996; Sabine et al., 1999; Feely et al. 2002;]. Results (Fig. 5, open square) show that NTA^{pre} increases gradually with depth from an average surface value of ~2305 μmol kg⁻¹ to ~2353 μmol kg⁻¹ at 2000 m, and then remains constant from 2000 to 3000 m. The increase in NTA^{pre} with depth therefore accounts, in part, for the observed nutrient-type distribution of NTA (NTA^{meas}) in the water column at SEATS site.

The component “TA^{org}” in Equation (1) represents the change of TA due to production and/or remineralization of organic matters. During production of organic, the reduction of nutrients (mainly nitrate) will consume protons, thus raising TA. On the contrary, when organic matter is decomposed, the oxidation reaction will release protons, and decreases TA [Brewer and Goldman, 1976; Chen et al., 1982]. Conventionally, the net effect between organic production and decomposition on TA changes is estimated by AOU instead of attempting to determine the changes in nutrients. In this study, we adapt a coefficient of 0.119 proposed by Feely et al. [2002] to calculate the TA^{org}, where

$$TA^{org} = -0.119 * AOU \quad (5)$$

The above conversion has included the contributions from nitrate, organic

phosphorus and sulfur and assumed an N/AOU ratio of 16/170 [Anderson and Sarmiento, 1994]. The negative sign in equation (5) indicates an increase of a unit of AOU at the expense of a unit of TA. As it would be expected, the TA^{org} trend resembles the depth profile of AOU because it is converted from AOU (Fig. 2c). In addition, changes in NTA due to the oxidation of organic matter can be regarded as the difference between the NTA^{pre} (open squares; Fig. 5) and $(NTA^{pre} + TA^{org})$ (open triangles; Fig. 5).

As formulated in equation (1), “ TA^{carb} ” can be readily computed by subtracting $(NTA^{pre} + TA^{org})$ from NTA^{meas} . As shown graphically in Fig. 5, NTA^{meas} (open circles) increases sharply, while NTA^{pre} (open square) and $(NTA^{pre} + TA^{org})$ (open triangles) increase mildly with increasing depth at SEATAS station, and are indistinguishable in upper 200 m of the water column. The profiles further reveal that TA^{carb} [$NTA^{meas} - (NTA^{pre} + TA^{org})$] increases sharply with depth due to carbonate dissolution and is responsible for the large (NTA^{meas}) increase below 200 m in the water column. In this regard, oxidation of organic matter tends to mitigate the vertical gradient of NTA^{meas} .

3.2.2. $NTCO_2$

Referring to equation (2), “ $NTCO_2^{meas}$ ” is the sum of “ $NTCO_2^{pre}$ ”, “ TCO_2^{org} ”,

and “ $\text{TCO}_2^{\text{carb}}$ ”, in which “ $\text{TCO}_2^{\text{org}}$ ” can be evaluated from the AOU on the basis of the constant stoichiometric ratio (C/AOU) of 117/170 [Anderson and Sarmiento; 1994]:

$$\text{TCO}_2^{\text{org}} = 117/170 * \text{AOU} \quad (6)$$

For “ $\text{TCO}_2^{\text{carb}}$ ”, it can be calculated from TA^{carb} because of the fact that dissolution of CaCO_3 results in an increase of TA and TCO_2 at a ratio of 2/1, i.e. $\text{TCO}_2^{\text{carb}} = 0.5 \times \text{TA}^{\text{carb}}$. Substituting equation (1) and equation (6) into this relationship, and rearranging the equation, the term “ $\text{TCO}_2^{\text{carb}}$ ” can be computed as follows.

$$\begin{aligned} \text{TCO}_2^{\text{carb}} &= 0.5 \times \text{TA}^{\text{carb}} = 0.5 \times (\text{NTA}^{\text{meas}} - \text{NTA}^{\text{pre}} - \text{TA}^{\text{org}}) \\ &= 0.5 \times (\text{NTA}^{\text{meas}} - \text{NTA}^{\text{pre}}) + 0.0593 \times \text{AOU} \end{aligned} \quad (7)$$

Finally, $\text{NTCO}_2^{\text{pre}}$ can be calculated by subtracting $(\text{TCO}_2^{\text{org}} + \text{TCO}_2^{\text{carb}})$ from $\text{NTCO}_2^{\text{meas}}$ (ref. equation 2). Results from these calculations are depicted graphically in Fig. 6. As seen, $\text{NTCO}_2^{\text{pre}}$, $\text{TCO}_2^{\text{org}}$ (corresponding to the difference between $(\text{NTCO}_2^{\text{pre}} + \text{TCO}_2^{\text{org}})$ and $\text{NTCO}_2^{\text{pre}}$), and $\text{TCO}_2^{\text{carb}}$ all increase with depth. Thus, the observed depth distribution of $\text{NTCO}_2^{\text{meas}}$ in the upper 300 m is mainly due to the increase in $\text{NTCO}_2^{\text{pre}}$ and $\text{TCO}_2^{\text{org}}$, while $\text{TCO}_2^{\text{carb}}$ together with $\text{NTCO}_2^{\text{pre}}$ and $\text{TCO}_2^{\text{org}}$ accounts, in larger extent, for the continuous increase of $\text{NTCO}_2^{\text{meas}}$ below

300 m in the water column.

Furthermore, in order to assess the relative contribution of carbonate dissolution and decomposition of organic matter to the observed depth variation of TCO_2 , ratios of IC/OC ($\text{TCO}_2^{\text{carb}}/\text{TCO}_2^{\text{org}}$) are calculated and plotted in Fig. 7. As shown, IC/OC increases from ~ 0.1 at 300 m to ~ 0.4 at 1500m, then remains constant below 1500 m. The value of 0.4 suggests that approximately 30% of TCO_2 in waters deeper than 1500 m at the SEATS site is due to carbonate dissolution. The estimated $\sim 30\%$ of carbonate dissolution in this study is consistent with those report previously by Tsunogai [1972], Kroopnick [1974], and Chen [1990] in the Pacific. The high IC/OC ratio of ~ 0.4 found in the deep waters of SCS also reflects the fact that they are originated from the oldest and hence most corrosive water mass, i.e. the North Pacific Deep Water (Stuiver et al., 1983). The increasing IC/OC ratios with depth further reveal that carbonate dissolution increases as a function of depth relative to the rate of organic decomposition that is higher in the upper water at SEATS site.

To gain further insight of the status of carbonate saturation in SCS, we have calculated $\Omega_{\text{aragonite}}$ and Ω_{calcite} , in which $\Omega = [\text{Ca}^{2+}] \times [\text{CO}_3^{2-}]/K_{\text{sp}}$, using the program developed by Lewis and Wallace [1998], and results are shown in Fig. 8. As seen, deep waters in SCS are under-saturated with respect to aragonite and calcite. Fig. 8

also shows that saturation depths of aragonite and calcite can be placed at about 600 m and 2500 m, respectively, at SEATS site. The calculated depths are in consistence with those reported in the same latitude of western North Pacific by Feely et al. [2002], and are comparable to those documented during WOCE/JGOFS era.

Finally, in order to better assess the depth levels where carbonate dissolution actually takes place in water column at SEATS site, we have superimposed the depth distribution of $\text{TCO}_2^{\text{carb}}$ (ref. Equation 2 and Fig. 6; $\text{TCO}_2^{\text{carb}} = \text{NTCO}_2^{\text{meas}} - (\text{NTCO}_2^{\text{pre}} + \text{TCO}_2^{\text{org}})$; termed as TA^* by Feely et al., 2002) on $\Omega_{\text{aragonite}}$ and Ω_{calcite} depth profiles in Fig. 8. It is found that appreciable $\text{TCO}_2^{\text{carb}}$ is present in waters well above the calcite saturation depth (~2500m), even at depths shallower than the aragonite saturation depth (~600m). In other words, $\text{TCO}_2^{\text{carb}}$ data indicate that dissolution of carbonate minerals has taken place at depths shallower than those assessed by saturation data. Although the general consensus has been that appreciable carbonate dissolution occur only at greater depths in the ocean because most surface waters are supersaturated with respect to both aragonite and calcite, recent studies suggest that dissolution of carbonates indeed occurs in shallow waters. For instance, on the basis of sediment trap data, Milliman et al. [1999] reported that as much as 60-80% of carbonates exported from the surface layer was remineralized

in the upper 500-1000m of the ocean. Feely et al. [2002] and Sabine et al. [2002b] found that excess TA did exist in the shallow water well above the calcite lysocline in the Pacific and the Indian Oceans. Our results at SEATS station in SCS thus support their contentions. Nevertheless, it should note that estimates from excess TA data represent the uppermost limit of dissolution, because other sources, such as non-carbonate sedimentary detritus [Chen, 2002], could contribute also to the observed TA in the water column. Moreover, mechanisms such as dissolution of CaCO_3 in the guts of zooplankton [Harris, 1994; Pond et al., 1995], enhanced dissolution during bacterial oxidation of organic matter [Milliman et al., 1999], and presence of more soluble carbonate phases [Byrne et al., 1984] have been proposed to help elucidate such a phenomenon in the oceans.

3.2.3. $\delta^{13}\text{C}_{\text{TCO}_2}$

In order to evaluate the respective contribution of $\delta^{13}\text{C}^{\text{pre}}$, $\delta^{13}\text{C}^{\text{org}}$ and $\delta^{13}\text{C}^{\text{carb}}$ to $\delta^{13}\text{C}^{\text{meas}}$, we rewrite the equation (3) in a mass-balance form:

$$\delta^{13}\text{C}^{\text{meas}} \times \text{TCO}_2^{\text{meas}} = \delta^{13}\text{C}^{\text{pre}} \times \text{TCO}_2^{\text{pre}} + \delta^{13}\text{C}^{\text{org}} \times \text{TCO}_2^{\text{org}} + \delta^{13}\text{C}^{\text{carb}} \times \text{TCO}_2^{\text{carb}} \quad (8)$$

where $\delta^{13}\text{C}^{\text{meas}}$, $\delta^{13}\text{C}^{\text{org}}$, and $\delta^{13}\text{C}^{\text{carb}}$ represent $\delta^{13}\text{C}$ in $\text{TCO}_2^{\text{meas}}$, $\text{TCO}_2^{\text{org}}$ and $\text{TCO}_2^{\text{carb}}$, respectively. In this study, values of -20‰ for $\delta^{13}\text{C}^{\text{org}}$ [Goericke and Fry,

1994] and +2‰ for $\delta^{13}\text{C}^{\text{carb}}$ [Bonneau et al., 1980] are adopted in our calculations.

Rearranging equation (8), $\delta^{13}\text{C}^{\text{pre}}$ then can be computed by the following equation:

$$\delta^{13}\text{C}^{\text{pre}} \text{ (in ‰)} = (\delta^{13}\text{C}^{\text{meas}} \times \text{TCO}_2^{\text{meas}} + 20 \times \text{TCO}_2^{\text{org}} - 2 \times \text{TCO}_2^{\text{carb}}) / (\text{TCO}_2^{\text{pre}}) \quad (9)$$

Results show that $\delta^{13}\text{C}^{\text{pre}}$ increases progressively from $\sim 0.7\text{‰}$ at the surface to $\sim 1.2\text{‰}$ at 700 m, and then remains in a narrow range ($1.2 \pm 0.1\text{‰}$) throughout the water column to 3000 m (open squares in Fig. 9). The low $\delta^{13}\text{C}^{\text{pre}}$ in the surface waters mainly reflects the fact that the carbon isotopic composition of anthropogenic CO_2 is much lighter than $\delta^{13}\text{C}$ of seawater (-22 to -32‰ ; Tans, 1981; Andres et al., 1996). Additionally, as mentioned earlier, deep waters in SCS, which is originated from the West Philippine Sea deep waters, is old and bears less negative $\delta^{13}\text{C}^{\text{pre}}$ values during the time when they outcrop in the surface at high latitudes before sinking downward to enter the SCS. Moreover, as revealed by Gruber et al. [1999] and Quay et al. [2003], values of the present-day $\delta^{13}\text{C}$ in surface waters of the Pacific increase with latitudes from 30° to 60° N. Sinking and subsequent import of waters from high latitudes in northern Pacific to SCS will also contribute to the observed increase of $\delta^{13}\text{C}^{\text{pre}}$ at deep. A further discussion of effects of anthropogenic CO_2 on the observed $\delta^{13}\text{C}$ trend will be presented in the next section.

To further evaluate the net changes in $\delta^{13}\text{C}$ due to the addition of $\text{TCO}_2^{\text{org}}$

during organic decomposition, we have assumed the effect of carbonate dissolution is negligible. The assumption is made because, as shown by the calculated IC/OC ratios in previous section, TCO₂ in SCS is mainly derived from the decomposition of organic matter, which is characteristic of lower $\delta^{13}\text{C}$ than carbonates ($\sim -20\text{‰}$ vs. $\pm 1\text{‰}$). Thus, $\delta^{13}\text{C}^{\text{org}}$ can be readily calculated by the following mass balance equation:

$$\delta^{13}\text{C}^{\text{org}} = [(\delta^{13}\text{C}^{\text{pre}} \times \text{TCO}_2^{\text{pre}}) + (-20 \times \text{TCO}_2^{\text{org}})] / (\text{TCO}_2^{\text{pre}} + \text{TCO}_2^{\text{org}}) - \delta^{13}\text{C}^{\text{pre}}$$

Fig. 9 (open triangles) shows the depth profile of the calculated $\delta^{13}\text{C}^{\text{org}}$ plus $\delta^{13}\text{C}^{\text{pre}}$. As seen, they are nearly the same as $\delta^{13}\text{C}^{\text{meas}}$ (open circles). In other words, the observed decrease of $\delta^{13}\text{C}$ with depth at SEATS station is principally owing to the addition of TCO₂^{org}, while dissolution of carbonates has little effect on the change of $\delta^{13}\text{C}$.

3.3 The penetration of anthropogenic CO₂ at the SEATS station

Estimate of the penetration and storage of anthropogenic CO₂ (Excess CO₂) in the ocean can be derived from the conventional “carbon chemistry (mainly TCO₂ and TA)” methods or the $\delta^{13}\text{C}$ data [Wallace, 2001; Quay et al., 2003]. The carbon chemistry method has long been recognized as a direct approach because ocean’s TCO₂ contents response directly to the increment of atmospheric pCO₂ and the

resulting greater net air-to-sea CO₂ flux. Likewise, addition of anthropogenic CO₂ in air can result in a reduction of $\delta^{13}\text{C}$ in seawater because anthropogenic CO₂ is depleted in ^{13}C [Friedli et al., 1986; Keeling et al., 1989]. In this study, we apply both carbon chemistry method and $\delta^{13}\text{C}$ data, which have been measured concurrently, to estimate the penetration of anthropogenic CO₂ at the SEATS station. The use of these paired data sets has the advantage to directly compare results obtained from these two independent methods, thus providing an internal check on our estimates. In addition, $\delta^{13}\text{C}$ data provide a quantitative means to better assess the constraint on the size of exchange between seawaters and the overlying atmosphere reservoirs on the basis of ratios of “ $\delta^{13}\text{C}$ decrease to TCO₂ increase, i.e. $\Delta\delta^{13}\text{C}/\Delta\text{TCO}_2$,” [Keir et al., 1998; Körtzinger et al., 2003].

During the past decade, several techniques on the basis of carbon chemistry data have been proposed to estimate the magnitude of anthropogenic CO₂ in the ocean, including the “back calculation”, “ ΔC^* ”, “multiparametric mixing analysis (MIX)”, and “time-series” methods [Wallace; 2001]. However, for a single site such as the SEATS station in this study, the back calculation method is the only one that can be applied, because ΔC^* method requires information on water ages along a fixed isopycnal surface to estimate the term of air-sea disequilibrium [Gruber et al., 1996; Gruber, 1998]. The MIX method relies on a detailed knowledge of different

water sources and a complicated analysis of mixing among them [Goyet et al., 1999; Coatanoan et al., 2001]. Although the time-series method seems to best fit for a single site, in which two historical TCO₂ data sets are compared in a suitable time interval (generally longer than ten years) [Sabine et al., 1999; Ono et al., 2000; Wallace, 2001], the lack of historical data at the SEATS station has impeded such an effort.

In this study, we have utilized the back calculation method of Chen and Millero [1979] to estimate the influence of anthropogenic CO₂ on TCO₂ and its carbon isotopic compositions in the water column at the SEATS site. A similar technique was also proposed by Brewer [1978]. The underlying principle of this method is that the NTCO₂^{pre} for a given water parcel can be calculated after corrections of organic oxidation and carbonate dissolution (see section 3.2.2 for the details; the “NTCO₂^{pre}” denoted as NTCO₂^{pre}_{old} in the following discussion). The present NTCO₂^{pre} (NTCO₂^{pre}_{present}) of the same water mass can be derived from the potential temperature (θ) because they are well correlated in a given ocean basin. The signal of anthropogenic CO₂ (termed as “anthropogenic CO₂” or “excess CO₂” by different researchers) can be assessed by the difference between these two preformed values, i.e. (NTCO₂^{pre}_{old} - NTCO₂^{pre}_{present}). According to Chen et al. [1986] and Chen and Huang [1995], the NTCO₂^{pre}_{present} can be calculated as follows.

For the deep and bottom waters:

$$\text{NTCO}_2^{\text{pre}}_{\text{present}} (\mu\text{mol kg}^{-1}) = 2219 - 11 \times \delta (\pm 16)$$

For waters above and at the salinity minimum:

$$\text{NTCO}_2^{\text{pre}}_{\text{present}} (\mu\text{mol kg}^{-1}) = 2242 - 12.08 \times \delta (\pm 18)$$

At depth where the salinity minimum waters mix with deep waters, the δ/S plot is further used to estimate the relative contribution from each. For surface waters, the “anthropogenic CO_2 ” is estimated from the difference between measured NTCO_2 and the “preindustrial NTCO_2 ”, which is computed from the measured TA and hydrographical data assuming that pCO_2 equal to 280 ppmv and is at equilibrium.

Results of these calculations are depicted in Fig. 10. As shown, concentrations of anthropogenic CO_2 decrease exponentially with depth and have the highest values at surface. Below 1000 m, they remain constant throughout the water column, suggesting penetration of the anthropogenic CO_2 has reached to this depth. Such a penetration depth is in good agreement with other studies reported previously in the North Pacific [Chen, 1987; 1993; Feely et al., 1999; Sabine et al., 2002a]. Nonetheless, the concentration ($\sim 60 \mu\text{mol kg}^{-1}$) of anthropogenic CO_2 in the surface water is higher than that reported by Sabine et al. [2002] in subtropical surface water

of the North Pacific Ocean (between 40-50 $\mu\text{mol kg}^{-1}$). It should be pointed out that the estimate of Sabine et al. is based on WOCE/JGOFS data set, which has collected in early 1990s (principally from 1991 to 1994). The data used in this study are collected in 2002 and 2003. Taking a TCO_2 increasing rate in surface water as 1.18 $\mu\text{mol kg}^{-1} \text{yr}^{-1}$ (the rate at the Hawaii Ocean Time-series station from 1988 to 1999; Dore et al., 2002) for the past 10 years, our estimation falls well within the range of Sabine et al. [2002a]. The total column inventory of anthropogenic CO_2 thus is estimated to be $\sim 18 \text{ mol m}^{-2}$ at the SEATS site, which is close to $\sim 20 \text{ mol m}^{-2}$ reported by Sabine et al. [2002a] for the same latitude in the western North Pacific. The minor discrepancy may be due to the upwelling circulation in SCS that tends to reduce its capacity in absorbing both natural and anthropogenic CO_2 . If the estimated column inventory of “anthropogenic CO_2 ” at the SEATS site were extrapolated to the entire SCS ($3.5 \times 10^6 \text{ km}^2$), the total anthropogenic CO_2 in SCS is estimated to be from 0.5 to 0.6 Pg C in 2002.

Conventionally, estimates of anthropogenic CO_2 penetration based on $\delta^{13}\text{C}$ data can be furnished directly by the observed temporal changes in $\delta^{13}\text{C}$ (Quay et al., 1992; Gruber et al., 1999; Sonnerup et al., 1999; Sonnerup et al., 2000; Quay et al., 2003) or indirectly using the the concurrent $\delta^{13}\text{C}$ -nutrient method [Broecker and Peng, 1982; Keir et al., 1998; Ortiz et al., 2000]. We have adopted the latter to assess the

influence of anthropogenic CO₂ in this study because of the lack of historical measurements of $\delta^{13}\text{C}$ at SEATS site as mentioned earlier. As discussed previously in section 3.2.3, vertical distribution of $\delta^{13}\text{C}$ is primarily controlled by the biological cycling of ^{13}C depleted organic matter in the water column, and an inverse correlation between $\delta^{13}\text{C}$ and nutrients should be existed. According to Broecker and Maier-Reimer [1992], the slope in the plot of $\delta^{13}\text{C}$ vs. phosphate is about -1.1, providing there is no isotope exchange between seawaters and overlying atmosphere (i.e. the measured $\delta^{13}\text{C}$ is only affected by the biological processes in the ocean). The correlation between $\delta^{13}\text{C}$ and phosphate at the SEATS site is plotted in Fig. 11. As seen, $\delta^{13}\text{C}$ inversely correlates with phosphate, and the slopes of correlation are much less negative (-0.21 and -0.63 for waters below and above 100 m, respectively) than the expected biological trend (-1.1). The deviation thus suggests that processes other than biological cycling, such as isotopic fractionations and uptake of anthropogenic CO₂, must have involved in decoupling the expected correlation between $\delta^{13}\text{C}$ and phosphate [Lynch-Stieglitz et al., 1995]. To elucidate this complication, we first quantify the air-sea exchange signature on $\delta^{13}\text{C}$ and then separate it from the effect of anthropogenic uptake.

It has been known that thermodynamic and kinetic effects during the air-sea exchange can result in large variations of $\delta^{13}\text{C}$ in the global surface ocean.

According to Mook et al., (1974) and Zhang et al. (1995), the temperature-dependent isotopic fractionation of $\delta^{13}\text{C}$ associated with the air-sea exchange is about $-0.1\text{‰} \text{ } ^\circ\text{K}^{-1}$. As a result, thermodynamic effect tends to make $\delta^{13}\text{C}$ in cold surface water higher than that in the warm surface water. Besides, kinetic effects will cause surface waters enriched in ^{13}C in source areas, whereas depleted in sink areas [Lynch-Stieglitz et al., 1995]. According to Broecker and Maier-Reimer [1992], effects of the air-sea exchange on the surface ocean $\delta^{13}\text{C}$ can be derived from the following relationship:

$$\delta^{13}\text{C}_{\text{as}} = \delta^{13}\text{C}^{\text{meas}} - (2.7 - 1.1 \times [\text{PO}_4^{3-}]) \quad (10)$$

where $\delta^{13}\text{C}_{\text{as}}$ stands for $\delta^{13}\text{C}$ that is affected by the air-sea exchange. It was originally denoted as $\Delta\delta^{13}\text{C}$ by Broecker and Maier-Reimer [1992], but later was renamed by Lynch-Stieglitz et al. [1995] to distinguish it from “the gradient of $\delta^{13}\text{C}$ ” commonly used in paleoceanographic community. The term in parenthesis on the right hand side of equation (10) is the mean ocean biological trend. By definition, a $\delta^{13}\text{C}_{\text{as}} = 0\text{‰}$ implies that a given water mass has the same air-sea signature as the mean ocean deep water. A positive $\delta^{13}\text{C}_{\text{as}}$ indicates a greater effect of air-sea exchange at low temperature and/or an evasion of CO_2 from surface water than the mean ocean deep water, whereas a negative $\delta^{13}\text{C}_{\text{as}}$ value suggests the contrary.

Fig. 11 shows that the trend of the plot of $\delta^{13}\text{C}$ vs. phosphate at the SEATS site departs appreciably from the hypothetical mean ocean biological trend. It further reveals that the offset, i.e. the $\delta^{13}\text{C}_{\text{as}}$ in equation 10, is negative for the waters shallower than ~800 m (phosphate $< 2.6 \mu\text{mol kg}^{-1}$), while it is slightly positive for waters below. The negative $\delta^{13}\text{C}_{\text{as}}$ in shallow waters, however, cannot be attributed to thermodynamic and kinetic effects alone. Instead, portion of the negative $\delta^{13}\text{C}_{\text{as}}$ signal must come from the anthropogenic CO_2 which is depleted in ^{13}C and has penetrated to a depth of ~1000 m as revealed previously (ref. Fig. 10).

To further assess the magnitude of the contribution of anthropogenic CO_2 to $\delta^{13}\text{C}_{\text{as}}$, denoted as $\delta^{13}\text{C}_{\text{p}}$, we have followed the pre-anthropogenic model of Keir et al. [1998] and Ortiz et al. [2000] with minor modification. We first assume that waters below 2000m contain no anthropogenic CO_2 , because the deep and bottom waters in the SCS are originated from the North Pacific Deep Water, the oldest water mass in the global oceans, so that they are unlikely to have outcropped at or near the sea surface to contact with the subsequently released anthropogenic CO_2 after industrialization. We further assume that the surface water $\delta^{13}\text{C}$ has decreased by 1.0 ‰ from pre-anthropogenic era to the present time. This assumption is made because the fact that $\delta^{13}\text{C}$ in the surface ocean waters is decreased by about 0.8 ‰ from the last 200 years to the end of 1992 [Böhm et al., 1996] and a rate of $\delta^{13}\text{C}$

decrease during the past decade in the surface water of the North Pacific is estimated to be 0.2 ‰ [Sonnerup et al., 1999]. Moreover, as shown in Fig. 10, the anthropogenic CO₂ content of the surface water at the SEATS site is about 60 μmol kg⁻¹. The assumed 1 ‰ decrease in δ¹³C will give a Δδ¹³C/ ΔTCO₂ ratio of about -0.017 ‰(μmol kg⁻¹)⁻¹, which falls well within the range of the modeling results (-0.016 to -0.019 ‰(μmol kg⁻¹)⁻¹) from Heimann and Maier-Reimer [1996]. δ¹³C_p now can be estimated by the following expression and shown in Fig. 11 (solid line):

$$\delta^{13}\text{C}_p = -0.67 \times [\text{PO}_4^{3-}] + 1.73$$

As pointed out by Ortiz et al. [2000], the slope of the above pre-anthropogenic trend (-0.67) would be very close to its current near-surface value, because it is very insensitive to anthropogenic changes in ocean chemistry and different ventilation. The slope of δ¹³C to phosphate derived from this study for the waters shallower than 100m at the SEATS site is ~-0.63 (Fig 11) and is in good agreement with that of pre-anthropogenic trend (-0.67). The consistency between these two values, therefore, supports the validity of our pre-anthropogenic model.

The offset between δ¹³C_p and δ¹³C^{meas}, denoted as Δδ¹³C_{a-p}, represents the magnitude of the “Suess effect” on δ¹³C_{as} and is plotted versus depth in Fig. 12. As seen, the depth distribution of Δδ¹³C_{a-p} indicates that the signature of “Suess effect”

has penetrated to a depth of at least 1000 m in the water column at SEATS site, and is almost identical to the anthropogenic CO₂ depth profile (Fig. 10) estimated above from concurrent TCO₂ and TA data. In addition, an averaged $\Delta\delta^{13}\text{C}/\Delta\text{TCO}_2$ ratio of $-0.024 \text{‰}(\mu\text{mol kg}^{-1})^{-1}$ throughout the penetration depth can be obtained by dividing the depth-integrated $\Delta\delta^{13}\text{C}_{\text{a-p}}$ ($\sim 440 \text{‰m}$) with the depth-integrated “excess CO₂” ($\sim 180000 \mu\text{mol kg}^{-1} \text{ m}$). This value is very close to the $\Delta\delta^{13}\text{C}/\Delta\text{TCO}_2$ ratio ($-0.024\text{‰}(\mu\text{mol kg}^{-1})^{-1}$) estimated from the temporal changes of TCO₂ and $\delta^{13}\text{C}$ at HOT [Winn et al., 1998; Gruber et al., 1999] and the North Atlantic Ocean [Körtzinger et al., 2003]. It differs, however, from ratios between -0.007 and $-0.015\text{‰}(\mu\text{mol kg}^{-1})^{-1}$ in the Southern Ocean [McNeill et al., 2001] and a value of $-0.016\text{‰}(\mu\text{mol kg}^{-1})^{-1}$ in the northeastern Atlantic [Keir et al., 1998]. The discrepancy of these estimates suggests that this ratio can be considerably variable in different regions of the oceans, and more efforts should be made in order to gain a better global perspective of the influence of anthropogenic CO₂ on $\delta^{13}\text{C}$ of TCO₂ in oceans.

4. Conclusions

In this study, we have thoroughly investigated the vertical distributions of NTA, NTCO₂ and $\delta^{13}\text{C}_{\text{TCO}_2}$ in the water column at SEATS site, northern South China Sea,

which are collected from seven different cruises spanning from March 2002 to August 2003. The depth profiles are then compiled to document their general distributions in the SCS. Furthermore, in order to better understand processes controlling their variations and to better quantify the influence of the anthropogenic CO₂ upon their distributions, we have deconvoluted the profiles into different components using various techniques that have been used widely in marine biogeochemical community. The effort thus ensures our results to be able to be compared with data from other studies for a better coverage of carbon synthesis in the world oceans.

Our results reveal that depth distributions of NTA, NTCO₂ and $\delta^{13}\text{C}_{\text{TCO}_2}$ in the water column at SEATS site are all controlled, in different extent, by production/decomposition of organic matters, production/dissolution of carbonates, and difference in their respective preformed values. The increase of NTA at shallow waters is resulted principally from the augmentation of preformed values, but in the deep waters carbonate dissolution becomes increasingly important for the continuous rise in NTA. For NTCO₂, increments of preformed values and organic oxidation with depth are responsible for the observed increasing trend. The decrease of $\delta^{13}\text{C}_{\text{TCO}_2}$ with depth, however, is attributed mostly to organic oxidation in water column. Calculations further reveal that an approximately 30% of TCO₂ added to

the deep waters is resulted from carbonate dissolution. Such a high percentage is among the greatest values reported in the world oceans and can be attributed to the fact that deep waters in the SCS is originated from the oldest water mass, i.e. the North Pacific Deep Water. Moreover, the depth distributions of $\text{TCO}_2^{\text{carb}}$ (TA^*) show that considerable carbonate dissolution may have taken place at depths shallower than those hypothetically estimated from calcite and aragonite saturations, providing that contributions from other non-carbonate sources are insignificant.

We also estimate the depth of anthropogenic CO_2 penetration in the water column using “anthropogenic CO_2 ” and “ $\Delta\delta^{13}\text{C}_{\text{a-p}}$ ” data, which are derived from the “back-calculation” and “ $\delta^{13}\text{C}$ vs. phosphate” methods, respectively. Results show that anthropogenic CO_2 has penetrated to a depth slightly deeper than 1000 m at SEATS site. Since more anthropogenic CO_2 is expected to continuously add into atmosphere, results from this study will provide a baseline for future studies of the impacts of anthropogenic CO_2 on the carbon system in the SCS.

Acknowledgments

We are grateful to the Captains, crew and technicians of *R/V Ocean Research I* and *III* for assistance with deck operations and shipboard sampling, and to F. S. Lee and S. G. Lin for laboratory assistance. We appreciate K. K. Liu, L. S. Wen, F. K.

Shiah, and staff of the National Center for Ocean Research (NCOR) for cruise participation and logistic supports during the course of this research. This work was supported by the National Science Council grants (NSC90-2611-M-110-025-OP1, NSC91-2611-M-110-003 and NSC92-2119-M-110-001) to D. D. Sheu. The study is a contribution to the SEATS (South East Asia Time-series Study) program sponsored by NCOR, National Science Council, Republic of China.

References:

- Anderson, L. A., On the hydrogen and oxygen content of marine phytoplankton, *Deep Sea Res. I*, 42, 1675-1680, 1995.
- Anderson, L. A., and J. L. Sarmiento, Redfield ratios of remineralization determined by nutrient data analysis, *Global Biogeochem. Cycles*, 8, 65-80, 1994.
- Andres, R. J., G. Marland, and S. Bischoff, Global and latitudinal estimates of $\delta^{13}\text{C}$ from fossil fuel consumption and cement manufacture, *Carbon Dioxide Inf. Anal. Cent., CDIAC Communications*, 22, Oak Ridge Natl. Lab., Oak Ridge, Tenn., 1996.
- Bates, N. R., Interannual variability of oceanic CO_2 and biogeochemical properties in the Western North Atlantic subtropical gyre. *Deep-Sea Res. II*, 48, 1507-1528, 2001.

- Benson, B. B., and D. Krause, The concentration and isotopic fractionation of oxygen dissolved in freshwater and seawater in equilibrium with the atmosphere. *Limnol. and Oceanogr.*, 29, 620-632, 1984.
- Böhm, F., M. M. Joachimski, H. Lehnert, G. Morgenroth, W. Kretschmer, J. Vacelet, W. C. Dullo, Carbon isotope records from extant Caribbean and South Pacific sponges: Evolution of $\delta^{13}\text{C}$ in surface water DIC, *Earth Planet. Sci. Lett.*, 139, 291-303, 1996.
- Bonneau, M. C., C. Bergnaud-Grazzini, and W. H. Berger, Stable isotope fractionation and differential dissolution in recent planktonic foraminifera from Pacific box cores, *Oceanol. Acta*, 3, 377-382, 1980.
- Boulahdid, M., and J. F. Minster, Oxygen consumption and nutrient regeneration ratios along isopycnal horizons in the Pacific Ocean, *Mar. Chem.*, 26, 133-153, 1989.
- Bradshaw, A. L., P. G. Brewer, D. K. Shafer, and R. T. William, Measurement of total carbon dioxide and alkalinity by potentiometric titration in the GEOSECS program. *Earth and Planet. Sci. Lett.*, 55, 99-115, 1981.
- Brewer, P.G., Direct measurement of the oceanic CO_2 increase, *Geophys. Res. Lett.*, 5, 997-1000, 1978.
- Brewer, P. G., and J. C. Goldman, Alkalinity changes generated by phytoplankton

- growth, *Limnol. Oceanogr.*, 21, 108-117, 1976.
- Broecker, W. S., "NO₃," a conservative water-mass tracer, *Earth Planet. Sci. Lett.*, 23, 100-107, 1974.
- Broecker, W. S., and T. H. Peng, *Tracers in the Sea*, 690 pp., Lamont-Doherty Earth Observatory, Palisades, N. Y., 1982.
- Broecker, W. S., and E. Maier-Reimer, The influence of air and sea exchange on the carbon isotope distribution in the sea, *Global Biogeochem. Cycles*, 6, 315-320, 1992.
- Butler, J. N., Alkalinity titration in seawater: how accurately can the data be fitted by an equilibrium model? *Mar. Chem.*, 38, 251-282, 1992.
- Byrne, R. H., J. G. Acker, P. R. Betzer, R. A. Feely, and M. H. Cates, Water column dissolution of aragonite in the Pacific Ocean, *Nature*, 312, 321-326, 1984.
- Chen, C. T. A., Decomposition of calcium carbonate and organic carbon in the deep oceans, *Science*, 201, 735-736, 1978.
- Chen, C. T. A., On the depth of anthropogenic CO₂ penetration in the Atlantic and Pacific Oceans, *Oceanol. Acta*, 97-102, 1987.
- Chen, C. T. A., Rates of calcium carbonate dissolution and organic carbon decomposition in the North Pacific Ocean, *J. Oceanogr. Soc. Jpn.*, 46, 201-210, 1990.

- Chen, C. T. A., Anthropogenic CO₂ distribution in the North Pacific Ocean, *J. Oceanogr.*, 49, 257-270, 1993.
- Chen, C. T. A., Shelf- vs. dissolution-generated alkalinity above the chemical lysocline, *Deep Sea Res. II*, 49, 5365-5375, 2002.
- Chen, C.T.A., and F.J. Millero, Gradual increase of oceanic CO₂, *Nature*, 277, 205-206, 1979.
- Chen, C. T. A., R. M. Pytkowicz, and E. J. Olson, Evaluation of the calcium problem in the South Pacific, *Geochem. J.*, 16, 1-10, 1982.
- Chen, C.T.A., M. R. Rodmam, C. L. Wei, E. J. Olson, and R. A. Feely, Carbonate Chemistry of the North Pacific Ocean. US Department of Energy Technical Report, *DOE/NBB-0079*, p. 176, 1986.
- Chen, C. T. A., and M. H. Huang, Carbonate chemistry and the anthropogenic CO₂ in the South China Sea, *Acta Oceanol. Sinica*, 14, 47-57, 1995.
- Chen, C. T. A., and M. H. Huang, A mid-depth front separating the South China Sea Water and the Philippine Sea Water, *J. of Oceanog.*, 52, 17-25, 1996.
- Chen, C. T. A., and S. L. Wang, Influence of intermediate water in the western Okinawa Trough by the outflow from the South China Sea, *J. of Geophys. Res.*, 103, 12,683- 12, 688, 1998.
- Chen, C. T. A., S. L. Wang, B. J. Wang, and S. C. Pai, Nutrient budgets for the South

China Sea basin, *Mar. Chem.*, 75, 281- 300, 2001.

Craig, H., Isotopic standards for carbon and oxygen and correction factors for mass-spectrometric analysis of carbon dioxide. *Geochim. Cosmochim. Acta*, 12, 133-149, 1957.

Chou, W. C., D. D. Sheu, C. T. A. Chen, S. L. Wang, and C. M. Tseng, Preliminary investigation on seasonal variability of mixed-layer CO₂, alkalinity, and fCO₂ at SEATS time-series station, northern South China Sea. (submitted to *Deep-Sea Res. I*)

Coatanoan, C., C. Goyet, N. Gruber, C. L. Sabine, and M. Warner, Comparison of two approaches to quantify anthropogenic CO₂ in the ocean: Results from the northern Indian Ocean, *Global Biogeochem. Cycles*, 15, 11-25, 2001.

Deutsch, C., N. Gruber, R. M. Key, J. L. Sarmiento, and A. Ganachaud, Denitrification and N₂ fixation in the Pacific Ocean, *Global Biogeochem. Cycles*, 15, 483-506, 2001.

DOE, Handbook of methods for the analysis of the various parameters of the carbon dioxide system in seawater, in *U.S. Department of Energy CO₂ science Team Report, version 2*, edited by A. G. Dickson A.G. and C. Goyet C., 1994.
(unpublished manuscript).

Dore, J. E., C. J. Carrillo, D. V. Hebel, and D. M. Karl, Carbon cycle observations at

the Hawaii Ocean Time-series Station ALOHA, in *Proceedings of the PICES North Pacific CO₂ Data Synthesis Symposium*, edited by Y. Nojiri, and R. Feely, Tsukuba, Japan, October 2000, 2002.

Dore, J. E., R. Lukas, D. W. Sadler, and D. M. Karl, Climate-driven changes to the atmospheric CO₂ sink in the subtropical North Pacific Ocean. *Nature*, 24, 754-757, 2003.

Emerson, S., Seasonal oxygen cycles and biological new production in surface waters of the subarctic Pacific Ocean, *J. Geophys. Res.*, 92(C6), 6535-6544, 1987.

Feely, R. A., C. L. Sabine, R. M. Key, and T. H. Peng, CO₂ survey synthesis results: Estimating the anthropogenic carbon dioxide sink in the Pacific Ocean, *U. S. JGOFS News*, 9, 1-4, 1999.

Feely, R. A., C. L. Sabine, K. Lee, F. L. Millero, M. F. Lamb, D. Greeley, J. L. Bullister, R. M. Key, T. H. Peng, A. Kozyr, T. Ono, and C. S. Wong, In situ calcium carbonate dissolution in the Pacific Ocean, *Global Biogeochem. Cycles*, 16, doi:10.1029/2002GB001866, 2002.

Friedli, H., H. Löttscher, H. Oeschger, U. Siegenthaler, and B. Stauffer, Ice core record of the ¹³C/¹²C ratio of atmospheric CO₂ in the past two centuries, *Nature*, 324, 237-238, 1986.

Goericke, R., and B. Fry, Variations of marine plankton δ¹³C with latitude,

temperature, and dissolved CO₂ in the world ocean, *Global Biogeochem. Cycles*, 8, 85-90, 1994.

Gong, G. C., K. K. Liu, C. T. Liu, and S. C. Pai, The chemical hydrography of the South China Sea west of Luzon and a comparison with the West Philippine Sea, *Terr. Atmos. Oceanic Sci.*, 3, 587-602, 1992.

González-Dávila, M., J. M. Santana-Casiano, M. J Rueda, O. Linás, E. F.

González-Dávila, Seasonal and interannual variability of sea-surface carbon dioxide species at the European station for time-series in the ocean at the Canary Islands (ESTOC) between 1996 and 2000, *Global Biogeochem. Cycles*, 17, doi:10.1029/2002GB001993, 2003.

Goyet, C., C. Coatanoan, G. Eiseheid, T. Amaoka, K. Okuda, R. Healy, and S.

Tsunogai, Spatial variation of total CO₂ and total alkalinity in the northern Indian Ocean: A novel approach for the quantification of anthropogenic CO₂ in seawater, *J. Mar. Res.*, 57, 135-163, 1999.

Gruber, N., Anthropogenic CO₂ in the Atlantic Ocean, *Global Biogeochem. Cycles*, 12, 165-191, 1998.

Gruber, N., J. L. Samiento, and T. F. Stocker, An improved method for detecting anthropogenic CO₂ in the oceans, *Global Biogeochem. Cycles*, 10, 809-837, 1996.

Gruber, N., and J. L. Samiento, Global patterns of marine nitrogen fixation and

denitrification, *Global Biogeochem. Cycles*, *11*, 235-256, 1997.

Gruber, N., C. D. Keeling, R. B. Bacastow, P. R. Guenther, T. J. Lueker, M. Wahlen,

H. A. J. Meijer, W. G. Mook, and T. F. Stocker, Spatiotemporal patterns of carbon-13 in the global surface oceans and the oceanic Suess effect, *Global Biogeochem. Cycles*, *13*, 307-335, 1999.

Gruber, N., C. D. Keeling, and N. R. Bates, Interannual variability in the North

Atlantic ocean carbon sink, *Science*, *298*, 2374-2378, 2002.

Harris, R. P., Zooplankton grazing on the coccolithophore *Emiliana huxleyi* and its

role in inorganic carbon flux, *Mar. Biol.*, *119*, 431-439, 1994.

Heimann, M., and E. Maier-Reimer, On the relations between the ocean uptake of

CO₂ and its carbon isotopes, *Global Biogeochem. Cycles*, *10*, 89-110, 1996.

Jenkins, W. J., and J. C. Goldman, Seasonal oxygen cycling and primary production

in the Sargasso Sea, *J. Mar. Res.*, *43*, 465-491, 1985.

Johnson, K. M., K. D. Wills, D. B. Butler, W. K. Johnson, and C. S. Wong, C.S.,

Coulometric total carbon dioxide analysis for marine studies: maximizing the performance of an automated gas extraction system and coulometric detector, *Mar. Chem.*, *44*, 167-188, 1993.

Karl, D. M., R. Letelier, D. V. Hebel, D. F. Bird, and C. D. Winn, Trichodesmium

blooms and new production in the North Pacific gyre, in *Marine Pelagic*

Cyanobacteria: Trichodesmium and Other Diazotrophs, edited by E. J. Carpenter, pp. 219-237, Kluwer Acad. Norwell, Mass., 1992.

Karl, D. M., R. Letelier, L. Tupas, J. Dore, J. Christian, and D. Hebel, The role of nitrogen fixation in biogeochemical cycling in the subtropical North Pacific Ocean, *Nature*, 388, 533-538, 1997.

Karl, D. M., N. R. Bates, S. Emerson, P. J. Harrison, C. Jeandel, O. Llinás, K. K. Liu, J-C Marty, A. F. Michaels, J. C. Miquel, S. Neuer, N. Nojiri, and C. S. Wong, Temporal studies of biogeochemical processes determined from ocean time-series observations during the JGOFS era, in *Ocean Biogeochemistry: the role of the ocean carbon cycle in global change*, edited by M. J. R. Fasham, pp. 239-267, Springer, Berlin, 2003.

Keeling, C. D., R. B. Bacastow, A. F. Carter, S. C. Piper, T. P. Whorf, M. Heimann, W. G. Mook, and H. Roeloffzen, A three-dimensional model of atmospheric CO₂ transport based on observed winds, 1, Analysis of observational data, in *Aspects of Climate Variability in the Pacific and thw Western Americas*, *Geophys. Monogr. Ser.*, vol. 55, edited by D. H. Peterson, pp. 165-236, AGU, Washington, D. C., 1989.

Keir, R., G. Rehder, and E. Suess, The $\delta^{13}\text{C}$ anomaly in the Northeastern Atlantic, *Global Biogeochem. Cycles*, 12, 467-477, 1998.

- Körtzinger, A., P. D. Quay, and R. E. Sonnerup, Relationship between anthropogenic CO₂ and ¹³C Suess effect in the North Atlantic Ocean, *Global Biogeochem. Cycles*, *17*, doi:10.1029/2001GB001427, 2003.
- Kroopnick, P., The dissolved O₂-CO₂-¹³C system in the eastern equatorial Pacific, *Deep-Sea Res.*, *21*, 211-227, 1974.
- Kroopnick, P., R. F. Weiss, and H. Craig, Total CO₂, ¹³C, and dissolved oxygen-¹⁸O at GEOSECS II in the North Atlantic, *Earth and Planet. Sci. Lett.*, *16*, 1972.
- Kroopnick, P. M., The distribution of ¹³C of SCO₂ in the world oceans, *Deep Sea Res.*, *32*, 57-84, 1985.
- Lewis, E., and D. W. R. Wallace, Program developed for CO₂ system calculations, Rep. 105, 33pp., Oak Ridge Natl. Lab., U.S. Dep. of Energy, Oak Ridge, Tenn., 1998.
- Lin, H. L., L. W. Wang, C. H. Wang, and G. C. Gong, Vertical distribution of δ¹³C of dissolved inorganic carbon in the Northeastern South China Sea, *Deep Sea Res. I*, *46*, 757-775, 1999.
- Lynch-Stieglitz, J., T. F. Stocker, W. S. Broecker, and R. G. Fairbanks, The influence of air-sea exchanges on the isotopic composition of oceanic carbon: Observations and modeling, *Global Biogeochem. Cycles*, *9*, 653-666, 1995.
- McNichol, A. P., and E. R. M. Druffel, Variability of the δ¹³C of dissolved inorganic

- carbon at a site in the north Pacific Ocean. *Geochim. Cosmochim. Acta*, *56*, 3589-3592, 1992.
- McNeill, B. I., R. J. Matear, and B. Tilbrook, Does carbon 13 track anthropogenic CO₂ in the Southern Ocean? *Global Biogeochem. Cycles*, *15*, 597-614, 2001.
- Millero, F. J., J. Z. Zhang, K. Lee, D. Campelle, Titration alkalinity of seawater. *Mar. Chem.*, *44*, 269-280, 1993.
- Millero, F. J., K. Lee, and M. Roche, Distribution of alkalinity in the surface waters of the major oceans, *Mar. Chem.*, *60*, 111-130, 1998.
- Milliman, J. D., P. J. Troy, W. M. Balch, A. K. Adams, Y. H. Li, and F. T. Mackenzie, Biological mediated dissolution of calcium carbonate above the chemical lysocline, *Deep Sea Res. I*, *46*, 1653-1669, 1999.
- Minster, J., and M. Boulahdid, Redfield ratios along isopycnal surface- A complimentary study, *Deep Sea Res., Part A*, *34*, 1981-2003, 1987.
- Mook, W. G., J. C. Bommerson, and W. H. Staverman, Carbon isotope fractionation between dissolved bicarbonate and gaseous carbon dioxide, *Earth Planet. Sci. Lett.*, *22*, 169-176, 1974.
- Murphy, J., and J. P. Riley, A modified single solution method for the determination of phosphate in natural waters. *Anal. Chim. Acta*, *27*, 31-36, 1962.
- Ono, T., Y. W. Watanabe, and S. Watanabe, Recent increase of DIC in the western

- North Pacific, *Mar. Chem.*, 72, 317-328, 2000.
- Ortiz, J. D., A. C. Mix, P. A. Wheeler, and R. M. Key, Anthropogenic CO₂ invasion into the northeast Pacific based on concurrent $\delta^{13}\text{C}_{\text{DIC}}$ and nutrient profiles from the California Current, *Global Biogeochem. Cycles*, 14, 917-929, 2000.
- Pai, S.C., C. C. Yang, and J. P. Riley, Formation kinetics of the pink azo dye in the determination of nitrite in natural waters. *Anal. Chim. Acta*, 232, 345-349, 1990a.
- Pai, S.C., C. C. Yang, and J. P. Riley, Effects of acidity and molybdate concentration on the kinetics of the formation of the phosphoantimonymolybdenum blue complex. *Anal. Chim. Acta*, 229, 115-120, 1990b.
- Pai, S. C., G. C. Gong, and K. K. Liu, Determination of dissolved oxygen in seawater by direct spectrophotometry of total iodine. *Mar. Chem.*, 41, 343-351, 1993.
- Pai, S. C., and J. P. Riley, Determination of nitrate in the presence of nitrite in natural waters by flow injection analysis with a non-quantitative on-line cadmium reductor. *Int. J. Environmental Analytical Chemistry*, 57, 263-277, 1994.
- Peng, T. H., and W. S. Broecker, C/P ratios in marine detritus, *Global Biogeochem. Cycles*, 1, 155-161, 1987.
- Pond, D. W., R. P. Harris, and C. A. Brownlee, Microinjection technique using a pH sensitive dye to determine the gut pH of *Calanus helgolandicus*, *Mar. Biol.*, 123, 75-79, 1995.

Quay, P. D., B. Tilbrook, and C. S. Wong, Oceanic uptake of fossil fuel CO₂:

Carbon-13 evidence, *Science*, 256, 74-79, 1992.

Quay, P., R. Sonnerup, T. Westby, J. Stutsman, and A. McNichol, Changes in the

¹³C/¹²C of dissolved inorganic carbon in the ocean as a tracer of anthropogenic

CO₂ uptake, *Global Biogeochem. Cycles*, 17, doi:10.1029/2001GB001817, 2003.

Redfield, A. C., B. H. Ketchum, and F. A. Richards, The influence of organisms on

the composition of sea water, in *The Sea*, vol. 2, edited by M. N. Hill, pp. 26-77,

Interscience, New York, 1963.

Sabine, C. L., F. T. Mackenzie, C. Winn, D. M. Karl, Geochemistry of carbon dioxide

in seawater at the Hawaii ocean time series station, ALOHA, *Global Biogeochem.*

Cycles, 9, 637-651, 1995.

Sabine, C. L., R. M. Key, K. M. Johnson, F. L. Millero, A. Poisson, J. L. Samiento, D.

W. R. Wallace, and C. D. Winn, Anthropogenic CO₂ inventory of the Indian

Ocean, *Global Biogeochem. Cycles*, 13, 179-198, 1999.

Sabine, C. L., R. A. Feely, R. M. Key, J. L. Bullister, F. L. Millero, K. Lee, T. H.

Peng, B. Tilbrook, and C. S. Wong, Distribution of anthropogenic CO₂ in the

Pacific Ocean, *Global Biogeochem. Cycles*, 16, doi:10.1029/2001GB001639,

2002a.

Sabine, C. L., R. M. Key, R. A. Feely, and D. Greeley, Inorganic carbon in the Indian

Ocean: distribution and dissolution processes, *Global Biogeochem. Cycles*, 16,

doi:10.1029/2002GB001869, 2002b.

Sheu, D. D., W. Y. Lee, C. H. Wang, C. L. Wei, C. T. A. Chen, C. Cherng, M. H.

Huang, Depth distribution of $\delta^{13}\text{C}$ of dissolved CO_2 in seawater off eastern

Taiwan: effects of the Kuroshio current and its associated upwelling phenomenon.

Cont. Shelf Res., 16, 1609-1619, 1996.

Sonnerup, R. E., P. D. Quay, A. P. McNichol, J. L. Bullister, T. A. Westby, and H. L.

Anderson, Reconstructing the oceanic ^{13}C Suess effect, *Global Biogeochem.*

Cycles, 13, 857-872, 1999.

Sonnerup, R. E., P. D. Quay, A. P. McNichol, , The Indian Ocean ^{13}C Suess effect,

Global Biogeochem. Cycles, 14, 903-916, 2000.

Strickland, J. D. H., and T. R. Parsons, *A practical handbook of seawater analysis.*

Fisheries Research Board of Canada, Ottawa, Canada, 310pp., 1972.

Stuiver, M., P. D. Quay, and H. G. Ostlund, Abyssal water carbon-14 distribution and

the age of the world oceans, *Science*, 219, 849-851, 1983.

Takahashi, T., W. S. Broecker, and S. Langer, Redfield ratio based on chemical data

from isopycnal surface, *J. Geophys. Res.*, 90, 6907-6924, 1985.

Tans, P., A compilation of bomb ^{14}C data for use in global carbon model calculation,

in *SCOPE 16: Carbon Cycles Modelling*, edited by B. Bolin, pp. 131-137, John

Wiley, New York, 1981.

Tsunogai, S., An estimate of the rate of decomposition of organic matter in the deep water of the Pacific Ocean, in *Biological Oceanography of the Northern North Pacific Ocean*, edited by Y. Takenouti and I. Shoten, pp. 517-533, Tokyo, 1972..

Tsurushima, N., Y. Nojiri, K. Imai, and S. Watanabe, Seasonal variations of carbon dioxide system and nutrients in the surface mixed layer at station KNOT (44° N, 155° E) in the subarctic western North Pacific. *Deep-Sea Res. II*, 49, 5377-5394, 2002.

Wallace, D.W.R. Introduction to special section: Ocean measurements and models of carbon sources and sinks, *Global Biogeochem. Cycles*, 15, 3-10, 2001.

Winn, C. D., Y. H. Li, F. T. Mackenzie, and D. M. Karl, Rising surface ocean dissolved inorganic carbon at the Hawaii Ocean Time-series site. *Mar. Chem.*, 60, 33-47, 1998.

Wong, C. S., and Y. H. Chan, Temporal variations in the partial pressure and flux of CO₂ at ocean Station P in the subarctic northeast Pacific Ocean. *Tellus*, 43B, 206-223, 1991.

Wong, G. T. F., S. W. Chung, F. K. Shiah, C. C. Chen, L. S. Wen, and K. K. Liu, Nitrate anomaly in the upper nutricline in the northern South China Sea- Evidence for nitrogen fixation, *Geophys. Res. Lett.*, 29,

doi:10.1029/2002GL015796, 2002.

Zhang, J., P. D. Quay, and D. O. Wilbur, Carbon isotope fractionation during
gas-water exchange and dissolution of CO₂, *Geochim. Cosmochim. Acta*, 59,
107-114, 1995.

FIGURE CAPTIONS

- Fig. 1. Bathymetric map showing the location of the SEATS (South East Asia Time-series Study) time-series station ($18^{\circ}15'N$, $115^{\circ}35'E$). Contours are in meters.
- Fig. 2. Depth profiles of PO_4^{3-} (a), NO_3^- (b), AOU (c), NTA (d), $NTCO_2$ (e), and $\delta^{13}C_{TCO_2}$ (f) at the SEATS station.
- Fig. 3. Plots of PO_4^{3-} vs. AOU (a), NO_3^- vs. AOU (b), and NO_3^- vs. PO_4^{3-} (c) at the SEATS station. Open circles represent samples taken from depths shallower than 100 m, whereas solid circles stand for those deeper than 100 m.
- Fig. 4. Depth profiles of N^* at the SEATS station, which is calculated from N^* ($\mu\text{mol kg}^{-1}$) = nitrate $-16 \times$ phosphate $+ 2.9$ [Gruber and Samiento, 1997; Deutsch et al., 2001].
- Fig. 5. Depth profiles of measured NTA (NTA^{meas}), preformed NTA (NTA^{pre}), and $NTA^{\text{pre}} + TA^{\text{org}}$ at the SEATS station. See details in text for the definitions and calculations of TA^{org} and TA^{carb} .
- Fig. 6. Depth profiles of measured $NTCO_2$ ($NTCO_2^{\text{meas}}$), preformed $NTCO_2$ ($NTCO_2^{\text{pre}}$), and $NTCO_2^{\text{pre}} + TCO_2^{\text{org}}$ at the SEATS station. See text for the definitions and calculations of TCO_2^{org} and TCO_2^{carb} in details.
- Fig. 7. Depth profiles of IC/OC ratio at the SEATS station, which implies the relative contribution of carbonate dissolution and organic decomposition to TCO_2 production in deep waters.
- Fig. 8. Depth profiles of aragonite ($\Omega_{\text{aragonite}}$) and calcite (Ω_{calcite}) saturation levels at the SEATS station. Superimposed is the depth profile of TCO_2^{carb} (TCO_2 produced from carbonate dissolution).
- Fig. 9. Depth profiles of measured $\delta^{13}C$ ($\delta^{13}C^{\text{meas}}$), preformed $\delta^{13}C$ ($\delta^{13}C^{\text{pre}}$), and $\delta^{13}C^{\text{pre}} + \delta^{13}C^{\text{org}}$ at the SEATS station. See details in text for the definition and calculation of $\delta^{13}C^{\text{org}}$.

Fig. 10. Depth profiles of anthropogenic CO₂ at the SEATS station.

Fig. 11. The correlation between $\delta^{13}\text{C}_{\text{TCO}_2}$ and phosphate at the SEATS station. Superimposed are two regression lines calculated separately from water samples above (open circles) and below (solid circles) 100 m. In addition, the dotted and solid lines denote respectively the hypothetical mean ocean biological trend and that derived from the pre-anthropogenic model. See details in text for the definitions and calculations of the mean ocean biological trend and the pre-anthropogenic model.

Fig. 12. Depth profiles of $\Delta\delta^{13}\text{C}_{\text{a-p}}$ at the SEATS station. See text for the definition and calculation of “ $\Delta\delta^{13}\text{C}_{\text{a-p}}$ ” in details.

Fig. 1

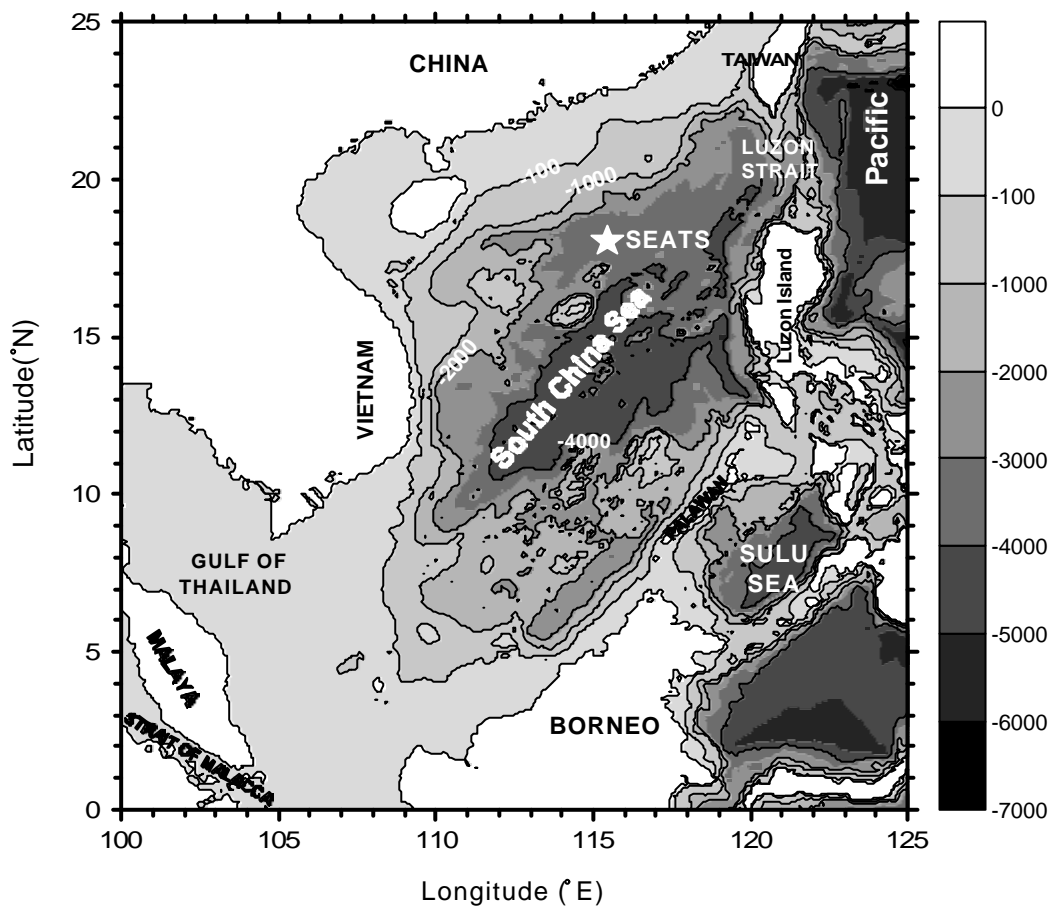


Fig. 2

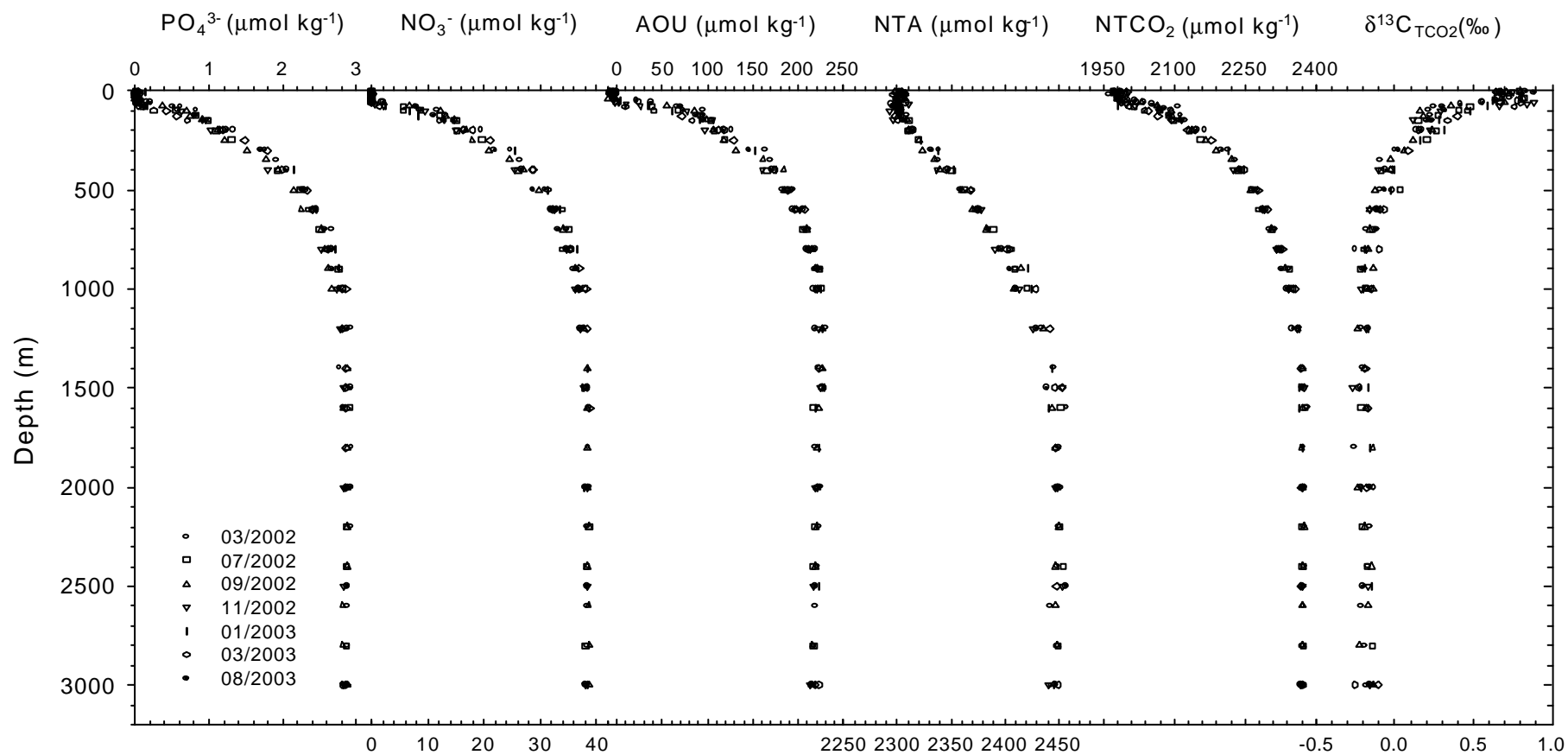


Fig. 3

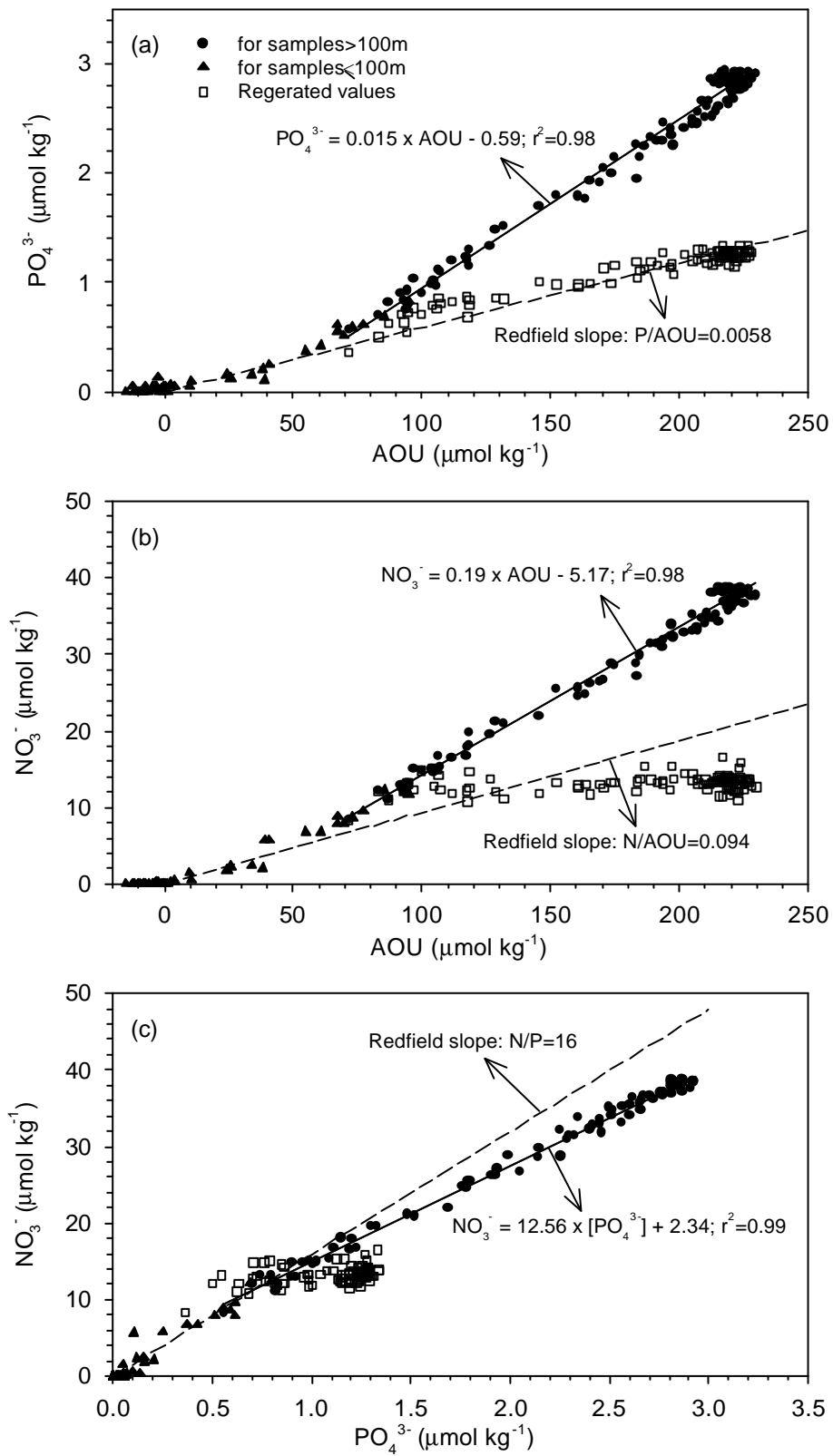


Fig. 4

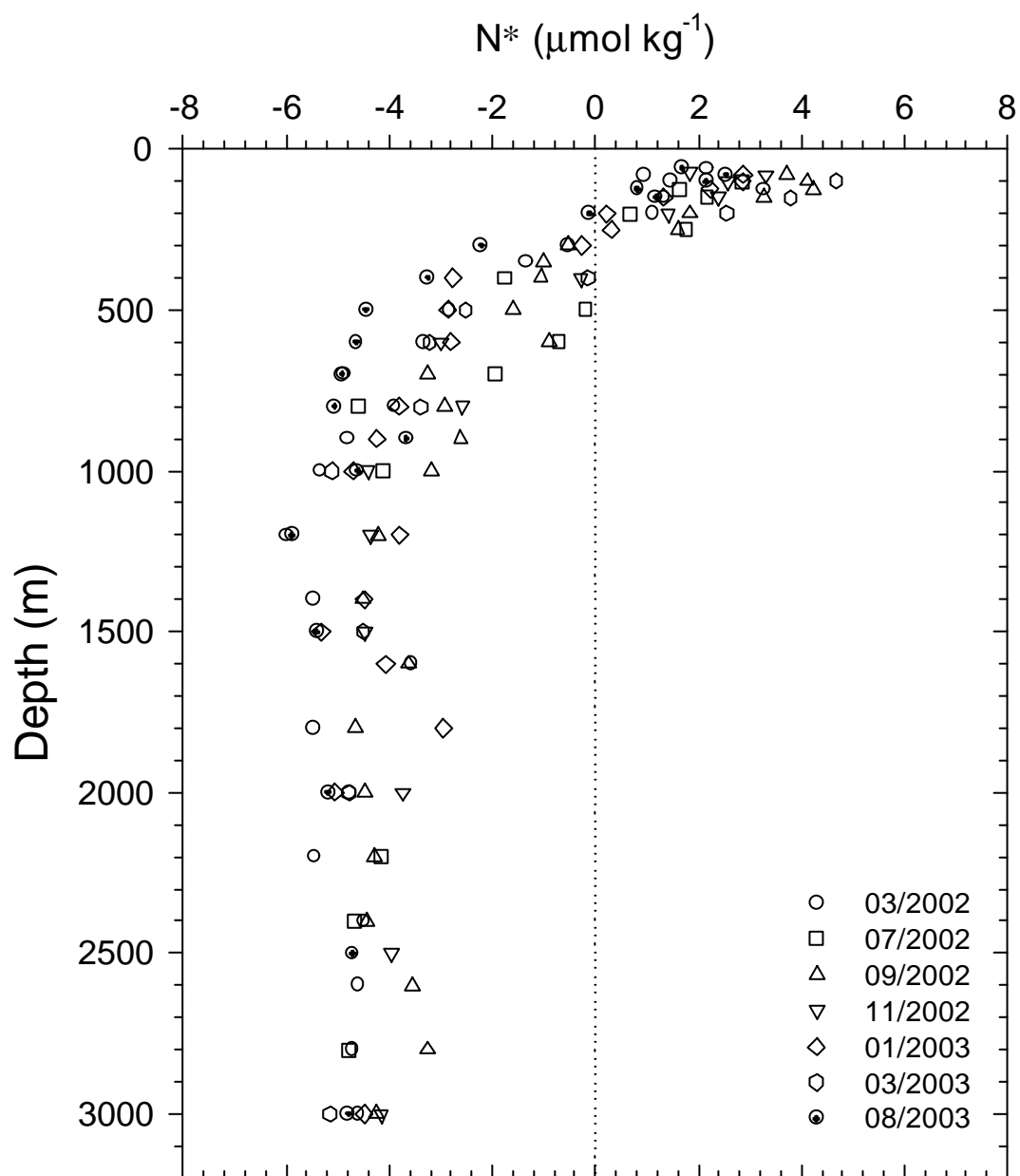


Fig. 5

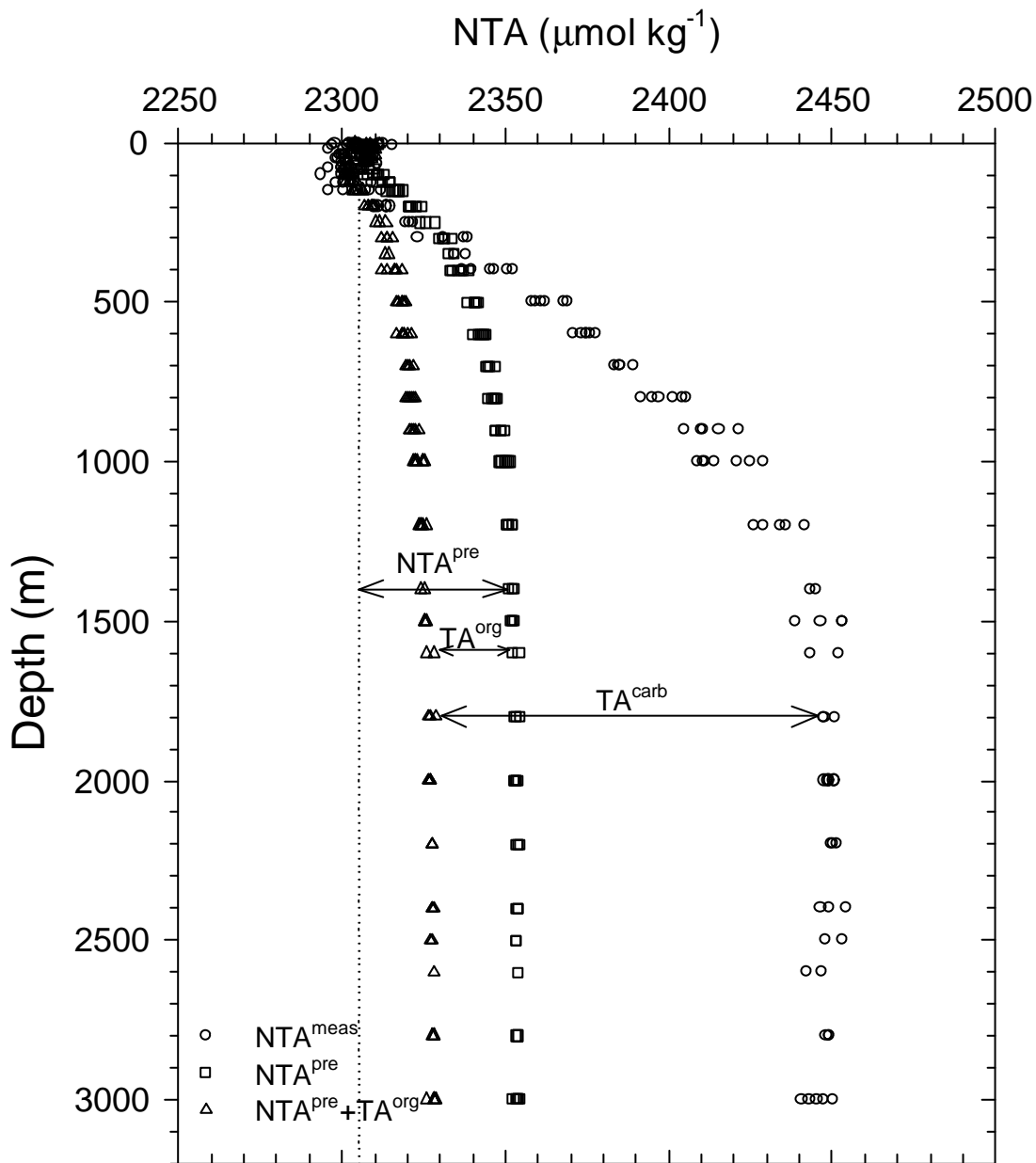


Fig. 6

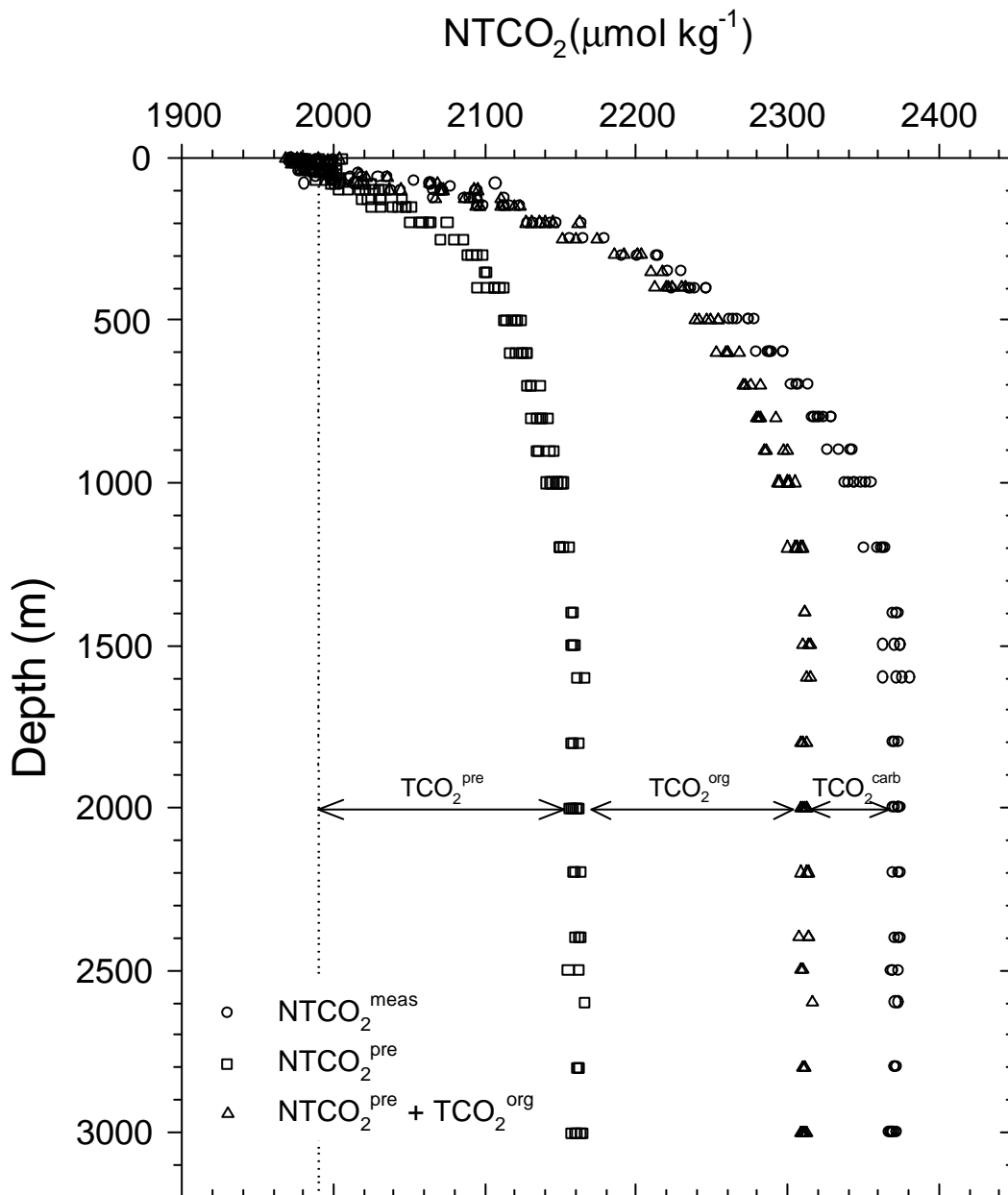
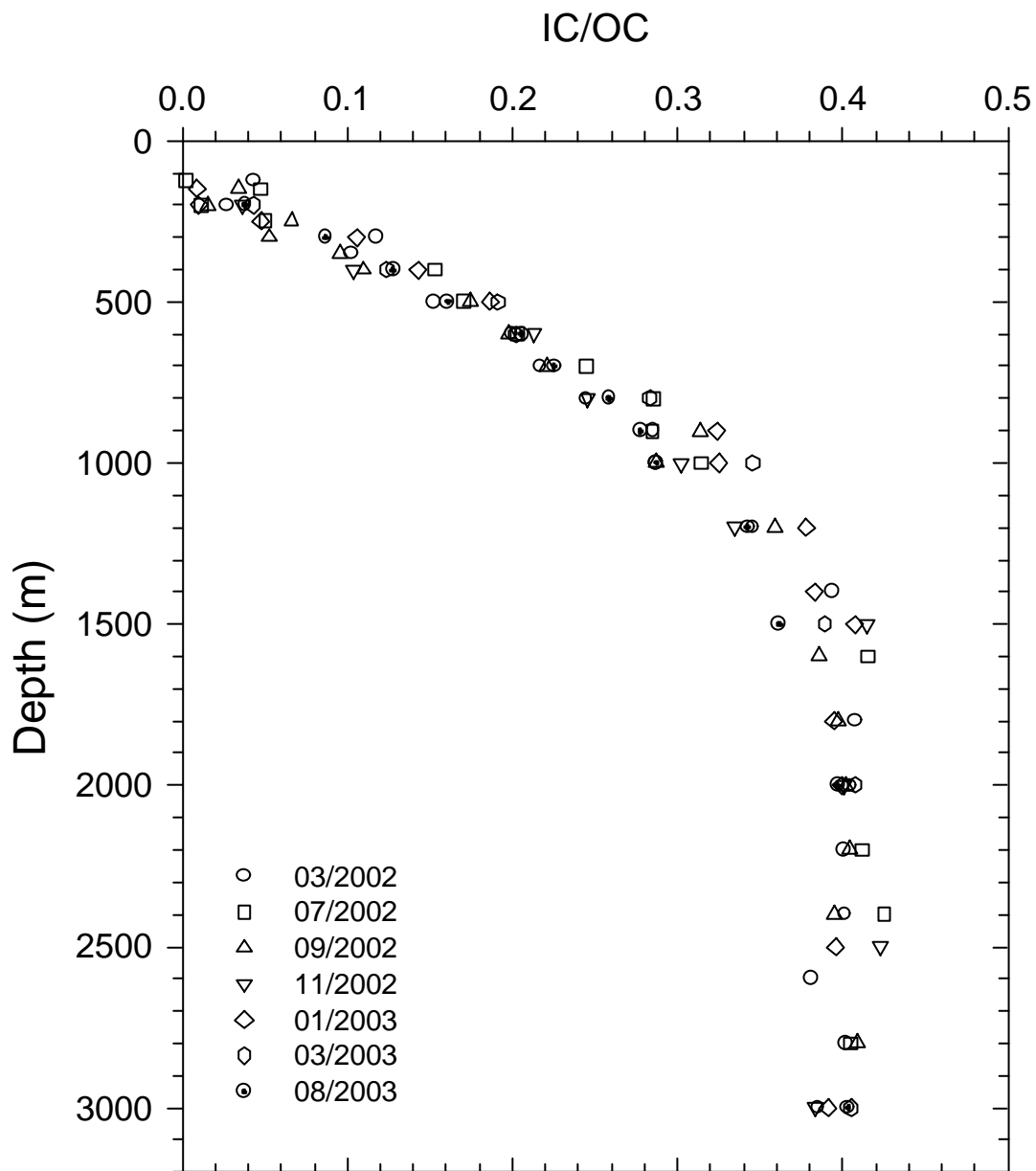


Fig. 7



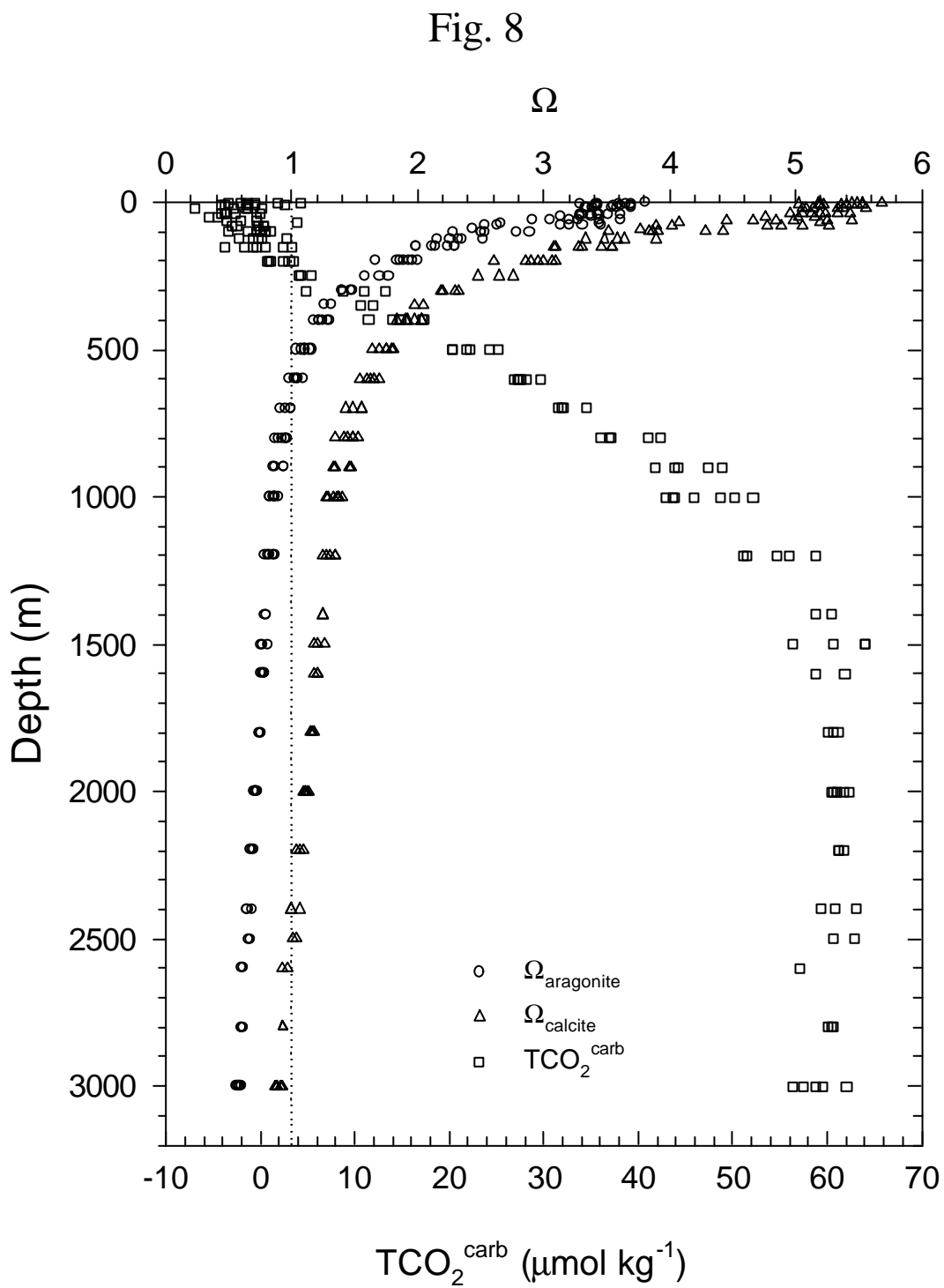


Fig. 9

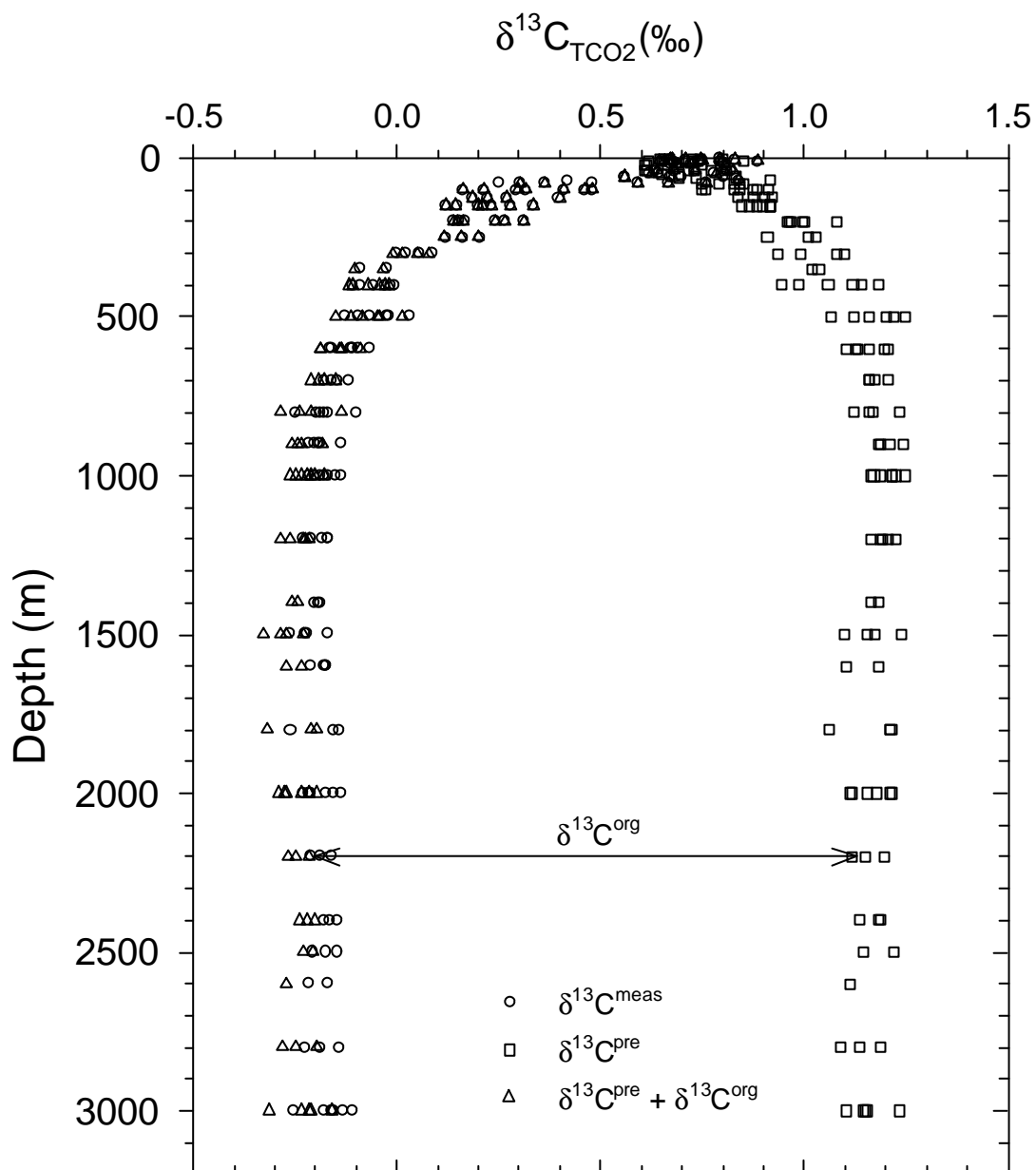


Fig. 10

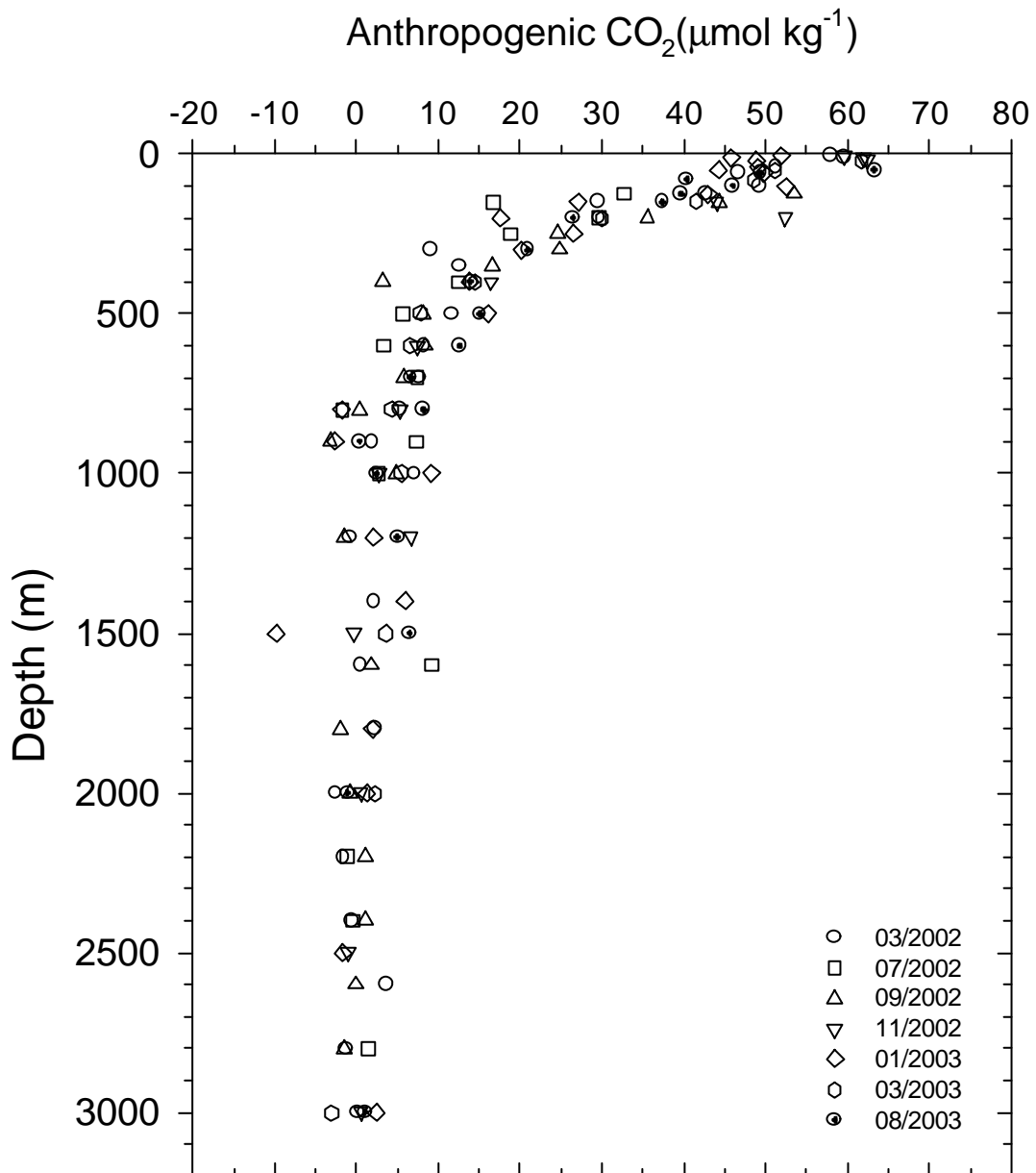


Fig. 11

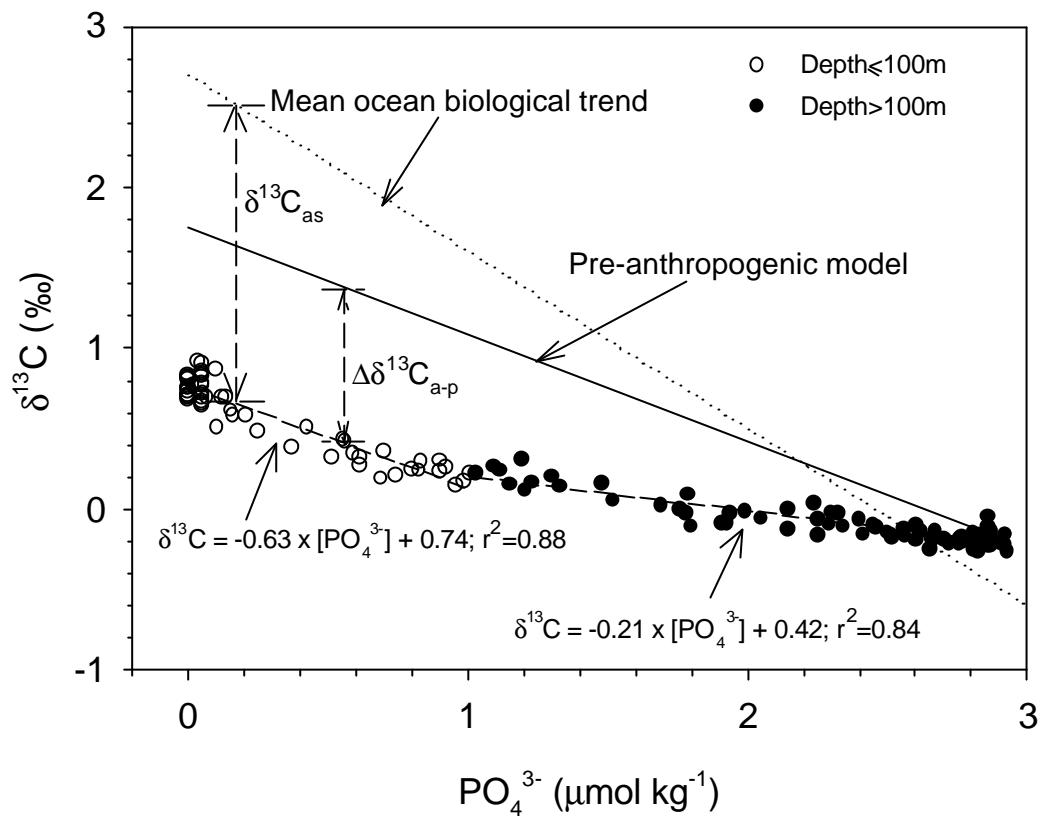
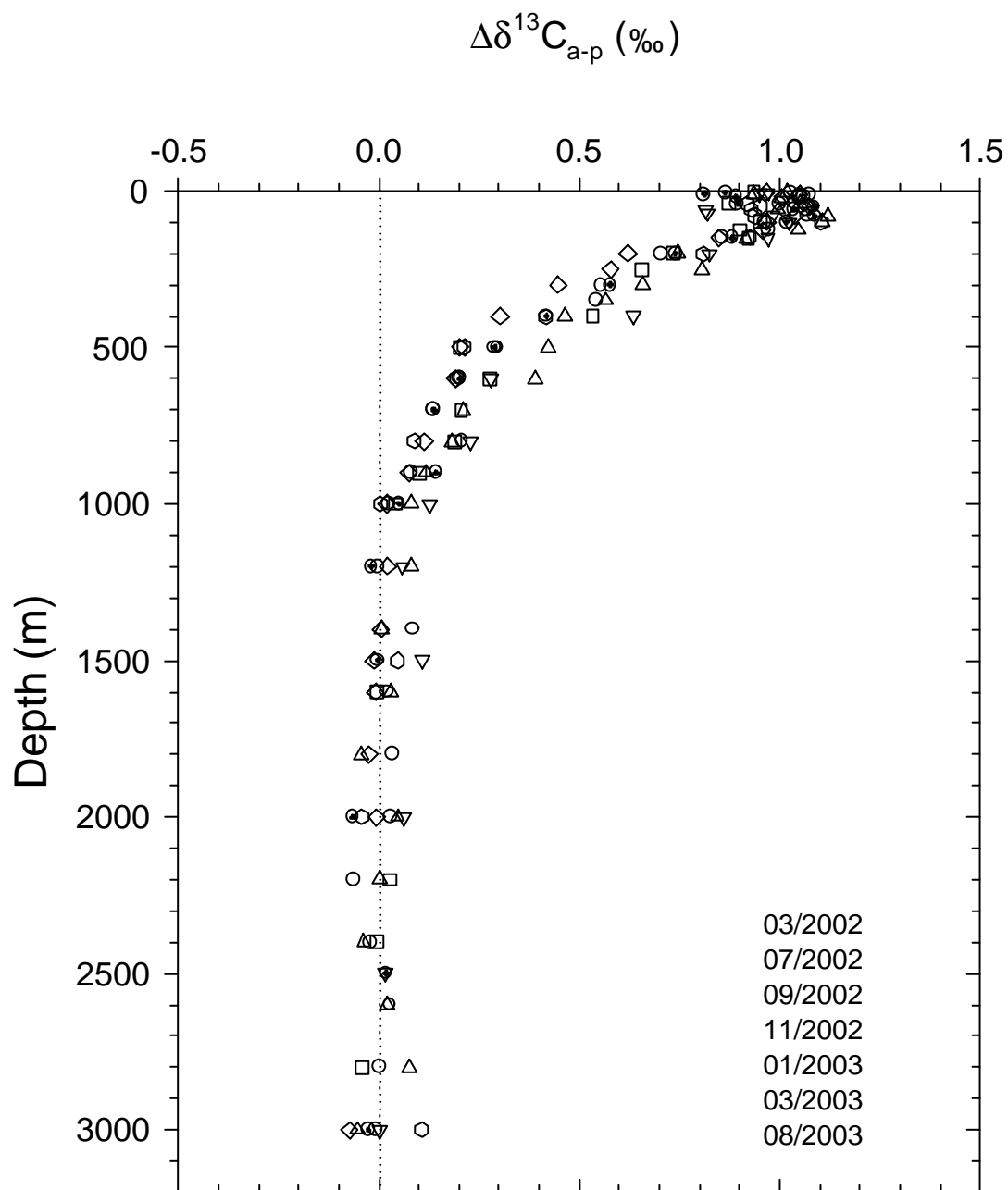


Fig. 12



作者簡介

姓名：周文臣

生日：民國 58 年 1 月 28 日

出生地：台灣 桃園

學歷：

國立中山大學海洋地質及化學研究所博士班 2000-present

法國巴黎第六大學地體構造系博士班研究 1998-1999

法國 Poitiers 大學法語密集班結業 1997-1998

國立中山大學海洋地質研究所碩士 1992-1994

國立中山大學海洋資源系學士 1988-1992

經歷：

私立實踐大學兼任講師 2000-2002

國立中山大學海洋地質研究所研究助理 1996-1997

著作：

一、期刊論文

1. Sheu, D.D., Jou, W.C., Chen, M.J., 1995. Evaluation on the precision of stable isotopic analysis of trace carbonate samples for paleotemperature estimate. *Acta Oceanographica Taiwanica* 34, 61-70.
2. Sheu, D.D., Jou, W.C., Chen, M.J., Lee, W.Y., Lin, S., 1995. Variations of calcium carbonate, organic carbon and their isotopic compositions in surface sediments of the East China Sea. *Terrestrial, Atmospheric and Oceanic Sciences* 6, 115-128.
3. Sheu, D.D., Jou, W.C., Chung, Y.C., Tang, T.Y., Hung, J.J., 1999. Geochemical and carbon isotopic characterization of particles collected in sediment traps from the East China Sea continental slope and the Okinawa Trough northeast of Taiwan. *Continental Shelf Research* 19, 183-203.
4. Chou, W.C., Sheu, D.D., Chen, C.T.A., Wang, S.L., Tseng, C.M., 2004. Preliminary investigation on seasonal variability of mixed-layer CO₂, alkalinity, and fCO₂ at the SEATStime-series site, northern South China Sea, Deep-Sea Research I. (submitted)
5. Chou, W.C., Sheu, D.D., Chen, C.T.A., Tseng, C.M., 2004. Vertical distributions of alkalinity, TCO₂, δ¹³C_{TCO₂} at South East Asia Time-series Study (SEATS) site: controlling processes and anthropogenic CO₂ influence. (in preparation)

二、研討會論文

01. 周文臣、許德惇、陳鎮東、李福祥、林信吉, 2001, 南海 $\delta^{18}\text{O}_{\text{SW}}$, $\delta^{13}\text{C}_{\text{DIC}}$ 及 $\delta^{18}\text{O}_{\text{DO}}$ 深度變化和混合層厚薄關係之研究, 2001 年地球科學聯合學術研討會: 海洋科學成果發表會論文集, 2001 年 9 月 25~27 日, A124-A125 頁。
02. 張志成、許德惇、周文臣、詹森, 2001, 台灣海峽海水氧同位素組成之時空分佈變化, 2001 年地球科學聯合學術研討會: 海洋科學成果發表會論文集, 2001 年 9 月 25~27 日, A181 頁。
03. 周文臣、許德惇、林清芬、陳鎮東, 2002, 南海與西菲律賓海海水 $\delta^{18}\text{O}$ 與鹽度垂直分布的差異: 談南海水的來源, 2002 年海峽兩岸第 5 屆台灣臨近海域海洋科學研討會論文集, 2002 年 5 月 14~16 日, 164-166 頁。
04. 許德惇、周文臣, 2002, C-13 distribution of total dissolved CO_2 in seawater at the South China Sea SEAT station: Observations and interpretations, 2002 年海洋科學成果發表會論文摘要集, 2002 年 12 月 23~25 日, 20-23 頁。
05. 周文臣、許德惇、洪佳章、鍾玉嘉、洪國璋、Cindy Lee, 2002, 沉積物中胺基酸的分析方法及其應用: 以高屏溪及其河口沉積物與沉降顆粒為例, 2002 年海洋科學成果發表會論文摘要集, 2002 年 12 月 23~25 日, 273-275 頁。
06. Sheu, D.D., Chou, W.C., 2003. Seasonal variability of seawater $\delta^{13}\text{C}$ at the South China Sea time-series station. JGOFS Final Open Science Conference Program Abstracts, May 5-8, 2003, Washington, D.C., USA, p71.
07. 周文臣、許德惇、陳鎮東、曾鈞懋、孫震南、施詠嚴, 2004, Vertical distributions of alkalinity, TCO_2 and $\delta^{13}\text{C}_{\text{TCO}_2}$ at the South East Asia Time-series Station (SEATS): Controlling processes and anthropogenic CO_2 influences, 2004 年海洋科學成果發表會論文摘要集, 2004 年 5 月 17~19 日, 39 頁。
08. 曾鈞懋、李丙生、周文臣、許德惇、黃天福、劉康克, 2004, Temporal variability of upper-layer oceanic CO_2 species at SEATS, 2004 年海洋科學成果發表會論文摘要集, 2004 年 5 月 17~19 日, 40 頁。
09. Chou W.C., Sheu, D.D., Chen, C.T.A., Tseng, C.M., 2004. Depth variations of alkalinity, TCO_2 , and $\delta^{13}\text{C}_{\text{TCO}_2}$ at SEATS Time-series Station, Northern South China Sea, 2004 Western Pacific Geophysics Meeting Abstracts, August 16-20, 2004, Honolulu, Hawaii. (accepted)
10. Tseng, C.M., Lee, B.S., Chou, W.C., Sheu, D.D., Wong, G.T.F., Liu, K.K., 2004. Temporal variability of upper-layer oceanic CO_2 species at SEATS, 2004 Western Pacific Geophysics Meeting Abstracts, August 16-20, 2004, Honolulu, Hawaii. (accepted)
11. 周文臣、許德惇、陳鎮東、王樹倫、曾鈞懋, 2004, Preliminary study on seasonal variability of mixed-layer CO_2 , alkalinity, and fCO_2 , 海峽兩岸第 6 屆 (2004 年) 海洋科學研討會論文集, 2004 年 8 月 27~30 日。 (submitted)